



DIGITAL CONTROLLER DESIGN FOR SAMPLED-DATA NONLINEAR SYSTEMS

A THESIS SUBMITTED TO  
THE GRADUATE SCHOOL OF NATURAL AND APPLIED SCIENCES  
OF  
MIDDLE EAST TECHNICAL UNIVERSITY

BY

AHMET ÜSTÜNTÜRK

IN PARTIAL FULFILLMENT OF THE REQUIREMENTS  
FOR  
THE DEGREE OF DOCTOR OF PHILOSOPHY  
IN  
ELECTRICAL AND ELECTRONICS ENGINEERING

MARCH 2012

Approval of the thesis:

**DIGITAL CONTROLLER DESIGN FOR SAMPLED-DATA NONLINEAR SYSTEMS**

submitted by **AHMET ÜSTÜNTÜRK** in partial fulfillment of the requirements for the degree of **Doctor of Philosophy in Electrical and Electronics Engineering Department, Middle East Technical University** by,

Prof. Dr. Canan Özgen  
Dean, Graduate School of **Natural and Applied Sciences**

\_\_\_\_\_

Prof. Dr. İsmet Erkmen  
Head of Department, **Electrical and Electronics Engineering**

\_\_\_\_\_

Prof. Dr. Erol Kocaođlan  
Supervisor, **Electrical and Electronics Engineering Dept., METU**

\_\_\_\_\_

**Examining Committee Members:**

Prof. Dr. Kemal Leblebiciođlu  
Electrical and Electronics Engineering Dept., METU

\_\_\_\_\_

Prof. Dr. Erol Kocaođlan  
Electrical and Electronics Engineering Dept., METU

\_\_\_\_\_

Prof. Dr. Aydan Erkmen  
Electrical and Electronics Engineering Dept., METU

\_\_\_\_\_

Assist. Prof. Dr. Yakup Özkazanç  
Electrical and Electronics Engineering Dept., Hacettepe University

\_\_\_\_\_

Assist. Prof. Dr. Emre Tuna  
Electrical and Electronics Engineering Dept., METU

\_\_\_\_\_

**Date:**

\_\_\_\_\_

**I hereby declare that all information in this document has been obtained and presented in accordance with academic rules and ethical conduct. I also declare that, as required by these rules and conduct, I have fully cited and referenced all material and results that are not original to this work.**

Name, Last Name: AHMET ÜSTÜNTÜRK

Signature :

# ABSTRACT

DIGITAL CONTROLLER DESIGN FOR SAMPLED-DATA NONLINEAR SYSTEMS

Üstüntürk, Ahmet

Ph.D., Department of Electrical and Electronics Engineering

Supervisor : Prof. Dr. Erol Kocaođlan

March 2012, 155 pages

In this thesis, digital controller design methods for sampled-data nonlinear systems are considered. Although sampled-data nonlinear control has attracted much attention in recent years, the controller design methods for sampled-data nonlinear systems are still limited. Therefore, a range of controller design methods for sampled-data nonlinear systems are developed such as backstepping, adaptive and robust backstepping, reduced-order observer-based output feedback controller design methods based on the Euler approximate model. These controllers are designed to compensate the effects of the discrepancy between the Euler approximate model and exact discrete time model, parameter estimation error in adaptive control and observer error in output feedback control which behave as disturbance. A dual-rate control scheme is presented for output-feedback stabilization of sampled-data nonlinear systems. It is shown that the designed controllers semiglobally practically asymptotically (SPA) stabilize the closed-loop sampled-data nonlinear system. Moreover, various applications of these methods are given and their performances are analyzed with simulations.

Keywords: Nonlinear, sampled-data, backstepping, output feedback

# ÖZ

## DOĞRUSAL OLMAYAN KESİKLİ-ZAMAN SİSTEMLERİ İÇİN SAYISAL DENETLEYİCİ TASARIMI

Üstüntürk, Ahmet

Doktora, Elektrik ve Elektronik Mühendisliği Bölümü

Tez Yöneticisi : Prof. Dr. Erol Kocaoğlu

Mart 2012, 155 sayfa

Bu tezde, kesikli zaman doğrusal olmayan sistemler için sayısal denetleyici tasarım yöntemleri incelenmiştir. Son yıllarda, bu sistemlerin kontrolü çok ilgi görmesine karşın, denetleyici tasarım yöntemleri henüz sınırlı sayıdadır. Bu nedenle, söz konusu sistemler için Euler yaklaşık model kullanılarak geri adımlamalı, uyarlanabilir ve gürbüz geri adımlamalı, indirgenmiş dereceli gözleyiciye dayalı çıktı geri beslemeli denetleyici tasarım yöntemleri geliştirilmiştir. Bu denetleyiciler, Euler yaklaşık model ile tam model arasındaki farklılık, uyarlanabilir denetimde parametre tahmin hatası ve çıktı geri beslemeli denetimde gözleyici hatası gibi sisteme gürültü şeklinde etki eden etkenleri dengelemek amacıyla tasarlanmıştır. Kesikli zaman doğrusal olmayan sistemlerin çıktı geri beslemeli kontrolü için çift örnekleme zamanlı denetleme yöntemi verilmiştir. Bu denetleyicilerin, söz konusu sistemleri yarı global pratik asimtotik olarak kararlı hale getirdiği gösterilmiştir. Ayrıca, bu yöntemlerin çeşitli uygulamaları verilmiş olup, performansları benzetişimlerle irdelenmiştir.

Anahtar Kelimeler: Doğrusal olmayan, kesikli zaman, geri adımlamalı, çıktı geri besleme

*To my family...*

## **ACKNOWLEDGMENTS**

I would like to express sincere gratitude to Prof. Dr. Erol Kocaođlan for his support and guidance throughout this research. I would also like to thank to Prof. Dr. Kemal Leblebiciođlu and Assist. Prof. Dr. Yakup Özkazanç for their valuable comments and suggestions provided generously at all stages of my research.

Finally, I am indebted deeply to my wife, Fatmanur and son, Beşir Kerem for their endless support and patience throughout this work.

# TABLE OF CONTENTS

|  |      |
|--|------|
| ABSTRACT . . . . .   | iv   |
| ÖZ . . . . .   | v    |
| ACKNOWLEDGMENTS . . . . .  | vii  |
| TABLE OF CONTENTS . . . . .                                      | viii |
| LIST OF FIGURES . . . . .  | xi   |
| CHAPTERS   |      |
| 1 INTRODUCTION . . . . .   | 1    |
| 1.1 Stabilization of Sampled-Data Nonlinear Systems . . . . .    | 1    |
| 1.1.1 Continuous-Time Design . . . . .                           | 2    |
| 1.1.2 Direct Discrete-Time Design . . . . .                      | 3    |
| 1.1.3 Sampled-Data Design . . . . .                              | 6    |
| 1.1.4 Multi-rate Sampling . . . . .                              | 6    |
| 1.1.5 Output-Feedback Control . . . . .                          | 7    |
| 1.2 Purpose of this Research . . . . .                           | 7    |
| 1.3 Outline . . . . .  | 7    |
| 1.4 Contributions . . . . .                                      | 9    |
| 1.5 Publications from This Work . . . . .                        | 10   |
| 2 THEORETICAL BACKGROUND . . . . .                               | 11   |
| 2.1 Introduction . . . . .                                       | 11   |
| 2.2 Notations and Definitions . . . . .                          | 11   |
| 2.3 Backstepping . . . . .                                       | 16   |
| 2.3.1 Continuous-Time Backstepping . . . . .                     | 16   |
| 2.3.2 Continuous-Time Adaptive Backstepping . . . . .            | 17   |
| 2.3.3 The Euler Model-Based Discrete-Time Backstepping . . . . . | 19   |

|       |  |    |
|-------|--|----|
| 3     | SPA STABILIZATION OF SAMPLED-DATA NONLINEAR SYSTEMS VIA BACKSTEPPING . . . . .   | 21 |
| 3.1   | Introduction . . . . .   | 21 |
| 3.2   | Preliminaries . . . . .  | 22 |
| 3.3   | Main Results . . . . .   | 24 |
| 3.4   | Applications . . . . .   | 27 |
| 3.4.1 | Dynamically Positioned Ship . . . . .  | 28 |
| 3.4.2 | Two-Link Robot Manipulator . . . . .   | 31 |
| 3.4.3 | Attitude Control of Rigid Artificial Satellite . . . . .   | 35 |
| 3.4.4 | Second-Order Single-Input System . . . . .   | 39 |
| 3.4.5 | Jet Engine Stall . . . . .   | 43 |
| 3.5   | Conclusions . . . . .  | 45 |
| 4     | ADAPTIVE BACKSTEPPING FOR THE EULER APPROXIMATE MODEL OF SAMPLED-DATA NONLINEAR SYSTEMS . . . . .                                | 47 |
| 4.1   | Introduction . . . . .   | 47 |
| 4.2   | Preliminaries . . . . .  | 48 |
| 4.3   | Main Results . . . . .   | 50 |
| 4.4   | Applications . . . . .   | 58 |
| 4.4.1 | Second-Order System . . . . .  | 58 |
| 4.4.2 | Aircraft Wing Rock . . . . .   | 66 |
| 4.5   | Conclusions . . . . .  | 72 |
| 5     | ROBUST BACKSTEPPING FOR THE EULER APPROXIMATE MODEL OF SAMPLED-DATA NONLINEAR SYSTEMS . . . . .                                  | 73 |
| 5.1   | Introduction . . . . .   | 73 |
| 5.2   | Preliminaries . . . . .  | 74 |
| 5.3   | Main Results . . . . .   | 76 |
| 5.4   | Application . . . . .  | 80 |
| 5.5   | Conclusions . . . . .  | 84 |
| 6     | REDUCED ORDER OBSERVER BASED OUTPUT-FEEDBACK CONTROL FOR THE EULER APPROXIMATE MODEL OF SAMPLED-DATA NONLINEAR SYSTEMS . . . . . | 86 |
| 6.1   | Introduction . . . . .   | 86 |

|       |  |     |
|-------|--|-----|
| 6.2   | Preliminaries . . . . .  | 87  |
| 6.3   | Main Results . . . . .   | 89  |
| 6.4   | Applications . . . . .   | 95  |
| 6.4.1 | Dynamically Positioned Ship . . . . .  | 95  |
| 6.4.2 | Two-Link Robot Manipulator . . . . .   | 101 |
| 6.4.3 | Attitude Control of Rigid Artificial Satellite . . . . .   | 105 |
| 6.4.4 | Second-Order Single-Input System . . . . .   | 109 |
| 6.5   | Conclusions . . . . .  | 113 |
| 7     | OUTPUT-FEEDBACK STABILIZATION OF NONLINEAR DUAL-RATE<br>SAMPLED-DATA SYSTEMS VIA APPROXIMATE DISCRETE-TIME MODEL | 115 |
| 7.1   | Introduction . . . . .   | 115 |
| 7.2   | Preliminaries . . . . .  | 117 |
| 7.3   | Main Results . . . . .   | 121 |
| 7.4   | Applications . . . . .   | 127 |
| 7.4.1 | Dynamically Positioned Ship . . . . .  | 127 |
| 7.4.2 | Two-Link Robot Manipulator . . . . .   | 132 |
| 7.4.3 | Attitude Control of Rigid Artificial Satellite . . . . .   | 136 |
| 7.4.4 | Second-Order Single-Input System . . . . .   | 141 |
| 7.5   | Conclusions . . . . .  | 145 |
| 8     | CONCLUSIONS & FURTHER RESEARCH . . . . .   | 146 |
| 8.1   | Conclusions . . . . .  | 146 |
| 8.2   | Further Research . . . . .   | 148 |
|       | REFERENCES . . . . .   | 150 |
|       | CURRICULUM VITAE . . . . .   | 155 |

## LIST OF FIGURES

### FIGURES

|   |    |
|---|----|
| Figure 1.1 General sampled-data system configuration. . . . .   | 2  |
| Figure 3.1 Time responses of the yaw angle $\psi$ , the North position $n$ and the East position $e$ with $T = 0.2$ . Dotted line:controller $u_E$ . Solid line:designed controller $u_T$ . . . . .                         | 29 |
| Figure 3.2 Time responses of yaw angle $\psi$ , the North position $n$ and the East position $e$ with $T = 0.4$ . Dotted line:controller $u_E$ . Solid line:designed controller $u_T$ . . . . .                             | 29 |
| Figure 3.3 Time responses of yaw angle $\psi$ , the North position $n$ and the East position $e$ with $T = 0.2$ and large initial conditions. Dotted line:controller $u_E$ . Solid line:designed controller $u_T$ . . . . . | 30 |
| Figure 3.4 Responses of the system for the first trajectory with $T = 0.1$ . Dotted line:controller $u_E$ . Solid line:designed controller $u_T$ . Dash-dotted line:desired trajectory. . . . .                             | 33 |
| Figure 3.5 Responses of the system for the first trajectory with $T = 0.2$ . Dotted line:controller $u_E$ . Solid line:designed controller $u_T$ . Dash-dotted line:desired trajectory. . . . .                             | 33 |
| Figure 3.6 Responses of the system for the second trajectory with $T = 0.1$ . Dotted line:controller $u_E$ . Solid line:designed controller $u_T$ . Dash-dotted line:desired trajectory. . . . .                            | 34 |
| Figure 3.7 Responses of the system for the second trajectory with $T = 0.15$ . Dotted line:controller $u_E$ . Solid line:designed controller $u_T$ . Dash-dotted line:desired trajectory. . . . .                           | 34 |
| Figure 3.8 Time responses of $\rho$ and $w$ with $T = 0.1$ . Dotted line:controller $u_E$ . Solid line:designed controller $u_T$ . . . . .  | 36 |

|   |    |
|---|----|
| Figure 3.9 Time responses of $\rho$ and $w$ with $T = 0.4$ . Dotted line:controller $u_E$ . Solid line:designed controller $u_T$ . . . . .  | 37 |
| Figure 3.10 Time responses of $\rho$ and $w$ with $T = 0.1$ and initial conditions doubled. Dotted line:controller $u_E$ . Solid line:designed controller $u_T$ . . . . .   | 38 |
| Figure 3.11 Time responses of $\eta, \xi$ and $u$ with $T = 0.6$ . Solid line:controller $u_T$ . Dash-dotted line:controller $u_{NT}$ . Dotted line:controller $u_{ct}$ . . . . .   | 40 |
| Figure 3.12 Time responses of $\eta, \xi$ and $u$ with $T = 0.9$ . Solid line:controller $u_T$ . Dash-dotted line:controller $u_{NT}$ . Dotted line:controller $u_{ct}$ . . . . .   | 40 |
| Figure 3.13 Time responses of $\eta, \xi$ and $u$ with $T = 0.6$ and the initial condition $(\eta(0), \xi(0)) = (-1, -30)$ . Solid curve:controller $u_T$ . Dash-dotted line:controller $u_{NT}$ . Dotted line:controller $u_{ct}$ . . . . .                | 41 |
| Figure 3.14 Domain of attraction estimates with $T = 0.6$ . Diamond:controller $u_T$ . Star:controller $u_{NT}$ . . . . .   | 41 |
| Figure 3.15 Time responses of $\phi$ and $\psi$ with $T = 0.01$ . Solid curve:controller $u_T$ . Dash-dotted line:controller $u_{NT}$ . Dotted line:controller $u_{ct}$ . . . . .   | 44 |
| Figure 3.16 Time responses of $\phi$ and $\psi$ with $T = 0.5$ . Solid curve:controller $u_T$ . Dash-dotted line:controller $u_{NT}$ . Dotted line:controller $u_{ct}$ . . . . .  | 44 |
| Figure 3.17 Time responses of $\phi$ and $\psi$ with the initial conditions $(R(0), \phi(0), \psi(0)) = (5, 4, 4)$ and $T = 0.01$ . Solid curve:controller $u_T$ . Dash-dotted line:controller $u_{NT}$ . Dotted line:controller $u_{ct}$ . . . . .         | 45 |
| Figure 4.1 Time responses of $x_1, \hat{\theta}$ and $u$ with $T = 0.002$ . Dotted line:Continuous-time controller. Dash-dotted line:Emulation controller. Solid line:Designed controller. . . . .  | 59 |
| Figure 4.2 Time responses of $x_1, \hat{\theta}$ and $u$ with $T = 0.1$ . Dotted line:Continuous-time controller. Dash-dotted line:Emulation controller. Solid line:Designed controller. . . . .  | 59 |
| Figure 4.3 Time responses of $x_1, \hat{\theta}$ and $u$ with the doubled initial conditions $x_1(0) = x_2(0) = 6$ and $T = 0.002$ . Dotted line:Continuous-time controller. Dash-dotted line:Emulation controller. Solid line:Designed controller. . . . . | 61 |
| Figure 4.4 Domain of attraction estimates with $T = 0.002$ . Diamond:controller $u_T$ . Star:controller $u_E$ . . . . .   | 61 |

|             |  |    |
|-------------|--|----|
| Figure 4.5  | Time responses of $x_1, \hat{\theta}$ and $u$ with $T = 0.05$ . Dotted line:Continuous-time controller. Dash-dotted line:Emulation controller. Solid line:Designed controller. . . . .   | 63 |
| Figure 4.6  | Time responses of $x_1, \hat{\theta}$ and $u$ with $T = 0.15$ . Dotted line:Continuous-time controller. Dash-dotted line:Emulation controller. Solid line:Designed controller. . . . .   | 63 |
| Figure 4.7  | Time responses of $x_1, \hat{\theta}$ and $u$ with the initial conditions $x_1(0) = x_2(0) = 5$ and $T = 0.05$ . Dotted line:Continuous-time controller. Dash-dotted line:Emulation controller. Solid line:Designed controller. . . . .  | 64 |
| Figure 4.8  | Domain of attraction estimates with $T = 0.05$ . Diamond:controller $u_T$ . Star:controller $u_E$ . . . . .  | 64 |
| Figure 4.9  | Time responses of $x_1, \hat{\theta}$ and $u$ with $T = 0.05$ . Dotted line:Continuous-time controller. Dash-dotted line:Emulation controller. Solid line:Designed controller. . . . .   | 65 |
| Figure 4.10 | Time responses of $x_1, x_2, x_3$ with $T = 0.1$ . Dotted line:Continuous-time controller. Dash-dotted line:Emulation controller. Solid line:Designed controller. . . . .  | 68 |
| Figure 4.11 | Time responses of $x_1, x_2, x_3$ with $T = 0.15$ . Dotted line:Continuous-time controller. Dash-dotted line:Emulation controller. Solid line:Designed controller. . . . .   | 68 |
| Figure 4.12 | Time responses of $x_1, x_2, x_3$ with the initial conditions doubled and $T = 0.1$ . Dotted line:Continuous-time controller. Dash-dotted line:Emulation controller. Solid line:Designed controller. . . . .                             | 69 |
| Figure 4.13 | Time responses of $x_1, x_2, x_3$ with $T = 0.1$ . Dotted line:Continuous-time controller. Dash-dotted line:Emulation controller. Solid line:Designed controller. . . . .  | 70 |
| Figure 4.14 | Time responses of $x_1, x_2, x_3$ with $T = 0.15$ . Dotted line:Continuous-time controller. Dash-dotted line:Emulation controller. Solid line:Designed controller. . . . .   | 70 |
| Figure 4.15 | Time responses of $x_1, x_2, x_3$ with the initial conditions $x_1(0) = 0.8, x_2(0) = x_3(0) = 0$ and $T = 0.1$ . Dotted line:Continuous-time controller. Dash-dotted line:Emulation controller. Solid line:Designed controller. . . . . | 71 |
| Figure 4.16 | Time responses of $x_1, x_2, x_3$ with $T = 0.1$ . Dotted line:Continuous-time controller. Dash-dotted line:Emulation controller. Solid line:Designed controller. . . . .  | 71 |
| Figure 5.1  | Time responses of $\eta, \xi$ and $u$ with $T = 0.005$ . . . . .   | 81 |
| Figure 5.2  | Time responses of $\eta, \xi$ and $u$ with $T = 0.02$ . . . . .  | 81 |

|   |     |
|---|-----|
| Figure 5.3 Time responses of $\eta, \xi$ and $u$ with the initial conditions $\eta(0) = \xi(0) = 3$ and $T = 0.005$ . . . . .   | 83  |
| Figure 5.4 Domain of attraction estimates with $T = 0.005$ . Diamond:controller $u_T$ . Star:controller $u_P$ . . . . .   | 83  |
| Figure 5.5 Time responses of $\eta, \xi$ and $u$ with the initial conditions $\eta(0) = \xi(0) = 3$ and $T = 0.005$ . . . . .   | 84  |
| Figure 6.1 Time responses of observer errors with $T = 0.2$ . Solid curve:observer (6.39). Dotted line:observer (6.37)-(6.38). . . . .  | 97  |
| Figure 6.2 Time responses of observer errors with $T = 0.4$ . Solid curve:observer (6.39). Dotted line:observer (6.37)-(6.38). . . . .  | 98  |
| Figure 6.3 Time responses of yaw angle $\psi$ , the North position $n$ and the East position $e$ with $T = 0.2$ . Dotted line:controller $u_E$ . Solid line:designed controller $u_T$ . . . . .                             | 99  |
| Figure 6.4 Time responses of yaw angle $\psi$ , the North position $n$ and the East position $e$ with $T = 0.4$ . Dotted line:controller $u_E$ . Solid line:designed controller $u_T$ . . . . .                             | 99  |
| Figure 6.5 Time responses of yaw angle $\psi$ , the North position $n$ and the East position $e$ with $T = 0.2$ and large initial conditions. Dotted line:controller $u_E$ . Solid line:designed controller $u_T$ . . . . . | 100 |
| Figure 6.6 Responses of the system for the first trajectory with $T = 0.08$ . Dotted line:controller $u_E$ . Solid line:designed controller $u_T$ . Dash-dotted line:desired trajectory. . . . .                            | 102 |
| Figure 6.7 Responses of the system for the first trajectory with $T = 0.12$ . Dotted line:controller $u_E$ . Solid line:designed controller $u_T$ . Dash-dotted line:desired trajectory. . . . .                            | 102 |
| Figure 6.8 Responses of the system for the second trajectory $T = 0.05$ . Dotted line:controller $u_E$ . Solid line:designed controller $u_T$ . Dash-dotted line:desired trajectory. . . . .                                | 103 |
| Figure 6.9 Responses of the system for the second trajectory $T = 0.1$ . Dotted line:controller $u_E$ . Solid line:designed controller $u_T$ . Dash-dotted line:desired trajectory. . . . .                                 | 103 |
| Figure 6.10 Time responses of $\rho$ and $\tilde{w}$ with $T = 0.1$ . Dotted line:controller $u_E$ . Solid line:designed controller $u_T$ . . . . .   | 106 |

|  |     |
|--|-----|
| Figure 6.11 Time responses of $\rho$ and $\tilde{w}$ with $T = 0.2$ . Dotted line:controller $u_E$ . Solid line:designed controller $u_T$ . . . . .  | 107 |
| Figure 6.12 Time responses of $\rho$ and $\tilde{w}$ with $T = 0.1$ and doubled initial conditions. Dotted line:controller $u_E$ . Solid line:designed controller $u_T$ . . . . .  | 108 |
| Figure 6.13 Time responses of $\eta$ , $\hat{\xi}$ and $u$ with $T = 0.6$ . Solid line:controller $u_T$ . Dotted line:controller $u_E$ . . . . .   | 111 |
| Figure 6.14 Time responses of $\eta$ , $\hat{\xi}$ and $u$ with $T = 0.9$ . Solid line:controller $u_T$ . Dotted line:controller $u_E$ . . . . .   | 111 |
| Figure 6.15 Time responses of $\eta$ , $\hat{\xi}$ and $u$ with $T = 0.9$ and the initial condition $(\eta(0), \xi(0)) = (5, 5)$ . Solid line:controller $u_T$ . Dotted line:controller $u_E$ . . . . .  | 112 |
| Figure 6.16 Domain of attraction estimates with $T = 0.6$ . Diamond:controller $u_T$ . Star:controller $u_E$ . . . . .   | 112 |
|  |     |
| Figure 7.1 Time responses of yaw angle $x_3$ , the North position $x_1$ , the East position $x_2$ and the observer errors for $x_4$ , $x_5$ and $x_6$ with $T_m = 0.6$ , $T_i = 0.2$ , $h = 0.005$ and $T = 0.6$ . Dotted line: Single-rate controller. Solid line: Dual-rate controller. . . . .                                  | 129 |
| Figure 7.2 Time responses of yaw angle $x_3$ , the North position $x_1$ , the East position $x_2$ and the observer errors for $x_4$ , $x_5$ and $x_6$ with $T_m = 0.8$ , $T_i = 0.2$ , $h = 0.005$ and $T = 0.8$ . Dotted line and right y-axis: Single-rate controller. Solid line and left y-axis: Dual-rate controller. . . . . | 130 |
| Figure 7.3 Time responses of yaw angle $x_3$ , the North position $x_1$ , the East position $x_2$ and the observer errors for $x_4$ , $x_5$ and $x_6$ with and large initial conditions, $T_m = 0.6$ , $T_i = 0.2$ , $h = 0.005$ and $T = 0.6$ . Dotted line: Single-rate controller. Solid line: Dual-rate controller. . . . .    | 131 |
| Figure 7.4 Responses of the system for the first trajectory with $T_m = 0.15$ , $T_i = 0.01$ , $h = 0.001$ and $T = 0.15$ . Dotted line: Single-rate controller. Solid line: Dual-rate designed controller. Dash-dotted line:desired trajectory. . . . .   | 134 |
| Figure 7.5 Responses of the system for the first trajectory with $T_m = 0.3$ , $T_i = 0.03$ , $h = 0.003$ and $T = 0.3$ . Dotted line: Single-rate controller. Solid line: Dual-rate designed controller. Dash-dotted line:desired trajectory. . . . .   | 134 |

|  |     |
|--|-----|
| Figure 7.6 Responses of the system for the second trajectory with $T_m = 0.1$ , $T_i = 0.01$ , $h = 0.001$ and $T = 0.1$ . Dotted line: Single-rate controller. Solid line: Dual-rate designed controller. Dash-dotted line:desired trajectory. . . . .                            | 135 |
| Figure 7.7 Responses of the system for the second trajectory with $T_m = 0.2$ , $T_i = 0.005$ , $h = 0.0005$ and $T = 0.2$ . Dotted line: Single-rate controller. Solid line: Dual-rate designed controller. Dash-dotted line:desired trajectory. . . . .                          | 135 |
| Figure 7.8 Time responses of $\rho$ and $\tilde{w}$ with $T_m = 0.5$ , $T_i = 0.1$ , $h = 0.001$ and $T = 0.5$ . Dotted line: Single-rate controller. Solid line: Dual-rate controller. . . .  | 138 |
| Figure 7.9 Time responses of $\rho$ and $\tilde{w}$ with $T_m = 0.8$ , $T_i = 0.1$ , $h = 0.001$ and $T = 0.8$ . Dotted line: Single-rate controller. Solid line: Dual-rate controller. . . .  | 139 |
| Figure 7.10 Time responses of $\rho$ and $\tilde{w}$ with 1.5-fold initial conditions and $T_m = 0.5$ , $T_i = 0.1$ , $h = 0.001$ , $T = 0.5$ . Dotted line: Single-rate controller. Solid line: Dual-rate controller. . . . .   | 140 |
| Figure 7.11 Time responses of $\eta$ , the observer error $\tilde{\xi}$ and $u$ with $T_m = 0.8$ , $T_i = 0.1$ , $h = 0.05$ and $T = 0.8$ . Solid line: Dual-rate controller. Dotted line: Single-rate controller. . . . .   | 142 |
| Figure 7.12 Time responses of $\eta$ , the observer error $\tilde{\xi}$ and $u$ with $T_m = 0.9$ , $T_i = 0.1$ , $h = 0.05$ and $T = 0.9$ . Solid line: Dual-rate controller. Dotted line: Single-rate controller. . . . .   | 142 |
| Figure 7.13 Time responses of $\eta$ , the observer error $\tilde{\xi}$ and $u$ with the initial conditions $(\eta(0), \xi(0)) = (-3, -5)$ and $T_m = 0.8$ , $T_i = 0.1$ , $h = 0.05$ , $T = 0.8$ . Solid line: Dual-rate controller. Dotted line: Single-rate controller. . . . . | 143 |
| Figure 7.14 Domain of attraction estimates with $T_m = 0.8$ , $T_i = 0.1$ , $h = 0.05$ , $T = 0.8$ . Diamond: Dual-rate controller. Star: Single-rate controller. . . . .  | 143 |

# CHAPTER 1

## INTRODUCTION

This thesis considers the controller design methods for sampled-data nonlinear systems. Although sampled-data nonlinear control has attracted much attention in recent years, the controller design methods for sampled-data nonlinear systems are still limited. The aim of this research is to provide a range of controller design methods for sampled-data nonlinear systems, present various applications of the methods obtained and analyze their performances through simulation based analyses.

In this chapter, the background and purpose of this research are presented. Then, a short overview of contributions and outline of the thesis are introduced. Finally, publications from the work done are given.

### 1.1 Stabilization of Sampled-Data Nonlinear Systems

Because of technological advances in computer technology, nowadays controllers are implemented using a digital computer in most control engineering systems. Therefore sampled-data systems has received much attention in recent years. A sampled-data system involves both continuous-time system and digital controller which is implemented with the computer. In Figure 1.1, a sampled-data system is shown schematically [5].

In sampled-data control system, a digital controller is applied using analog-to-digital (A/D) converter and digital-to-analog (D/A) converter. In Figure 1.1, the output from the process  $y(t)$  is converted to digital form by the A/D converter which is often called as sampler device. The conversion is done at the sampling time,  $t_k$ . The A/D converter sends the sampled output

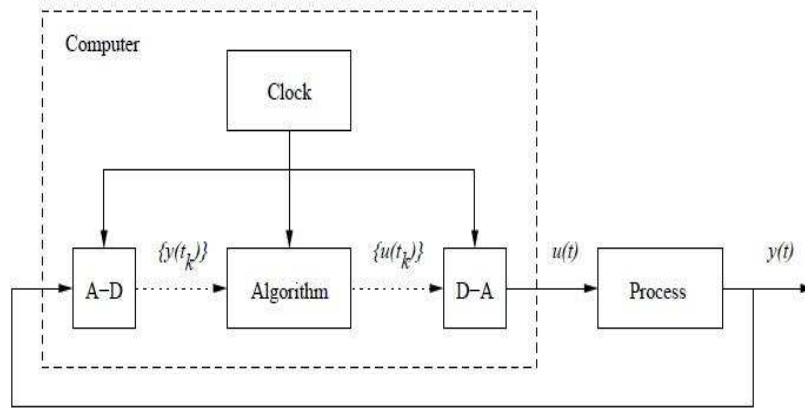


Figure 1.1: General sampled-data system configuration.

$\{y(t_k)\}$  to the controller. Then, the controller produces the control sequence  $\{u(t_k)\}$ . Later this sequence is converted to piecewise continuous control signal  $u(t)$  by D/A converter which is often referred as hold device. This control signal is then applied to the process. An internal clock is used to synchronize the operation of the system.

Most plants are nonlinear in nature. A linear approximation around a prescribed operating point can be used for analysis and controller design of these nonlinear plants. However, the nonlinearities cannot be neglected (see [60] for details) in many situations. Therefore, in these cases, controller is designed using a nonlinear model. Moreover, the system which includes a nonlinear plant and digital controller is classified as sampled-data nonlinear control system. There are many applications for sampled-data nonlinear control systems such as ship or submarine control, biochemical reactors, manoeuvre control of an aircraft, position control for robotic systems, etc.

Controllers can be designed for sampled-data nonlinear systems using three different approaches which are described in [32] as continuous-time design (CTD), direct discrete-time design and sampled-data design.

### 1.1.1 Continuous-Time Design

One way to design a digital controller is CTD method, often referred to as emulation, based on continuous-time model of the plant. First, a continuous-time controller is designed using

continuous-time plant model and any continuous-time design tools. In this step, sampling is completely ignored. Secondly, the designed continuous-time controller is discretized using one of the discretization methods such as Euler, Tustin, other Runge-Kutta methods and matched pole-zero discretization. Then, the discretized controller is implemented using sampler and hold devices under sufficiently fast sampling rates.

Since there exist many design tools for continuous-time systems (see for instance [27, 30, 60, 62]) and there is no need to consider sampling at design stage, CTD method is rather popular. In [5, 13, 53], various techniques of emulation design are given.

A general and unified framework for designing controllers for sampled-data nonlinear systems with disturbances using emulation technique was presented in [36]. In [36], it is shown that if the continuous-time closed-loop system satisfies a certain dissipation inequality with a continuous-time controller, then a similar dissipation inequality is satisfied in a semiglobal practical sense for the discrete-time model of the sampled-data closed-loop system with the emulation controller.

Emulation controllers work well under sufficiently fast sampling (see [7, 36, 54, 59, 67]). The reference [49] provided a formula to compute the largest sampling period to stabilize a sampled-data nonlinear system with an emulation controller.

There are some advantages of emulation design. First, there are many tools for controller design in continuous-time domain. Second, the sampling is taken into account at the implementation stage. Therefore, the controller design problem is separated from the problem of choosing a sampling period. However, some disadvantages may arise during the application of this method. Since the performance of the continuous-time controller can only be recovered under very fast sampling condition, because of hardware restrictions it may be impossible to reduce sampling period to a sufficiently small value to ensure desired performance. Therefore, in these cases direct discrete-time design is a better alternative which is based on discrete-time model of the plant.

### **1.1.2 Direct Discrete-Time Design**

The second way to design a digital controller is direct discrete-time design which is based on discrete-time model of the plant. This method involves designing a controller for the discrete-

time plant model. Sampling is considered at the design stage.

There are two approaches in the literature regarding the discrete-time plant model. The first one is based on the assumption of the availability of the exact discrete-time models. While in the second one, it is assumed that the exact models are unknown. Although the assumption of the availability of the exact models usually holds for linear systems, this almost never holds for nonlinear systems. Since the computation of the exact discrete-time model of nonlinear system involves solving analytically a nonlinear differential equation over one sampling interval, which is impossible in general, the exact model of the nonlinear system cannot be computed in general. Because of this, approximate discrete-time models are commonly used in practice.

The controller is designed in three steps using approximate model based direct discrete-time design. The first design step is discretization of the continuous-time model to obtain the approximate model of the plant. The approximate model is usually parameterized by the sampling period  $T$ , which may be left as a parameter to be determined later. In the second step, a discrete-time controller is designed for the approximate model of the plant to satisfy certain stability and robustness criteria for closed-loop discrete-time system. At this stage,  $T$  is determined to achieve a satisfactory performance for the system. As the final step, the designed controller is implemented using sampled and hold devices under sufficiently fast sampling rates.

To obtain the approximate discrete-time model of continuous-time plant, numerical methods are generally used. Approximation by these methods causes discrepancy between exact and approximate models. Since controller is designed using the approximate model and stability is checked for the exact model, there is no guarantee for the stability of the exact model [46, 50]. Therefore, design verification needs to be done before implementing the controller to the original continuous-time plant.

A more general framework for stabilization of sampled-data nonlinear systems using approximate discrete-time models was presented in the recent papers [43, 45, 46, 47, 50, 32]. References [46, 50] give a set of general and sufficient conditions that guarantee the stabilization of exact model with the family of controllers which stabilizes the approximate model. Although [46, 50] provide a framework for controller design using approximate models, they did not explain how the controller design can be carried out within this framework. Since

the results in [46, 50] are prescriptive they can be used as guide when designing a controller based on the approximate model. [43, 45] generalize the results in [46, 50] for input-to-state (ISS) stabilization and ISS stabilization of sampled-data nonlinear systems with disturbance, respectively. Controller design within this framework is also addressed in [47, 35].

There are several ways to design controllers satisfying the conditions given in [46, 50]. In [48], two integrator backstepping designs were presented for sampled-data nonlinear systems in strict feedback form using Euler approximate model. Applications of the direct discrete-time design to jet engine stall and two link manipulator were given in [32]. Also [63] shows that a direct discrete-time controller guarantees asymptotic stability of the closed-loop system that is not achieved by the emulation controller for two link manipulator system with Slotine and Lie controller. In [58], robust backstepping for sampled-data nonlinear system in strict feedback form using Euler approximate model was presented. Receding horizon control, also known as model predictive control, of sampled-data nonlinear system using approximate discrete-time model was addressed in [11]. Simulations in these papers show that the controllers designed by direct discrete-time design method outperform the emulation controllers.

Redesigning an emulation controller using direct discrete-time design is another way to obtain some improvements. In [44], a redesign method based on Fliess expansions of the Lyapunov difference for the sampled-data system was presented. [17] investigates the sampled-data feedback laws to minimize the difference between the continuous-time system and sampled-data system after one sampling interval. In addition, a continuous-time controller was redesigned for a robotic manipulator in [32] using the Euler model. It was shown in [32] that the redesigned controller yielded better performance when compared to the emulation controller.

There are some advantages of the direct discrete-time design. First, the sampling is considered from the beginning of the design process. Therefore, better performance can be achieved by the controller obtained by direct discrete-time design comparing to emulation controller. Second, larger sampling periods may be applied to the controller designed by direct discrete-time design. However, there also exist some disadvantages of this method. Since the continuous-time model is discretized at the beginning of the design process, the discretization may destroy some important properties of the continuous-time model such as feedback linearizability [2, 8] and minimum phase properties [41]. Therefore, analysis and design using this method are usu-

ally harder. Moreover, intersample behaviour is not taken into account in direct discrete-time design. This limitation may cause ripple in the response of the systems. This disadvantage can be eliminated by careful design and the choice of sampling period. Another way to take the intersample behaviour into account is sampled-data design.

### **1.1.3 Sampled-Data Design**

The third way to design a digital controller is sampled-data design based on the sampled-data model of the plant. Because of the use of sampled-data model, intersample behaviour is taken into account. This approach has been developed since 1990's for linear systems [8]. However, because of the complexity of nonlinear sampled-data model, results on this method for nonlinear systems are scarce. [55] proposed a sampled-data design method for solving the sampled-data stabilization problem of the general class of nonlinear Lipschitz continuous systems. This method was applied to robot manipulator in [55].

Sampled-data design method uses exact sampled-data model of the system and controller is designed using this model. Since this method does not involve approximation of the plant or controller, stability and performance are maintained by this method for arbitrarily large sampling periods  $T$ .

### **1.1.4 Multi-rate Sampling**

Although the emulation and direct discrete-time design allow multi-rate sampled-data systems, design methods using these approaches are single-rate in general, i.e. input and measurement sampling rates are assumed to be equal. In practical applications, hardware restrictions on input and measurement sampling rate can be different. Moreover, it is assumed that measurement results and the corresponding controller signals are available instantaneously. This assumption is unrealistic. Therefore, the use of multi-rate control scheme for sampled-data systems was proposed in [1, 37, 38, 56] so that several sample rates co-exist to achieve better performances.

### **1.1.5 Output-Feedback Control**

In many applications, only a part of the state vector is available from measurement. Thus control using output-feedback or dynamic feedback is necessary. The dynamic feedback bases the input signal on output history. Since dynamic feedback controller has its own state called as controller internal state, it can be thought as a dynamic system itself. The output feedback is based on the partial information about the state vector. Output feedback controller reads some output signal which is a known function of all or some of the state variables. Then it builds the input signal accordingly. Moreover, designing an observer for unmeasured states is a useful method to be used for constructing an output-feedback controller.

The problem of output feedback stabilization of sampled-data nonlinear systems was considered in [10, 28, 65, 3]. A framework for designing a discrete-time observer based on approximate discrete-time model of the plant was presented in [3]. [10, 28] show that the obtained sampled-data controllers using high gain observers can recover the performance of the continuous-time state feedback controllers.

## **1.2 Purpose of this Research**

In this thesis, the problem of controller design for sampled-data nonlinear systems is considered. Although there exist a comprehensive set of tools for analysis and controller design of continuous-time nonlinear systems, the controller design methods are still limited for their sampled-data counterparts. The purpose of this research is to provide a range of controller design tools for sampled-data nonlinear systems. In particular, backstepping, adaptive backstepping and reduced order observer based output-feedback control design methods for sampled-data nonlinear systems are investigated. A multi-rate control scheme for output-feedback stabilization of sampled-data nonlinear systems is developed. Moreover, the design tools developed in the study conducted is applied to some examples arising from engineering practice and their performances are analyzed with simulations.

## **1.3 Outline**

The organization of this research can be summarized as shown below:

**Chapter 2:** In this chapter, technical preliminaries are provided. Common notation and definitions which will be used throughout the thesis are presented. Various important results from the literature which will be used to compare with the results of the work conducted are also cited.

**Chapter 3:** The problem of backstepping control of sampled-data nonlinear systems in strict feedback form based on the Euler approximate model is considered. A backstepping design method is presented to compensate the effects of the discrepancy between the Euler approximate model and exact discrete time model. Also numerical examples are given to illustrate the design methods.

**Chapter 4:** This chapter considers the problem of adaptive backstepping control of sampled-data nonlinear systems in strict feedback form based on the Euler approximate model. Two adaptive backstepping design methods are presented to compensate the effects of the error in parameter estimation. Also numerical examples are given to illustrate the design methods.

**Chapter 5:** The robust backstepping control of sampled-data nonlinear systems in strict feedback form based on the Euler approximate model is discussed. A robust backstepping design method which is modified version of the method given in [58] is presented to compensate the effect of difference between disturbance or model uncertainty and its bound. Also a numerical example is given to illustrate the design method.

**Chapter 6:** This chapter considers the problem of reduced order observer-based output feedback control of sampled-data nonlinear systems in strict feedback form based on the Euler approximate model. A reduced order observer design which is an extension of the reduced order observer given in [33] to a general class of multi-input nonlinear systems is presented. Then, a reduced-order observer-based backstepping method is given to compensate the effect of observer error. Also numerical examples are given to illustrate the design methods.

**Chapter 7:** In this chapter, the problem of dual-rate output feedback stabilization of sampled-data nonlinear systems is studied under the low measurement rate constraint. The dual-rate control scheme is presented based on estimation of the missing output values between measured output samples using approximate discrete-time model. It is shown that if one designs a single-rate observer-based output feedback controller which semiglobally practically asymptotically (SPA) stabilizes the sampled-data nonlinear system, then the dual-rate observer-

based output feedback controller will also SPA stabilize the exact discrete-time plant model. Then, numerical examples are given to illustrate the design method.

**Chapter 8:** The concluding remarks and future work related to the research are presented.

## 1.4 Contributions

1. A range of controller design tools for sampled-data nonlinear systems are proposed. The designed controllers SPA stabilize sampled-data nonlinear systems in strict feedback form and are based on the Euler approximate model. In particular,

- A backstepping design method is developed for sampled-data nonlinear systems in strict feedback form. Different from the backstepping controller given in [48], the controller in this thesis is designed for multi-input sampled-data nonlinear systems to compensate the effects of the discrepancy between the Euler approximate model and exact discrete time model by adding a nonlinear damping term. Simulation results show that the designed controller outperforms the controllers given in [48] and [26].
- Two adaptive backstepping design methods are presented for sampled-data nonlinear systems in strict feedback form. The controllers are designed to compensate the effect of the error in parameter estimation. Simulation results show that the designed controllers outperform the emulation controllers.
- A robust backstepping method is developed for sampled-data nonlinear systems in strict feedback form. This controller is a modified version of the controller given in [58]. Different from the controller in [58], the controller in this thesis is designed to compensate the effect of difference between disturbance or model uncertainty and their bounds. Simulation results show that the designed controller outperforms the controller given in [58].
- A reduced-order observer-based SPA stabilizing backstepping method is given for sampled-data nonlinear systems in strict feedback form. Different from the backstepping controller given in [25], the controller in this thesis is designed to compensate the effects of observer error. Simulation results show that the designed controller outperforms the controller given in [25].

2. A reduced order observer design is presented, which is an extension of the reduced order observer given in [33] to a general class of multi-input nonlinear systems. It is shown by simulations that observer error converges to zero by the designed observer when compared to the observer given in [25].
3. For the problem of dual-rate output feedback stabilization of sampled-data nonlinear systems under the low measurement rate constraint, a dual-rate control scheme is presented based on estimation of the missing output values between measured output samples using approximate discrete-time model. It is shown that if one designs a single-rate observer-based output feedback controller which SPA stabilizes the sampled-data nonlinear system, then the SPA stability property will be preserved by the dual-rate observer-based output feedback controller. Simulation results show that the designed dual-rate controller gives faster results when compared to the single-rate controller.
4. The design tools developed in this research are applied to several practical examples and the resulting performances are analyzed.

## **1.5 Publications from This Work**

The followings are submitted to journals:

1. Üstüntürk, A., Output-feedback stabilization of nonlinear dual-rate sampled-data systems via approximate discrete-time model, Accepted by Automatica, 2011.
2. Üstüntürk, A., Kocaođlan, E., Backstepping designs for the stabilization of nonlinear sampled-data systems via approximate discrete-time model, Submitted to International Journal of Control, 2011, Under review.

## CHAPTER 2

### THEORETICAL BACKGROUND

#### 2.1 Introduction

This chapter provides technical preliminaries. Common notation and definitions which will be used throughout the thesis are presented. Various important results from the literature which will be used to compare with the results of this thesis in simulations are also cited.

#### 2.2 Notations and Definitions

The sets of real, natural and nonnegative integer numbers are denoted as  $\mathbb{R}$ ,  $\mathbb{N}$  and  $\mathbb{Z}^+$ , respectively.  $\mathcal{SN}$  denotes the class of all smooth nondecreasing functions  $q : \mathbb{R}_{\geq 0} \rightarrow \mathbb{R}_{\geq 0}$  which satisfy  $q(t) > 0$  for all  $t > 0$ . A function  $\gamma : \mathbb{R}_{\geq 0} \rightarrow \mathbb{R}_{\geq 0}$  is called class  $\mathcal{G}$  if it is continuous, zero at zero and strictly increasing. The classes of functions are defined in [27] as follows.

**Definition 2.2.1** [27] *A continuous function  $\alpha : [0, a) \rightarrow [0, \infty)$  is said to belong to class  $\mathcal{K}$  if it is strictly increasing and  $\alpha(0) = 0$ . It is said to belong to class  $\mathcal{K}_\infty$  if  $a = \infty$  and  $\alpha(r) \rightarrow \infty$  as  $r \rightarrow \infty$ . Functions of class  $\mathcal{K}_\infty$  are invertible.*

**Definition 2.2.2** [27] *A continuous function  $\beta : [0, a) \times [0, \infty) \rightarrow [0, \infty)$  is said to belong to class  $\mathcal{KL}$  if, for each fixed  $s$ , the mapping  $\beta(r, s)$  belongs to class  $\mathcal{K}$  with respect to  $r$  and, for each fixed  $r$ , the mapping  $\beta(r, s)$  is decreasing with respect to  $s$  and  $\beta(r, s) \rightarrow 0$  as  $s \rightarrow \infty$ .*

The notation  $|\cdot|$  always denotes the Euclidean norm for a vector and the Frobenius norm for a matrix given by  $|A| = \sqrt{\text{trace}(A^T A)}$ . The symbol  $\sum_{i,j=1}^{q,n}$  means  $\sum_{i=1}^q \sum_{j=1}^n$ . For the sake

of simplicity, the notation  $x$  will be used to denote  $x(kT)$  where  $k \in \mathbb{N}, T > 0$ .  $\varepsilon_s(i) = (0, \dots, 0, 1, 0, \dots, 0)^T \in \mathbb{R}^s, i = 1, \dots, s, s \geq 1$  is a vector of the canonical basis of the vectorial space  $\mathbb{R}^s$  where  $i$  shows the location of 1 in the vector. The set  $Co(a, b) = \{\lambda a + (1 - \lambda)b : \lambda \in [0, 1]\}$  is the convex hull of  $\{a, b\}$  where  $a, b \in \mathbb{R}^n$ . Throughout the thesis, the units of the sampling periods and time axes in all figures are in seconds.

Consider the continuous-time nonlinear system

$$\dot{x} = f(x(t), u(t)), \quad y = Cx(t) \quad (2.1)$$

where  $x \in \mathbb{R}^n$  is the state,  $u \in \mathbb{R}^m$  is the control input,  $y \in \mathbb{R}^l$  is the output,  $C$  is a constant matrix of appropriate dimension and the function  $f$  is locally Lipschitz. The control input  $u$  is realized through a zero-order hold such that  $u(t) = u(kT) := u(k), \forall t \in [kT, (k+1)T), k \in \mathbb{N}$  and the output  $y$  is measured at sampling instants  $kT$ ; that is  $y(k) := y(kT)$  where  $T > 0$  is the sampling period.

The difference equation corresponding to the exact discrete-time model of (2.1) and its approximate discrete-time model are represented by:

$$x(k+1) = F_T^e(x(k), u(k)), \quad y(k) = Cx(k) \quad (2.2)$$

$$x(k+1) = F_T^a(x(k), u(k)), \quad y(k) = Cx(k), \quad (2.3)$$

respectively.

The exact discrete-time model  $F_T^e$  is obtained as the exact solution of initial value problem of the continuous-time model over sampling interval. The approximate discrete-time model  $F_T^a$  is obtained via numerical approximation. As mentioned in Chapter 1, exact discrete-time model is not available for nonlinear systems in general and approximate discrete-time model is used. Since, in general, discretization with numerical approximation obviously involves inaccuracy, this leads to discrepancies between the exact model and the approximate model. Therefore, sampled-data systems cannot achieve identical properties as what their continuous-time counterparts have. If continuous-time systems achieve the properties such as asymptotic stability, input-to-state stability and dissipativity for the whole state space and the whole input space (in a global sense), this case is not satisfied for sampled-data systems in general. Sampling might destroy global properties of the systems, so that the properties hold in a weaker (semiglobal practical) sense. Indeed, semiglobal practical property is common in sampled-data systems. Semiglobal practical asymptotical (SPA) stability and SPA stability Lyapunov

functions are defined in [48] as follows:

**Definition 2.2.3** [48] *The family of controllers  $u_T$  SPA stabilizes  $F_T$  if there exists  $\beta \in \mathcal{KL}$  such that for any pair of strictly positive real numbers  $(D, v)$  there exists  $T^* > 0$  such that for each  $T \in (0, T^*)$  the solutions of  $x(k+1) = F_T(x(k), u_T(x(k)))$  satisfy:  $|x(k, x(0))| \leq \beta(|x(0)|, kT) + v$ , for all  $k \geq 0$ , whenever  $|x(0)| \leq D$ .*

**Definition 2.2.4** [48] *Let  $\hat{T} > 0$  be given and for each  $T \in (0, \hat{T})$  let functions  $V_T : \mathbb{R}^n \rightarrow \mathbb{R}_{\geq 0}$  and  $u_T : \mathbb{R}^n \rightarrow \mathbb{R}^m$  be defined. The pair of families  $(u_T, V_T)$  is a SPA stabilizing pair for  $F_T$  if there exist  $\alpha_1, \alpha_2, \alpha_3 \in \mathcal{K}_\infty$  such that for any pair of strictly positive real numbers  $(\Delta, \delta)$  there exists a triple of strictly positive real numbers  $(T^*, L, M)$ , with  $T^* \leq \hat{T}$ , such that for all  $x, z \in \mathbb{R}^n$  with  $\max\{|x|, |z|\} \leq \Delta$  and  $T \in (0, T^*)$ , and the following conditions are satisfied:*

$$\alpha_1(|x|) \leq V_T(x) \leq \alpha_2(|x|) \quad (2.4)$$

$$V_T(F_T(x, u_T(x))) - V_T(x) \leq -T\alpha_3(|x|) + T\delta \quad (2.5)$$

$$|V_T(x) - V_T(z)| \leq L|x - z| \quad (2.6)$$

$$|u_T(x)| \leq M \quad (2.7)$$

Consistency is an important property for the approximate model to be a good approximation of the exact model. This property is used to measure the discrepancy between the exact model and the approximate model. One step consistency property is given in [46] as follows:

**Definition 2.2.5** ([46]) *The family  $F_T^a(x, u)$  is said to be one-step consistent with the exact discrete-time model  $F_T^e(x, u)$  if, for each compact set  $\Omega \subset \mathbb{R}^n \times \mathbb{R}^m$ , there exists a class- $\mathcal{K}$  function  $\rho(\cdot)$  and a constant  $T_0 > 0$  such that,  $|F_T^e(x, u) - F_T^a(x, u)| \leq T\rho(T)$  for all  $(x, u) \in \Omega$  and  $T \in (0, T_0]$ .*

A sufficient condition for one-step consistency is the following whose proof is given in [36].

**Lemma 2.2.6** [36] *Consider  $F_T^e$  and  $F_T^a$ . If*

1.  $F_T^a$  is one-step consistent with  $F_T^{Euler}$  where  $F_T^{Euler} = x + Tf(x, u)$ ,
2. given any strictly positive real numbers  $(\Delta_x, \Delta_u)$ , there exists  $\rho_1 \in \mathcal{K}_\infty$ ,  $M > 0$ ,  $T^* > 0$ , such that, for all  $T \in (0, T^*)$  and for all  $|x| \leq \Delta_x$ ,  $|u| \leq \Delta_u$ ,

- (a)  $\max_{|x| \leq \Delta_x, |u| \leq \Delta_u} |f(x, u)| \leq M$   
(b)  $|f(x_1, u) - f(x_2, u)| \leq \rho_1(|x_1 - x_2|)$

then  $F_T^a$  is one-step consistent with  $F_T^e$

By Lemma 2.2.6, it can be shown that Euler approximate model is one-step consistent with the exact model, whose proof is given in [36]. Moreover, if the approximate model (2.3) is consistent with the exact model (2.2), stability properties for (2.2) can be deduced from the stability analysis of (2.3) according to the following theorem which is a direct consequence of Theorem 3.2 in [45].

**Theorem 2.2.7** [45, 50, 51] *If system (2.3) is SPA stable with the pair of families  $(u_T, V_T)$  and  $u_T$  is uniformly locally bounded, then the exact discretized system (2.2) is SPA stable.*

Then, stability properties of the sampled-data system (2.1) can be deduced from those of exact discretized system under mild conditions [51].

**Definition 2.2.8 (Uniformly locally bounded)** [32]  *$u_T$  is said to be uniformly locally bounded if for any  $\Delta_x > 0$  there exist strictly positive numbers  $T^*$  and  $\Delta_u > 0$  such that for all  $T \in (0, T^*)$  and all  $|x| \leq \Delta_x$  we have  $|u_T| \leq \Delta_u$ .*

Consider now the following family of observers for (2.2)

$$\hat{x}(k+1) = G_T(\hat{x}(k), y(k), u(k)) \quad (2.8)$$

SPA stable observers and Lyapunov functions for SPA stable observers are defined in the following definitions. These definitions will be used later to prove the SPA stability of designed observer.

**Definition 2.2.9** [33] *The family of observers (2.8) is SPA stable observer for  $x(k+1) = F_T(x(k), u(k))$ , if for any compact sets  $\mathcal{X} \subset \mathbb{R}^n$ ,  $\hat{\mathcal{X}} \subset \mathbb{R}^p$ ,  $\mathcal{U} \subset \mathbb{R}^m$ ,  $\mathcal{Y} \subset \mathbb{R}^l$  and any strictly positive number  $\nu$ , there exists  $T^* > 0$  such that the followings hold.*

1. *For all  $x_0 \in \mathcal{X}$ ,  $u \in \mathcal{U}$ ,  $y_0 \in \mathcal{Y}$  and  $T \in (0, T^*]$ , there exists  $\hat{x}_0 \in \hat{\mathcal{X}}$  such that  $|\hat{x}(k) - x(k)| \leq T\nu, \forall k \geq 1$ .*

2. For all  $x_0 \in \mathcal{X}$ ,  $\hat{x}_0 \in \hat{\mathcal{X}}$ ,  $u \in \mathcal{U}$ ,  $y_0 \in \mathcal{Y}$  and all  $T \in (0, T^*]$ ,  $\limsup_{k \rightarrow \infty} |\hat{x}(k) - x(k)| \leq T\nu$ .

where  $x_0 = x(0)$ ,  $\hat{x}_0 = \hat{x}(0)$  and  $y_0 = y(0)$ .

**Definition 2.2.10** [3] *The family of observers (2.8) is SPA stable as in Definition 2.2.9 if there exists a family of Lyapunov functions  $V_T(x, \hat{x})$  and class- $\mathcal{K}_\infty$  functions  $\alpha_1(\cdot)$ ,  $\alpha_2(\cdot)$ ,  $\alpha_3(\cdot)$  such that for any compact sets  $\mathcal{X} \subset \mathbb{R}^n$ ,  $\hat{\mathcal{X}} \subset \mathbb{R}^p$ ,  $\mathcal{U} \subset \mathbb{R}^m$ ,  $\mathcal{Y} \subset \mathbb{R}^l$  and any strictly positive number  $\nu$ , there exist constants  $T^* > 0$  and  $M > 0$ , such that for all  $x, x_1, x_2 \in \mathcal{X}$ ,  $\hat{x} \in \hat{\mathcal{X}}$ ,  $u \in \mathcal{U}$ ,  $y \in \mathcal{Y}$ , and  $T \in (0, T^*]$ ,*

$$|V_T(x_1, \hat{x}) - V_T(x_2, \hat{x})| \leq M|x_1 - x_2|, \quad (2.9)$$

$$\alpha_1(|e|) \leq V_T(x, \hat{x}) \leq \alpha_2(|e|), \quad (2.10)$$

$$\frac{V_T(F_T(x, y, u), G_T(\hat{x}, y, u)) - V_T(x, \hat{x})}{T} \leq -\alpha_3(|e|) + \nu \quad (2.11)$$

where  $e$  is the observer error defined by the difference between the actual states and their estimates. Moreover, if  $F_T^a$  is consistent with  $F_T^e$  as in Definition 2.2.5 and the family of observers (2.8) is SPA stable observer for (2.3), then the family of observers (2.8) is also SPA stable observer for (2.2).

Delta operator  $\delta$  is defined as  $\delta(x(k)) = \frac{x(k+1) - x(k)}{T}$ , for any sequence  $x(k) \in \mathbb{R}^n$  for all  $k$  and  $T$  is the sampling period. Using this definition, one has  $\delta(g_1^T g_1) = 2g_1^T \delta g_1 + T(\delta g_1)^T \delta g_1$  for any sequence  $g_1(k) \in \mathbb{R}^n$  for all  $k$ .

**Theorem 2.2.11 (Mean Value Theorem)** *Assume that  $f : \mathbb{R}^n \rightarrow \mathbb{R}$  is continuously differentiable at each point  $x$  of an open set  $S \subset \mathbb{R}^n$ . Let  $x$  and  $y$  be two points of  $S$  such that the line segment  $L(x, y) \subset S$ . Then there exists a point  $z$  of  $L(x, y)$  such that*

$$f(y) - f(x) = \left. \frac{\partial f}{\partial x} \right|_{x=z} (y - x).$$

*The line segment  $L(x, y)$  joining two distinct points  $x$  and  $y$  in  $\mathbb{R}^n$  is*

$$L(x, y) = \{z | z = \theta x + (1 - \theta)y, 0 < \theta < 1\}$$

The differential mean value theorem (DMVT) for higher dimensional vector valued functions is defined in [66] as follows:

**Definition 2.2.12** [66] Let  $f : \mathbb{R}^n \rightarrow \mathbb{R}^q$ . Let  $a, b \in \mathbb{R}^n$ . It is assumed that  $f$  is differentiable on  $Co(a, b)$ . Then there are constant vectors  $c_1, \dots, c_q \in Co(a, b)$ ,  $c_i \neq a, c_i \neq b$  for  $i = 1, \dots, q$  such that:

$$f(a) - f(b) = \left( \sum_{i,j=1}^{q,n} \varepsilon_q(i) \varepsilon_n^T(j) \frac{\partial f_i}{\partial x_j}(c_i) \right) (a - b).$$

## 2.3 Backstepping

Backstepping is a recursive design method. In this method, appropriate functions of state variables are selected as virtual-control inputs for lower dimension subsystems of the overall system recursively. In each step of the method, a new virtual control law expressed as a function of the virtual control law in the previous steps is obtained. The algorithm terminates when the overall system is reached. The resulting feedback controller is then obtained to achieve the original control objective.

The backstepping technique can be applied for systems in strict feedback form as follows:

$$\begin{aligned} \dot{x} &= f(x) + g(x)\xi_1 \\ \dot{\xi}_1 &= f_1(x, \xi_1) + g_1(x, \xi_1)\xi_2 \\ &\dots \\ \dot{\xi}_i &= f_i(x, \xi_1, \dots, \xi_i) + g_i(x, \xi_1, \dots, \xi_i)\xi_{i+1} \\ &\dots \\ \dot{\xi}_m &= f_m(x, \xi_1, \dots, \xi_m) + g_m(x, \xi_1, \dots, \xi_m)u \end{aligned} \tag{2.12}$$

This technique can also be applied to a more general feedback form or even for a larger class of systems that do not follow any formal feedback forms. The detailed procedure for backstepping design is presented in [30].

### 2.3.1 Continuous-Time Backstepping

Consider the following continuous-time plant of the strict feedback form:

$$\begin{aligned} \dot{x} &= f(x) + g(x)\xi \\ \dot{\xi} &= u \end{aligned} \tag{2.13}$$

where  $x \in \mathbb{R}^n$  and  $\xi \in \mathbb{R}$  are the states,  $f(0) = 0$ ,  $f, g$  are differentiable sufficiently many times and  $u \in \mathbb{R}$  is the control input.

**Assumption 2.3.1** [32] Consider the system

$$\dot{x} = f(x) + g(x)u \quad (2.14)$$

where  $x \in \mathbb{R}^n$  is the state and  $u \in \mathbb{R}$  is the control input. There exist a continuously differentiable feedback control law

$$u = \alpha(x), \quad \alpha(0) = 0, \quad (2.15)$$

and a smooth, positive definite, radially unbounded function  $W : \mathbb{R}^n \rightarrow \mathbb{R}$  such that

$$\frac{\partial W}{\partial x}(x)[f(x) + g(x)\alpha(x)] \leq -\Omega(x), \quad \forall x \in \mathbb{R}^n, \quad (2.16)$$

where  $\Omega : \mathbb{R}^n \rightarrow \mathbb{R}$  is positive definite.

Under this assumption, the following lemma on integrator backstepping is given together with its proof in [30].

**Lemma 2.3.2** [30] Consider the system (2.13), which is an augmentation of (2.14) with an integrator. Suppose that all conditions on Assumption 2.3.1 are satisfied by the upper subsystem of (2.13) with control  $\xi \in \mathbb{R}$ . Then

$$V(x, \xi) = W(x) + \frac{1}{2}[\xi - \alpha(x)]^2 \quad (2.17)$$

is a control Lyapunov function (clf) for the full system (2.13). That is, there exists a feedback control  $u = \alpha^a(x; \xi)$  which renders  $x = 0, \xi = 0$  the globally asymptotically stable (GAS) equilibrium of (2.13). One such control is

$$u = -c(\xi - \alpha(x)) + \frac{\partial \alpha}{\partial x}(x)[f(x) + g(x)\xi] - \frac{\partial W}{\partial x}(x)g(x), \quad c > 0. \quad (2.18)$$

### 2.3.2 Continuous-Time Adaptive Backstepping

Consider the following parametric strict feedback system

$$\dot{x} = Ax + B\xi + \phi^T \theta \quad (2.19)$$

$$\dot{\xi} = u + \phi_n^T(x_1, \dots, x_{n-1}, \xi)\theta \quad (2.20)$$

where

$$A = \begin{bmatrix} 0 & 1 & 0 & \dots & \dots & 0 \\ 0 & 0 & 1 & 0 & \dots & 0 \\ \dots & \dots & \dots & \dots & \dots & \dots \\ \dots & \dots & \dots & \dots & \dots & \dots \\ 0 & \dots & \dots & \dots & 0 & 1 \\ 0 & \dots & \dots & \dots & \dots & 0 \end{bmatrix}, B = \begin{bmatrix} 0 \\ \dots \\ \dots \\ \dots \\ 0 \\ 1 \end{bmatrix}, \phi = \begin{bmatrix} \phi_1(x_1) & \phi_2(x_1, x_2) & \dots & \dots & \phi_{n-1}(x_1, \dots, x_{n-1}) \end{bmatrix}$$

and  $x \in \mathbb{R}^{n-1}$ ,  $\xi \in \mathbb{R}$ ,  $u \in \mathbb{R}$  and  $\phi_i \in \mathbb{R}^p$  is a vector of known smooth nonlinear functions with  $\phi_i(0, \dots, 0) = 0$ ,  $i = 1, \dots, n$ ,  $\theta \in \mathbb{R}^p$  is a vector of unknown constant parameters. It is assumed that there exists a known constant  $\bar{\theta}$  such that  $|\theta| \leq \bar{\theta}$ .

Using adaptive backstepping based on tuning function technique given in [30] a continuous-time adaptive controller can be designed for plant (2.19)-(2.20) as follows:

$$u = -c_n z_n - z_{n-1} + \sum_{m=1}^{n-1} \frac{\partial \alpha_{n-1}}{\partial x_m} x_{m+1} - w_n^T \hat{\theta} + \frac{\partial \alpha_{n-1}}{\partial \hat{\theta}} \Gamma \tau_n + v_n \quad (2.21)$$

where  $z_1 = x_1$ ,  $\alpha_1 = -c_1 z_1 - \phi_1^T \hat{\theta}$ ,  $x_n = \xi$ ,  $v_2 = 0$  and for  $i = 2, 3, \dots, n$

$$z_i = x_i - \alpha_{i-1}, \quad (2.22)$$

$$\alpha_i(x_1, \dots, x_i, \hat{\theta}) = -z_{i-1} - c_i z_i + \sum_{m=1}^{i-1} \frac{\partial \alpha_{i-1}}{\partial x_m} x_{m+1} - w_i^T \hat{\theta} + \frac{\partial \alpha_{i-1}}{\partial \hat{\theta}} \Gamma \tau_i + v_i \quad (2.23)$$

$$\tau_i(x_1, \dots, x_i, \hat{\theta}) = \tau_{i-1} + z_i w_i \quad (2.24)$$

$$w_i(x_1, \dots, x_i, \hat{\theta}) = \phi_i - \sum_{m=1}^{i-1} \frac{\partial \alpha_{i-1}}{\partial x_m} \phi_m \quad (2.25)$$

$$v_i(x_1, \dots, x_i, \hat{\theta}) = \sum_{m=1}^{i-2} z_{m+1} \frac{\partial \alpha_{i-1}}{\partial \hat{\theta}} \Gamma w_i, \quad i = 3, \dots, n \quad (2.26)$$

and  $c_i$  are any positive real numbers.

The parameter estimator is obtained as:

$$\dot{\hat{\theta}} = \Gamma W(z, \hat{\theta}) z \quad (2.27)$$

where  $z := [z_1, \dots, z_n]^T$ ,  $W(z, \hat{\theta}) = [w_1, \dots, w_n]$  and  $\Gamma = \Gamma^T$  is any arbitrary positive definite matrix.

Moreover, another adaptive backstepping method based on immersion and invariance principle is introduced in [22]. Using the algorithm in [22] an adaptive state feedback control law

for system (2.19)-(2.20) can be designed as follows:

$$x_{i+1}^* = -\sigma_i(x_1, \dots, x_i, \hat{\theta}_1, \dots, \hat{\theta}_i) - \phi_i(x_1, \dots, x_i)^T \times (\hat{\theta}_i + \beta_i(x_1, \dots, x_i)) \\ + \sum_{k=1}^{i-1} \frac{\partial x_i^*}{\partial x_k} [x_{k+1} + \phi_k(x_1, \dots, x_k)^T \times (\hat{\theta}_k + \beta_k(x_1, \dots, x_k))] + \sum_{k=1}^{i-1} \frac{\partial x_i^*}{\partial \hat{\theta}_k} \dot{\hat{\theta}}_k + x_1^{*(i)}, \quad (2.28)$$

$$u = x_{n+1}^* \quad (2.29)$$

with  $i = 1, \dots, n$  and  $x_n = \xi$ ,

$$\sigma_1 = \left(c_1 + \frac{\varepsilon}{2}\right) (x_1 - x_1^*) \quad (2.30)$$

$$\sigma_i = \left(c_i + \frac{\varepsilon}{2}\right) (x_i - x_i^*) + \frac{\varepsilon}{2} \sum_{k=1}^{i-1} \left(\frac{\partial x_i^*}{\partial x_k}\right)^2 (x_i - x_i^*) + (x_{i-1} - x_{i-1}^*) \quad (2.31)$$

for  $i = 2, \dots, n$  where  $c_i > 0$  and  $\varepsilon > 0$  are constants.

To obtain the adaptive law define the estimation errors

$$z_i = \hat{\theta}_i - \theta + \beta_i(x_1, \dots, x_i), \quad i = 1, \dots, n \quad (2.32)$$

where  $\hat{\theta}_i$  are the estimator states and  $\beta_i : \mathbb{R}^i \rightarrow \mathbb{R}^p$  are  $C^{n-i}$  functions. The functions  $\beta_i$  are selected as:

$$\beta_i(x_1, \dots, x_i) = \gamma_i \int_0^{x_i} \phi_i(x_1, \dots, x_{i-1}, \chi) d\chi + \delta_i(x_i) \quad (2.33)$$

where  $\gamma_i > 0$  are constants and  $\delta_i(x_i)$  are  $C^{n-i}$  functions with  $\delta_1(x_1) = 0$ . From the dynamics of  $z_i$ , the adaptive law is obtained as:

$$\dot{\hat{\theta}}_i = - \sum_{k=1}^i \frac{\partial \beta_i}{\partial x_k} (x_{k+1} + \phi_k(x_1, \dots, x_k)^T (\hat{\theta}_i + \beta_i)), \quad i = 1, \dots, n \quad (2.34)$$

### 2.3.3 The Euler Model-Based Discrete-Time Backstepping

The Euler model-based discrete-time backstepping method is developed for single-input sampled-data nonlinear systems in [48] and extended to multi-input sampled-data nonlinear systems in [24, 25, 26]. Consider a continuous-time plant of the strict feedback form:

$$\dot{\eta} = f(\eta) + g(\eta)\xi \quad (2.35)$$

$$\dot{\xi} = u \quad (2.36)$$

where  $\eta \in \mathbb{R}^n$  and  $\xi \in \mathbb{R}^m$  are the state vectors,  $f(0) = 0$ ,  $f, g$  are differentiable sufficiently many times, and the control input  $u \in \mathbb{R}^m$  is realized through a zero order hold such that

$u(t) = u(kT) := u(k), \forall t \in [kT, (k+1)T), k \in \mathbb{N}$  and the state measurements  $\eta(k) := \eta(kT)$  and  $\xi(k) := \xi(kT)$  are available at sampling instants  $kT, k \in \mathbb{N}$  where  $T > 0$  is the sampling period.

Then the Euler approximate discrete-time model of (2.35)-(2.36) is given by

$$\eta(k+1) = r_T(\eta(k), \xi(k)) \quad (2.37)$$

$$\xi(k+1) = \xi(k) + Tu(k) \quad (2.38)$$

where  $r_T = \eta + T[f(\eta) + g(\eta)\xi]$ . The following theorem provides the SPA stabilizing controller design based on backstepping via Euler approximate discrete-time model of sampled-data nonlinear system.

**Theorem 2.3.3** [48, 26] *Assume that there exist  $\hat{T} > 0$  and a pair  $(\phi_T, W_T)$  that is defined for each  $T \in (0, \hat{T})$  and that is a SPA stabilizing pair for the subsystem (2.37) with  $\xi \in \mathbb{R}^m$  regarded as its control. Suppose also that:*

1.  $\phi_T$  and  $W_T$  are continuously differentiable for any  $T \in (0, \hat{T})$ ;
2. there exists  $\varphi \in \mathcal{K}_\infty$  such that  $|\phi_T(\eta)| \leq \varphi(|\eta|)$  for all  $\eta \in \mathbb{R}^n, T \in (0, \hat{T})$ ;
3. for any  $\tilde{\Delta} > 0$  there exists a pair of strictly positive numbers  $(\tilde{T}, \tilde{M})$  such that  $\max\{|\frac{\partial W_T}{\partial \eta}|, |\frac{\partial \phi_T}{\partial \eta}|\} \leq \tilde{M}$  for each  $T \in (0, \tilde{T})$  and  $|\eta| \leq \tilde{\Delta}$ .

Then there exists a SPA stabilizing pair  $(\phi_T, V_T)$  for (2.37)-(2.38) as:

$$u = -c(\xi - \phi_T(\eta)) - \frac{\Delta \tilde{W}_T(x)}{T} + \frac{\Delta \phi_T}{T} \quad (2.39)$$

$$V_T(x) = W_T(\eta) + \frac{1}{2}|\xi - \phi_T(\eta)|^2 \quad (2.40)$$

where  $c > 0$  is arbitrary,  $x = [\eta^T \quad \xi^T]^T$  and

$$\begin{aligned} \Delta \bar{\phi}_T &= \phi_T(r_T) - \phi_T(\eta) \\ \Delta \tilde{W}_T(x) &= \begin{cases} \frac{\Delta \tilde{W}_T(x)[\xi - \phi_T(\eta)]}{|\xi - \phi_T(\eta)|^2}, & \xi \neq \phi_T(\eta) \\ Tg^T(\eta) \left( \frac{\partial W_T}{\partial \eta} \right)^T(r_T), & \xi = \phi_T(\eta) \end{cases} \\ \Delta \bar{W}_T(x) &= W_T(r_T) - W_T(r_T^\phi) \\ r_T^\phi &= \eta + T[f(\eta) + g(\eta)\phi_T(\eta)]. \end{aligned}$$

## CHAPTER 3

# SPA STABILIZATION OF SAMPLED-DATA NONLINEAR SYSTEMS VIA BACKSTEPPING

### 3.1 Introduction

In this chapter, a digital controller design method is proposed. In this method, the controller is designed by backstepping based on the approximate discrete-time model. This controller semiglobally practically asymptotically (SPA) stabilizes the sampled-data nonlinear systems in strict feedback form.

In Chapter 1, digital controller design methods for sampled-data nonlinear systems were classified as continuous-time design, often referred to as emulation, direct discrete-time design and sampled-data design. As the performance of the continuous-time controller can only be recovered under very fast sampling condition, it may be impossible to reduce sampling period to a sufficiently small value to ensure desired performance due to the hardware restrictions. Moreover, sampling is taken into account at the design process in direct discrete-time design. Therefore, direct discrete-time method may outperform the emulation design [32, 48, 63]. Direct discrete-time design method involves designing a controller for the discrete-time plant model. In this method, the first step is the discretization of the continuous-time model. To obtain the exact discrete-time model it is needed to solve a nonlinear differential equation explicitly. Therefore, the exact discrete-time model of the plant cannot be computed in general. This has motivated research on controller design using direct discrete-time design via approximate discrete-time models. Hence, a more general framework for stabilization of sampled-data nonlinear systems using approximate discrete-time models was presented in the recent papers [43, 45, 46, 47, 50, 32]. In [46, 50], it is shown that the stabilization of exact model

with the family of controllers which stabilizes the approximate model is guaranteed under certain conditions. In [48], two integrator backstepping designs were presented for sampled-data nonlinear systems in strict feedback form using Euler approximate model within this framework. The controller in [48] was extended to multi-input sampled-data nonlinear systems in [26].

In this chapter, the problem of backstepping controller design is considered for sampled-data nonlinear systems in strict feedback form using direct discrete-time design. The controller design is based on the Euler approximate model. In this problem, the discrepancy between the Euler approximate model and exact discrete time model behaves as disturbance. It is known that even exponentially decaying disturbances can destabilize the sampled-data nonlinear system. Hence, in this chapter, the controller is designed to compensate the effects of this factor. This is the main difference from the controllers in [48] and [26]. It is shown that the designed controller SPA stabilizes the closed-loop sampled-data system based on the framework proposed in [46]. Also numerical examples are given to illustrate the design method. Simulation results show that the designed controller outperforms the controllers given in [48] and [26].

The chapter is organized as follows. In Section 3.2 preliminaries are given. The main results are stated and proved in Section 3.3. Then, in Section 3.4, application examples are provided to illustrate the design method. Finally, conclusions are presented in the last section.

## 3.2 Preliminaries

This section provides technical preliminaries. Common definitions which will be used throughout this chapter are presented. For the sake of clarity and easy reading, some notions and definitions that have been introduced in Chapter 2 are repeated when necessary.

Consider the following continuous-time nonlinear system

$$\dot{x} = f(x(t), u(t)) \tag{3.1}$$

where  $x \in \mathbb{R}^n$  is the state,  $u \in \mathbb{R}^m$  is the control input and the function  $f$  is locally Lipschitz. The control input  $u$  is realized through a zero-order hold such that  $u(t) = u(kT) := u(k), \forall t \in [kT, (k+1)T), k \in \mathbb{N}$  where  $T > 0$  is the sampling period.

The difference equation corresponding to the exact discrete-time model of (3.1) and its ap-

proximate discrete-time model are represented by:

$$x(k+1) = F_T^e(x(k), u(k)) \quad (3.2)$$

$$x(k+1) = F_T^a(x(k), u(k)), \quad (3.3)$$

respectively.

To measure the discrepancy between the exact model and the approximate model, one step consistency property, as defined in [46], is used:

**Definition 3.2.1** [46] *The family  $F_T^a(x, u)$  is said to be one-step consistent with the exact discrete-time model  $F_T^e(x, u)$  if, for each compact set  $\Omega \subset \mathbb{R}^n \times \mathbb{R}^m$ , there exists a class- $\mathcal{K}$  function  $\rho(\cdot)$  and a constant  $T_0 > 0$  such that,  $|F_T^e(x, u) - F_T^a(x, u)| \leq T\rho(T)$  for all  $(x, u) \in \Omega$  and  $T \in (0, T_0]$ .*

SPA stability and SPA stability Lyapunov functions are defined in [48] as follows.

**Definition 3.2.2** [48] *The family of controllers  $u_T$  SPA stabilizes  $F_T$  if there exists  $\beta \in \mathcal{KL}$  such that for any pair of strictly positive real numbers  $(D, v)$  there exists  $T^* > 0$  such that for each  $T \in (0, T^*)$  the solutions of  $x(k+1) = F_T(x(k), u_T(x(k)))$  satisfy:  $|x(k, x(0))| \leq \beta(|x(0)|, kT) + v$ , for all  $k \geq 0$ , whenever  $|x(0)| \leq D$ .*

**Definition 3.2.3** [48] *Let  $\hat{T} > 0$  be given and for each  $T \in (0, \hat{T})$  let functions  $V_T : \mathbb{R}^n \rightarrow \mathbb{R}_{\geq 0}$  and  $u_T : \mathbb{R}^n \rightarrow \mathbb{R}^m$  be defined. The pair of families  $(u_T, V_T)$  is a SPA stabilizing pair for  $F_T$  if there exist  $\alpha_1, \alpha_2, \alpha_3 \in \mathcal{K}_\infty$  such that for any pair of strictly positive real numbers  $(\Delta, \delta)$  there exists a triple of strictly positive real numbers  $(T^*, L, M)$ , with  $T^* \leq \hat{T}$ , such that for all  $x, z \in \mathbb{R}^n$  with  $\max\{|x|, |z|\} \leq \Delta$  and  $T \in (0, T^*)$ , and the following conditions are satisfied:*

$$\alpha_1(|x|) \leq V_T(x) \leq \alpha_2(|x|) \quad (3.4)$$

$$V_T(F_T(x, u_T(x))) - V_T(x) \leq -T\alpha_3(|x|) + T\delta \quad (3.5)$$

$$|V_T(x) - V_T(z)| \leq L|x - z| \quad (3.6)$$

$$|u_T(x)| \leq M \quad (3.7)$$

**Theorem 3.2.4** [45, 50, 51] *If  $(u_T, V_T)$  is a SPA stabilizing pair for  $F_T^a$ , then  $u_T$  stabilizes  $F_T^e$ .*

Then, stability properties of the sampled-data system (3.1) can be deduced from those of exact discretized system under certain conditions [51].

### 3.3 Main Results

In this section, the design of SPA stabilizing backstepping controller based on the Euler approximate model is presented for sampled-data nonlinear system in strict feedback form. The controller is designed to compensate the effect of the discrepancy between the Euler and the exact discrete-time model which behaves as disturbance. This is the main difference from the controllers given in [48] and [26].

Consider the following strict feedback nonlinear system

$$\dot{\eta} = f(\eta) + g(\eta)\xi \quad (3.8)$$

$$\dot{\xi} = \alpha(\eta, \xi) + \beta(\eta)u \quad (3.9)$$

where  $\eta \in \mathbb{R}^n$  and  $\xi \in \mathbb{R}^m$  are the state vectors,  $f(0) = 0$ ,  $f, g, \alpha$  are differentiable sufficiently many times,  $\beta(\eta) \neq 0, \forall \eta$ , the control input  $u \in \mathbb{R}^m$  is realized through a zero order hold such that  $u(t) = u(kT) := u(k), \forall t \in [kT, (k+1)T), k \in \mathbb{N}$  and the state measurements  $\eta(k) := \eta(kT)$  and  $\xi(k) := \xi(kT)$  are available at sampling instants  $kT, k \in \mathbb{N}$  where  $T > 0$  is the sampling period.

The difference equations corresponding to the exact discrete-time model of the system (3.8)-(3.9) are denoted by:

$$\eta(k+1) = F_{\eta,T}^e(\eta, \xi, u) \quad (3.10)$$

$$\xi(k+1) = F_{\xi,T}^e(\eta, \xi, u). \quad (3.11)$$

Then the Euler approximate discrete-time model of (3.8)-(3.9) is given by:

$$\eta(k+1) = F_{\eta,T}^a(\eta, \xi, u) = \eta + T(f(\eta) + g(\eta)\xi) \quad (3.12)$$

$$\xi(k+1) = F_{\xi,T}^a(\eta, \xi, u) = \xi + T(\alpha(\eta, \xi) + \beta(\eta)u). \quad (3.13)$$

Using the Euler model, the exact discrete-time model (3.10)-(3.11) can be written as:

$$\eta(k+1) = \eta + T(f(\eta) + g(\eta)\xi) + F_{\eta,T}^e(\eta, \xi, u) - F_{\eta,T}^a(\eta, \xi, u) \quad (3.14)$$

$$\xi(k+1) = \xi + T(\alpha(\eta, \xi) + \beta(\eta)u) + F_{\xi,T}^e(\eta, \xi, u) - F_{\xi,T}^a(\eta, \xi, u) \quad (3.15)$$

**Hypothesis 3.3.1** [48] *There exist  $\hat{T} > 0$  and a pair  $(\phi_T, W_T)$  that is defined for each  $T \in (0, \hat{T})$  and that is a SPA stabilizing pair for the subsystem (3.14) with  $\xi \in \mathbb{R}^m$  regarded as its control. Suppose also that the followings hold:*

1.  $\phi_T$  and  $W_T$  are twice differentiable for any  $T \in (0, \hat{T})$ ;
2. there exists  $\varphi \in \mathcal{K}_\infty$  such that  $|\phi_T(\eta)| \leq \varphi(|\eta|)$  for all  $\eta \in \mathbb{R}^n$ ,  $T \in (0, \hat{T})$ ;
3. for any  $\tilde{\Delta} > 0$  there exists a pair of strictly positive numbers  $(\tilde{T}, \tilde{M}_1)$  such that  $\max\{|\frac{\partial W_T}{\partial \eta}|, |\frac{\partial \phi_T}{\partial \eta}|, |\frac{\partial^2 \phi_T}{\partial \eta^2}|, |\frac{\partial^2 W_T}{\partial \eta^2}|\} \leq \tilde{M}_1$  for each  $T \in (0, \tilde{T})$  and  $|\eta| \leq \tilde{\Delta}$ .

The following theorem provides the SPA stabilizing controller design based on backstepping via Euler approximate discrete-time model of sampled-data nonlinear system and one-step consistency of the Euler model with the exact model.

**Theorem 3.3.2** *Assuming that Hypothesis 3.3.1 holds, the system (3.14)-(3.15) is SPA stable with the following controller*

$$u = \beta^{-1}(\eta)(-c(\xi - \phi_T(\eta)) - g(\eta)^T (\frac{\partial W_T}{\partial \eta}(\bar{\eta}_0^+))^T - d \left| \left( \frac{\partial \phi_T}{\partial \eta}(\eta_0^+) \right) \right|^2 (\xi - \phi_T(\eta)) + \frac{\Delta \phi_T}{T} - \alpha(\eta, \xi)) \quad (3.16)$$

where  $c, d > 0$ ,  $\Delta \phi_T = \phi_T(\eta_0^+) - \phi_T(\eta)$ ,  $\eta_0^+ = \eta + T(f(\eta) + g(\eta)\xi)$  and  $\bar{\eta}_0^+ = \eta + T(f(\eta) + g(\eta)\phi_T)$ .

**Proof.** Let  $\Delta, \mu, \hat{\mu} \in \mathbb{R}_{>0}$ ,  $\rho_\eta, \rho_\xi \in \mathcal{K}_\infty$ ,  $x = [\eta^T \ z^T]^T \in \mathbb{R}^{n+m}$  with  $|x| \leq \Delta$ ,  $z = \xi - \phi_T$  and  $c = c_1 + c_2$ . Consider the system (3.14). According to Hypothesis 3.3.1, there exists  $\hat{T} > 0$  such that condition (3.5) holds for  $T \in (0, \hat{T})$  with  $\tilde{\alpha}_3 \in \mathcal{K}_\infty$  and  $\hat{\mu}$  when  $\xi = \phi_T$  as input such that,

$$\Delta W_T = W_T(\bar{\eta}^+) - W_T(\eta) \leq -T\tilde{\alpha}_3(|\eta|) + T\hat{\mu} \quad (3.17)$$

where  $\bar{\eta}^+ = \eta + T(f(\eta) + g(\eta)\phi_T) + F_{\eta,T}^e(\eta, \phi_T, u) - F_{\eta,T}^a(\eta, \phi_T, u)$ . Then, using delta operator the exact discrete-time models (3.14)-(3.15) can be written as:

$$\delta \eta = f(\eta) + g(\eta)(z + \phi_T) + \frac{F_{\eta,T}^e - F_{\eta,T}^a}{T} \quad (3.18)$$

$$\delta z = \alpha(\eta, \xi) + \beta(\eta)u - \frac{\phi_T(\eta^+) - \phi_T(\eta)}{T} + \frac{F_{\xi,T}^e - F_{\xi,T}^a}{T} \quad (3.19)$$

with  $\eta^+ = \eta + T(f(\eta) + g(\eta)\xi) + F_{\eta,T}^e - F_{\eta,T}^a$ . Let  $\Delta_1 = \sup_{|x| \leq \Delta, T \in (0, \hat{T})} \max\{|\eta^+|, |\eta_0^+|, |\bar{\eta}_0^+|, |\bar{\eta}^+|\}$  that is well defined since functions  $f, g, \phi_T$  are continuous. Let  $\bar{\Delta} = \max\{\Delta, \Delta_1\}$  generates  $\tilde{T}, \tilde{M}_1$  such that inequality 3 in Hypothesis 3.3.1 holds. Let  $\tilde{M} = \sup_{|x| \leq \Delta, T \in (0, \hat{T})} \max\{|\xi - \phi_T|, |f(\eta) + g(\eta)\xi|, |g(\eta)|, |\tilde{M}_1|, |\beta(\eta)|, |\alpha(\eta, \xi)|, \rho_\eta, \rho_\xi\}$  which is well defined since all the considered functions are continuous over the given compact set. Let  $T^* > 0$  and for each  $T \in (0, T^*)$  let the Lyapunov function  $V_T$  be defined as  $V_T(\eta, \xi) = W_T(\eta) + \frac{1}{2}z^T z$ . It is obvious that conditions (3.4) and (3.6) are satisfied, (see [48]) and hence, to prove SPA stability, it is enough to show that conditions (3.5) and (3.7) are satisfied. First, it will be shown that condition (3.5) holds:

$$\delta V_T = \frac{\Delta V_T}{T} = \frac{V_T(k+1) - V_T(k)}{T} = \delta W_T + z^T \delta z + \frac{T}{2}((\delta z)^T \delta z).$$

$\delta W_T$  can be written, using the mean value theorem, as:

$$\begin{aligned} \delta W_T &= \frac{W_T(\eta^+) - W_T(\bar{\eta}^+) + W_T(\bar{\eta}^+) - W_T(\eta)}{T} \\ &= \frac{\Delta W_T}{T} + (\xi - \phi_T(\eta))^T g(\eta)^T \left( \frac{\partial W_T}{\partial \eta}(\eta^\diamond) \right)^T \end{aligned} \quad (3.20)$$

where  $\eta^\diamond = \bar{\eta}^+ + T\theta_1 g(\eta)(\xi - \phi_T(\eta))$  and  $\theta_1 \in (0, 1)$ .

Then,  $\delta V_T$  can be written, using (3.18), (3.19) and (3.20), as:

$$\begin{aligned} \delta V_T &\leq \frac{\Delta W_T}{T} - cz^T z + z^T \Lambda + \frac{T}{2}((\delta z)^T \delta z) + z^T \left( \frac{F_{\xi,T}^e - F_{\xi,T}^a}{T} \right) \\ &\quad + z^T g(\eta)^T \left( \left( \frac{\partial W_T}{\partial \eta}(\eta^\diamond) \right)^T - \left( \frac{\partial W_T}{\partial \eta}(\bar{\eta}_0^+) \right)^T \right) \end{aligned}$$

with  $\Lambda = \frac{\phi_T(\eta_0^+) - \phi_T(\eta^+)}{T} - d \left| \left( \frac{\partial \phi_T}{\partial \eta}(\eta_0^+) \right) \right|^2 z$ .

Using the mean value theorem, the term  $z^T g(\eta)^T \left( \left( \frac{\partial W_T}{\partial \eta}(\eta^\diamond) \right)^T - \left( \frac{\partial W_T}{\partial \eta}(\bar{\eta}_0^+) \right)^T \right)$  can be written as:

$$z^T g(\eta)^T \left( \left( \frac{\partial W_T}{\partial \eta}(\eta^\diamond) \right)^T - \left( \frac{\partial W_T}{\partial \eta}(\bar{\eta}_0^+) \right)^T \right) \leq T \tilde{M}^4. \quad (3.21)$$

Using the mean value theorem, it can be obtained that

$$\frac{\phi_T(\eta_0^+) - \phi_T(\eta^+)}{T} = - \left( \frac{\partial \phi_T}{\partial \eta}(\eta^*) \right) \left( \frac{F_{\eta,T}^e - F_{\eta,T}^a}{T} \right) \quad (3.22)$$

where  $\eta^* = \eta_0^+ + \ell_1 F_{\eta,T}^e - F_{\eta,T}^a$  and  $\ell_1 \in (0, 1)$ .

Then, using the differential mean value theorem (DMVT) and (3.22),  $\Lambda$  can be written as:

$$\begin{aligned}\Lambda &= \left( \left( \frac{\partial \phi_T}{\partial \eta}(\eta_0^+) \right) - \left( \frac{\partial \phi_T}{\partial \eta}(\eta^*) \right) - \left( \frac{\partial \phi_T}{\partial \eta}(\eta_0^+) \right) \right) \left( \frac{F_{\eta,T}^e - F_{\eta,T}^a}{T} \right) - d \left| \left( \frac{\partial \phi_T}{\partial \eta}(\eta_0^+) \right) \right|^2 z \\ &= - \left( \frac{\partial^2 \phi_T}{\partial \eta^2}(\eta^{**}) \right) \ell_1 \Omega \left( \frac{F_{\eta,T}^e - F_{\eta,T}^a}{T} \right) - \left( \frac{\partial \phi_T}{\partial \eta}(\eta_0^+) \right) \left( \frac{F_{\eta,T}^e - F_{\eta,T}^a}{T} \right) - d \left| \left( \frac{\partial \phi_T}{\partial \eta}(\eta_0^+) \right) \right|^2 z\end{aligned}\quad (3.23)$$

where  $\Omega = [\Omega_1^T, \Omega_2^T, \dots, \Omega_n^T]^T$ ,  $\Omega_i = F_{\eta,T}^e - F_{\eta,T}^a$ ,  $\eta^{**} = \eta_0^+ + \ell_1 \ell_2 F_{\eta,T}^e - F_{\eta,T}^a$  and  $\ell_2 \in (0, 1)$ .

From one-step consistency of the Euler model with the exact model, there exist  $\rho_\eta, \rho_\xi \in \mathcal{K}_\infty$  such that,

$$\left| F_{\eta,T}^e - F_{\eta,T}^a \right| \leq T \rho_\eta(T) \quad (3.24)$$

$$\left| F_{\xi,T}^e - F_{\xi,T}^a \right| \leq T \rho_\xi(T). \quad (3.25)$$

Then, using (3.17), (3.21), (3.23)-(3.25) and Young's inequality,  $\delta V_T$  can be written as:

$$\begin{aligned}\delta V_T &\leq \frac{\Delta W_T}{T} + T \tilde{M}^4 + |z^T \frac{\partial^2 \phi_T}{\partial \eta^2}(\eta^{**}) \ell_1 \Omega| \rho_\eta(T) - (c_1 + c_2) z^T z + |z^T| \rho_\xi(T) + \frac{1}{4d} (\rho_\eta(T))^2 \\ &\quad - (\sqrt{d} \left| \left( \frac{\partial \phi_T}{\partial \eta}(\eta_0^+) \right) z \right| + \frac{1}{2\sqrt{d}} \rho_\eta(T))^2 + \frac{T}{2} |-(c_1 + c_2)z - \left( \frac{\partial^2 \phi_T}{\partial \eta^2}(\eta^{**}) \right) \ell_1 \Omega| \rho_\eta(T) \\ &\quad - g(\eta)^T \left( \frac{\partial W_T}{\partial \eta}(\bar{\eta}_0^+) \right)^T - \left| \left( \frac{\partial \phi_T}{\partial \eta}(\eta_0^+) \right) \rho_\eta(T) - d \left| \left( \frac{\partial \phi_T}{\partial \eta}(\eta_0^+) \right) \right|^2 z + \rho_\xi(T) \right|^2 \\ &\leq -\tilde{\alpha}_3(|\eta|) + \hat{\mu} + T \tilde{M}^4 - c_1 z^T z + \left( \frac{1}{4c_2} + \frac{1}{4d} \right) \tilde{M}^2 + \frac{T}{2} ((c+1)\tilde{M} + 2\tilde{M}^2 + d\tilde{M}^3)^2 \\ &\leq -\tilde{\alpha}_3(|\eta|) - c_1 z^T z + \mu.\end{aligned}$$

Then, from Proposition 1 in [48], there exists  $\bar{\alpha}_3 \in \mathcal{K}_\infty$  such that  $\Delta V_T \leq -T \bar{\alpha}_3(|x|) + T\mu$ .

Finally, the following equation shows that condition (3.7) holds:

$$\begin{aligned}|u| &\leq |\beta(\eta)^{-1}| (c|\xi - \phi_T(\eta)| + |g(\eta)^T \left( \frac{\partial W_T}{\partial \eta}(\bar{\eta}_0^+) \right)^T| + |d| \left| \frac{\partial \phi_T}{\partial \eta}(\eta_0^+) \right|^2 |\xi - \phi_T(\eta)|) \\ &\quad + \left| \frac{\Delta \phi_T}{T} \right| + |\alpha(\eta, \hat{\xi})| \leq c + 1 + 2\tilde{M} + d\tilde{M}^2 = \bar{M}.\end{aligned}$$

Consequently, one can easily conclude that system (3.14)-(3.15) with the controller (3.16) is SPA stable. ■

### 3.4 Applications

In this section, the design method given in Theorem 3.3.2 is applied to various systems and the simulation results are analyzed.

### 3.4.1 Dynamically Positioned Ship

In the dynamic positioning problems, the speed of a ship is quite small. Hence it can be assumed that the damping forces are linear [12]. Then, consider the following equation of motion for the moored tanker in Example 11.4 in [12]

$$\dot{\eta} = R(\psi(t))v \quad (3.26)$$

$$\dot{v} = A_1\eta + A_2v + Bu \quad (3.27)$$

where  $\eta = [n \ e \ \psi]^T$ ,  $v = [\mu \ v \ r]^T$ ,  $u = [u_1 \ u_2 \ u_3]^T$ ,  $A_1 = -M^{-1}K$ ,  $A_2 = -M^{-1}D$ ,  $B = M^{-1}$  and

$$M = \begin{bmatrix} 1.0852 & 0 & 0 \\ 0 & 2.0575 & -0.4087 \\ 0 & -0.4087 & 0.2153 \end{bmatrix}, \quad R(\psi) = \begin{bmatrix} \cos \psi & -\sin \psi & 0 \\ \sin \psi & \cos \psi & 0 \\ 0 & 0 & 1 \end{bmatrix},$$

$$D = \begin{bmatrix} 0.0865 & 0 & 0 \\ 0 & 0.0762 & 0.1510 \\ 0 & 0.0151 & 0.0031 \end{bmatrix}, \quad K = \text{diag}\{0.0389, 0.0266, 0\}$$

as given in [25].

The control law  $\phi_T(\eta) = -R^T(\psi)L\eta$  and the Lyapunov function  $W_T(\eta) = \frac{1}{2}\eta^T\eta$  are a SPA stabilizing pair for the subsystem (3.26), where  $L$  can be chosen such that  $L = \text{diag}\{l_1, l_2, l_3\}$  with  $|1 - Tl_i| < 1$  and  $l_i > 0$  for sufficiently small  $T > 0$ . Using this pair, the controllers  $u_T$  and  $u_E$  are designed. The controller  $u_T$  is designed using (3.16) in Theorem 3.3.2. The controller  $u_E$  is obtained using the method given in [26] which was also presented in Theorem 2.3.3. The following simulation parameters are set:  $L = \text{diag}\{0.5, 0.5, 0.5\}$  and  $c = 1$ . Then, simulations have been performed in order to compare the performances of the controllers  $u_T$  and  $u_E$  with different sampling periods and initial conditions.

First, the controllers  $u_T$  and  $u_E$  are applied to the system (3.26)-(3.27) with the sampling period  $T = 0.2$  and the initial conditions,  $\eta(0) = [-2 \ 2 \ -\frac{\pi}{4}]^T$  and  $v(0) = 0_{3 \times 1}$ . Simulation results are given in Figure 3.1. As can be seen from figure, both controllers stabilize the system (3.26)-(3.27), but faster with  $u_T$ . Simulation results for the controller  $u_T$  show that as the parameter  $d$  increases, the performance of the controller  $u_T$  is faster. For  $d > 7$ , the controller  $u_T$  cannot stabilize the system (3.26)-(3.27).

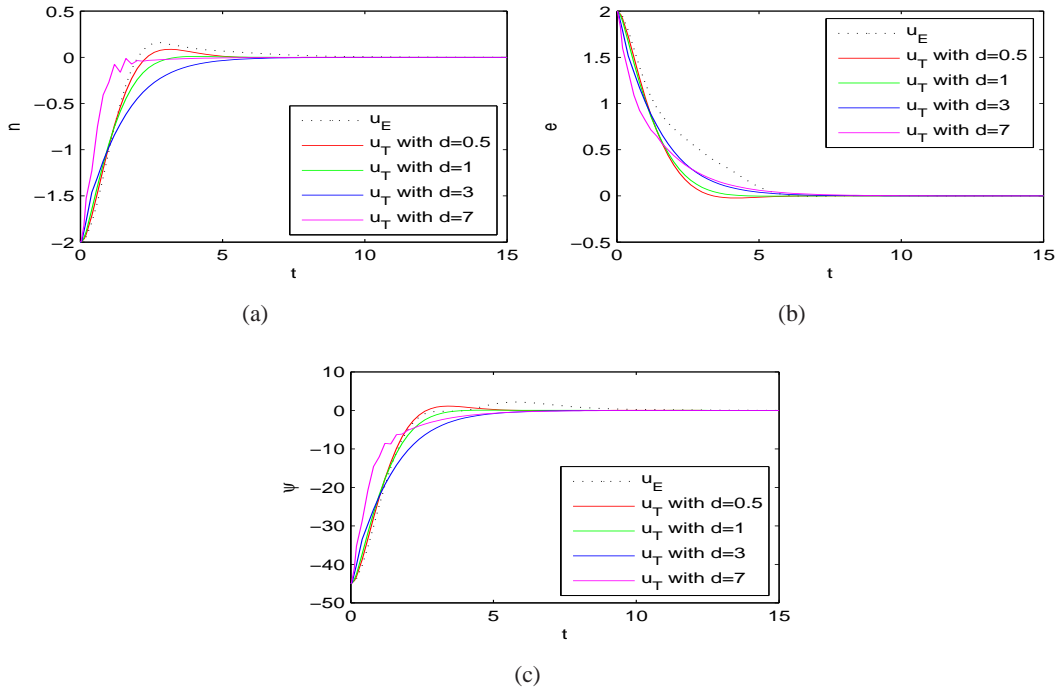


Figure 3.1: Time responses of the yaw angle  $\psi$ , the North position  $n$  and the East position  $e$  with  $T = 0.2$ . Dotted line:controller  $u_E$ . Solid line:designed controller  $u_T$ .

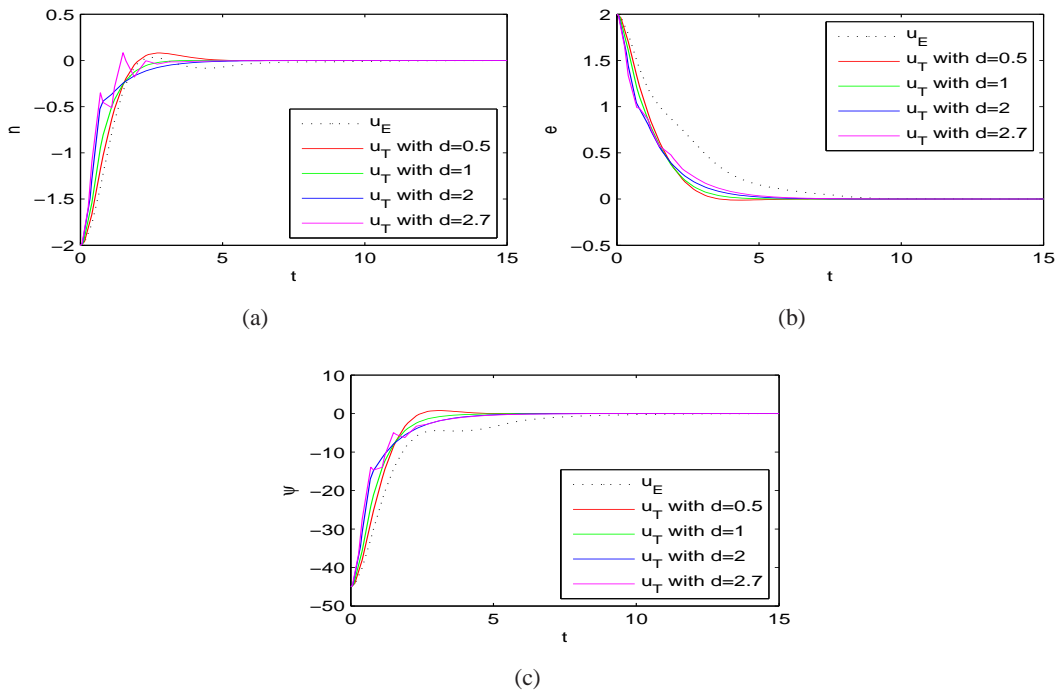


Figure 3.2: Time responses of yaw angle  $\psi$ , the North position  $n$  and the East position  $e$  with  $T = 0.4$ . Dotted line:controller  $u_E$ . Solid line:designed controller  $u_T$ .

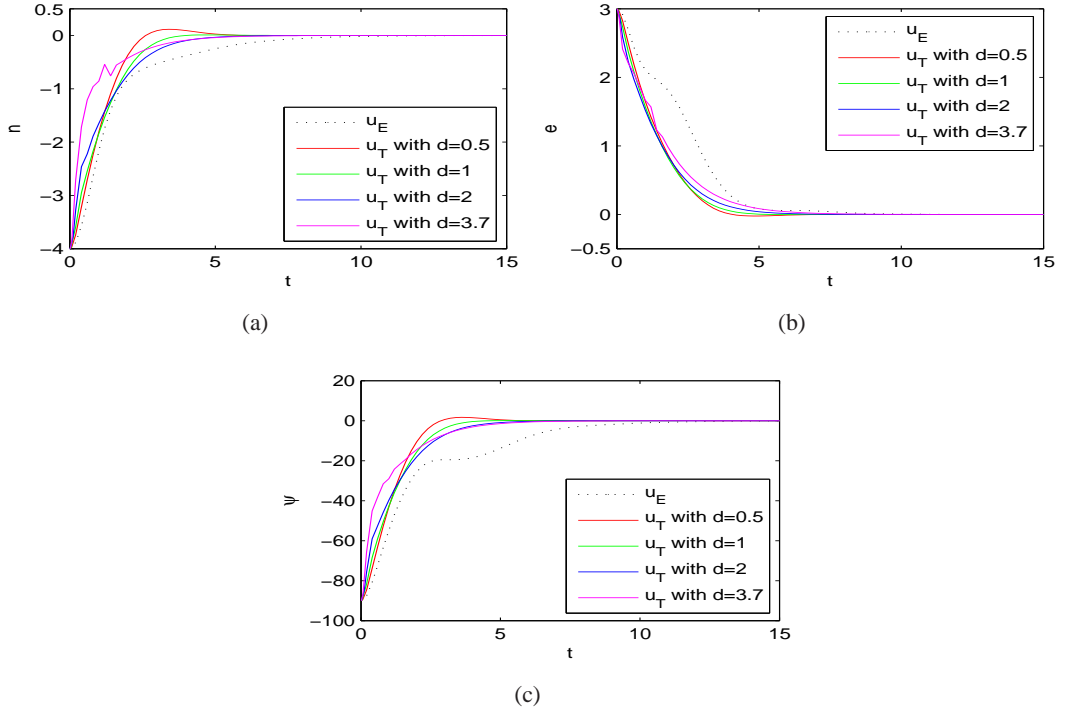


Figure 3.3: Time responses of yaw angle  $\psi$ , the North position  $n$  and the East position  $e$  with  $T = 0.2$  and large initial conditions. Dotted line:controller  $u_E$ . Solid line:designed controller  $u_T$ .

Then, the simulation is performed with the initial conditions given above and large sampling period  $T = 0.4$ . Simulation results are given in Figure 3.2. It is shown that both controllers stabilize the system (3.26)-(3.27), but faster with  $u_T$  again. Faster results are obtained with the controller  $u_T$  until  $d = 2.7$  and the performance worsens after  $d = 2.7$ . For  $d > 2.7$ , the controller  $u_T$  cannot stabilize the system (3.26)-(3.27). Simulation results for the controller  $u_E$  show that increase in the sampling period  $T$  results in slightly slow response. While the controller  $u_E$  cannot stabilize the system (3.26)-(3.27) for  $T > 0.9$  with the initial conditions above, the controller  $u_T$  can stabilize the system until  $T = 0.1$ .

Finally, the controllers are applied to the system (3.26)-(3.27) with the same sampling period  $T = 0.2$  as in the first simulation and large initial conditions,  $\eta(0) = [-4 \quad 3 \quad -\frac{\pi}{2}]^T$  and  $\nu(0) = 0_{3 \times 1}$ . Simulation results are given in Figure 3.3. It is shown that the controller  $u_T$  yields better results when compared to the controller  $u_E$  again.

Moreover, when the sampling period  $T$  or the initial conditions are increased, the controller  $u_T$  gives faster results for cases where the parameter  $d$  has smaller value.

### 3.4.2 Two-Link Robot Manipulator

In general, the dynamic model of n-link rigid-body robot manipulator can be written as given by the following matrix equation [9, 52]:

$$M(q)\ddot{q} + C(q, \dot{q})\dot{q} + G(q) = u$$

where the state  $q \in \mathbb{R}^n$  is the angular position vector of joint variable,  $M(q) \in \mathbb{R}^{n \times n}$  is the positive definite symmetric inertia matrix,  $C(q, \dot{q}) \in \mathbb{R}^{n \times n}$  is the Coriolis-centripetal matrix,  $G(q) \in \mathbb{R}^n$  is the gravity vector, and  $u \in \mathbb{R}^n$  is the control input vector. In the simulations, a two-link manipulator is considered with masses  $m_1$  and  $m_2$  [kg], lengths  $l_1$  and  $l_2$  [m], angles  $q_1$  and  $q_2$  [rad], torques  $u_1$  and  $u_2$  [Nm] for each link. Hence, defining the state vectors as  $\eta := [q_1 \quad q_2]^T$  and  $\xi := [\dot{q}_1 \quad \dot{q}_2]^T$ , the dynamic model of the two-link manipulator can be written as:

$$\dot{\eta} = \xi \quad (3.28)$$

$$\dot{\xi} = M^{-1}(\eta)(u - C(\eta, \xi)\xi - G(\eta)) \quad (3.29)$$

where  $M = \begin{bmatrix} M_1 & M_2 \\ M_3 & M_4 \end{bmatrix}$ ,  $C = \begin{bmatrix} C_1 & C_2 \\ C_3 & C_4 \end{bmatrix}$ ,  $G = \begin{bmatrix} G_1 \\ G_2 \end{bmatrix}$  and  $u = \begin{bmatrix} u_1 \\ u_2 \end{bmatrix}$  with  $M_1 = m_1 l_{c1}^2 + m_2(l_1^2 + l_{c2}^2 + 2l_1 l_{c2} \cos q_2)$ ,  $M_2 = M_3 = m_2 l_1 l_{c2} \cos q_2 + m_2 l_{c2}^2$ ,  $M_4 = m_2 l_{c2}^2$ ,  $C_1 = -m_2 l_2 l_{c2} \sin q_2 \dot{q}_2$ ,  $C_2 = -m_2 l_2 l_{c2} \sin q_2 (\dot{q}_1 + \dot{q}_2)$ ,  $C_3 = m_2 l_2 l_{c2} \sin q_2 \dot{q}_1$ ,  $C_4 = 0$ ,  $G_1 = m_1 g l_{c1} \cos q_1 + m_2 g (l_1 \cos q_1 + l_{c2} \cos(q_1 + q_2))$ ,  $G_2 = m_2 g l_{c2} \cos(q_1 + q_2)$ .  $l_{c1}$  and  $l_{c2}$  are the distances of the center of mass from the joint axes. The robot parameters are given as  $m_1 = m_2 = 5$  [kg],  $l_1 = l_2 = 0.5$  [m],  $l_{c1} = l_{c2} = 0.25$  [m]. The control objective is to solve the trajectory tracking problem. Hence, the joint position tracking error  $e$  is defined as  $e := \eta - \eta_d$  where  $\eta_d := \begin{bmatrix} q_{1d} \\ q_{2d} \end{bmatrix}$  is the desired position trajectory. Then, the system dynamics can be written as:

$$\dot{e} = \xi - \dot{\eta}_d \quad (3.30)$$

$$\dot{\xi} = M^{-1}(\eta)(u - C(\eta, \xi)\xi - G(\eta)). \quad (3.31)$$

The control law  $\phi_T(\eta) = \begin{bmatrix} -c_1(q_1 - q_{1d}) + \dot{q}_{1d} \\ -c_2(q_2 - q_{2d}) + \dot{q}_{2d} \end{bmatrix}$  and the Lyapunov function  $W_T(\eta) = \frac{1}{2}\eta^T \eta$  is a SPA stabilizing pair for the subsystem (3.30). Using this pair the controllers  $u_T$  and  $u_E$  are designed for the system (3.30)-(3.31). The controller  $u_T$  is designed using (3.16) in Theorem 3.3.2. The controller  $u_E$  is obtained using the method given in [26] which was also presented in Theorem 2.3.3. The following simulation parameters are set:  $c_1 = 2$ ,  $c_2 = 3$  and  $c = 1$ . Two different reference trajectories,  $q_{d1} = q_{d2} = \frac{5}{4} - \frac{5}{4}e^{-t}$  and  $q_{d1} = q_{d2} = \sin(t)$ , are

considered. Then, simulations have been performed in order to compare the performances of the controllers  $u_T$  and  $u_E$  with the initial conditions  $\eta(0) = \xi(0) = \begin{bmatrix} 0 \\ 0 \end{bmatrix}$  and different sampling periods.

First, the controllers  $u_T$  and  $u_E$  are applied to the system (3.28)-(3.29) with the first reference trajectory,  $q_{d1} = q_{d2} = \frac{5}{4} - \frac{5}{4}e^{-t}$ .

Simulation results with the sampling period  $T = 0.1$  are given in Figure 3.4. As can be seen from figure, both controllers track the desired trajectory, but the tracking error converges to zero faster with  $u_T$ . Simulation results for the controller  $u_T$  show that as the parameter  $d$  increases, the tracking error of the controller  $u_T$  is smaller. For  $d > 1.2$ , the controller  $u_T$  cannot stabilize the system (3.28)-(3.29).

Simulation results with large sampling period  $T = 0.2$  are given in Figure 3.5. It is shown that both controllers track the desired trajectory, but the tracking error converges to zero faster with  $u_T$  again. Results with smaller tracking error are obtained with the controller  $u_T$  until  $d = 0.5$ . For  $d > 0.5$ , the controller  $u_T$  cannot stabilize the system (3.28)-(3.29). Simulation results for the controller  $u_E$  show that increase in the sampling period  $T$  results in slower response. While the controller  $u_E$  cannot stabilize the system (3.28)-(3.29) for  $T > 0.22$ , the controller  $u_T$  can stabilize the system until  $T = 0.24$ .

Then, the controllers  $u_T$  and  $u_E$  are applied to the system (3.28)-(3.29) with the second reference trajectory,  $q_{d1} = q_{d2} = \sin(t)$ .

Simulation results with the sampling period  $T = 0.1$  are given in Figure 3.6. As can be seen from figure, the controller  $u_T$  tracks the desired trajectory with smaller tracking error when compared to the controller  $u_E$ . Simulation results for the controller  $u_T$  show that as the parameter  $d$  increases, the controller  $u_T$  tracks the desired trajectory with smaller error but for  $d = 1$  its performance is degraded. For  $d > 1$ , the controller  $u_T$  cannot stabilize the system (3.28)-(3.29).

Simulation results with large sampling period  $T = 0.15$  are given in Figure 3.7. It is shown that the tracking error increases for both controllers when compared to the results with  $T = 0.1$ , but tracking error of the controller  $u_T$  is smaller than that of the controller  $u_E$ . Results with smaller tracking error are obtained with the controller  $u_T$  until  $d = 0.6$ . The performance of the controller  $u_T$  worsens after  $d = 0.6$ . For  $d > 0.6$ , the controller  $u_T$  cannot stabilize

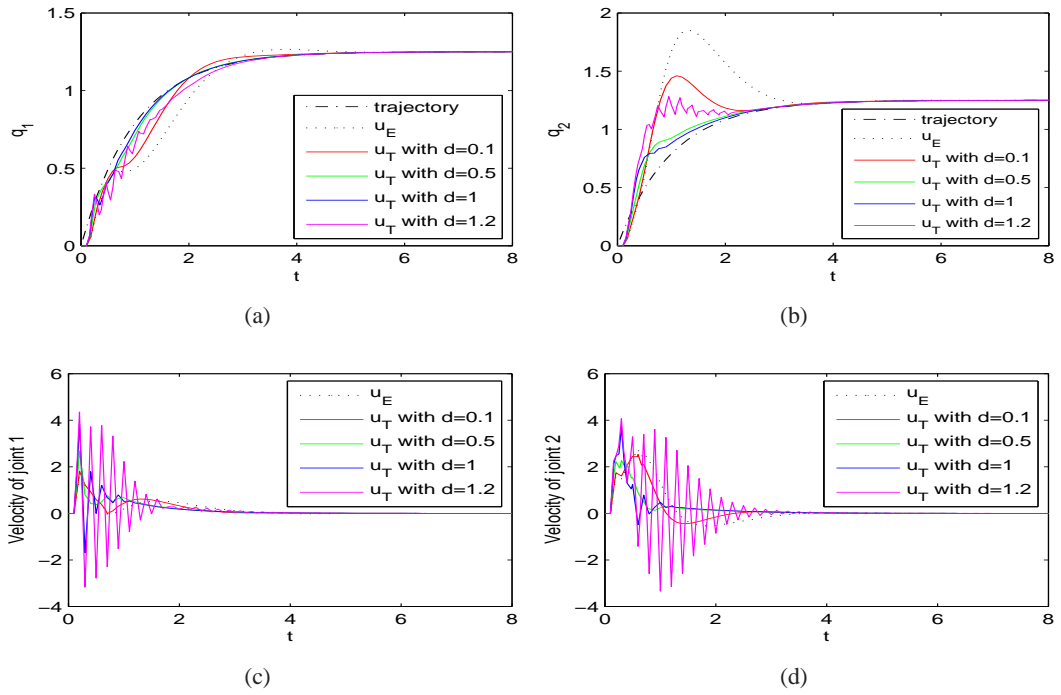


Figure 3.4: Responses of the system for the first trajectory with  $T = 0.1$ . Dotted line:controller  $u_E$ . Solid line:designed controller  $u_T$ . Dash-dotted line:desired trajectory.

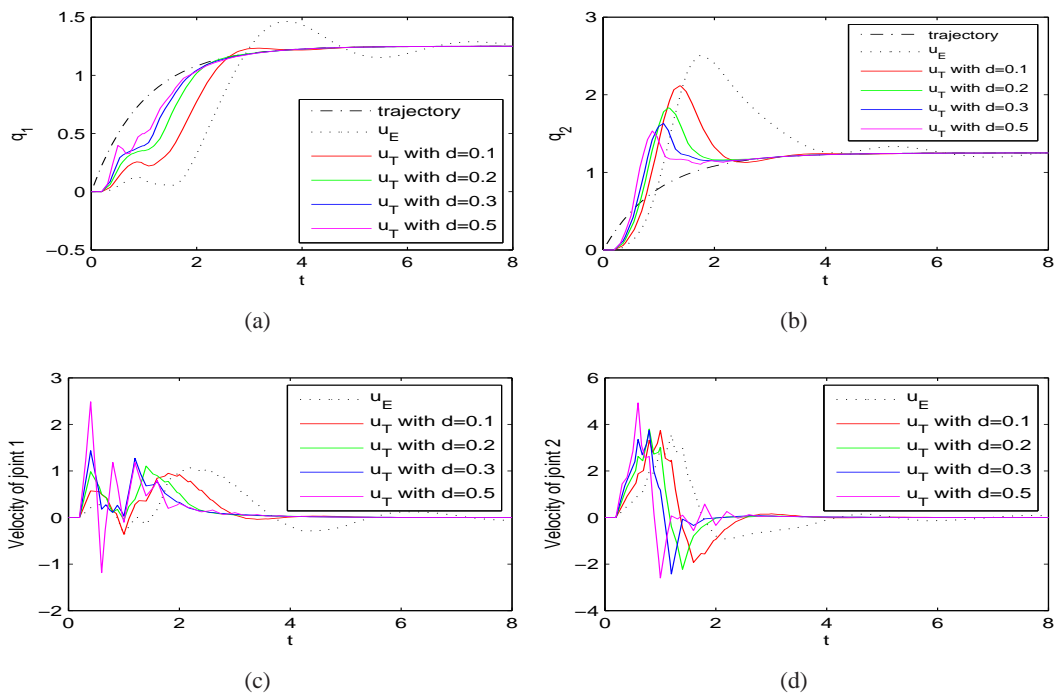


Figure 3.5: Responses of the system for the first trajectory with  $T = 0.2$ . Dotted line:controller  $u_E$ . Solid line:designed controller  $u_T$ . Dash-dotted line:desired trajectory.

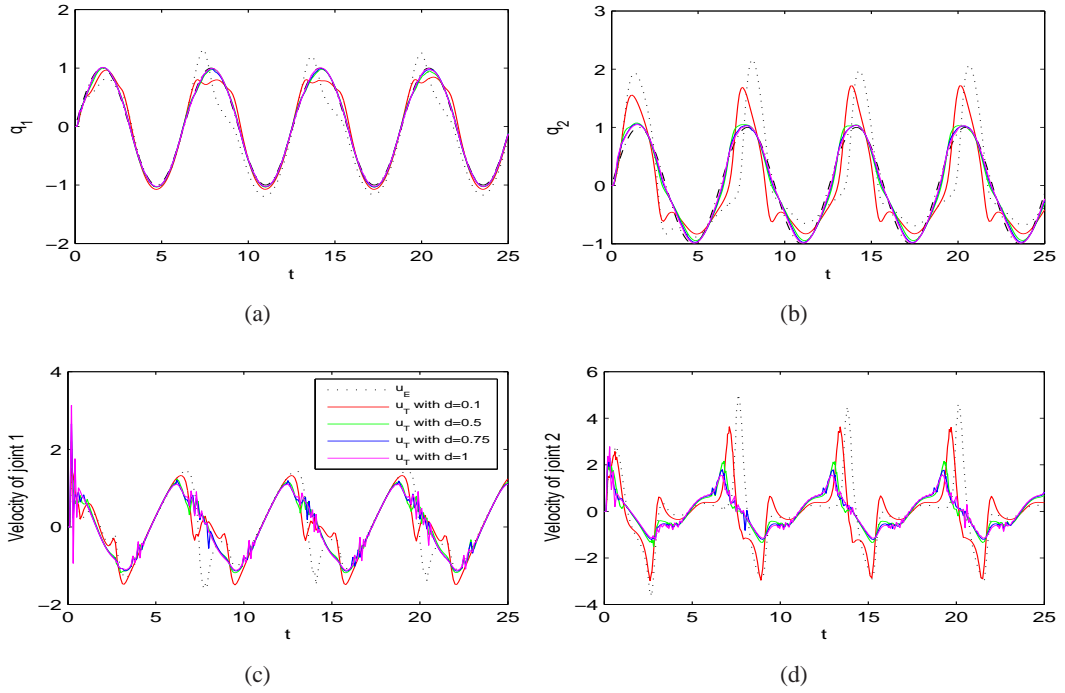


Figure 3.6: Responses of the system for the second trajectory with  $T = 0.1$ . Dotted line:controller  $u_E$ . Solid line:designed controller  $u_T$ . Dash-dotted line:desired trajectory.

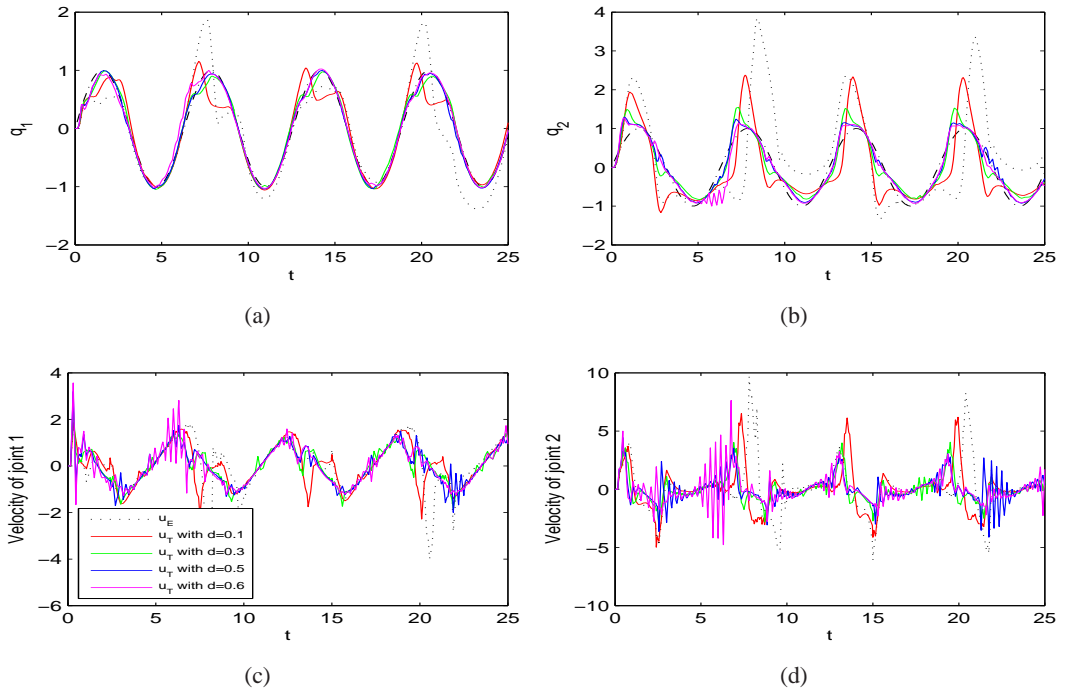


Figure 3.7: Responses of the system for the second trajectory with  $T = 0.15$ . Dotted line:controller  $u_E$ . Solid line:designed controller  $u_T$ . Dash-dotted line:desired trajectory.

the system (3.28)-(3.29). While the controller  $u_E$  cannot stabilize the system (3.28)-(3.29) for  $T > 0.18$ , the controller  $u_T$  can stabilize the system until  $T = 0.2$ .

Moreover, as the sampling period  $T$  increases, the controller  $u_T$  shows good performance for cases where the parameter  $d$  has smaller value.

### 3.4.3 Attitude Control of Rigid Artificial Satellite

In this part, a digital attitude control of a rigid artificial satellite is considered. Its attitude motion is modeled by the following nonlinear differential equations

$$\dot{\rho} = H(\rho)w, \quad (3.32)$$

$$\dot{w} = J^{-1}S(w)Jw + J^{-1}u \quad (3.33)$$

where  $w := [w_1 \ w_2 \ w_3]^T \in \mathbb{R}^3$  is the angular velocity vector of the body in a body-fixed frame,  $\rho \in \mathbb{R}^3$  is the Cayley-Rodrigues parameters describing the body orientation,  $u \in \mathbb{R}^3$  is the control torque vector of the body,  $J = J^T = \text{diag}\{10, 15, 20\}$  is the inertia matrix of the body [31],  $S(w)$  is the skew-symmetric matrix given by  $S(w) = \begin{bmatrix} 0 & w_3 & -w_2 \\ -w_3 & 0 & w_1 \\ w_2 & -w_1 & 0 \end{bmatrix}$  and  $H(\rho) = \frac{1}{2}(I - S(\rho) + \rho\rho^T)$ .

The control law  $\phi_T(\rho) = -H^{-1}(\rho)L\rho$  and the Lyapunov function  $W_T(\eta) = \frac{1}{2}\rho^T\rho$  is a SPA stabilizing pair for the subsystem (3.32) where  $L$  can be chosen such that  $L = \text{diag}\{l_1, l_2, l_3\}$  with  $|1 - Tl_i| < 1$  and  $l_i > 0$  for sufficiently small  $T > 0$ . Using this pair, the controllers  $u_T$  and  $u_E$  are designed for the system (3.32)-(3.33). The controller  $u_T$  is designed using (3.16) in Theorem 3.3.2. The controller  $u_E$  is obtained using the method given in [26] which was also presented in Theorem 2.3.3. The following simulation parameters are set:  $L = \text{diag}\{0.5, 0.5, 0.5\}$  and  $c = 1$ . Then, simulations have been performed in order to compare the performances of the controllers  $u_T$  and  $u_E$  with different sampling periods and initial conditions.

First, the initial conditions are chosen as  $\rho(0) = [1.4735 \ 0.6115 \ 2.5521]^T$  and  $w(0) = 0_{3 \times 1}$ . Simulation results with the sampling period  $T = 0.1$  are given in Figure 3.8. As can be seen from figure, both controllers stabilize the system (3.32)-(3.33), but faster with  $u_T$ . As the parameter  $d$  increases, the performance of the controller  $u_T$  is faster but for  $d = 1$  performance degradation starts. For  $d > 7$ , the controller  $u_T$  cannot stabilize the system (3.32)-(3.33).

Then, the simulation is performed with the initial conditions given above and large sampling

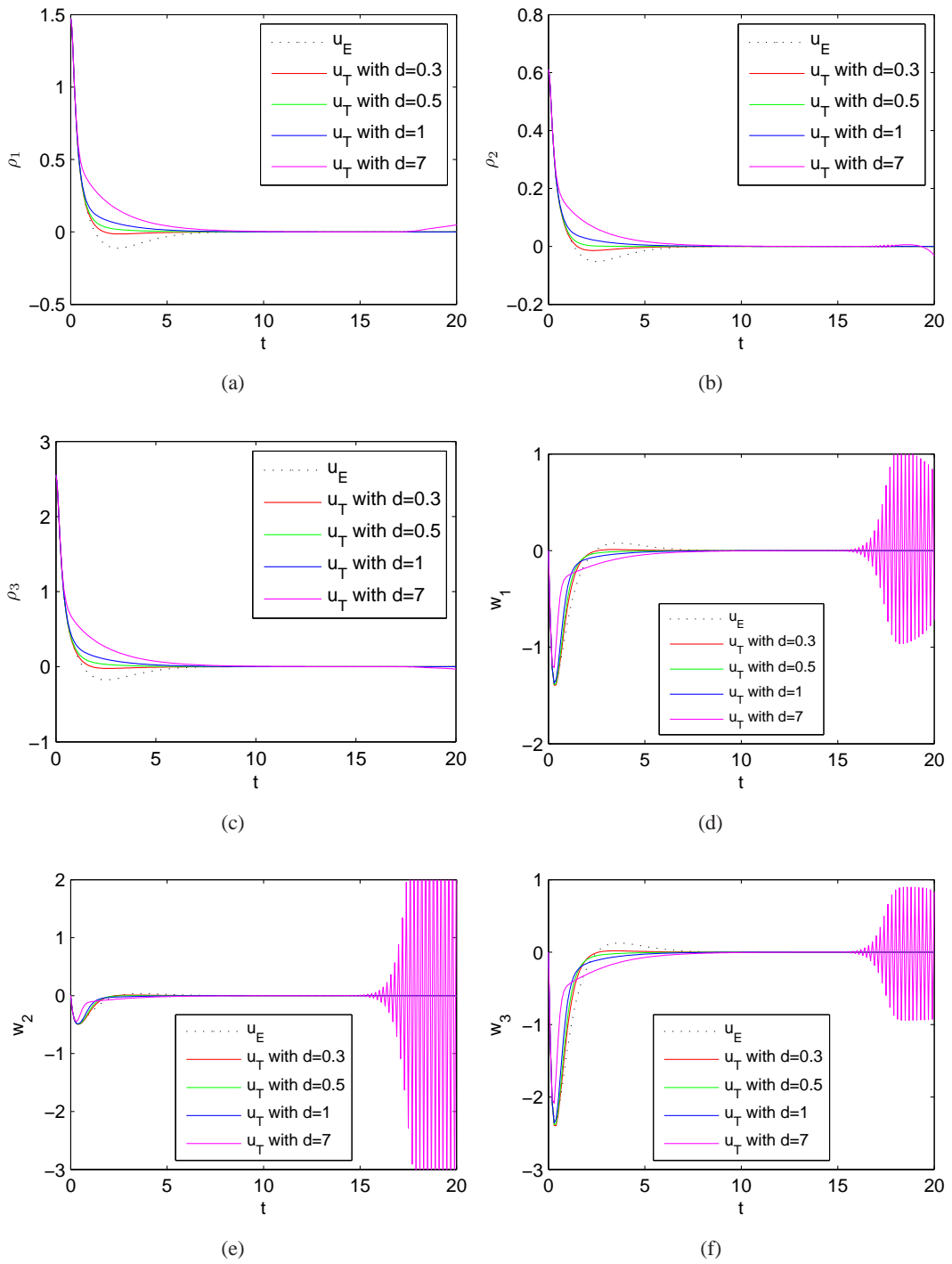


Figure 3.8: Time responses of  $\rho$  and  $w$  with  $T = 0.1$ . Dotted line:controller  $u_E$ . Solid line:designed controller  $u_T$ .

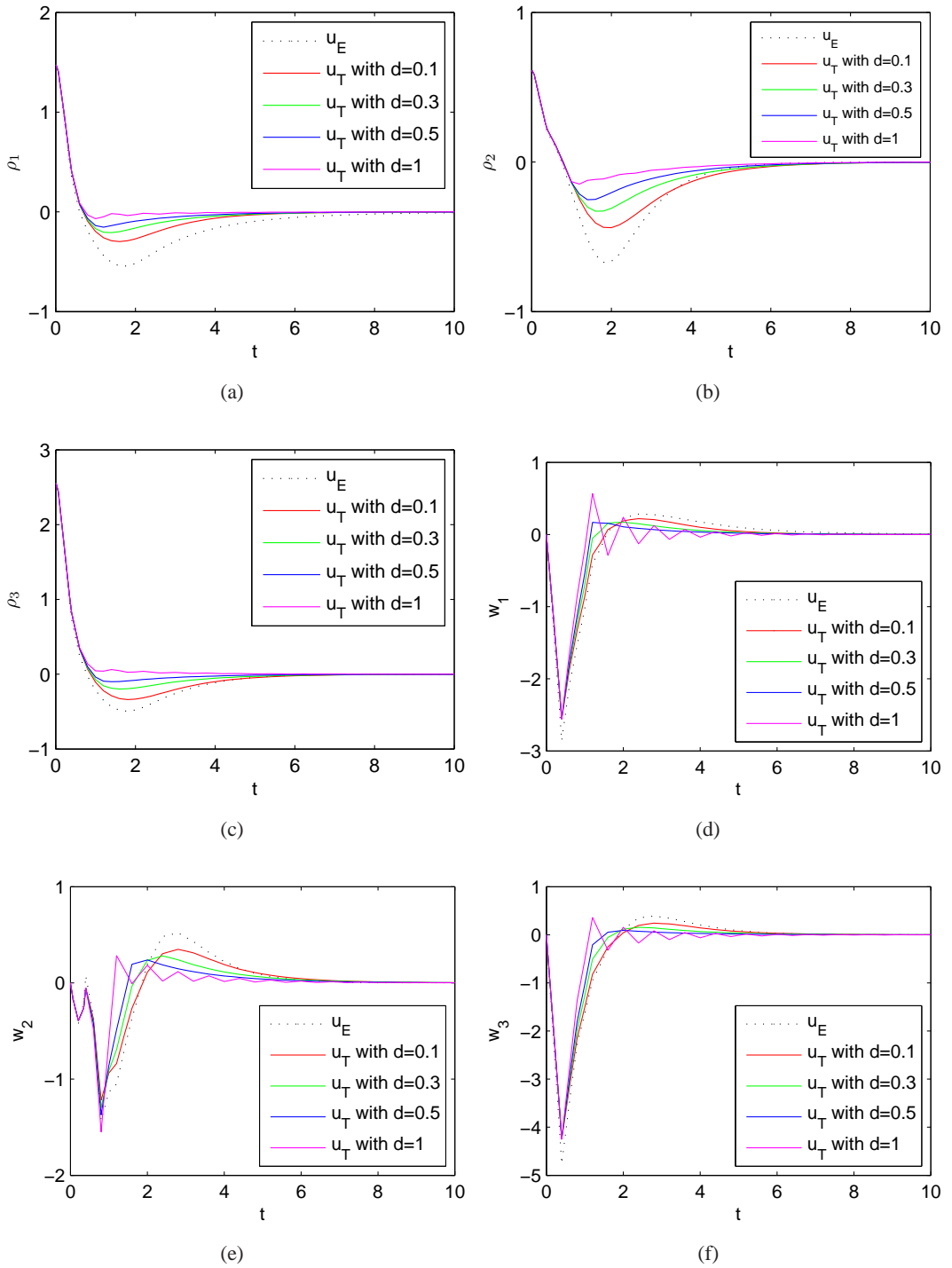


Figure 3.9: Time responses of  $\rho$  and  $w$  with  $T = 0.4$ . Dotted line:controller  $u_E$ . Solid line:designed controller  $u_T$ .

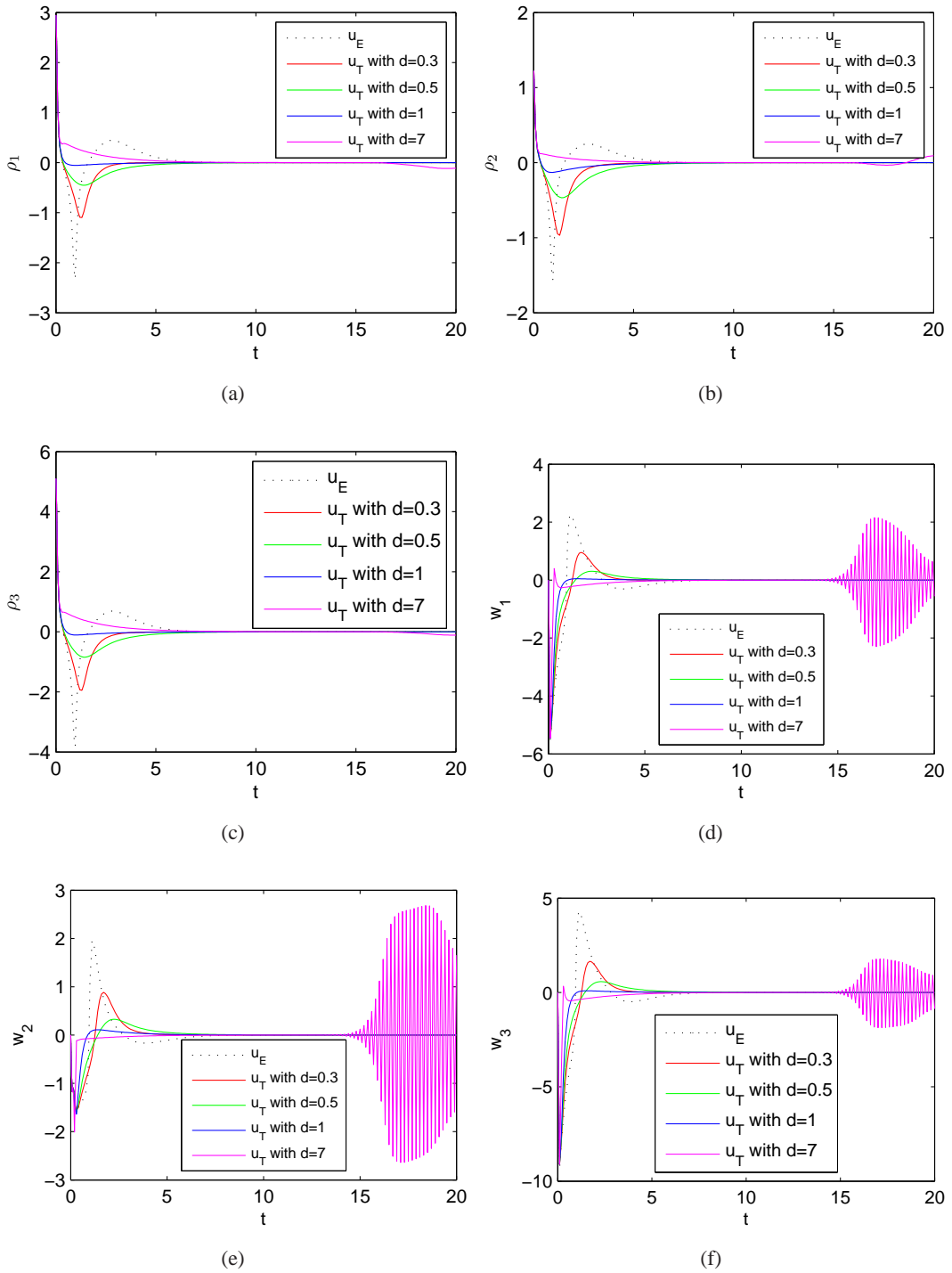


Figure 3.10: Time responses of  $\rho$  and  $w$  with  $T = 0.1$  and initial conditions doubled. Dotted line:controller  $u_E$ . Solid line:designed controller  $u_T$ .

period  $T = 0.4$ . Simulation results are given in Figure 3.9. It is shown that the controller  $u_T$  gives faster results when compared to the controller  $u_E$ . The controller  $u_T$  shows a good performance until  $d = 1$ . For  $d > 1$ , the controller  $u_T$  cannot stabilize the system (3.32)-(3.33). The controller  $u_E$  gives slower response with larger overshoots when compared to results with  $T = 0.1$ . While the controller  $u_E$  cannot stabilize the system (3.32)-(3.33) for  $T > 0.47$ , the controller  $u_T$  can stabilize the system until  $T = 0.51$ .

Finally, the controllers are applied to the system (3.32)-(3.33) with the same sampling period  $T = 0.1$  as in the first simulation and initial conditions doubled. Simulation results are given in Figure 3.10. It is shown that the controller  $u_T$  gives faster results when compared to the controller  $u_E$  again.

Moreover, when the sampling period  $T$  or the initial conditions are increased, the controller  $u_T$  gives faster results for cases where the parameter  $d$  has smaller value.

#### 3.4.4 Second-Order Single-Input System

Now, as a different example, consider the following second-order continuous-time plant with single input:

$$\dot{\eta} = \eta^2 + \xi \quad (3.34)$$

$$\dot{\xi} = u \quad (3.35)$$

where  $\eta \in \mathbb{R}$  and  $\xi \in \mathbb{R}$  are the state vectors and  $u \in \mathbb{R}$  is the control input.

First, continuous-time backstepping controller  $u_{ct}$  is designed for system (3.34)-(3.35) using the backstepping method given in [30]. The controller  $u_{ct}$  is obtained as  $u_{ct} = -2\eta - \eta^2 - \xi - (2\eta + 1)(\xi + \eta^2)$  with  $\phi_T = -\eta^2 - \eta$ , the Lyapunov function  $W(\eta) = \frac{1}{2}\eta^2$  and  $c = 1$ . Then, the controller  $u_T$  is designed using (3.16) in Theorem 3.3.2 with  $\phi_T = -\eta^2 - \eta$ , the Lyapunov function  $W_T(\eta) = \frac{1}{2}\eta^2$  and  $c = 1$ . The controller  $u_{NT}$  is designed using the method given in [48] which was also presented in Theorem 2.3.3. Then, simulations have been performed in order to compare the performances of the controllers  $u_T$  and  $u_E$  with different sampling periods and initial conditions.

In the first simulation, the initial conditions are chosen as  $(\eta(0), \xi(0)) = (1.6, 0.5)$ . Simulation results for the time responses of  $\eta$ ,  $\xi$  and  $u$  with the sampling period  $T = 0.6$  are given in

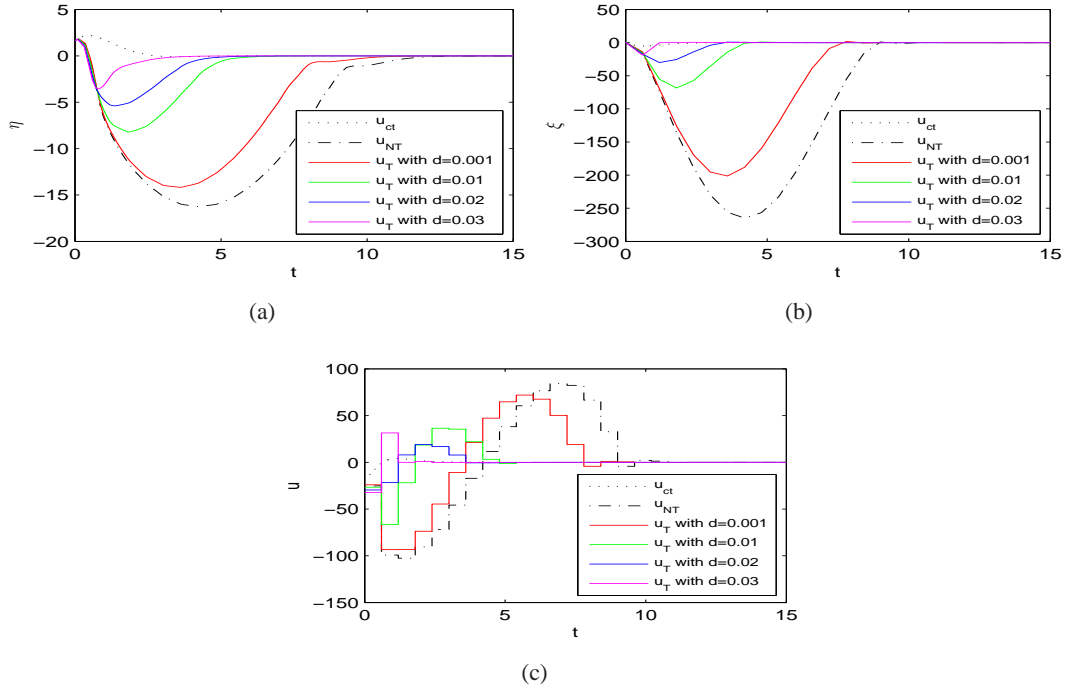


Figure 3.11: Time responses of  $\eta$ ,  $\xi$  and  $u$  with  $T = 0.6$ . Solid line:controller  $u_T$ . Dash-dotted line:controller  $u_{NT}$ . Dotted line:controller  $u_{ct}$ .

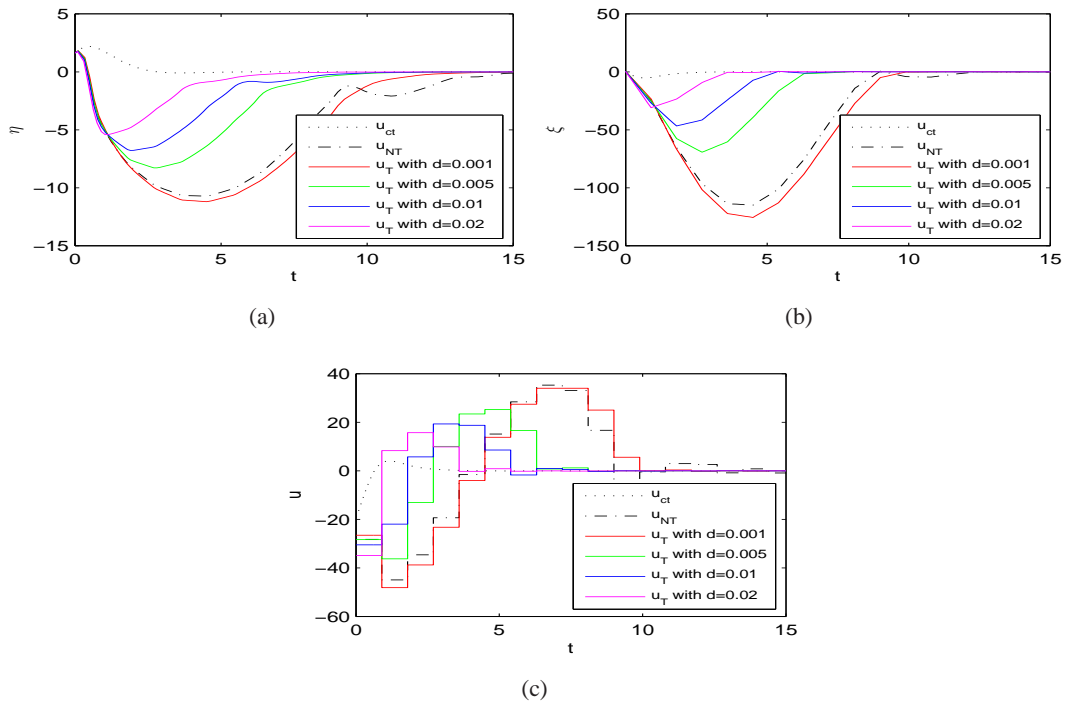


Figure 3.12: Time responses of  $\eta$ ,  $\xi$  and  $u$  with  $T = 0.9$ . Solid line:controller  $u_T$ . Dash-dotted line:controller  $u_{NT}$ . Dotted line:controller  $u_{ct}$ .

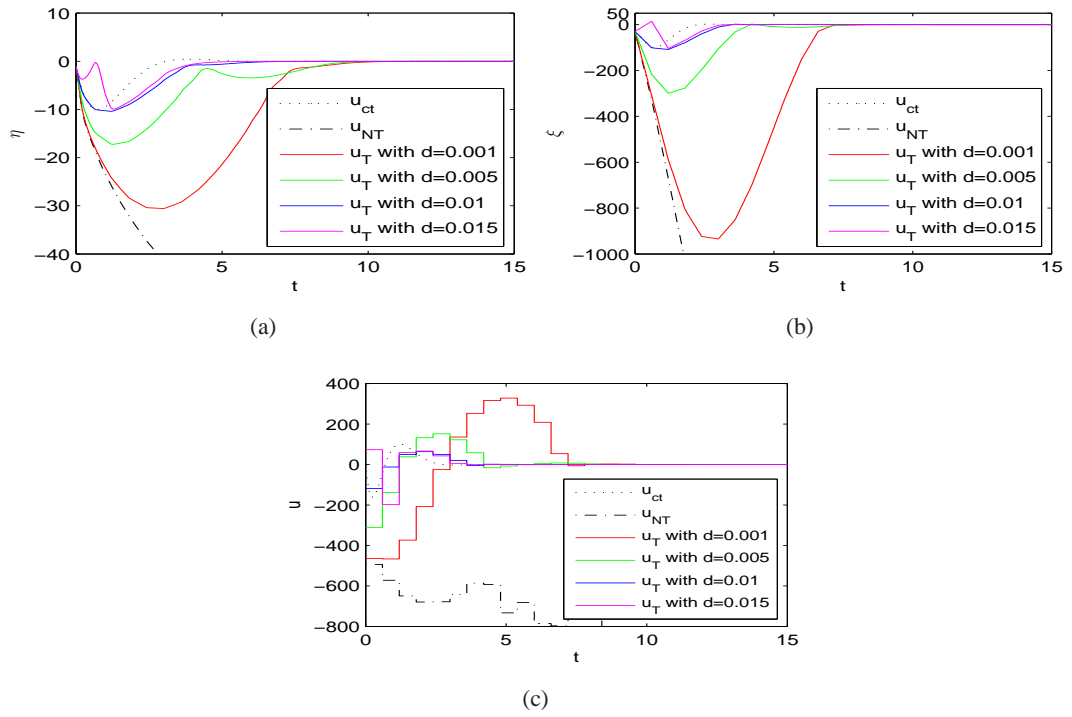


Figure 3.13: Time responses of  $\eta$ ,  $\xi$  and  $u$  with  $T = 0.6$  and the initial condition  $(\eta(0), \xi(0)) = (-1, -30)$ . Solid curve:controller  $u_T$ . Dash-dotted line:controller  $u_{NT}$ . Dotted line:controller  $u_{ct}$ .

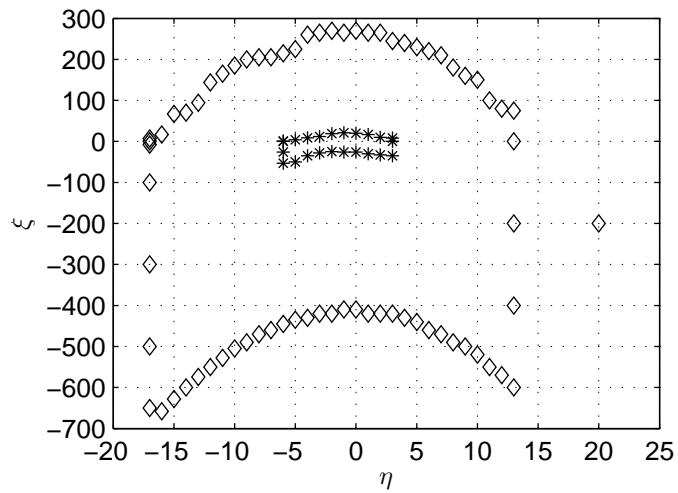


Figure 3.14: Domain of attraction estimates with  $T = 0.6$ . Diamond:controller  $u_T$ . Star:controller  $u_{NT}$ .

Figure 3.11. It is shown that the designed controller  $u_T$  works well and is faster than the controller  $u_{NT}$ . As the parameter  $d$  increases, the performance of the controller  $u_T$  is faster but for  $d = 0.03$  performance degradation starts. For  $d > 0.03$ , the controller  $u_T$  cannot stabilize the system (3.34)-(3.35).

Next, the simulation is performed with the initial conditions given above and large sampling period  $T = 0.9$ . Simulation results are given in Figure 3.12. It is shown that the controller  $u_T$  gives faster results when compared to the controller  $u_{NT}$ . The controller  $u_T$  shows a good performance until  $d = 0.02$  and the performance worsens after  $d = 0.02$ . For  $d > 0.02$ , the controller  $u_T$  cannot stabilize the system (3.34)-(3.35). The controller  $u_{NT}$  gives slower response as the sampling period  $T$  is increased. While the controller  $u_{NT}$  cannot stabilize the system (3.34)-(3.35) for  $T > 0.95$ , the controller  $u_T$  can stabilize the system until  $T = 1$ .

Then, the controllers are applied to the system (3.34)-(3.35) with the same sampling period  $T = 0.6$  as in the first simulation and large initial conditions  $(\eta(0), \xi(0)) = (-1, -30)$ . Simulation results are given in Figure 3.13. As can be seen from figure, while the controller  $u_{NT}$  cannot stabilize the system the designed controller  $u_T$  stabilizes the system successfully.

As can be seen from figures, the control input  $u_T$  is produced with less energy when compared to the control input  $u_{NT}$ . Therefore, the proposed method requires less control effort. Simulation results also show that when the parameter  $d$  is increased, energy of the control input  $u_T$  decreases in general.

Moreover, when the sampling period  $T$  or the initial conditions are increased, the controller  $u_T$  gives faster results for cases where the parameter  $d$  has smaller value.

Finally, by applying the controllers to the system (3.34)-(3.35) with different initial conditions, domain of attraction (DOA) estimates with the controllers  $u_T$  and  $u_{NT}$  for the sampling period  $T = 0.6$  are given in Figure 3.14. In DOA estimate with the controller  $u_T$ , the parameter  $d$  is chosen as  $d = 0.001$ . As can be seen from figure, DOA for the system with the controller  $u_T$  is much larger than that with the controller  $u_{NT}$ . For different controller parameters and sampling periods, much larger DOA estimate may be obtained with the controller  $u_T$  when compared to the estimate given in figure.

### 3.4.5 Jet Engine Stall

As a last example, consider the jet engine model given in [30]:

$$\dot{R} = -\sigma R^2 - \sigma R(2\phi + \phi^2) \quad (3.36)$$

$$\dot{\phi} = -\psi - \frac{3}{2}\phi^2 - \frac{1}{2}\phi^3 - 3R\phi - 3R \quad (3.37)$$

$$\dot{\psi} = -u \quad (3.38)$$

where  $\phi$  is the mass flow,  $\psi$  is the pressure rise and  $R$  is the normalized stall squared amplitude. As  $R \geq 0$ , the stabilization of the subsystem (3.36) is obvious by inspection. Choosing simply a virtual control  $\phi = \alpha(R) = 0$  yields  $\dot{R} = -\sigma R^2$ , which means that  $R(t) \rightarrow 0$  as  $t \rightarrow \infty$ . Therefore the backstepping procedure can be shortened from a three-step design to a two-step design [30].

Consider (3.37) as the upper subsystem, and (3.38) as the lower subsystem with  $\psi$  regarded as the virtual control for the upper subsystem. The upper subsystem can be stabilized with the virtual control  $\alpha(\phi, R) = c_1\phi - \frac{3}{2}\phi^2 - 3R$ . Then using Lyapunov function  $W = \frac{1}{2}\phi^2$ , continuous-time backstepping controller is obtained as  $u_{ct} = c(\psi - c_1\phi + \frac{3}{2}\phi^2 + 3R) - \phi - (c_1 - 3\phi)(-\psi - \frac{3}{2}\phi^2 - \frac{1}{2}\phi^3 - 3R\phi - 3R) + 3\sigma R(-R - 2\phi - \phi^2)$ . Using (3.16) in Theorem 3.3.2, the controller  $u_T$  is obtained with control law  $\alpha(\phi, R) = c_1\phi - \frac{3}{2}\phi^2 - 3R$  and Lyapunov function  $W_T = \frac{1}{2}\phi^2$ . The controller parameters are chosen such that  $c = c_1 = 1, \sigma = 7$ . Simulations have been performed to compare performances of the designed controller  $u_T$  and the controller  $u_{NT}$  designed in [32] using the method given in [48].

First, the initial conditions are chosen as  $(R(0), \phi(0), \psi(0)) = (0, -1, -6)$ . Simulation results for the time responses of  $\phi$  and  $\psi$  with the sampling period  $T = 0.01$  are given in Figure 3.15. It is shown that the designed controller  $u_T$  works well and is faster than the controller  $u_{NT}$ . As the parameter  $d$  increases, the performance of the controller  $u_T$  is faster but for  $d = 6$  performance degradation starts. For  $d > 13$ , the controller  $u_T$  cannot stabilize the system (3.36)-(3.38).

Then, the simulation is performed with the initial conditions given above and large sampling period  $T = 0.5$ . Simulation results are given in Figure 3.16. It is shown that the controller  $u_T$  yields faster results when compared to the controller  $u_{NT}$ . The controller  $u_T$  shows a good performance until  $d = 0.1$ . For  $d > 0.1$ , the controller  $u_T$  cannot stabilize the system (3.36)-

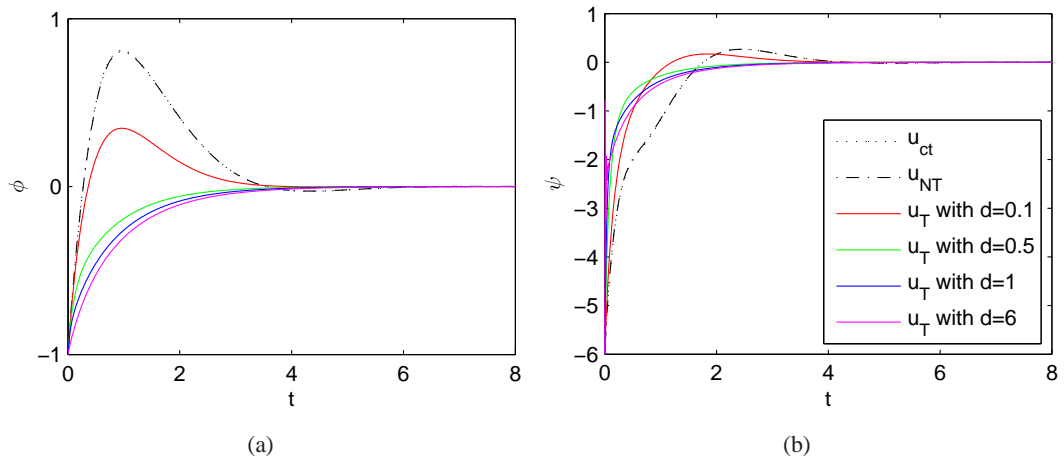


Figure 3.15: Time responses of  $\phi$  and  $\psi$  with  $T = 0.01$ . Solid curve:controller  $u_T$ . Dash-dotted line:controller  $u_{NT}$ . Dotted line:controller  $u_{ct}$ .

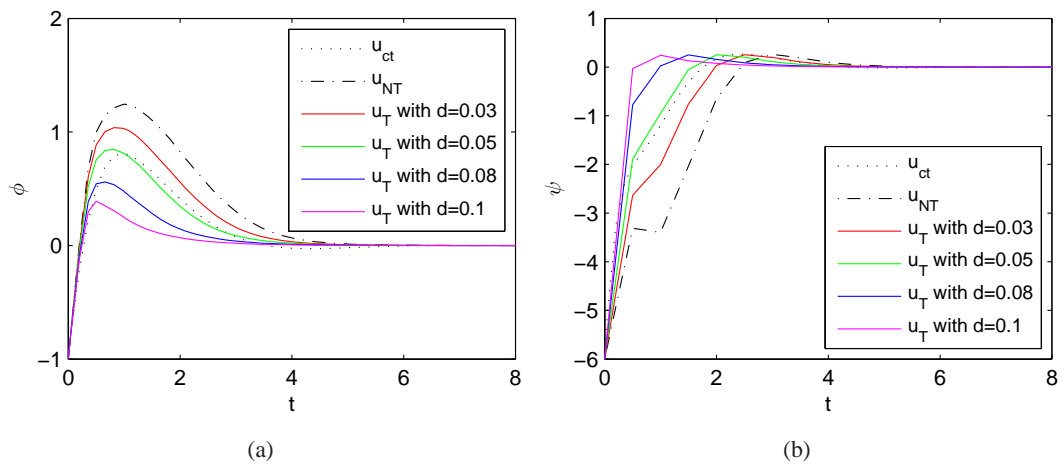


Figure 3.16: Time responses of  $\phi$  and  $\psi$  with  $T = 0.5$ . Solid curve:controller  $u_T$ . Dash-dotted line:controller  $u_{NT}$ . Dotted line:controller  $u_{ct}$ .

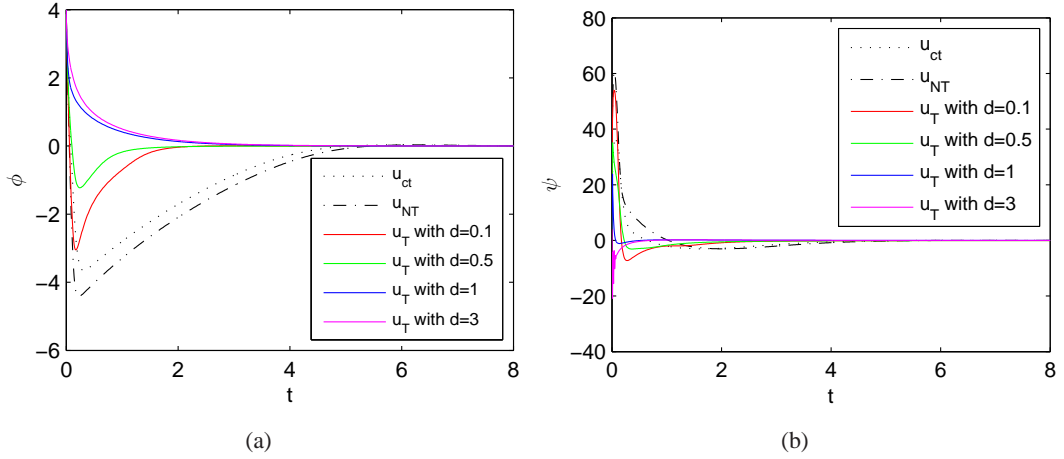


Figure 3.17: Time responses of  $\phi$  and  $\psi$  with the initial conditions  $(R(0), \phi(0), \psi(0)) = (5, 4, 4)$  and  $T = 0.01$ . Solid curve:controller  $u_T$ . Dash-dotted line:controller  $u_{NT}$ . Dotted line:controller  $u_{ct}$ .

(3.38). The controller  $u_{NT}$  gives response with larger overshoots as the sampling period  $T$  is increased. While the controller  $u_{NT}$  cannot stabilize the system (3.36)-(3.38) for  $T > 0.85$ , the controller  $u_T$  can stabilize the system until  $T = 1$ .

Finally, the controllers are applied to the system (3.36)-(3.38) with the same sampling period  $T = 0.01$  as in the first simulation and large initial conditions  $(R(0), \phi(0), \psi(0)) = (5, 4, 4)$ . Simulation results are given in Figure 3.17. As can be seen from Figure 3.17, both controllers stabilize the system successfully, but faster with  $u_T$ .

Moreover, when the sampling period  $T$  or the initial conditions are increased, the controller  $u_T$  gives faster results for cases where the parameter  $d$  has smaller value.

### 3.5 Conclusions

In this chapter, the problem of backstepping controller design has been considered for sampled-data nonlinear systems in strict feedback form. A backstepping design method has been presented based on the Euler approximate model. It has been shown that the designed controllers SPA stabilize the closed-loop sampled-data system based on the framework proposed in [46]. The proposed design has been applied to several examples arising from the engineering practice. Their performances were analyzed with simulations.

For the problem considered, the discrepancy between the Euler approximate model and exact discrete time model behaves as disturbance. It is known that even exponentially decaying disturbances can destabilize the sampled-data nonlinear systems. Hence, in this chapter, the controllers were designed to compensate the effects of this factor. The results obtained are, of course, different from the controllers in [48] and [26]. Using simulations, the performance of the designed controller has been compared with the controllers given in [48] and [26]. It was shown that the designed controller yielded better performance when compared to the controllers given in [48] and [26].

Moreover, in case of unstable results, the controllers given in [48] and [26] can be tuned to obtain stable results by adapting the controller gain. However, the controller designed by the proposed method can also be tuned adapting another parameter in addition to the controller gain. So the proposed method gives an additional flexibility for tuning the controller. Another advantage of the designed controller is that the controller designed by the proposed method can stabilize the systems with larger sampling periods when compared to the controllers given in [48] and [26].

## CHAPTER 4

# ADAPTIVE BACKSTEPPING FOR THE EULER APPROXIMATE MODEL OF SAMPLED-DATA NONLINEAR SYSTEMS

### 4.1 Introduction

In this chapter, two adaptive digital controller design methods are proposed. In these methods, the controllers are designed by adaptive backstepping based on the approximate discrete-time model. These controllers semiglobally practically asymptotically (SPA) stabilize the sampled-data nonlinear systems.

In many cases, a desired control performance cannot be satisfied with a nonadaptive controller because of parameter uncertainties. For these cases, the adaptive design methods are used. Generally the adaptive design method is based on the design of a parameter adaptive law, i.e. estimates of the parameters are made to converge to the true value of uncertain parameters for plants by controllers.

The problem of adaptive control of continuous-time nonlinear systems have been widely studied in the last years and many design tools have been proposed (see [21, 22, 30, 40, 61, 62] and references therein). The class of feedback linearizable systems that depend linearly on the unknown parameters are most widely studied (see [30, 40, 61] and references therein). In [30], the design of a backstepping adaptive controller has been well studied for continuous-time nonlinear systems in the parametric strict-feedback form. In [22], an alternative adaptive backstepping design for continuous-time nonlinear systems in the parametric strict-feedback form was proposed using the nonlinear adaptive stabilization tools developed in [4, 23].

On the other hand, adaptive control of sampled-data nonlinear systems has drawn little attention. In [19], a controller based on higher order approximations is developed using an overparametrization. A sampled-data scheme using continuous-time adaptive controller with  $\sigma$ -modification based on emulation approach is given in [64]. In [57], considering high order approximations for a general class of nonlinear systems, the design of high order adaptive discrete-time controllers using the truncated Fliess series of the Lyapunov difference equation is developed. In [34], an adaptive controller for sampled-data nonlinear systems is developed based on [22].

In this chapter, the problem of adaptive backstepping controller design is considered for sampled-data nonlinear systems in strict feedback form using direct discrete-time design. The controller design is based on the Euler approximate model. In this problem, the error in parameter estimation behaves as disturbance. Even exponentially decaying disturbances can destabilize the sampled-data nonlinear system. Hence, in the work that follows, the design methods to compensate the effects of this factor are presented. It is shown that the designed controllers SPA stabilize the closed-loop sampled-data system based on the framework proposed in [46]. Also numerical examples are given to illustrate the design methods. Simulation results show that the designed controllers outperform the emulation controllers.

The chapter is organized as follows. In Section 4.2 preliminaries are given. The main results are stated and proved in Section 4.3. Then, in Section 4.4, application examples are provided to illustrate the design method. Finally, conclusions are presented.

## 4.2 Preliminaries

This section provides technical preliminaries. Common definitions which will be used throughout the chapter are presented. For the sake of clarity and easy reading, some notions and definitions that have been introduced in Chapter 2 are repeated when necessary.

Consider the following continuous-time nonlinear system

$$\dot{x} = f(x(t), u(t)) \tag{4.1}$$

where  $x \in \mathbb{R}^n$  is the state,  $u \in \mathbb{R}^m$  is the control input and the function  $f$  is locally Lipschitz. The control input  $u$  is realized through a zero-order hold such that  $u(t) = u(kT) := u(k), \forall t \in$

$[kT, (k + 1)T), k \in \mathbb{N}$  where  $T > 0$  is the sampling period.

The difference equation corresponding to the exact discrete-time model of (4.1) and its approximate discrete-time model are represented by:

$$x(k + 1) = F_T^e(x(k), u(k)) \quad (4.2)$$

$$x(k + 1) = F_T^a(x(k), u(k)) \quad (4.3)$$

respectively.

To measure the difference between the exact model and the approximate model, one step consistency property, as defined in [46], is used:

**Definition 4.2.1** ([46]) *The family  $F_T^a(x, u)$  is said to be one-step consistent with the exact discrete-time model  $F_T^e(x, u)$  if, for each compact set  $\Omega \subset \mathbb{R}^n \times \mathbb{R}^m$ , there exists a class- $\mathcal{K}$  function  $\rho(\cdot)$  and a constant  $T_0 > 0$  such that,  $|F_T^e(x, u) - F_T^a(x, u)| \leq T\rho(T)$  for all  $(x, u) \in \Omega$  and  $T \in (0, T_0]$ .*

SPA stability and SPA stability Lyapunov functions are defined in [48] as follows.

**Definition 4.2.2** [48] *The family of controllers  $u_T$  SPA stabilizes  $F_T$  if there exists  $\beta \in \mathcal{KL}$  such that for any pair of strictly positive real numbers  $(D, \nu)$  there exists  $T^* > 0$  such that for each  $T \in (0, T^*)$  the solutions of  $x(k + 1) = F_T(x(k), u_T(x(k)))$  satisfy:  $|x(k, x(0))| \leq \beta(|x(0)|, kT) + \nu$ , for all  $k \geq 0$ , whenever  $|x(0)| \leq D$ .*

**Definition 4.2.3** [48] *Let  $\hat{T} > 0$  be given and for each  $T \in (0, \hat{T})$  let functions  $V_T : \mathbb{R}^n \rightarrow \mathbb{R}_{\geq 0}$  and  $u_T : \mathbb{R}^n \rightarrow \mathbb{R}$  be defined. The pair of families  $(u_T, V_T)$  is a SPA stabilizing pair for  $F_T$  if there exist  $\alpha_1, \alpha_2, \alpha_3 \in \mathcal{K}_\infty$  such that for any pair of strictly positive real numbers  $(\Delta, \hat{\delta})$  there exists a triple of strictly positive real numbers  $(T^*, L, M)$ , with  $T^* \leq \hat{T}$ , such that for all  $x, x_1, x_2 \in \mathbb{R}^n$  with  $\max\{|x|, |x_1|, |x_2|\} \leq \Delta$  and  $T \in (0, T^*)$ , and the following conditions are satisfied:*

$$\alpha_1(|x|) \leq V_T(x) \leq \alpha_2(|x|) \quad (4.4)$$

$$V_T(F_T(x, u_T(x))) - V_T(x) \leq -T\alpha_3(|x|) + T\hat{\delta} \quad (4.5)$$

$$|V_T(x_1) - V_T(x_2)| \leq L|x_1 - x_2| \quad (4.6)$$

$$|u_T(x)| \leq M \quad (4.7)$$

**Theorem 4.2.4** [45, 50, 51] *If  $(u_T, V_T)$  is a SPA stabilizing pair for  $F_T^a$ , then  $u_T$  stabilizes  $F_T^e$ .*

Then, stability properties of the sampled-data system (4.1) can be deduced from those of exact discretized system under certain conditions [51].

### 4.3 Main Results

In this section, two adaptive backstepping controller designs are presented for sampled-data nonlinear system in strict feedback form. The controller designs are based on the Euler approximate model. The controllers are designed to compensate the effects of the error in parameter estimation which behaves as disturbance and SPA stabilize the sampled-data nonlinear systems.

Consider the following parametric strict feedback system:

$$\dot{x} = Ax + B\xi + \phi^T \theta \quad (4.8)$$

$$\dot{\xi} = u + \phi_n^T(x_1, \dots, x_{n-1}, \xi)\theta \quad (4.9)$$

where

$$A = \begin{bmatrix} 0 & 1 & 0 & \dots & \dots & 0 \\ 0 & 0 & 1 & 0 & \dots & 0 \\ \dots & \dots & \dots & \dots & \dots & \dots \\ \dots & \dots & \dots & \dots & \dots & \dots \\ 0 & \dots & \dots & \dots & 0 & 1 \\ 0 & \dots & \dots & \dots & \dots & 0 \end{bmatrix}, B = \begin{bmatrix} 0 \\ \dots \\ \dots \\ \dots \\ 0 \\ 1 \end{bmatrix}, \phi = \begin{bmatrix} \phi_1(x_1) & \phi_2(x_1, x_2) & \dots & \dots & \phi_{n-1}(x_1, \dots, x_{n-1}) \end{bmatrix}$$

and  $x \in \mathbb{R}^{n-1}$ ,  $\xi \in \mathbb{R}$ ,  $u \in \mathbb{R}$  and  $\phi_i \in \mathbb{R}^p$  is a vector of known smooth nonlinear functions with  $\phi_i(0, \dots, 0) = 0$ ,  $i = 1, \dots, n$ ,  $\theta \in \mathbb{R}^p$  is a vector of unknown constant parameters, the control input  $u(t) = u(kT) =: u(k)$ ,  $\forall t \in [kT, (k+1)T)$ ,  $k \in \mathbb{N}$  which is realized through a zero order hold where  $T > 0$  is the sampling period and the state measurements  $x(k) := x(kT)$  and  $\xi(k) := \xi(kT)$  are available at sampling instants  $kT$ ,  $k \in \mathbb{N}$ . It is assumed that there exists a known constant  $\bar{\theta}$  such that  $|\theta| \leq \bar{\theta}$ .

The difference equations corresponding to the exact discrete-time model of (4.8)-(4.9) are

represented by

$$x(k+1) = F_{x,T}^e(x, \xi, u, \theta) \quad (4.10)$$

$$\xi(k+1) = F_{\xi,T}^e(x, \xi, u, \theta). \quad (4.11)$$

Then the Euler approximate model of (4.8)-(4.9) is given by

$$x(k+1) = x + T(Ax + B\xi + \phi^T \theta) \quad (4.12)$$

$$\xi(k+1) = \xi + T(u + \phi_n^T \theta). \quad (4.13)$$

The first adaptive backstepping controller design will be presented for the Euler approximate model (4.12)-(4.13) below. The controller design is based on the Euler approximate model of the parameter estimator obtained using the algorithm given in [30] and stated in Chapter 2.

**Hypothesis 4.3.1** [48] *There exist  $\hat{T} > 0$ , a pair  $(\alpha_T, W_T)$  and parameter estimator  $\hat{\theta}_x(k+1)$  that are defined for each  $T \in (0, \hat{T})$  and that SPA stabilize the subsystem (4.12) with  $\xi \in \mathbb{R}$  regarded as its control where the parameter estimator  $\hat{\theta}_x(k+1)$  is the Euler approximate model of the estimator  $\dot{\hat{\theta}}_x$  which is obtained during the design of  $\alpha_T$  using tuning function technique given in [30]. Suppose also that the followings hold:*

1. *for any  $\tilde{\Delta} > 0$  there exists  $\bar{\Delta} > 0$  such that  $|\phi_i| \leq \bar{\Delta}$  for all  $|x| \leq \tilde{\Delta}$  and  $i = 1, 2, \dots, n$ ,*
2.  *$\alpha_T$  and  $W_T$  are twice differentiable for any  $T \in (0, \hat{T})$ ;*
3. *there exists  $\varphi \in \mathcal{K}_\infty$  such that  $|\alpha_T(\tilde{x})| \leq \varphi(|\tilde{x}|)$  for all  $\tilde{x} = [x^T \quad \hat{\theta}_x^T]^T \in \mathbb{R}^{n+p-1}$  and  $T \in (0, \hat{T})$  where  $x \in \mathbb{R}^{n-1}$  and  $\hat{\theta}_x \in \mathbb{R}^p$ ;*
4. *for any  $\tilde{\Delta} > 0$  there exists a pair of strictly positive numbers  $(\tilde{T}, \tilde{M}_1)$  such that  $\max\{|\frac{\partial W_T}{\partial x}|, |\frac{\partial \alpha_T}{\partial x}|, |\frac{\partial^2 \alpha_T}{\partial x^2}|, |\frac{\partial^2 W_T}{\partial x^2}|\} \leq \tilde{M}_1$  for each  $T \in (0, \tilde{T})$ ,  $|x| \leq \tilde{\Delta}$ ,  $|\tilde{\theta}_x| \leq \Delta_p$  and  $|\theta| \leq \bar{\theta}$  where  $\tilde{\theta}_x = \theta - \hat{\theta}_x$ .*

The following theorem provides the SPA stabilizing adaptive backstepping controller design based on the Euler approximate discrete-time model of sampled-data nonlinear system.

**Theorem 4.3.2** *Assuming that Hypothesis 4.3.1 holds, the system (4.12)-(4.13) is SPA stable with the following controller and parameter estimators for  $\theta$  and so is the exact discretized*

system (4.10)-(4.11).

$$u = -c(\xi - \alpha_T(x, \hat{\theta}_x)) - \left( \frac{\partial W_T}{\partial x}(\bar{x}_0^+) \right) B + \frac{\Delta \alpha_T}{T} - \phi_n^T \hat{\theta}_\xi - d(\xi - \alpha_T(x, \hat{\theta}_x)) \left| \left( \frac{\partial \alpha_T}{\partial x}(x_0^+, \hat{\theta}_x^+) \right)^T \right|^2 \quad (4.14)$$

$$\hat{\theta}_x(k+1) = \hat{\theta}_x + Tg(x, \hat{\theta}_x) \quad (4.15)$$

$$\hat{\theta}_\xi(k+1) = \hat{\theta}_\xi + T\Gamma(\xi - \alpha_T(x, \hat{\theta}_x))\phi_n \quad (4.16)$$

where  $c, d > 0$ ,  $\Gamma$  is an arbitrary positive definite matrix,  $\Delta \alpha_T = \alpha_T(x_0^+, \hat{\theta}_x^+) - \alpha_T(x, \hat{\theta}_x)$ ,  $x_0^+ = x + T(Ax + B\xi + \phi^T \hat{\theta}_x)$ ,  $\bar{x}_0^+ = x + T(Ax + B\alpha_T(x, \hat{\theta}_x) + \phi^T \hat{\theta}_x)$ ,  $g(x, \hat{\theta}_x)$  is the estimator  $\hat{\dot{\theta}}_x$  obtained during the design of  $\alpha_T$  using tuning function technique given in [30], and (4.15)-(4.16) are the parameter estimators for  $\theta$  where (4.15) is obtained when designing the virtual control law  $\alpha_T$  and (4.16) is obtained when designing the control law  $u$ .

**Proof.** Let  $\Delta, \Delta_p, \mu, \hat{\mu} \in \mathbb{R}_{>0}$ ,  $\eta = [x^T \ \xi^T]^T \in \mathbb{R}^n$  with  $|\eta| \leq \Delta$ ,  $\hat{\eta} = [x^T \ \tilde{\theta}_x^T]^T \in \mathbb{R}^{n+p-1}$ ,  $\tilde{\eta} = [x^T \ z \ \tilde{\theta}^T]^T \in \mathbb{R}^{n+2p}$ ,  $z = \xi - \alpha_T$  and  $\tilde{\theta} = \theta - \hat{\theta} = [\hat{\theta}_x^T \ \tilde{\theta}_\xi^T]^T$  with  $\hat{\theta} = [\hat{\theta}_x^T \ \hat{\theta}_\xi^T]^T$ ,  $|\tilde{\theta}| \leq \Delta_p$  and  $|\theta| \leq \bar{\theta}$ . Consider the system (4.12). There exists  $\hat{T} > 0$  such that condition (4.5) holds for  $T \in (0, \hat{T})$  with  $\tilde{\alpha}_3 \in \mathcal{K}_\infty$  and  $\hat{\mu}$  when  $\xi = \alpha_T$  as input such that

$$\Delta W_T = W_T(\bar{x}^+, \tilde{\theta}_x^+) - W_T(x, \tilde{\theta}_x) \leq -T\tilde{\alpha}_3(|\hat{\eta}|) + T\hat{\mu} \quad (4.17)$$

where  $\bar{x}^+ = x + T(Ax + B\alpha_T(x, \hat{\theta}_x) + \phi^T \theta)$ . Then, using delta operator, the Euler approximate models of  $x, z$  and  $\tilde{\theta}_\xi$  can be written as:

$$\delta x = Ax + B(z + \alpha_T) + \phi^T \theta \quad (4.18)$$

$$\delta z = u - \frac{\alpha_T(x^+, \hat{\theta}_x^+) - \alpha_T(x, \hat{\theta}_x)}{T} + \phi_n^T \theta \quad (4.19)$$

$$\delta \tilde{\theta}_\xi = -\Gamma z \phi_n \quad (4.20)$$

Let  $\Delta_1 = \sup_{|\eta| \leq \Delta, |\theta| \leq \bar{\theta}, |\tilde{\theta}| \leq \Delta_p, T \in (0, \hat{T})} \max\{|x^+|, |x_0^+|, |\bar{x}_0^+|, |\bar{x}^+|\}$  that is well defined since functions  $\alpha_T, \phi_i$  are continuous. Let  $\bar{\Delta} = \max\{\Delta, \Delta_1\}$  generates  $\tilde{T}, \tilde{M}_1$  such that inequality 4 in Hypothesis 4.3.1 holds. Let  $\tilde{M} = \sup_{|\eta| \leq \Delta, |\theta| \leq \bar{\theta}, |\tilde{\theta}| \leq \Delta_p, T \in (0, \hat{T})} \max\{|\xi - \alpha_T|, |Ax + B\xi + \phi^T \theta|, |\phi_i|, \tilde{M}_1, |\tilde{\theta}|, |\hat{\theta}|\}$  which is well defined since all the considered functions are continuous over the given compact set. Let  $T^* > 0$  and for each  $T \in (0, T^*)$  let the Lyapunov function  $V_T$  be defined as  $V_T(x, \xi, \tilde{\theta}) = W_T(x, \tilde{\theta}_x) + \frac{1}{2}z^2 + \frac{1}{2}\tilde{\theta}_\xi^T \Gamma^{-1} \tilde{\theta}_\xi$ . It is obvious that conditions (4.4) and (4.6) are satisfied, (see [48]) and hence, to prove SPA stability, it is enough to show that conditions (4.5)

and (4.7) are satisfied. First, it will be shown that condition (4.5) holds.

$$\delta V_T = \frac{\Delta V_T}{T} = \frac{V_T(k+1) + V_T(k)}{T} = \delta W_T + z\delta z + \tilde{\theta}_\xi^T \Gamma^{-1} \delta \tilde{\theta}_\xi + \frac{T}{2} ((\delta z)^2 + (\delta \tilde{\theta}_\xi)^T \Gamma^{-1} \delta \tilde{\theta}_\xi)$$

$\delta W_T$  can be written, using the mean value theorem, as:

$$\begin{aligned} \delta W_T &= \frac{W_T(x^+, \tilde{\theta}_x^+) - W_T(\bar{x}^+, \tilde{\theta}_x^+) + W_T(\bar{x}^+, \tilde{\theta}_x^+) - W_T(x, \tilde{\theta}_x)}{T} \\ &= \frac{\Delta W_T}{T} + \left( \frac{\partial W_T}{\partial x}(x^\diamond) \right) B(\xi - \alpha_T) \end{aligned} \quad (4.21)$$

where  $x^\diamond = \bar{x}^+ + T\ell_1 B(\xi - \alpha_T)$  and  $\ell_1 \in (0, 1)$ .

Then,  $\delta V_T$  can be written, using (4.18-4.20) and (4.21), as:

$$\begin{aligned} \delta V_T &= \frac{\Delta W_T}{T} + \left( \frac{\partial W_T}{\partial x}(x^\diamond) \right) Bz + z(u - \frac{\alpha_T(x^+, \hat{\theta}_x^+) - \alpha_T(x, \hat{\theta}_x)}{T} + \phi_n^T \theta) \\ &\quad - \tilde{\theta}_\xi^T z \phi_n + \frac{T}{2} ((\delta z)^2 + (\delta \tilde{\theta}_\xi)^T \Gamma^{-1} \delta \tilde{\theta}_\xi) \\ &= \frac{\Delta W_T}{T} + \left( \left( \frac{\partial W_T}{\partial x}(x^\diamond) \right) - \left( \frac{\partial W_T}{\partial x}(\bar{x}_0^+) \right) \right) Bz - cz^2 + z\Lambda \\ &\quad + \frac{T}{2} ((\delta z)^2 + (\delta \tilde{\theta}_\xi)^T \Gamma^{-1} \delta \tilde{\theta}_\xi) \end{aligned} \quad (4.22)$$

$$\text{with } \Lambda = \frac{\alpha_T(x_0^+, \hat{\theta}_x^+) - \alpha_T(x^+, \hat{\theta}_x)}{T} - dz \left| \left( \frac{\partial \alpha_T}{\partial x}(x_0^+, \hat{\theta}_x^+) \right)^T \right|^2.$$

Using the mean value theorem, the term  $\left( \left( \frac{\partial W_T}{\partial x}(x^\diamond) \right) - \left( \frac{\partial W_T}{\partial x}(\bar{x}_0^+) \right) \right) Bz$  can be written as:

$$\left( \left( \frac{\partial W_T}{\partial x}(x^\diamond) \right) - \left( \frac{\partial W_T}{\partial x}(\bar{x}_0^+) \right) \right) Bz \leq T\tilde{M}^3. \quad (4.23)$$

Using the mean value theorem, it can be obtained that

$$\frac{\alpha_T(x_0^+, \hat{\theta}_x^+) - \alpha_T(x^+, \hat{\theta}_x)}{T} = - \left( \frac{\partial \alpha_T}{\partial x}(x^*, \hat{\theta}_x^+) \right) \phi^T \tilde{\theta}_x \quad (4.24)$$

where  $x^* = x_0^+ + T\ell_2 \phi^T \tilde{\theta}_x$  and  $\ell_2 \in (0, 1)$ .

Then, using the mean value theorem and (4.24),  $\Lambda$  can be written as:

$$\begin{aligned} \Lambda &= \left( \left( \frac{\partial \alpha_T}{\partial x}(x_0^+, \hat{\theta}_x^+) \right) - \left( \frac{\partial \alpha_T}{\partial x}(x^*, \hat{\theta}_x^+) \right) - \left( \frac{\partial \alpha_T}{\partial x}(x_0^+, \hat{\theta}_x^+) \right) \right) \phi^T \tilde{\theta}_x - dz \left| \left( \frac{\partial \alpha_T}{\partial x}(x_0^+, \hat{\theta}_x^+) \right)^T \right|^2 \\ &= - \left( \frac{\partial^2 \alpha_T}{\partial x^2}(x^{**}, \hat{\theta}_x^+) \right) \ell_2 T (\phi^T \tilde{\theta}_x)^2 - \left( \frac{\partial \alpha_T}{\partial x}(x_0^+, \hat{\theta}_x^+) \right) \phi^T \tilde{\theta}_x - dz \left| \left( \frac{\partial \alpha_T}{\partial x}(x_0^+, \hat{\theta}_x^+) \right)^T \right|^2 \end{aligned} \quad (4.25)$$

where  $x^{**} = x_0^+ + T\ell_2 \ell_3 \phi^T \tilde{\theta}_x$  and  $\ell_3 \in (0, 1)$ .

Using (4.17), (4.23), (4.25) and Young's inequality,  $\delta V_T$  can be written as:

$$\begin{aligned}
\delta V_T &\leq \frac{\Delta W_T}{T} + |z| \left( \frac{\partial^2 \alpha_T}{\partial x^2}(x^{**}, \hat{\theta}_x^+) \right) \ell_2 T (\phi^T \tilde{\theta}_x)^2 + T \tilde{M}^3 - cz^2 + \frac{1}{4d} |\phi^T \tilde{\theta}_x|^2 \\
&\quad - |\sqrt{d} \left( \frac{\partial \alpha_T}{\partial x}(x_0^+, \hat{\theta}_x^+) \right)^T z + \frac{1}{2\sqrt{d}} \phi^T \tilde{\theta}_x|^2 + \frac{T}{2} ((c|z| + \left| \left( \frac{\partial^2 \alpha_T}{\partial x^2}(x^{**}, \hat{\theta}_x^+) \right) \ell_2 T (\phi^T \tilde{\theta}_x)^2 \right| \\
&\quad + \left| \left( \frac{\partial W_T}{\partial x}(\bar{x}_0^+) \right) B \right| + \left| \left( \frac{\partial \alpha_T}{\partial x}(x_0^+, \hat{\theta}_x^+) \right) \phi^T \tilde{\theta}_x \right| + d \left| \left( \frac{\partial \alpha_T}{\partial x}(x_0^+, \hat{\theta}_x^+) \right)^T \right|^2 |z| + |\phi_n^T \tilde{\theta}_\xi|^2 + |\Gamma| |z \phi_n|^2) \\
&\leq -\tilde{\alpha}_3(|\hat{\eta}|) + \hat{\mu} + T \tilde{M}^3 - cz^2 + \frac{1}{4d} \tilde{M}^4 + \frac{T}{2} (((c+1)\tilde{M} + \tilde{M}^2 + (d+1)\tilde{M}^3)^2 + |\Gamma| \tilde{M}^4) \\
&\leq -\tilde{\alpha}_3(|\hat{\eta}|) - cz^2 + \mu.
\end{aligned}$$

Then, from Proposition 1 in [48], there exists  $\bar{\alpha}_3 \in K_\infty$ , such that  $\Delta V_T \leq -T \bar{\alpha}_3(|\hat{\eta}|) + T\mu$ .

Finally, the following equation shows that condition (4.7) holds,

$$\begin{aligned}
|u| &\leq c|\xi - \alpha_T| + \left| \left( \frac{\partial W_T}{\partial x}(\bar{x}_0^+) \right) \right| |B| + \left| \frac{\Delta \alpha_T}{T} \right| + |\phi_n^T \tilde{\theta}_\xi| + d \left| \left( \frac{\partial \alpha_T}{\partial x}(x_0^+, \hat{\theta}_x^+) \right)^T \right|^2 |z| \\
&\leq (c+1)\tilde{M} + 2\tilde{M}^2 + d\tilde{M}^3 = \bar{M}.
\end{aligned}$$

Consequently, system (4.12)-(4.13) with the controller (4.14) and parameter estimators (4.15) and (4.16) is SPA stable and since the Euler approximate model is one-step consistent with the exact model the same property holds for the exact discretized system (4.10)-(4.11).  $\blacksquare$

Considering the system (4.8)-(4.9), another adaptive backstepping controller design will be presented for the Euler approximate model (4.12)-(4.13) below. Different from the controller in Theorem 4.3.2, the controller design in this case is based on the Euler approximate models of the parameter estimators obtained using the algorithm given in [22] and stated in Chapter 2.

**Hypothesis 4.3.3** [48] *There exist  $\hat{T} > 0$ , a pair  $(\alpha_T, W_T)$  and parameter estimators  $\hat{\theta}_i(k+1)$  for  $i = 1, \dots, n-1$  that are defined for each  $T \in (0, \hat{T})$  and that SPA stabilize the subsystem (4.12) with  $\xi \in \mathbb{R}$  regarded as its control where the parameter estimators  $\hat{\theta}_i(k+1)$  are the Euler approximate models of  $\hat{\theta}_i$  which are obtained during the design of  $\alpha_T$  using the technique given in [22]. Suppose also that the followings hold:*

1. for any  $\tilde{\Delta} > 0$  there exists  $\bar{\Delta} > 0$  such that  $|\phi_i| \leq \bar{\Delta}$  for each  $|x| \leq \tilde{\Delta}$  and  $i = 1, 2, \dots, n$ ,
2.  $\alpha_T$  and  $W_T$  are twice differentiable for any  $T \in (0, \hat{T})$ ;

3. there exists  $\varphi \in \mathcal{K}_\infty$  such that  $|\alpha_T(\tilde{x})| \leq \varphi(|\tilde{x}|)$  for all  $\tilde{x}=[x^T \ \hat{\theta}_x^T]^T \in \mathbb{R}^{(n-1)(p+1)}$  and  $T \in (0, \hat{T})$  where  $x \in \mathbb{R}^{n-1}$  and  $\hat{\theta}_x = [\hat{\theta}_1, \hat{\theta}_2, \dots, \hat{\theta}_{n-1}]$  with  $\hat{\theta}_i \in \mathbb{R}^p$ ;
4. for any  $\tilde{\Delta} > 0$  there exists a pair of strictly positive numbers  $(\tilde{T}, \tilde{M}_1)$  such that  $\max\{|\frac{\partial W_T}{\partial x}|, |\frac{\partial \alpha_T}{\partial x}|, |\frac{\partial^2 \alpha_T}{\partial x^2}|, |\frac{\partial^2 W_T}{\partial x^2}|, |\frac{\partial \beta}{\partial x}|\} \leq \tilde{M}_1$  for each  $T \in (0, \tilde{T})$  and  $|x| \leq \tilde{\Delta}$ ,  $|\tilde{\theta}| \leq \Delta_p$ ,  $|\theta| \leq \bar{\theta}$  where  $\beta = [\beta_1, \beta_2, \dots, \beta_n]$  and  $\tilde{\theta}_x = [\tilde{\theta}_1, \tilde{\theta}_2, \dots, \tilde{\theta}_n]$  with  $\tilde{\theta}_i = \hat{\theta}_i - \theta + \beta_i$ .

The following theorem provides the SPA stabilizing adaptive backstepping controller design. The controller design is based on the Euler approximate model (4.12)-(4.13).

**Theorem 4.3.4** *Assuming that Hypothesis 4.3.3 holds, the system (4.12)-(4.13) is SPA stable with the following controller and the adaptive laws for  $\theta$  and so is the exact discretized system (4.10)-(4.11).*

$$u = -c(\xi - \alpha_T(x, \hat{\theta}_x)) - \left( \frac{\partial W_T}{\partial x}(\bar{x}_0^+) \right) B + \frac{\Delta \alpha_T}{T} - \phi_n^T(\hat{\theta}_n + \beta_n) - d(\xi - \alpha_T(x, \hat{\theta}_x)) \left| \left( \frac{\partial \alpha_T}{\partial x}(x_0^+, \hat{\theta}_x^+) \right)^T \right|^2 \quad (4.26)$$

$$\hat{\theta}_i(k+1) = \hat{\theta}_i - T \sum_{m=1}^i \frac{\partial \beta_i}{\partial x_m}(x_{m+1} + \phi_m^T(\hat{\theta}_i + \beta_i)) \quad (4.27)$$

for  $i = 1, \dots, n$  where  $c, d > 0$ ,  $x_n = \xi$ ,

$$\beta_i(x_1, \dots, x_i) = \gamma_i \int_0^{x_i} \phi_i(x_1, \dots, x_{i-1}, \chi) d\chi + \delta_i(x_i)$$

where  $\gamma_i > 0$  are constants and  $\delta_i(x_i)$  are  $C^{n-i}$  functions with  $\delta_1(x_1) = 0$  and

$$\Delta \alpha_T = \alpha_T(x_0^+, \hat{\theta}_x^+) - \alpha_T(x, \hat{\theta}_x), \quad (4.28)$$

$$x_0^+ = x + T(Ax + B\xi + \phi^T(\beta_x + \hat{\theta}_x)), \quad (4.29)$$

$$\bar{x}_0^+ = x + T(Ax + B\alpha_T + \phi^T(\beta_x + \hat{\theta}_x)) \quad (4.30)$$

with  $\beta_x = [\beta_1, \beta_2, \dots, \beta_{n-1}]$ ,  $\hat{\theta}_x = [\hat{\theta}_1, \hat{\theta}_2, \dots, \hat{\theta}_{n-1}]$  with  $\hat{\theta}_i \in \mathbb{R}^p$ .

**Proof.** Let  $\Delta, \Delta_p, \mu, \hat{\mu} \in \mathbb{R}_{>0}$ ,  $\eta=[x^T \ \xi^T]^T \in \mathbb{R}^n$  with  $|\eta| \leq \Delta$ ,  $\hat{\eta}=[x^T \ \tilde{\theta}_x^T]^T \in \mathbb{R}^{(n-1)(p+1)}$  with  $|\hat{\eta}| \leq \Delta$ ,  $\tilde{\eta}=[x^T \ z \ \tilde{\theta}^T]^T \in \mathbb{R}^{(n+1)p}$ ,  $z = \xi - \alpha_T$  and  $\tilde{\theta} = [\tilde{\theta}_x, \tilde{\theta}_n]$  with  $\tilde{\theta}_x = [\tilde{\theta}_1, \tilde{\theta}_2, \dots, \tilde{\theta}_{n-1}]$ ,  $\tilde{\theta}_i = \hat{\theta}_i - \theta + \beta_i$ ,  $|\tilde{\theta}| \leq \Delta_p$ ,  $|\theta| \leq \bar{\theta}$  and  $c = c_1 + c_2$ . There exists  $\hat{T} > 0$  such that condition (4.5) holds for  $T \in (0, \hat{T})$  with  $\hat{\mu}$  and  $\tilde{\alpha}_3 \in \mathcal{K}_\infty$  considering system (4.12) when  $\xi = \alpha_T$  as input such that

$$\Delta W_T = W_T(\bar{x}^+, \tilde{\theta}_x^+) - W_T(x, \tilde{\theta}_x) \leq -T\tilde{\alpha}_3(|\hat{\eta}|) + T\hat{\mu} \quad (4.31)$$

where  $\bar{x}^+ = x + T(Ax + B\alpha_T + \phi^T \theta)$ . Let  $\Delta_1 = \sup_{|\eta| \leq \Delta, |\theta| \leq \tilde{\theta}, |\hat{\theta}| \leq \Delta_p, T \in (0, \hat{T})} \max\{|x^+|, |x_0^+|, |\bar{x}_0^+|, |\bar{x}^+|\}$  that is well defined since functions  $\alpha_T, \phi_i, \beta_i$  are continuous. Let  $\bar{\Delta} = \max\{\Delta, \Delta_1\}$  generates  $\tilde{T}, \tilde{M}_1$  such that inequality 4 in Hypothesis 4.3.3 holds. Let  $\tilde{M} = \sup_{|\eta| \leq \Delta, |\theta| \leq \tilde{\theta}, |\hat{\theta}| \leq \Delta_p, T \in (0, \hat{T})} \max\{|\xi - \alpha_T|, |Ax + B\xi + \phi^T \theta|, |\phi_i|, \tilde{M}_1, |\tilde{\theta}|, |\hat{\theta}|, |\beta_i|\}$  which is well defined since all the considered functions are continuous over the given compact set. Let  $T^* > 0$  and for each  $T \in (0, T^*)$  let the Lyapunov function  $V_T$  be defined as  $V_T(x, \xi, \tilde{\theta}) = W_T(x, \tilde{\theta}_x) + \frac{1}{2}z^2 + \frac{1}{8c_2\gamma_n}\tilde{\theta}_n^2$ . It is obvious that the conditions (4.4) and (4.6) are satisfied and hence, to prove SPA stability, it is enough to show that conditions (4.5) and (4.7) are satisfied. First, it will be shown that condition (4.5) holds.

Using delta operator, the Euler approximate models of  $\tilde{\theta}_n$  can be written as

$$\delta\tilde{\theta}_n = - \sum_{m=1}^n \frac{\partial\beta_n}{\partial x_m} \phi_m^T \tilde{\theta}_n \quad (4.32)$$

$\delta W_T$  can be written, using the mean value theorem, as:

$$\begin{aligned} \delta W_T &= \frac{W_T(x^+, \tilde{\theta}_x^+) - W_T(\bar{x}^+, \tilde{\theta}_x^+) + W_T(\bar{x}^+, \tilde{\theta}_x^+) - W_T(x, \tilde{\theta}_x)}{T} \\ &= \frac{\Delta W_T}{T} + \left( \frac{\partial W_T}{\partial x}(x^\diamond) \right) B(\xi - \alpha_T) \end{aligned} \quad (4.33)$$

where  $x^\diamond = \bar{x}^+ + T\ell_1 B(\xi - \alpha_T)$  and  $\ell_1 \in (0, 1)$ .

Then, using (4.18), (4.19), (4.32), Remark 6 in [22] and applying the delta operator,  $\delta V_T$  can be written as:

$$\begin{aligned} \delta V_T &= \delta W_T + z\delta z + \frac{1}{4d_1\gamma_n}\tilde{\theta}_n\delta\tilde{\theta}_n + \frac{T}{2}((\delta z)^2 + \frac{1}{4c_2\gamma_n}(\delta\tilde{\theta}_n)^2) \\ &\leq \frac{\Delta W_T}{T} + \left( \frac{\partial W_T}{\partial x}(x^\diamond) \right) Bz + z(u - \frac{\alpha_T(x^+, \hat{\theta}_x^+) - \alpha_T(x, \hat{\theta}_x)}{T} + \phi_n^T \theta) \\ &\quad - \frac{1}{4c_2}(\phi_n^T \tilde{\theta}_n)^2 + \frac{T}{2}((\delta z)^2 + \frac{1}{4c_2\gamma_n}(\delta\tilde{\theta}_n)^2) \\ &\leq \frac{\Delta W_T}{T} - cz^2 + \left( \left( \frac{\partial W_T}{\partial x}(x^\diamond) \right) - \left( \frac{\partial W_T}{\partial x}(\bar{x}_0^+) \right) \right) Bz + z\Lambda \\ &\quad - z\phi_n^T \tilde{\theta}_n - \frac{1}{4c_2}(\phi_n^T \tilde{\theta}_n)^2 + \frac{T}{2}((\delta z)^2 + \frac{1}{4c_2\gamma_n}(\delta\tilde{\theta}_n)^2) \end{aligned}$$

with

$$\Lambda = \frac{\alpha_T(x_0^+, \hat{\theta}_x^+) - \alpha_T(x^+, \hat{\theta}_x)}{T} - dz \left| \left( \frac{\partial \alpha_T}{\partial x}(x_0^+, \hat{\theta}_x^+) \right)^T \right|^2.$$

Using the mean value theorem, the term  $\left( \left( \frac{\partial W_T}{\partial x}(x^\diamond) \right) - \left( \frac{\partial W_T}{\partial x}(\bar{x}_0^+) \right) \right) Bz$  can be written as:

$$\left( \left( \frac{\partial W_T}{\partial x}(x^\diamond) \right) - \left( \frac{\partial W_T}{\partial x}(\bar{x}_0^+) \right) \right) Bz \leq T\tilde{M}^3. \quad (4.34)$$

Using the mean value theorem, it can be obtained that

$$\frac{\alpha_T(x_0^+, \hat{\theta}_x^+) - \alpha_T(x^+, \hat{\theta}_x^+)}{T} = \left( \frac{\partial \alpha_T}{\partial x}(x^*, \hat{\theta}_x^+) \right) \phi^T \tilde{\theta}_x \quad (4.35)$$

where  $x^* = x_0^+ - T \ell_2 \phi^T \tilde{\theta}_x$  and  $\ell_2 \in (0, 1)$ .

Then, using the mean value theorem and (4.35),  $\Lambda$  can be written  $\left( \frac{\partial \alpha_T}{\partial x}(x_0^+, \hat{\theta}_x^+) \right) \phi^T \tilde{\theta}_x$  as:

$$\begin{aligned} \Lambda &= \left( \left( \frac{\partial \alpha_T}{\partial x}(x_0^+, \hat{\theta}_x^+) \right) - \left( \frac{\partial \alpha_T}{\partial x}(x^*, \hat{\theta}_x^+) \right) - \left( \frac{\partial \alpha_T}{\partial x}(x_0^+, \hat{\theta}_x^+) \right) \right) \phi^T \tilde{\theta}_x - dz \left| \left( \frac{\partial \alpha_T}{\partial x}(x_0^+, \hat{\theta}_x^+) \right) \right|^{T^2} \\ &= - \left( \frac{\partial^2 \alpha_T}{\partial x^2}(x^{**}, \hat{\theta}_x^+) \right) \ell_2 T (\phi^T \tilde{\theta}_x)^2 + \left( \frac{\partial \alpha_T}{\partial x}(x_0^+, \hat{\theta}_x^+) \right) \phi^T \tilde{\theta}_x - dz \left| \left( \frac{\partial \alpha_T}{\partial x}(x_0^+, \hat{\theta}_x^+) \right) \right|^{T^2} \end{aligned} \quad (4.36)$$

where  $x^{**} = x_0^+ - T \ell_2 \ell_3 \phi^T \tilde{\theta}_x$  and  $\ell_3 \in (0, 1)$ .

Using (4.31), (4.34), (4.36) and Young's inequality,  $\delta V_T$  can be written as:

$$\begin{aligned} \delta V_T &\leq \frac{\Delta W_T}{T} + |z| \left( \frac{\partial^2 \alpha_T}{\partial x^2}(x^{**}, \hat{\theta}_x^+) \right)^T \ell_2 T (\phi^T \tilde{\theta}_x)^2 + T \tilde{M}^3 - c_1 z^2 + \frac{1}{4d} (\phi^T \tilde{\theta}_x)^2 \\ &\quad - | \sqrt{d} \left( \frac{\partial \alpha_T}{\partial x}(x_0^+, \hat{\theta}_x^+) \right)^T z - \frac{1}{2\sqrt{d}} \phi^T \tilde{\theta}_x |^2 - (\sqrt{c_2} z - \frac{1}{2\sqrt{c_2}} \phi_n^T \tilde{\theta}_n)^2 + \frac{T}{2} (|c| |z| \\ &\quad + \left| \left( \frac{\partial W_T}{\partial x}(\bar{x}_0^+) \right) B \right| + \left| \left( \frac{\partial^2 \alpha_T}{\partial x^2}(x^{**}, \hat{\theta}_x^+) \right) \ell_2 T (\phi^T \tilde{\theta}_x)^2 \right| + \left| \left( \frac{\partial \alpha_T}{\partial x}(x_0^+, \hat{\theta}_x^+) \right) \phi^T \tilde{\theta}_x \right| \\ &\quad + d \left| \left( \frac{\partial \alpha_T}{\partial x}(x_0^+, \hat{\theta}_x^+) \right) \right|^{T^2} |z| + |\phi_n^T \tilde{\theta}_n|^2 + \frac{1}{4c_2 \gamma_n} \left( \sum_{m=1}^n \frac{\partial \beta_n}{\partial x_m} \phi_m^T \|\tilde{\theta}_n\| \right)^2 \\ &\leq -\tilde{\alpha}_3 (|\hat{\eta}|) + \hat{\mu} + T \tilde{M}^3 - c_1 z^2 + \frac{1}{4d} \tilde{M}^4 + \frac{T}{2} ((c+1)\tilde{M} + \tilde{M}^2 + (d+1)\tilde{M}^3)^2 + \frac{1}{4c_2 \gamma_n} \tilde{M}^6 \\ &\leq -\tilde{\alpha}_3 (|\hat{\eta}|) - c_1 z^2 + \mu. \end{aligned}$$

Then, from Proposition 1 in [48], there exists  $\bar{\alpha}_3 \in K_\infty$ , such that

$$\Delta V_T \leq -T \bar{\alpha}_3 (|\hat{\eta}|) + T \mu$$

Finally, the following equation shows that condition (4.7) holds,

$$\begin{aligned} |u| &\leq c|\xi - \alpha_T| + \left| \left( \frac{\partial W_T}{\partial x}(\bar{x}_0^+) \right) \right| |B| + \left| \frac{\Delta \alpha_T}{T} \right| + |\phi_n^T (\hat{\theta}_n + \beta_n)| + d \left| \left( \frac{\partial \alpha_T}{\partial x}(x_0^+, \hat{\theta}_x^+) \right) \right|^{T^2} |z| \\ &\leq (c+1)\tilde{M} + 3\tilde{M}^2 + d_2 \tilde{M}^3 = \bar{M} \end{aligned}$$

Consequently, system (4.12)-(4.13) with the controller (4.26) and parameter estimators (4.27) is SPA stable and since the Euler approximate plant model is one-step consistent with the exact model the same property holds for the exact discretized system (4.10)-(4.11).  $\blacksquare$

## 4.4 Applications

In this section, design methods given in Theorems 4.3.2 and 4.3.4 are applied to two different systems and the simulation results are analyzed.

### 4.4.1 Second-Order System

Consider the following plant

$$\dot{x}_1 = x_2 + x_1^2\theta \quad (4.37)$$

$$\dot{x}_2 = u. \quad (4.38)$$

where  $\theta$  is the unknown parameter.

First, the controller in Theorem 4.3.2 and the emulation of the continuous-time controller designed using the tuning function technique will be applied to the system (4.37)-(4.38).

For the system (4.37)-(4.38), the continuous-time adaptive backstepping controller is designed according to the adaptive backstepping method based on tuning function technique given in [30] as:

$$\dot{\hat{\theta}} = x_1^3 + (c_1x_1 + x_1^2\hat{\theta} + x_2)(2x_1\hat{\theta} + c_1)x_1^2 \quad (4.39)$$

$$u_{ct} = -x_1 - c_2(c_1x_1 + x_1^2\hat{\theta} + x_2) - (2x_1\hat{\theta} + c_1)(x_2 + x_1^2\hat{\theta}) - x_1^2\dot{\hat{\theta}} \quad (4.40)$$

Then, the controller  $u_T$  is obtained using (4.14) in Theorem 4.3.2 with the estimator  $\hat{\theta}(k+1) = \hat{\theta} + Tx_1^3$ ,  $\alpha_T = -c_1x_1 - x_1^2\hat{\theta}$  and the Lyapunov function  $W_T = \frac{1}{2}x_1^2 + \frac{1}{2}\tilde{\theta}^2$ . Simulations have been performed in order to compare performances of controller  $u_T$  and the emulation,  $u_E$  of continuous-time controller (4.39)-(4.40) with different sampling periods and initial conditions. In simulations, following parameters are used:  $c = c_1 = c_2 = 3$  and  $\theta = 1$ .

In the first simulation, the initial conditions are chosen as  $x_1(0) = x_2(0) = 3$  and  $\hat{\theta}(0) = 0$ . Simulation results for the time responses of  $x_1$  and the estimate of  $\theta$  with the sampling period  $T = 0.002$  are given in Figure 4.1. It is shown that both controllers stabilize the system (4.37)-(4.38), but faster with controller  $u_T$ . As the parameter  $d$  increases, the performance of the controller  $u_T$  is faster but further increase results in performance degradation. The controller  $u_T$  cannot stabilize the system for  $d > 14$ .

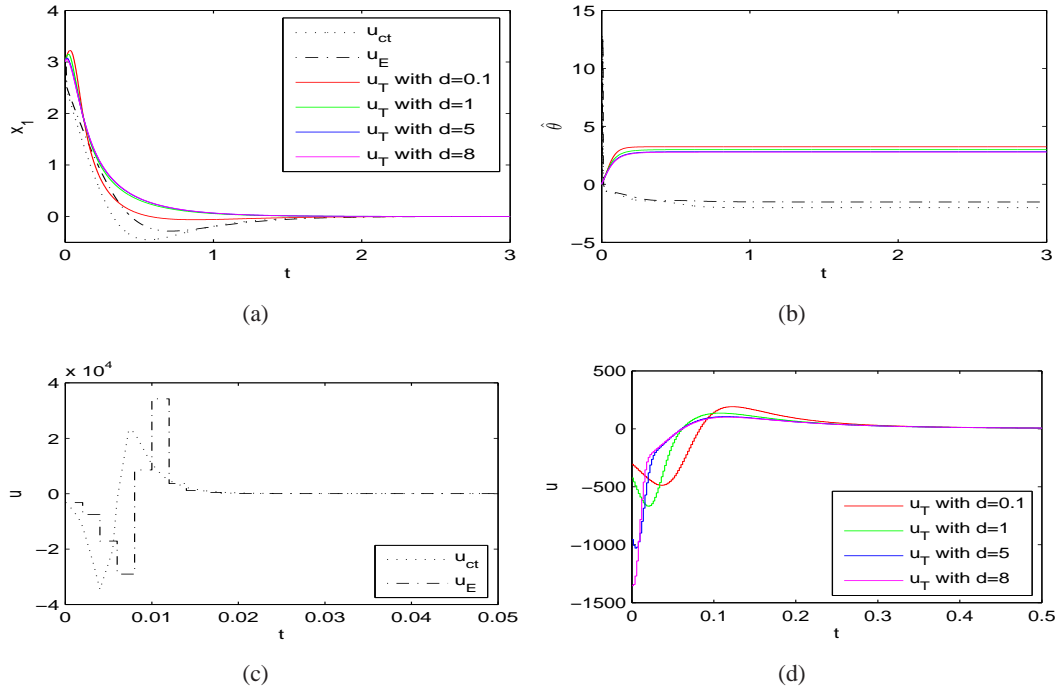


Figure 4.1: Time responses of  $x_1$ ,  $\hat{\theta}$  and  $u$  with  $T = 0.002$ . Dotted line:Continuous-time controller. Dash-dotted line:Emulation controller. Solid line:Designed controller.

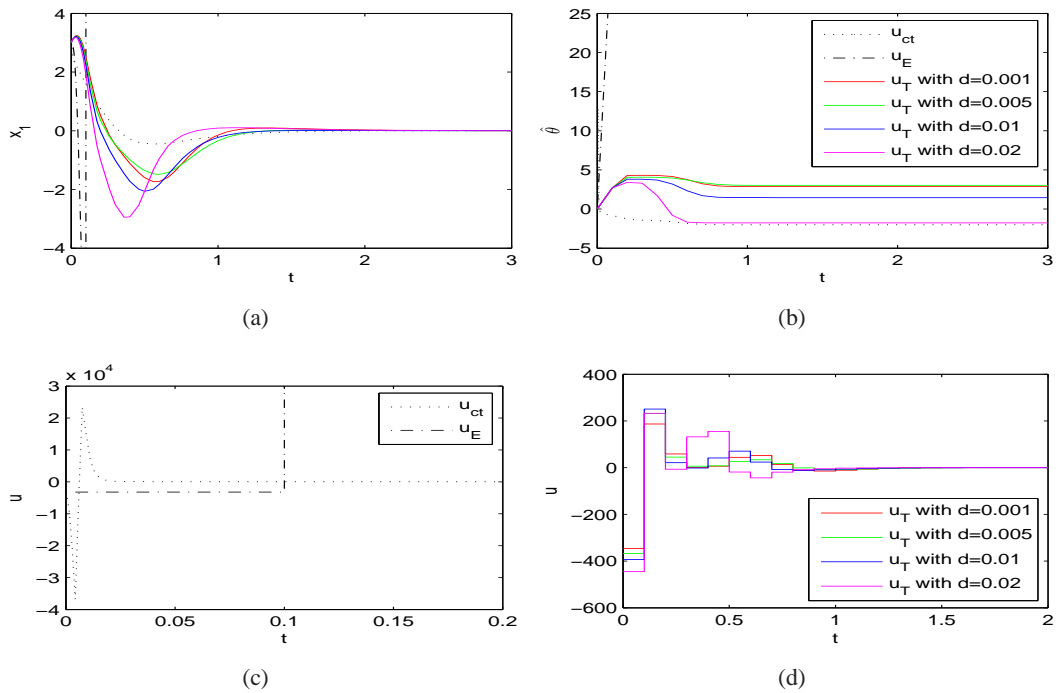


Figure 4.2: Time responses of  $x_1$ ,  $\hat{\theta}$  and  $u$  with  $T = 0.1$ . Dotted line:Continuous-time controller. Dash-dotted line:Emulation controller. Solid line:Designed controller.

Then, the simulation is performed with the initial conditions given above and large sampling period  $T = 0.1$ . Simulation results given in Figure 4.2 show that while the emulation controller  $u_E$  cannot stabilize the system, the controller  $u_T$  works well again. As the parameter  $d$  increases, the controller  $u_T$  yields faster results but further increase results in performance degradation. The controller  $u_T$  cannot stabilize the system for  $d > 0.04$ . While the emulation controller  $u_E$  cannot stabilize the system for  $T > 0.003$  the controller  $u_T$  stabilizes until  $T = 0.1$ .

Finally, the controllers are applied to the system (4.37)-(4.38) with the same sampling period  $T = 0.002$  as in the first simulation and initial conditions doubled  $x_1(0) = x_2(0) = 6$ . Simulation results are shown in Figure 4.3. While the emulation controller  $u_E$  cannot stabilize the system (4.37)-(4.38), the controller  $u_T$  still performs very well, even when compared to the continuous-time controller  $u_{ct}$ .

As can be seen from figures, it can be observed that the parameter estimate  $\hat{\theta}$  from the estimator  $\hat{\theta}(k+1) = \hat{\theta} + Tx_1^3$  designed for the controller  $u_T$  does not converge to the correct value of  $\theta$  although it is bounded. This is expected due to the practical stability, rather than global asymptotic stability property of the error dynamics of the estimator. However, the estimator error of the controller  $u_T$  is smaller than that of the emulation controller  $u_E$ .

Moreover, when the sampling period  $T$  or the initial conditions are increased, the controller  $u_T$  gives faster results for cases where the parameter  $d$  has smaller value.

As can be seen from figures, the control input  $u_T$  is produced with less energy when compared to the control input  $u_E$ . Therefore, the proposed method requires less control effort. Simulation results also show that when the parameter  $d$  is increased, energy of the control input  $u_T$  decreases in general.

Finally, by applying the controllers to the system (4.37)-(4.38) with different initial conditions, domain of attraction (DOA) estimates with the controllers  $u_T$  and  $u_E$  for the sampling period  $T = 0.002$  are given in Figure 4.4. In DOA estimate with the controller  $u_T$ , the parameter  $d$  is chosen as  $d = 0.1$ . As can be seen from figure, DOA for the system with the controller  $u_T$  is much larger than that with the controller  $u_E$ . For different controller parameters and sampling periods, DOA estimate with the controller  $u_T$  may be much larger than the estimate given in figure.

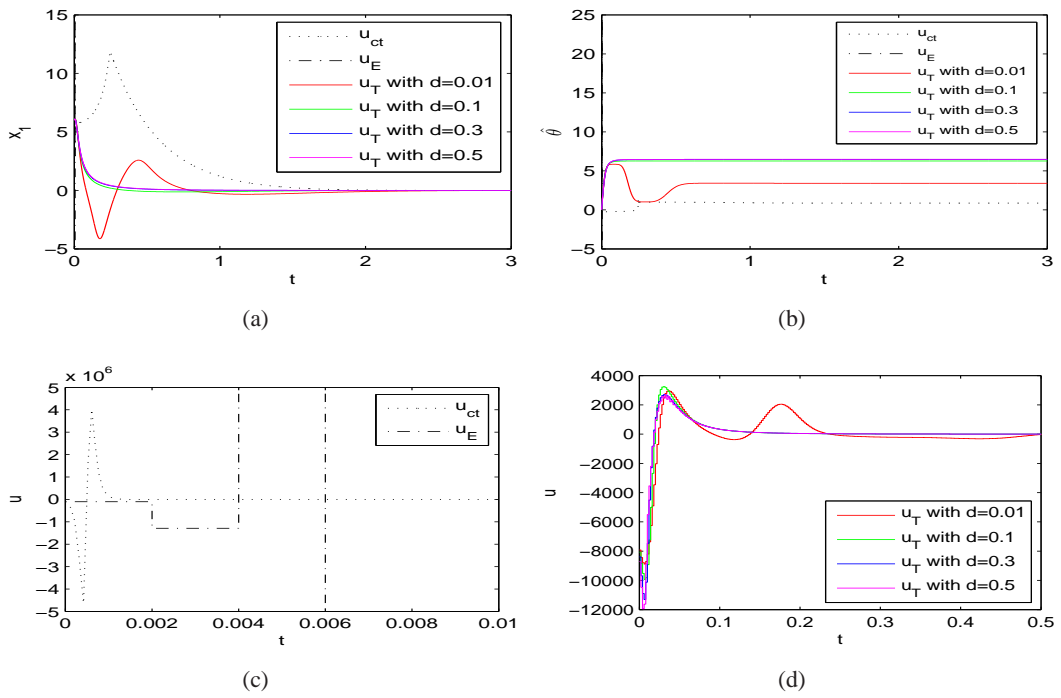


Figure 4.3: Time responses of  $x_1$ ,  $\hat{\theta}$  and  $u$  with the doubled initial conditions  $x_1(0) = x_2(0) = 6$  and  $T = 0.002$ . Dotted line:Continuous-time controller. Dash-dotted line:Emulation controller. Solid line:Designed controller.

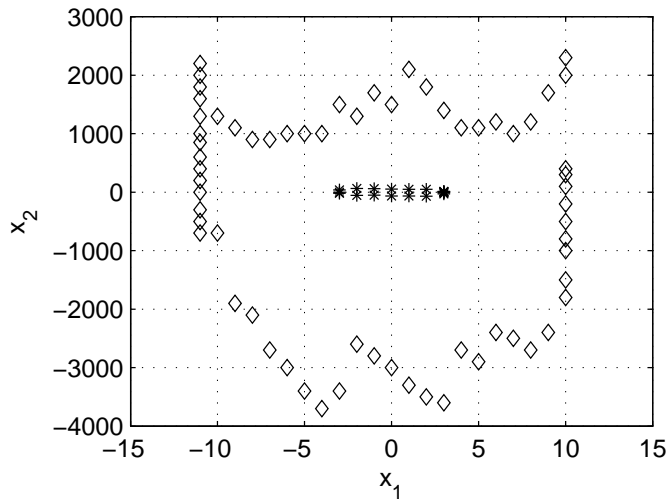


Figure 4.4: Domain of attraction estimates with  $T = 0.002$ . Diamond:controller  $u_T$ . Star:controller  $u_E$ .

Second, the controller in Theorem 4.3.4 and the emulation of the continuous-time controller designed using the technique in [22] will be applied to the system (4.37)-(4.38).

The continuous-time adaptive controller  $u_{ct}$  for system (4.37)-(4.38) is designed using the method given in [22] with  $\beta = \gamma_1 \frac{x_1^3}{3}$ . The controller  $u_T$  is obtained using (4.26) and (4.27) in Theorem 4.3.4 with  $\alpha_T = -(c_1 + \frac{\varepsilon}{2})x_1 - x_1^2(\hat{\theta} + \beta)$ , the Lyapunov function  $W_T = \frac{1}{2}x_1^2 + \frac{1}{(\gamma_1)}z_1^2$  and  $\beta = \gamma_1 \frac{x_1^3}{3}$  where  $z_1 = \hat{\theta} - \theta + \beta$ . Simulations have been performed in order to compare performances of the controller  $u_T$  and the emulation,  $u_E$  of continuous-time controller with different sampling periods and initial conditions. In simulations, following parameters are used:  $c = c_1 = c_2 = 3$ ,  $\varepsilon = 0.0002$ ,  $\gamma_1 = 0.05$  and  $\theta = 1$ .

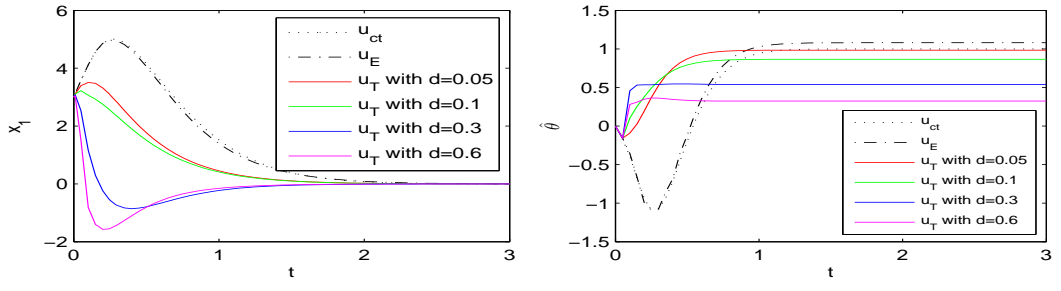
In the first simulation, the initial conditions are chosen as  $x_1(0) = x_2(0) = 3$  and  $\hat{\theta}(0) = 0$ . Simulation results for the time responses of  $x_1$  and the estimate of  $\theta$  with the sampling period  $T = 0.05$  are given in Figure 4.5. It is shown that both controllers stabilize the system (4.37)-(4.38), but faster with the controller  $u_T$ . As the parameter  $d$  increases, the performance of the controller  $u_T$  is faster but further increase results in performance degradation. The controller  $u_T$  cannot stabilize the system for  $d > 0.6$ .

Then, the simulation is performed with the initial conditions given above and large sampling period  $T = 0.15$ . As can be seen from Figure 4.6, the emulation controller  $u_E$  cannot stabilize the system with  $T = 0.15$ . On the other hand, the controller  $u_T$  stabilizes the system successfully. As the parameter  $d$  increases, the performance of the controller  $u_T$  is faster but further increase results in performance degradation. The controller  $u_T$  cannot stabilize the system  $d > 0.02$ . While the emulation controller  $u_E$  cannot stabilize the system for  $T > 0.1$  the controller  $u_T$  stabilizes until  $T = 0.15$ .

Next, the controllers are applied to the system (4.37)-(4.38) with the same sampling period  $T = 0.05$  as in the first simulation and large initial conditions  $x_1(0) = x_2(0) = 5$ . Simulation results are shown in Figure 4.7. Both controllers stabilize the system (4.37)-(4.38), but smoother and faster results are obtained with the controller  $u_T$  again.

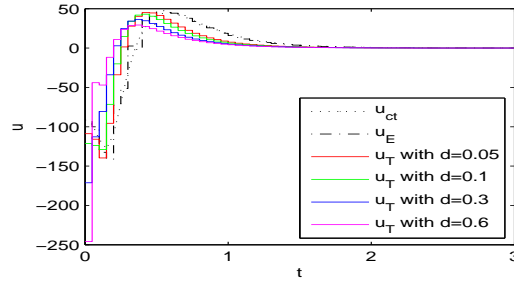
Moreover, when the sampling period  $T$  or the initial conditions are increased, the controller  $u_T$  gives faster results for cases where the parameter  $d$  has smaller value.

Finally, by applying the controllers to the system (4.37)-(4.38) with different initial conditions, domain of attraction (DOA) estimates with the controllers  $u_T$  and  $u_E$  for the sampling



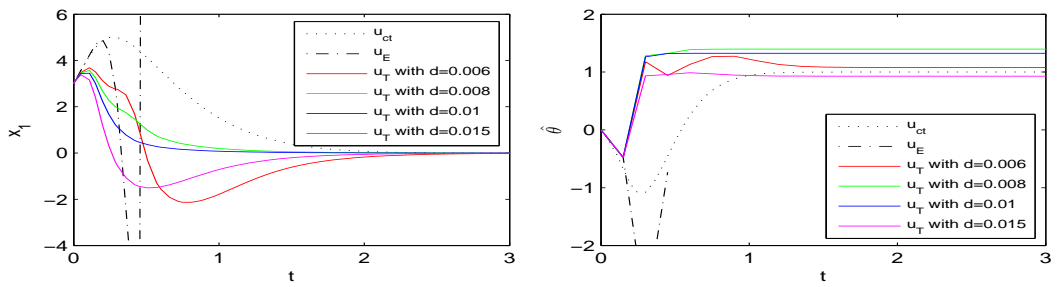
(a)

(b)



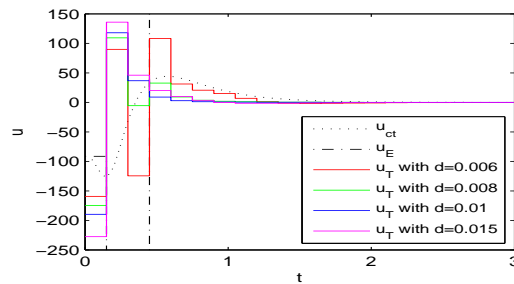
(c)

Figure 4.5: Time responses of  $x_1$ ,  $\hat{\theta}$  and  $u$  with  $T = 0.05$ . Dotted line: Continuous-time controller. Dash-dotted line: Emulation controller. Solid line: Designed controller.



(a)

(b)



(c)

Figure 4.6: Time responses of  $x_1$ ,  $\hat{\theta}$  and  $u$  with  $T = 0.15$ . Dotted line: Continuous-time controller. Dash-dotted line: Emulation controller. Solid line: Designed controller.

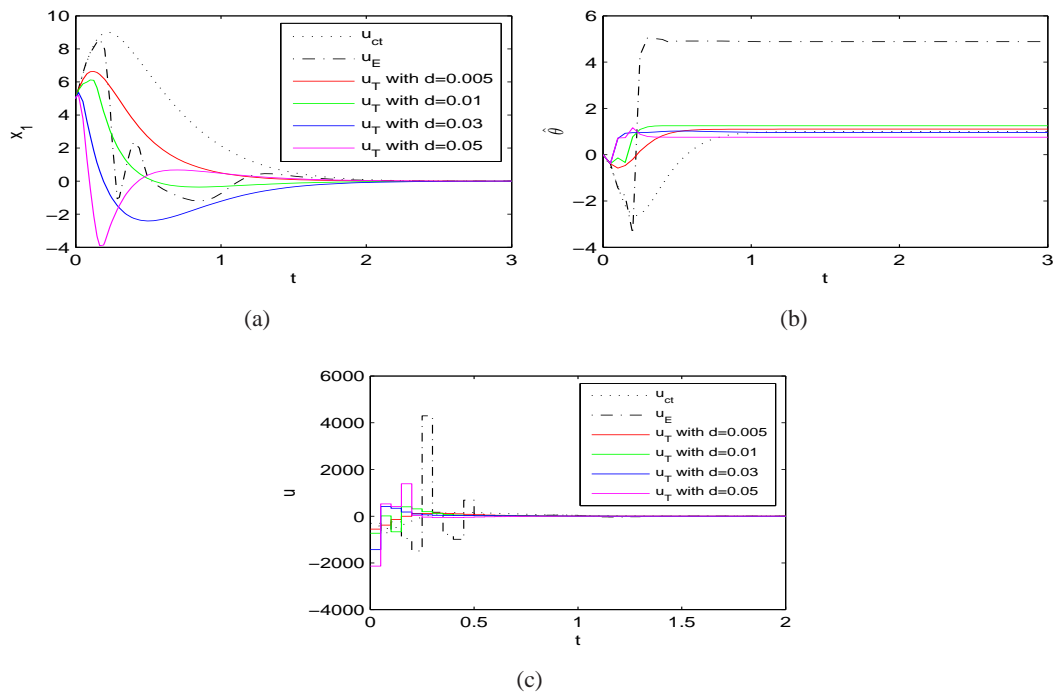


Figure 4.7: Time responses of  $x_1$ ,  $\hat{\theta}$  and  $u$  with the initial conditions  $x_1(0) = x_2(0) = 5$  and  $T = 0.05$ . Dotted line:Continuous-time controller. Dash-dotted line:Emulation controller. Solid line:Designed controller.

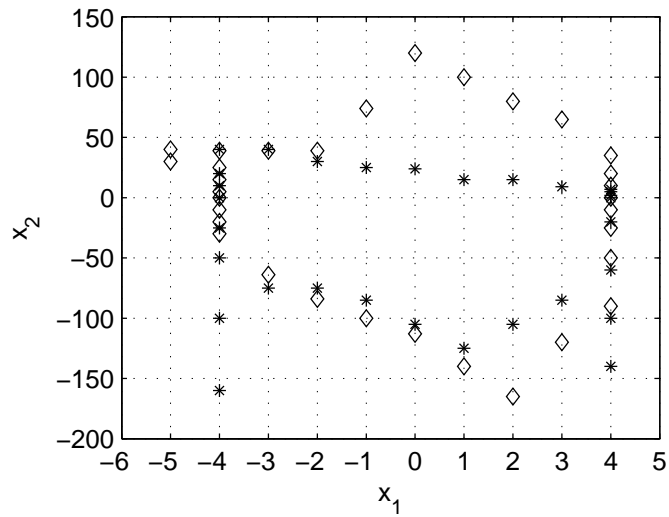


Figure 4.8: Domain of attraction estimates with  $T = 0.05$ . Diamond:controller  $u_T$ . Star:controller  $u_E$ .

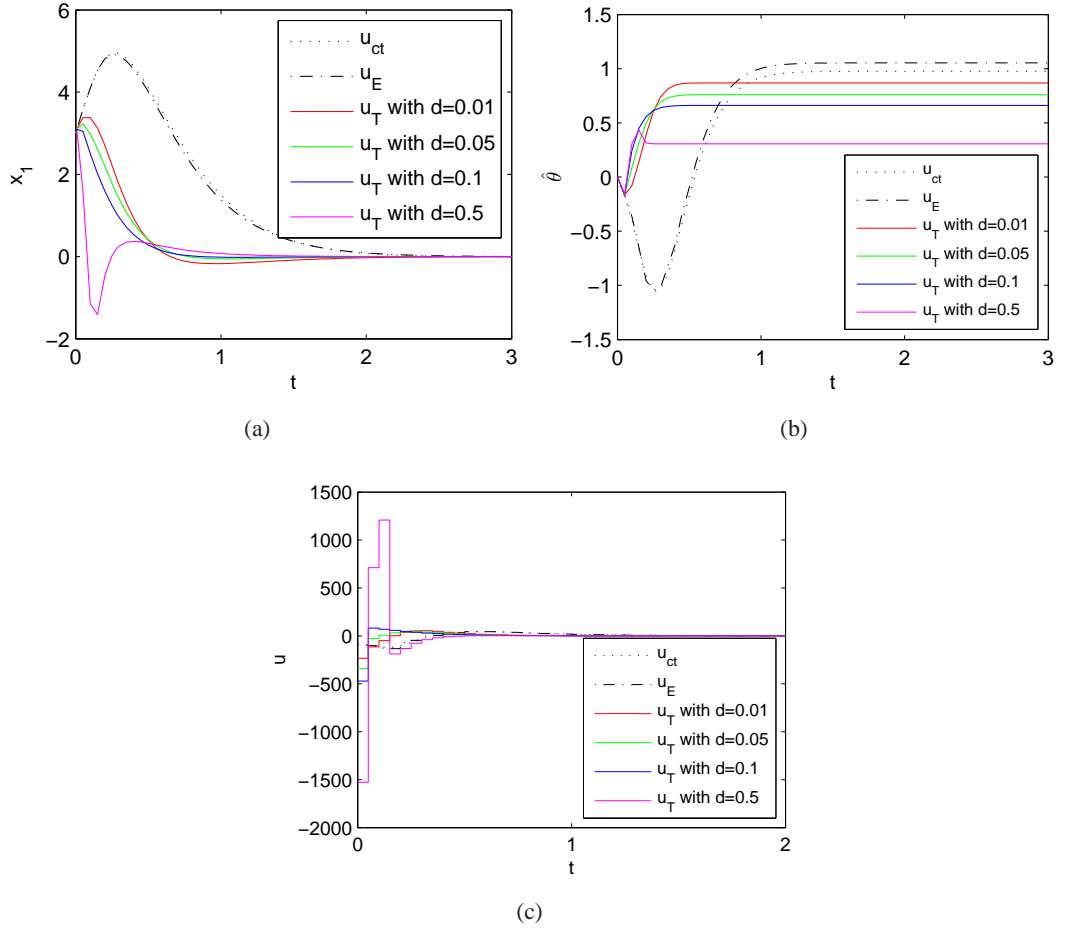


Figure 4.9: Time responses of  $x_1$ ,  $\hat{\theta}$  and  $u$  with  $T = 0.05$ . Dotted line:Continuous-time controller. Dash-dotted line:Emulation controller. Solid line:Designed controller.

period  $T = 0.05$  are given in Figure 4.8. In DOA estimate with the controller  $u_T$ , the parameter  $d$  is chosen as  $d = 0.001$ . As can be seen from figure, DOA for the system with the controller  $u_T$  is slightly larger than that with the controller  $u_E$ . For different controller parameters and sampling periods, much larger DOA estimate may be obtained with the controller  $u_T$  when compared to the estimate given in figure.

In addition, to see the effect of adding a constant to  $\beta$ , all the controllers are designed with  $\beta = \gamma_1(\frac{x_1^3}{3} + \gamma_2)$  and applied to the system (4.37)-(4.38). Simulation results with  $T = 0.05$ ,  $\gamma_2 = 0.5$  and the initial conditions  $x_1(0) = x_2(0) = 3$  can be seen from Figure 4.9. It is shown that results in this case are faster and with smaller overshoots when compared to the results in Figure 4.5.

As can be seen from figures, the control input  $u_T$  is produced with less energy when compared to the control input  $u_E$ . Therefore, the proposed method requires less control effort. Simulation results also show that when the parameter  $d$  is increased, energy of the control input  $u_T$  decreases in general.

Consequently, in this example, the controller designed using Theorem 4.3.4 gives stable results with larger sampling periods when compared to the controller designed using Theorem 4.3.2. Due to the structure of the parameter estimators in Theorem 4.3.4, parameter estimation error of the controller designed using Theorem 4.3.4 is smaller than that of the controller designed using Theorem 4.3.2

#### 4.4.2 Aircraft Wing Rock

In this part, the problem of wing rock elimination in high-performance aircraft is considered. Wing rock is a limit cycle oscillation which appears in the rolling motion of slender delta wings at high angles of attack (see [18, 20] and the references in Section 4.6 of [30]). Consider the following equations which describe the motion of the wing [30, 42]:

$$\dot{x}_1 = x_2 \quad (4.41)$$

$$\dot{x}_2 = x_3 + \phi_2(x_1, x_2)^T \theta \quad (4.42)$$

$$\dot{x}_3 = \frac{1}{\tau} u - \frac{1}{\tau} x_3 \quad (4.43)$$

where the states  $x_1$ ,  $x_2$  and  $x_3$  represent the roll angle, roll rate and aileron deflection angle, respectively,  $\tau$  is the aileron time constant,  $u$  is the control input,  $\theta \in \mathbb{R}^5$  is an unknown constant vector and  $\phi_2(x_1, x_2) = [1, x_1, x_2, |x_1|x_2, |x_2|x_2]^T$ .

First, the controller in Theorem 4.3.2 and the emulation of the continuous-time controller designed using the tuning function technique will be applied to the system (4.41)-(4.43).

For the system (4.41)-(4.43), the continuous-time adaptive backstepping controller is designed using the adaptive backstepping method based on tuning function technique given in [30]. Then, the controller  $u_T$  is obtained using (4.14) in Theorem 4.3.2 with the estimator  $\hat{\theta}(k+1) = \hat{\theta} + T\Gamma(x_2 + c_1 x_1)\phi_2$ ,  $\alpha_T = -c_2(x_2 + c_1 x_1) - \phi_2^T \hat{\theta}$  and the Lyapunov function  $W_T = \frac{1}{2}x_1^2 + \frac{1}{2}(x_2 + c_1 x_1)^2 + \frac{1}{2}\tilde{\theta}^T \Gamma^{-1} \tilde{\theta}$ . Simulations have been performed in order to compare performances of the controller  $u_T$  with the emulation,  $u_E$  of continuous-time controller with

different sampling periods and initial conditions. In simulations, following parameters are used:  $c = c_1 = c_2 = 5$ ,  $\tau = \frac{1}{15}$ ,  $\theta = [0, -26.67, 0.76485, -2.9225, 0]^T$  and  $\Gamma = 0.02I$  where  $I$  is the unit matrix.

In the first simulation, the initial conditions are chosen as  $x_1(0) = 0.4$ ,  $x_2(0) = x_3(0) = 0$  and  $\hat{\theta}(0) = 0$ . Simulation results for the time responses of  $x_1$ ,  $x_2$  and  $x_3$  with  $T = 0.1$  are given in Figure 4.10. It is shown that both controllers stabilize the system (4.41)-(4.43), but faster with controller  $u_T$ . As the parameter  $d$  increases, the performance of the controller  $u_T$  is faster but further increase results in performance degradation. The controller  $u_T$  cannot stabilize the system for  $d > 0.02$ .

Then, the simulation is performed with the initial conditions given above and large sampling period  $T = 0.15$ . Simulation results are given in Figure 4.11. It is shown that the controller  $u_T$  yields faster results when compared to the emulation controller  $u_E$ . As the parameter  $d$  increases, results of the controller  $u_T$  are faster. For  $d > 0.015$ , the controller  $u_T$  cannot stabilize the system (4.41)-(4.43). The emulation controller  $u_E$  yields slower results with larger overshoots when the sampling period  $T$  is increased. While the emulation controller  $u_E$  gives unstable results for  $T > 0.15$ , the controller  $u_T$  can stabilize until  $T = 0.2$ .

Finally, the controllers are applied to the system (4.41)-(4.43) with the same sampling period  $T = 0.1$  as in the first simulation and initial conditions doubled  $x_1(0) = 0.8$ ,  $x_2(0) = x_3(0) = 0$ . Simulation results are shown in Figure 4.12. While the emulation controller cannot stabilize the system (4.41)-(4.43), the controller  $u_T$  still performs very well.

Moreover, when the sampling period  $T$  or the initial conditions are increased, the controller  $u_T$  gives faster results for cases where the parameter  $d$  has smaller value.

Second, the controller in Theorem 4.3.4 and the emulation of the continuous-time controller designed using the technique in [22] will be applied to the system (4.41)-(4.43).

The continuous-time adaptive controller  $u_{ct}$  for system (4.41)-(4.43) is designed using the method given in [22] with  $\beta = \gamma_1 [x_2, x_1 x_2, \frac{1}{2} x_2^2, \frac{1}{2} |x_1| x_2^2, \frac{1}{3} |x_2| x_2^2]^T$ . The Euler based adaptive backstepping control law  $u_T$  is obtained using (4.26) and (4.27) in Theorem 4.3.4 with  $\alpha_T = -(x_1 + (c_2 + \frac{\epsilon}{2})(x_2 + c_1 x_1)) - \phi_2^T (\hat{\theta} + \beta)$ , Lyapunov function  $W_T = \frac{1}{2} x_1^2 + \frac{1}{2} (x_2 + c_1 x_1)^2 + \frac{2}{(\gamma_1 \epsilon)} z_2^T z_2$  and  $\beta = \gamma_1 [x_2, x_1 x_2, \frac{1}{2} x_2^2, \frac{1}{2} |x_1| x_2^2, \frac{1}{3} |x_2| x_2^2]^T$  where  $z_2 = \hat{\theta} - \theta + \beta$ . Simulations have been performed in order to compare performances of the controller  $u_T$  and the emulation,  $u_E$

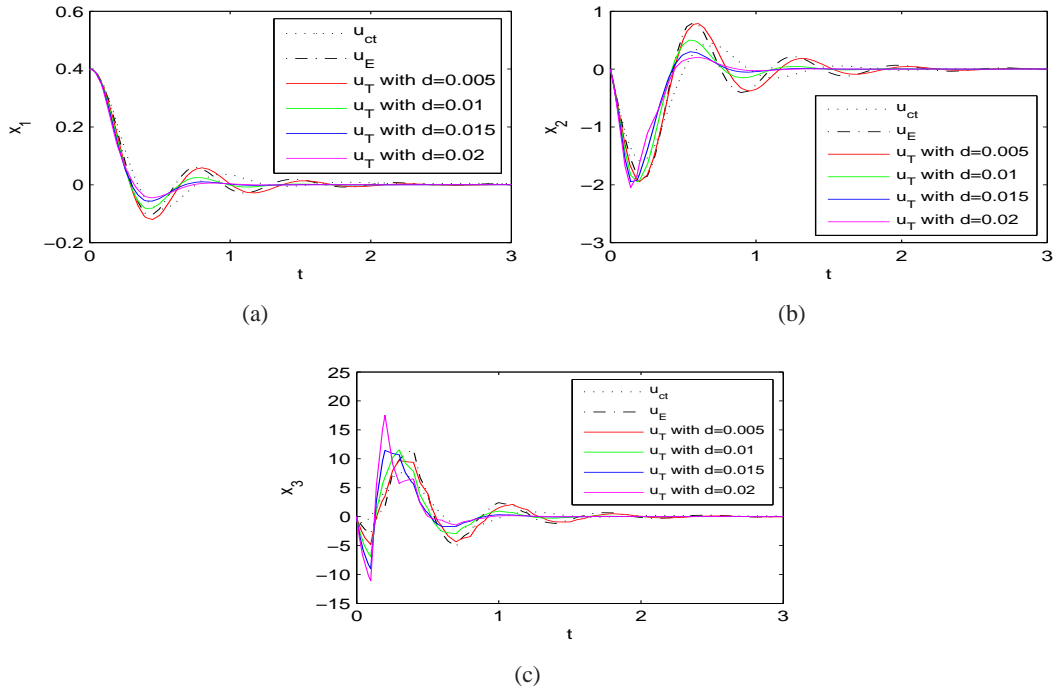


Figure 4.10: Time responses of  $x_1, x_2, x_3$  with  $T = 0.1$ . Dotted line:Continuous-time controller. Dash-dotted line:Emulation controller. Solid line:Designed controller.

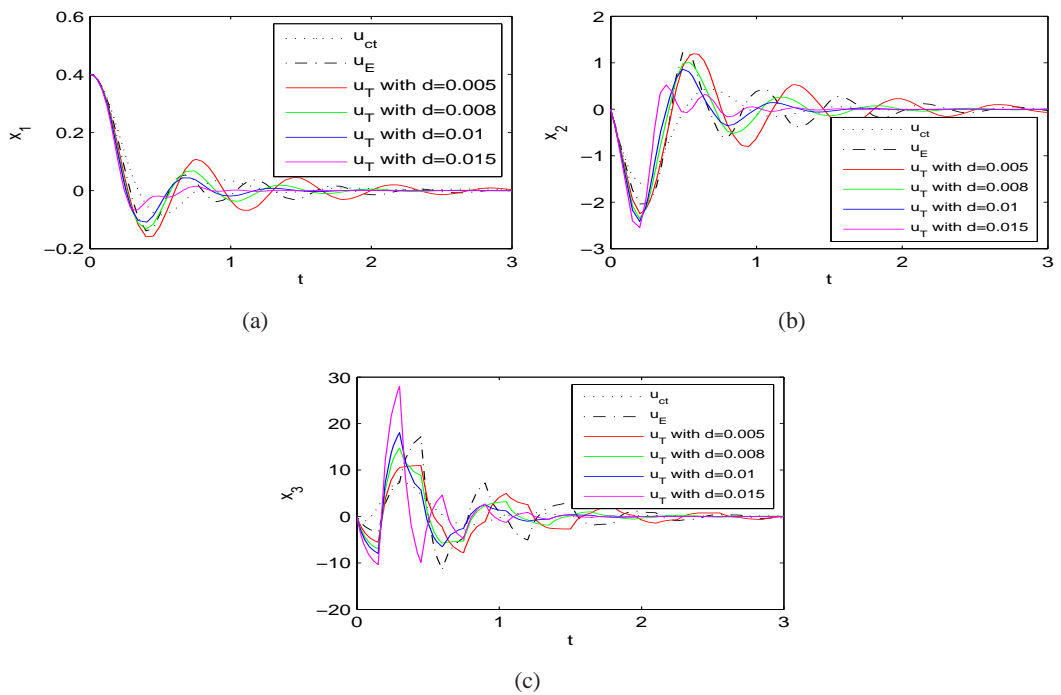


Figure 4.11: Time responses of  $x_1, x_2, x_3$  with  $T = 0.15$ . Dotted line:Continuous-time controller. Dash-dotted line:Emulation controller. Solid line:Designed controller.

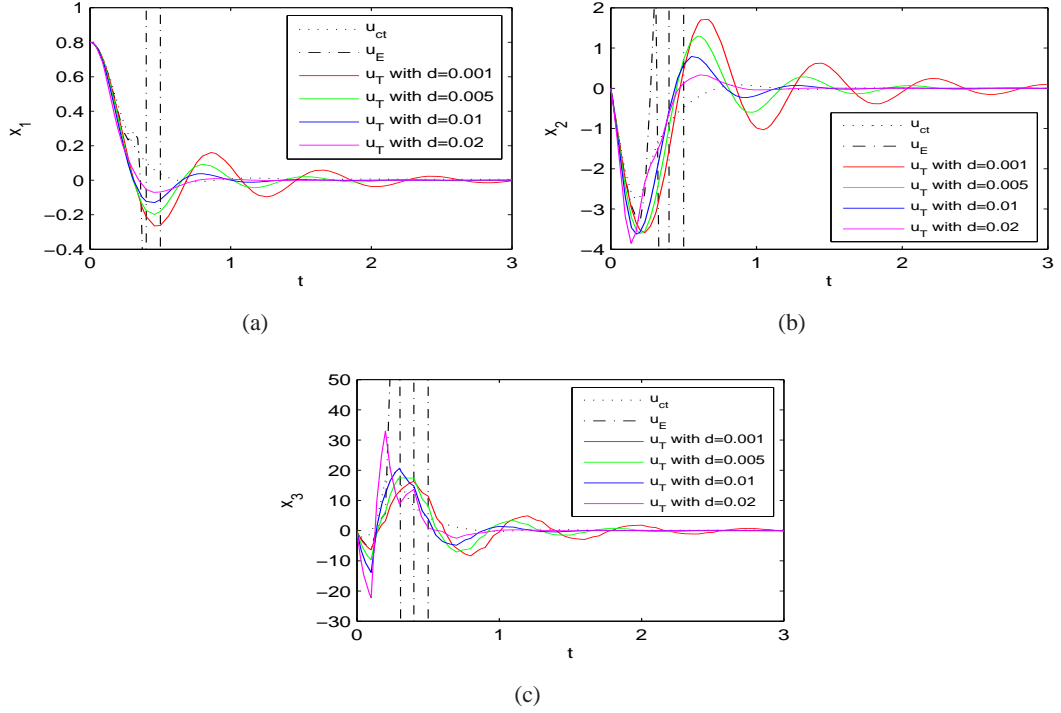


Figure 4.12: Time responses of  $x_1, x_2, x_3$  with the initial conditions doubled and  $T = 0.1$ . Dotted line:Continuous-time controller. Dash-dotted line:Emulation controller. Solid line:Designed controller.

of continuous-time controller. In simulations, following parameters are used:  $c = c_1 = c_2 = 5$ ,  $\varepsilon = 0.0002$ ,  $\gamma_1 = 0.01$ ,  $\tau = \frac{1}{15}$  and  $\theta = [0, -26.67, 0.76485, -2.9225, 0]^T$ .

In the first simulation, the initial conditions are chosen as  $x_1(0) = 0.4, x_2(0) = x_3(0) = 0$  and  $\hat{\theta}(0) = 0$ . Simulation results for the time responses of  $x_1, x_2$  and  $x_3$  with  $T = 0.1$  are given in Figure 4.13. It is shown that both controllers stabilize the system (4.41)-(4.43), but faster with controller  $u_T$ . As the parameter  $d$  increases, the performance of the controller  $u_T$  is faster but further increase results in performance degradation. The controller  $u_T$  cannot stabilize the system for  $d > 0.025$ .

Then, the simulation is performed with the initial conditions given above and large sampling period  $T = 0.15$ . Simulation results are given in Figure 4.14. It is shown that the controller  $u_T$  yields faster results when compared to the emulation controller  $u_E$ . As the parameter  $d$  increases, results of the controller  $u_T$  are faster. For  $d > 0.01$ , the controller  $u_T$  can not stabilize the system (4.41)-(4.43). The emulation controller  $u_E$  yields slower results with larger overshoots when the sampling period  $T$  is increased. Both controllers give unstable

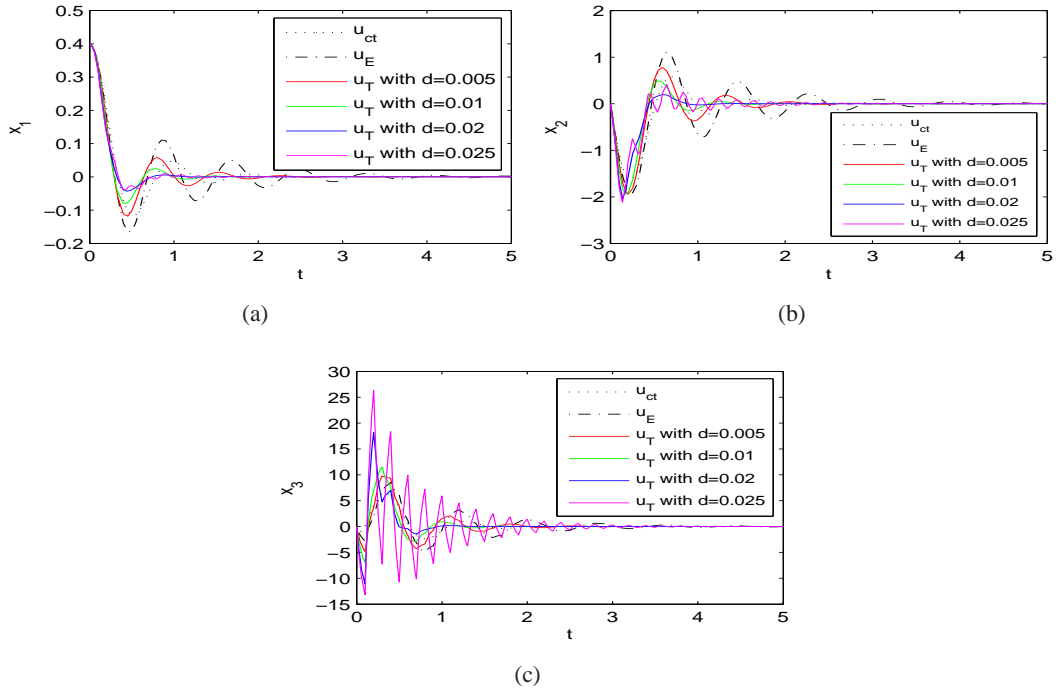


Figure 4.13: Time responses of  $x_1, x_2, x_3$  with  $T = 0.1$ . Dotted line:Continuous-time controller. Dash-dotted line:Emulation controller. Solid line:Designed controller.

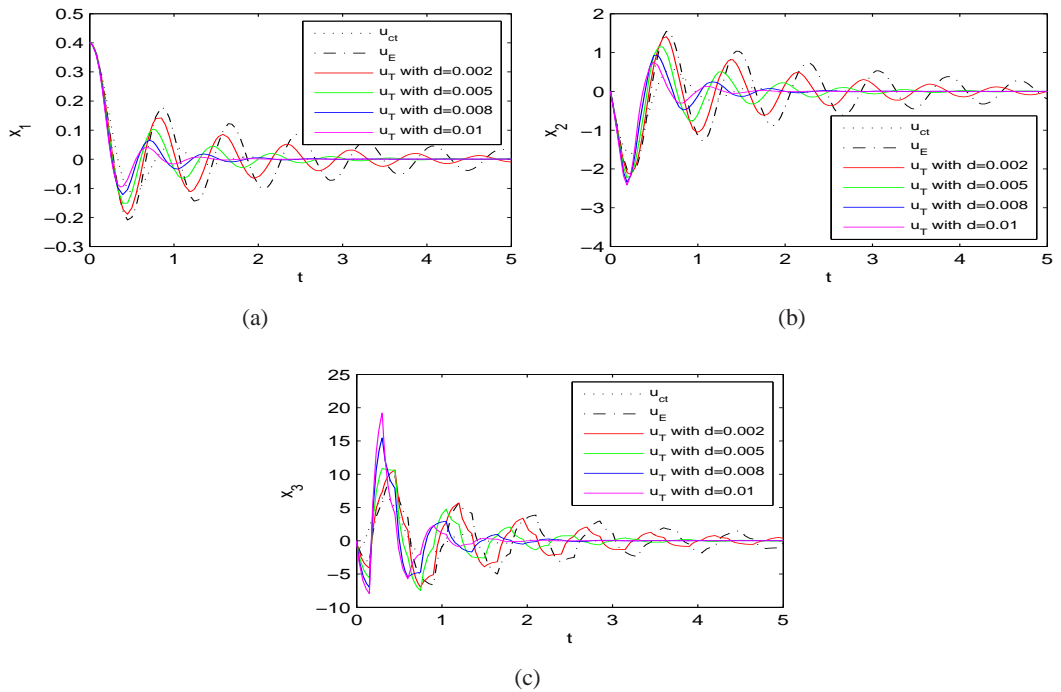


Figure 4.14: Time responses of  $x_1, x_2, x_3$  with  $T = 0.15$ . Dotted line:Continuous-time controller. Dash-dotted line:Emulation controller. Solid line:Designed controller.

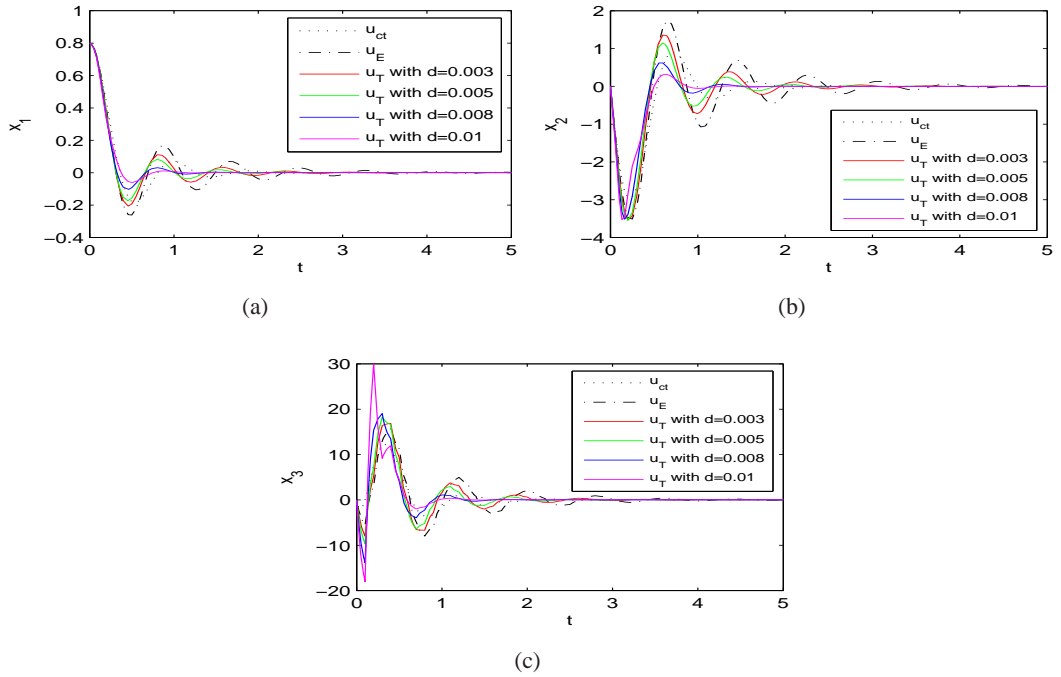


Figure 4.15: Time responses of  $x_1, x_2, x_3$  with the initial conditions  $x_1(0) = 0.8, x_2(0) = x_3(0) = 0$  and  $T = 0.1$ . Dotted line:Continuous-time controller. Dash-dotted line:Emulation controller. Solid line:Designed controller.

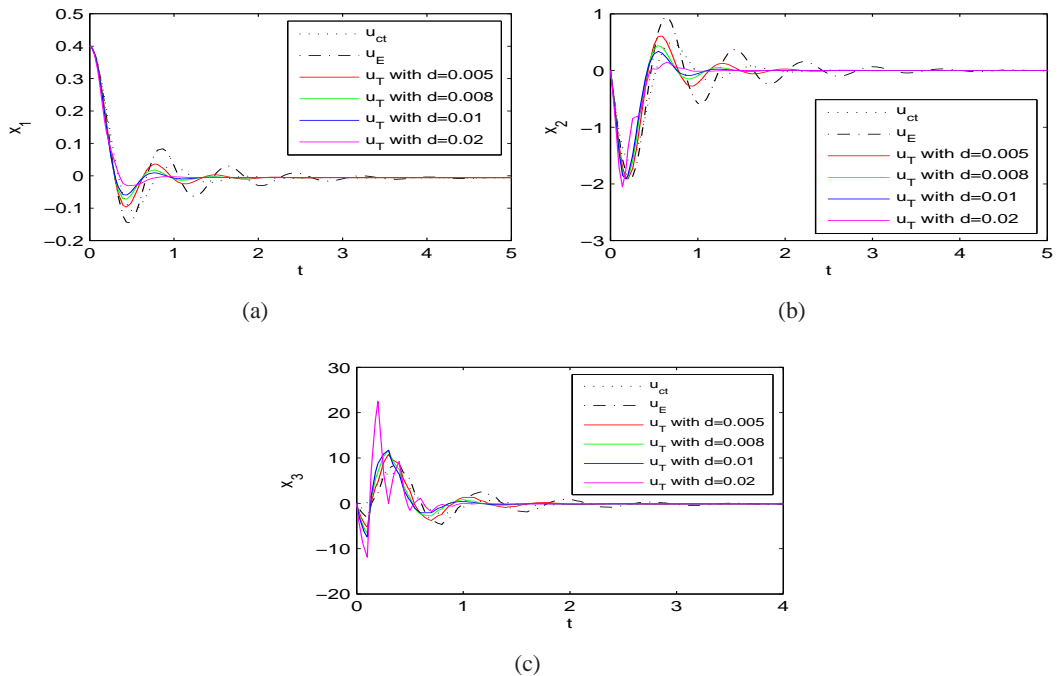


Figure 4.16: Time responses of  $x_1, x_2, x_3$  with  $T = 0.1$ . Dotted line:Continuous-time controller. Dash-dotted line:Emulation controller. Solid line:Designed controller.

results for  $T > 0.2$ .

Next, the controllers are applied to the system (4.41)-(4.43) with the same sampling period  $T = 0.1$  as in the first simulation and initial conditions doubled  $x_1(0) = 0.8, x_2(0) = x_3(0) = 0$ . Simulation results are shown in Figure 4.15. Both controllers stabilize the system (4.41)-(4.43) successfully, but faster with the controller  $u_T$ .

Moreover, when the sampling period  $T$  or the initial conditions are increased, the controller  $u_T$  gives faster results for cases where the parameter  $d$  has smaller value.

Finally, to see the effect of adding a constant to  $\beta$ , all the controllers are designed with  $\beta = \gamma_1 \left( \left[ x_2, x_1 x_2, \frac{1}{2} x_2^2, \frac{1}{2} |x_1| x_2^2, \frac{1}{3} |x_2| x_2^2 \right]^T + \gamma_2 \right)$  by adding a constant to  $\beta$  and applied to the system (4.41)-(4.43). Simulation results with  $T = 0.1, \gamma_2 = 25$  and the initial conditions  $x_1(0) = 0.4, x_2(0) = x_3(0) = 0$  can be seen from Figure 4.16. It is shown that results in this case are faster and with smaller overshoots when compared to the results in Figure 4.13.

## 4.5 Conclusions

In this chapter, the problem of adaptive backstepping controller design has been considered for sampled-data nonlinear systems in strict feedback form using direct discrete-time design. Two adaptive backstepping design methods has been presented based on the Euler approximate model. It has been shown that the designed controllers SPA stabilize the closed-loop sampled-data system based on the framework proposed in [46]. The proposed designs have been applied to two different examples. Their performances are analyzed with simulations.

For the problem considered, the error in parameter estimation behaves as disturbance. It is known that even exponentially decaying disturbances can destabilize the sampled-data nonlinear system. Hence, in this chapter, the controllers were designed to compensate the effects of this factor. As a result of this measure taken, the simulation results have shown that the controllers designed by the proposed methods outperform the emulation controllers.

While sampling is ignored prior to the implementation stage in emulation design, it is considered from the beginning of the design process in direct discrete-time design which is used in this chapter. Therefore, simulation results show that the designed controllers can stabilize the system with larger sampling periods when compared to the emulation controllers.

## CHAPTER 5

# ROBUST BACKSTEPPING FOR THE EULER APPROXIMATE MODEL OF SAMPLED-DATA NONLINEAR SYSTEMS

### 5.1 Introduction

In this chapter, a robust digital controller design method which is the modified version of the method given in [58] is proposed. In this method, the controller is designed by robust backstepping based on the approximate discrete-time model. This controller semiglobally practically asymptotically (SPA) stabilizes the sampled-data nonlinear systems.

Robust controller is designed to deal with model uncertainty and disturbances. Robust backstepping for continuous-time nonlinear systems have been widely studied in the last years (see [14, 15, 39, 16, 29] and references therein). With robust backstepping, [14, 15, 39, 16] achieved global stabilization in the presence of disturbances. The emergence of robust backstepping was described in [29].

On the other hand, the problem of stabilization of sampled-data nonlinear systems in the presence of disturbances has not received much attention. ISS (Input-to-State Stability) and IOSS (Input-to-Output-State Stability) properties are discussed in [45, 36, 35]. In [58], robust backstepping for sampled-data nonlinear system in strict feedback form using Euler approximate model is presented.

In this chapter, the problem of robust backstepping control of sampled-data nonlinear systems in strict feedback form based on the Euler approximate model is considered. The robust backstepping method given in [58] is modified to compensate the effect of difference between disturbance or model uncertainty and their bounds. It is shown that the designed controllers

SPA stabilize the closed-loop sampled-data system based on the framework proposed in [46]. Also a numerical example is given to illustrate the design method.

The chapter is organized as follows. In Section 5.2 preliminaries are given. The main results are stated and proved in Section 5.3. Then, in Section 5.4, an application example is provided to illustrate the design method. Finally, conclusions are presented.

## 5.2 Preliminaries

This section provides technical preliminaries. Common notation and definitions which will be used throughout the chapter are presented. For the sake of clarity and easy reading, some notions and definitions that have been introduced in Chapter 2 are repeated when necessary.

For a function  $d : \mathbb{R}_{\geq 0} \rightarrow \mathbb{R}^n$ ,  $d(k)$  denotes  $\{d(t) : t \in [kT, (k+1)T)\}$ ,  $k \in \mathbb{Z}^+$ ,  $n \in \mathbb{N}$ ,  $T \in \mathbb{R}_{\geq 0}$ .

It is said that  $d \in \mathcal{L}_\infty$  if  $d$  is Lebesgue measurable and there exists  $r \in \mathbb{R}_{\geq 0}$  such that  $\|d\|_\infty =$

$$\sup_{\tau \in \mathbb{R}_{\geq 0}} |d(\tau)| \leq r \text{ and } \|d_f\|_\infty \text{ denotes } \sup_{\tau \in [kT, (k+1)T)} |d(\tau)| \leq r, k \in \mathbb{Z}^+, T \in \mathbb{R}_{\geq 0}.$$

Consider the following continuous-time nonlinear system

$$\dot{x} = f(x(t), u(t), d(t)) \quad (5.1)$$

where  $x \in \mathbb{R}^n$  is the state,  $u \in \mathbb{R}$  is the control input,  $d \in \mathbb{R}^m$  is the exogenous disturbance and Lebesgue measurable and the function  $f$  is locally Lipschitz. The control input  $u$  is realized through a zero-order hold such that  $u(t) = u(kT) := u(k)$ ,  $\forall t \in [kT, (k+1)T)$ ,  $k \in \mathbb{N}$  where  $T > 0$  is the sampling period.

The difference equation corresponding to the exact discrete-time model of (5.1) and its approximate discrete-time model are represented by:

$$x(k+1) = F_T^e(x(k), u(k), d(k)) \quad (5.2)$$

$$x(k+1) = F_T^a(x(k), u(k), d(k)) \quad (5.3)$$

respectively.

To measure the discrepancy between the exact model and the approximate model, one step consistency property, as defined in [46], is used:

**Definition 5.2.1** ([46]) *The family  $F_T^a(x, u)$  is said to be one-step consistent with the exact discrete-time model  $F_T^e(x, u)$  if, for each compact set  $\Omega \subset \mathbb{R}^n \times \mathbb{R}^m$ , there exists a class- $\mathcal{K}$  function  $\rho(\cdot)$  and a constant  $T_0 > 0$  such that,  $|F_T^e(x, u) - F_T^a(x, u)| \leq T\rho(T)$  for all  $(x, u) \in \Omega$  and  $T \in (0, T_0]$ .*

The definition of SPA stability and SPA stability Lyapunov functions can be deduced from [45] as follows.

**Definition 5.2.2** [45] *The family of controllers  $u_T$  SPA stabilizes  $F_T$  if there exists  $\beta \in \mathcal{KL}$  such that for any strictly positive real numbers  $(\Delta_x, \Delta_d, v)$  there exists  $T^* > 0$  such that for each  $T \in (0, T^*)$  the solutions of  $x(k+1) = F_T(x(k), u_T(x(k)), d(k))$  satisfy:  $|x(k, x(0), d)| \leq \beta(|x(0)|, kT) + v$ , for all  $k \geq 0$ , whenever  $|x(0)| \leq \Delta_x$  and  $d \in \mathcal{L}_\infty$  with  $\|d\|_\infty \leq \Delta_d$ .*

**Definition 5.2.3** [45] *Let  $\hat{T} > 0$  be given and for each  $T \in (0, \hat{T})$  let functions  $V_T : \mathbb{R}^n \rightarrow \mathbb{R}_{\geq 0}$  and  $u_T : \mathbb{R}^n \rightarrow \mathbb{R}^m$  be defined. The pair of families  $(u_T, V_T)$  is a SPA stabilizing pair for  $F_T$  if there exist  $\alpha_1, \alpha_2, \alpha_3 \in \mathcal{K}_\infty$  such that for any pair of strictly positive real numbers  $(\Delta_x, \Delta_d, \delta)$  there exists a triple of strictly positive real numbers  $(T^*, L, M)$ , with  $T^* \leq \hat{T}$ , such that for all  $x, z \in \mathbb{R}^n$  with  $\max\{|x|, |z|\} \leq \Delta_x$ , all  $d \in \mathcal{L}_\infty$  with  $\|d\|_\infty \leq \Delta_d$  and  $T \in (0, T^*)$ , and the following conditions are satisfied:*

$$\alpha_1(|x|) \leq V_T(x) \leq \alpha_2(|x|) \quad (5.4)$$

$$V_T(F_T(x, u_T(x), d)) - V_T(x) \leq -T\alpha_3(|x|) + T\delta \quad (5.5)$$

$$|V_T(x) - V_T(z)| \leq L|x - z| \quad (5.6)$$

$$|u_T(x)| \leq M \quad (5.7)$$

If the approximate model (5.3) is consistent with the exact model (5.2), stability properties for (5.2) can be deduced from the stability analysis of (5.3) according to the following theorem which is a direct consequence of Theorem 3.2 in [45].

**Theorem 5.2.4** [45, 50, 51] *If  $(u_T, V_T)$  is a SPA stabilizing pair for  $F_T^a$ , then  $u_T$  stabilizes  $F_T^e$ .*

Then, stability properties of the sampled-data system (5.1) can be deduced from those of exact discretized system under certain conditions [51].

### 5.3 Main Results

In this section, the design of SPA stabilizing robust backstepping controller is presented for sampled-data nonlinear system in strict feedback form. The controller design which is modified version of the method given in [58] is based on the Euler approximate model. The controller is designed to compensate the effect of difference between disturbance or model uncertainty and their bounds. This is the main difference from the controller given in [58].

Consider the following parametric strict feedback system

$$\dot{\eta} = f(\eta) + g(\eta)\xi + d_1 \quad (5.8)$$

$$\dot{\xi} = \alpha(\eta, \xi) + \beta(\eta)u + d_2 \quad (5.9)$$

where  $x = [\eta^T \ \xi^T]^T$  with  $\eta \in \mathbb{R}^n$  and  $\xi \in \mathbb{R}^m$  is the state vector,  $f(0) = 0$ ,  $f, g, \alpha$  are differentiable sufficiently many times,  $\beta(\eta) \neq 0, \forall \eta$ , the control input  $u \in \mathbb{R}^m$  is realized through a zero order hold such that  $u(t) = u(kT) := u(k), \forall t \in [kT, (k+1)T), k \in \mathbb{N}$  and the state measurements  $\eta(k) := \eta(kT)$  and  $\xi(k) := \xi(kT)$  are available at sampling instants  $kT, k \in \mathbb{N}$  where  $T > 0$  is the sampling period and  $d = [d_1^T \ d_2^T]^T \in \mathcal{L}_\infty$  is unknown and models the uncertainties or perturbations acting on the system.

In this section some information on the uncertain terms is supposed to be available. The following type of hypothesis is given in [58] which is standard when dealing with perturbed strict feedback systems [15].

**Hypothesis 5.3.1** [58] *1.  $d_1 \in C^1([t_0, \infty) \times \mathbb{R}^{n+m}, \mathbb{R}^n)$  and  $d_2 \in C^1([t_0, \infty) \times \mathbb{R}^{n+m}, \mathbb{R}^m)$ .  
2. There exist known functions  $\rho_1 \in C^1(\mathbb{R}^n, \mathbb{R}_{\geq 0})$  with  $\rho_1(0) = 0, \rho_2 \in C^1([t_0, \infty) \times \mathbb{R}^{n+m}, \mathbb{R}^m)$  such that, for all  $(t, x) \in [t_0, \infty) \times \mathbb{R}^{n+m} : |d_1(t, x)| \leq \rho_1(\eta)$  and  $|d_2(t, x)| \leq \rho_2(x)$ .*

Suppose that family of exact discrete-time models of the system (5.8)-(5.9) is

$$\eta(k+1) = F_{\eta, T}^e(\eta, \xi, u, d_1) \quad (5.10)$$

$$\xi(k+1) = F_{\xi, T}^e(\eta, \xi, u, d_2). \quad (5.11)$$

Since the exact discrete-time models (5.10)-(5.11) are not available in general, approximate discrete-time models are used. Also condition (1) in Hypothesis 5.3.1 will be assumed to hold.

Hence the following Euler approximate discrete-time model of (5.8)-(5.9) is considered.

$$\eta(k+1) = \eta + T(f(\eta) + g(\eta)\xi + d_1) \quad (5.12)$$

$$\xi(k+1) = \xi + T(\alpha(\eta, \xi) + \beta(\eta)u + d_2) \quad (5.13)$$

The following functions are defined in [58] are going to be used in the sequel.

**Definition 5.3.2** [58] For any  $\varepsilon, T \in \mathbb{R}_{\geq 0}, n \in \mathbb{Z}^+$ , the function  $\text{sat}_{T\varepsilon, n}(z) : \mathbb{R}^n \rightarrow \mathbb{R}^n$  is defined as, for  $z = [z_1, \dots, z_n]^T \in \mathbb{R}^n$  :  $\text{sat}_{T\varepsilon, n}(z) = [\text{sat}_{T\varepsilon, 1}(z_1), \dots, \text{sat}_{T\varepsilon, 1}(z_n)]^T$  with

$$\text{sat}_{T\varepsilon, 1}(z_i) = \begin{cases} \text{sign}(z_i), & \text{if } |z_i| \geq \frac{T\varepsilon}{n} \\ p(z_i), & \text{otherwise} \end{cases}$$

where  $p : \mathbb{R} \mapsto \mathbb{R}, p(0) = 0$  and  $|p| \leq 1$  over  $[-\frac{T\varepsilon}{n}, \frac{T\varepsilon}{n}]$ ,  $yp(y) = 0$  for  $y \in [-\frac{T\varepsilon}{n}, \frac{T\varepsilon}{n}]$ , is such that function  $\text{sat}_{T\varepsilon, n}$  is  $C^1$  over  $\mathbb{R}^n$ .

**Hypothesis 5.3.3** [48] There exist  $\hat{T} > 0$  and a pair  $(\phi_T, W_T)$  that is defined for each  $T \in (0, \hat{T})$  and that is a SPA stabilizing pair for the subsystem (5.12) with  $\xi \in \mathbb{R}^m$  regarded as its control. Suppose also that the followings hold:

1.  $\phi_T$  and  $W_T$  are twice differentiable for any  $T \in (0, \hat{T})$ ;
2. there exists  $\varphi \in \mathcal{K}_\infty$  such that  $|\phi_T(\eta)| \leq \varphi(|\eta|)$  for all  $\eta \in \mathbb{R}^n, T \in (0, \hat{T})$ ;
3. for any  $\tilde{\Delta} > 0$  there exists a pair of strictly positive numbers  $(\tilde{T}, \tilde{M}_1)$  such that  $\max\{|\frac{\partial W_T}{\partial \eta}|, |\frac{\partial \phi_T}{\partial \eta}|, |\frac{\partial^2 \phi_T}{\partial \eta^2}|, |\frac{\partial^2 W_T}{\partial \eta^2}|\} \leq \tilde{M}_1$  for each  $T \in (0, \tilde{T})$  and  $|\eta| \leq \tilde{\Delta}$ .

The following theorem provides the SPA stabilizing robust backstepping controller design based on the Euler approximate discrete-time model of sampled-data nonlinear system.

**Theorem 5.3.4** Assuming that Hypotheses 5.3.1 and 5.3.3 hold, the system (5.12)-(5.13) is SPA stable with the following controller and so is the exact discretized system (5.10)-(5.11)

$$\begin{aligned} u = & \beta^{-1}(\eta)(-c(\xi - \phi_T(\eta)) - g(\eta)^T (\frac{\partial W_T}{\partial \eta}(\bar{\eta}_0^+))^T + \frac{\Delta \phi_T}{T} - \alpha(\eta, \xi) \\ & - \kappa \left| \left( \frac{\partial \phi_T}{\partial \eta}(\eta_0^+) \right) \right|^2 - \left( \frac{\partial \phi_T}{\partial \eta}(\eta_0^+) \right) \hat{d}_1 + \hat{d}_2 \end{aligned} \quad (5.14)$$

where  $c, \kappa > 0, \Delta \phi_T = \phi_T(\eta_0^+) - \phi_T(\eta), \eta_0^+ = \eta + T(f(\eta) + g(\eta)\xi), \bar{\eta}_0^+ = \eta + T(f(\eta) + g(\eta)\phi_T), \hat{d}_1 = \rho_1 \text{sat}_{T\varepsilon, n} \left\{ (\xi - \phi_T(\eta)) \frac{\partial \phi_T}{\partial \eta}(\eta_0^+) \right\}$  and  $\hat{d}_2 = -\rho_2 \text{sat}_{T\varepsilon, n} ((\xi - \phi_T(\eta)))$  with  $\varepsilon \in \mathbb{R}_{\geq 0}$ .

**Proof.** Let  $\Delta, \mu, \hat{\mu}, \varepsilon \in \mathbb{R}_{>0}$ ,  $\tilde{x} = [\eta^T \ z^T]^T \in \mathbb{R}^{n+m}$  with  $|\tilde{x}| \leq \Delta$  and  $z = \xi - \phi_T$ . Consider the system (5.12). There exists  $\hat{T} > 0$  such that condition (5.5) holds for  $T \in (0, \hat{T})$  with  $\tilde{\alpha}_3 \in K_\infty$  and  $\hat{\mu}$  when  $\xi = \phi_T$  as input such that,

$$\Delta W_T = W_T(\bar{\eta}^+) - W_T(\eta) \leq -T\tilde{\alpha}_3(|\eta|) + T\hat{\mu} \quad (5.15)$$

where  $\bar{\eta}^+ = \eta + T(f(\eta) + g(\eta)\phi_T + d_1)$ . Then, using delta operator the approximate discrete-time models (5.12)-(5.13) can be written as:

$$\delta\eta = f(\eta) + g(\eta)(z + \phi_T) + d_1 \quad (5.16)$$

$$\delta z = \alpha(\eta, \xi) + \beta(\eta)u - \frac{\phi_T(\eta^+) - \phi_T(\eta)}{T} + d_2 \quad (5.17)$$

with  $\eta^+ = \eta + T(f(\eta) + g(\eta)\xi + d_1)$ . Let  $\Delta_1 = \sup_{|\tilde{x}| \leq \Delta, T \in (0, \hat{T})} \max\{|\eta^+|, |\eta_0^+|, |\bar{\eta}_0^+|, |\bar{\eta}^+|\}$  that is well defined since functions  $f, g, \phi_T, d_1$  are continuous. Let  $\bar{\Delta} = \max\{\Delta, \Delta_1\}$  generates  $\tilde{T}, \tilde{M}_1$  such that inequality 3 in Hypothesis 5.3.3 holds. Let  $\tilde{M} = \sup_{|\tilde{x}| \leq \Delta, T \in (0, \hat{T})} \max\{|\xi - \phi_T|, |f(\eta) + g(\eta)\xi|, |g(\eta)|, \tilde{M}_1, |\beta(\eta)|, |\alpha(\eta, \xi)|, \rho_1, \rho_2\}$  which is well defined since all the considered functions are continuous over the given compact set. Let  $T^* > 0$  and for each  $T \in (0, T^*)$  let the Lyapunov function  $V_T$  be defined as  $V_T(\eta, \xi) = W_T(\eta) + \frac{1}{2}z^T z$ . It is obvious that conditions (5.4) and (5.6) are satisfied, (see [48]) and hence, to prove SPA stability, it is enough to show that conditions (5.5) and (5.7) are satisfied. First, it will be shown that condition (5.5) holds:

$$\delta V_T = \frac{\Delta V_T}{T} = \frac{V_T(k+1) - V_T(k)}{T} = \delta W_T + z^T \delta z + \frac{T}{2}((\delta z)^T \delta z).$$

$\delta W_T$  can be written, using the mean value theorem, as:

$$\begin{aligned} \delta W_T &= \frac{W_T(\eta^+) - W_T(\bar{\eta}^+) + W_T(\bar{\eta}^+) - W_T(\eta)}{T} \\ &= \frac{\Delta W_T}{T} + (\xi - \phi_T(\eta))^T g(\eta)^T \left( \frac{\partial W_T}{\partial \eta}(\eta^\diamond) \right)^T \end{aligned} \quad (5.18)$$

where  $\eta^\diamond = \bar{\eta}^+ + T\theta_1 g(\eta)(\xi - \phi_T(\eta))$  and  $\theta_1 \in (0, 1)$ .

Then,  $\delta V_T$  can be written, using (5.16), (5.17) and (5.18), as:

$$\begin{aligned} \delta V_T &\leq \frac{\Delta W_T}{T} - cz^T z + z^T (\Lambda + d_2 + \hat{d}_2) + \frac{T}{2}((\delta z)^T \delta z) \\ &\quad + z^T g(\eta)^T \left( \left( \frac{\partial W_T}{\partial \eta}(\eta^\diamond) \right)^T - \left( \frac{\partial W_T}{\partial \eta}(\bar{\eta}_0^+) \right)^T \right) \end{aligned}$$

with  $\Lambda = \frac{\phi_T(\eta_0^+) - \phi_T(\eta^+)}{T} - \kappa \left| \left( \frac{\partial \phi_T}{\partial \eta}(\eta_0^+) \right) \right|^2 - \left( \frac{\partial \phi_T}{\partial \eta}(\eta_0^+) \right) \hat{d}_1$ .

Using the mean value theorem, the term  $z^T g(\eta)^T \left( \left( \frac{\partial W_T}{\partial \eta}(\eta^\diamond) \right)^T - \left( \frac{\partial W_T}{\partial \eta}(\bar{\eta}_0^+) \right)^T \right)$  can be written as:

$$z^T g(\eta)^T \left( \left( \frac{\partial W_T}{\partial \eta}(\eta^\diamond) \right)^T - \left( \frac{\partial W_T}{\partial \eta}(\bar{\eta}_0^+) \right)^T \right) \leq T \tilde{M}^4. \quad (5.19)$$

Using the mean value theorem, it can be obtained that

$$\frac{\phi_T(\eta_0^+) - \phi_T(\eta^+)}{T} = - \left( \frac{\partial \phi_T}{\partial \eta}(\eta^*) \right) d_1 \quad (5.20)$$

where  $\eta^* = \eta_0^+ + T \ell_1 d_1$  and  $\ell_1 \in (0, 1)$ .

Then, using the differential mean value theorem (DMVT) and (5.20),  $\Lambda$  can be written,  $\left( \frac{\partial \phi_T}{\partial \eta}(\eta_0^+) \right) d_1$  as:

$$\begin{aligned} \Lambda &= \left( \left( \frac{\partial \phi_T}{\partial \eta}(\eta_0^+) \right) - \left( \frac{\partial \phi_T}{\partial \eta}(\eta^*) \right) - \left( \frac{\partial \phi_T}{\partial \eta}(\eta_0^+) \right) \right) d_1 - \left( \frac{\partial \phi_T}{\partial \eta}(\eta_0^+) \right) \hat{d}_1 - \kappa \left| \left( \frac{\partial \phi_T}{\partial \eta}(\eta_0^+) \right) \right|^2 \\ &= - \left( \frac{\partial^2 \phi_T}{\partial \eta^2}(\eta^{**}) \right) T \ell_1 \Omega d_1 - \left( \frac{\partial \phi_T}{\partial \eta}(\eta_0^+) \right) (d_1 + \hat{d}_1) - \kappa \left| \left( \frac{\partial \phi_T}{\partial \eta}(\eta_0^+) \right) \right|^2 \end{aligned} \quad (5.21)$$

where  $\Omega = [\Omega_1^T, \Omega_2^T, \dots, \Omega_n^T]^T$ ,  $\Omega_i = d_i$ ,  $\eta^{**} = \eta_0^+ + T \ell_1 \ell_2 d_1$  and  $\ell_2 \in (0, 1)$ .

Using Definition 5.3.2, it can be shown that the following inequalities hold:

$$|z^T (-d_1 - \hat{d}_1)| \leq 2T \tilde{M} \varepsilon \quad (5.22)$$

$$|z^T (d_2 + \hat{d}_2)| \leq 2T \tilde{M} \varepsilon. \quad (5.23)$$

Then, using (5.15), (5.19), (5.21)-(5.23) and Young's inequality,  $\delta V_T$  can be written as:

$$\begin{aligned} \delta V_T &\leq \frac{\Delta W_T}{T} + T \tilde{M}^4 + |z^T \frac{\partial^2 \phi_T}{\partial \eta^2}(\eta^{**}) T \ell_1 \Omega| \rho_1(\eta) - c z^T z + |z^T (d_2 + \hat{d}_2)| + \frac{1}{4\kappa} |z^T (-d_1 - \hat{d}_1)|^2 \\ &\quad - (\sqrt{\kappa} \left| \left( \frac{\partial \phi_T}{\partial \eta}(\eta_0^+) \right) \right| + \frac{1}{2\sqrt{\kappa}} |z^T (-d_1 - \hat{d}_1)|)^2 + \frac{T}{2} (c|z| - \left| \left( \frac{\partial^2 \phi_T}{\partial \eta^2}(\eta^{**}) \right) \right| \ell_1 \Omega| \rho_1(T) \\ &\quad + |g(\eta)^T \left( \frac{\partial W_T}{\partial \eta}(\bar{\eta}_0^+) \right)^T| + \left| \left( \frac{\partial \phi_T}{\partial \eta}(\eta_0^+) \right) \hat{d}_1 + \kappa \left| \frac{\partial \phi_T}{\partial \eta}(\eta_0^+) \right|^2 + |\hat{d}_2| \right)^2 \\ &\leq -\tilde{\alpha}_3(|\eta|) + \hat{\mu} + T \tilde{M}^4 + 2T \tilde{M} \varepsilon - c z^T z + \frac{1}{\kappa} T^2 \tilde{M}^2 \varepsilon^2 + \frac{T}{2} ((c+1)\tilde{M} + (2+\kappa)\tilde{M}^2)^2 \\ &\leq -\tilde{\alpha}_3(|\eta|) - c z^T z + \mu. \end{aligned}$$

Then, from Proposition 1 in [48], there exists  $\bar{\alpha}_3 \in K_\infty$  such that  $\Delta V_T \leq -T \bar{\alpha}_3(|x|) + T \mu$ .

Finally, the following equation shows that condition (5.7) holds,

$$\begin{aligned} |u| &\leq |\beta(\eta)^{-1}| (c|\xi - \phi_T(\eta)| + |g(\eta)^T \left( \frac{\partial W_T}{\partial \eta}(\bar{\eta}_0^+) \right)^T| + \kappa \left| \frac{\partial \phi_T}{\partial \eta}(\eta_0^+) \right|^2 + \left| \frac{\partial \phi_T}{\partial \eta}(\eta_0^+) \hat{d}_1 \right| + |\hat{d}_2| \\ &\quad + \left| \frac{\Delta \phi_T}{T} \right| + |\alpha(\eta, \hat{\xi})| \leq c + 2 + (\kappa + 3)\tilde{M} = \bar{M}. \end{aligned}$$

Consequently, the system (5.12)-(5.13) with the controller (5.14) is SPA stable and since the Euler approximate plant model is one-step consistent with the exact model the same property holds for the exact discretized system (5.10)-(5.11). ■

## 5.4 Application

In this section, design method given in Theorem 5.3.4 is applied to a second order system and the simulation results are analyzed.

Consider the following continuous-time plant:

$$\dot{\eta} = \eta^2 + \xi + d_1(x) \quad (5.24)$$

$$\dot{\xi} = u + d_2(x) \quad (5.25)$$

where  $d_1 : x \mapsto (1 + \sin(x_2))x_1^3$  is bounded by  $\rho_1 : x \mapsto 2|x_1|^3$  and  $d_2 : x \mapsto 1 + \cos(x_1)x_2^2$  by  $\rho_2 : x \mapsto 1 + x_2^2$ .

The control law  $\phi_T = -\eta - \eta^2 - 2\eta^3$  and the Lyapunov function  $W_T(\eta) = \frac{1}{2}\eta^2$  is SPA stabilizing pair for the subsystem (5.24). The robust controllers  $u_T$  and  $u_P$ , and their nonrobust versions  $u_{NT}$  and  $u_B$  are designed for the system (5.24)-(5.25) using the control law  $\phi_T$  and the Lyapunov function  $W_T$  which are given above. The controllers  $u_T$  and  $u_P$  are designed using (5.14) in Theorem 5.3.4 and Theorem 12 in [58], respectively. Then, the controllers  $u_B$  and  $u_{NT}$  are obtained using (3.16) in Theorem 3.3.2 and the method given in [48] which was also presented in Theorem 2.3.3, respectively. The following simulation parameters are set:  $\varepsilon = 0.01$  and  $c = 1$ . Then, simulations have been performed in order to compare performances of the obtained controllers with different sampling periods and initial conditions.

First, the obtained controllers are applied to the system (5.24)-(5.25) with the sampling period  $T = 0.005$  and the initial conditions  $\eta(0) = \xi(0) = 2$ . The parameter  $d$  in the controller  $u_B$  is chosen as  $d = 2$ . Simulation results for the time responses of  $\eta$ ,  $\xi$  and  $u$  are given in Figure 5.1. It is shown that while the controller  $u_{NT}$  cannot stabilize the system, the trajectories of the system with the controller  $u_B$  does not converge to the origin. On the other hand, the controllers  $u_T$  and  $u_P$  stabilize the system (5.24)-(5.25), but faster with controller  $u_T$ . As the parameter  $\kappa$  increases, the performance of the controller  $u_T$  is faster but further increase results in performance degradation. The controller  $u_T$  cannot stabilize the system for  $\kappa > 3$ .

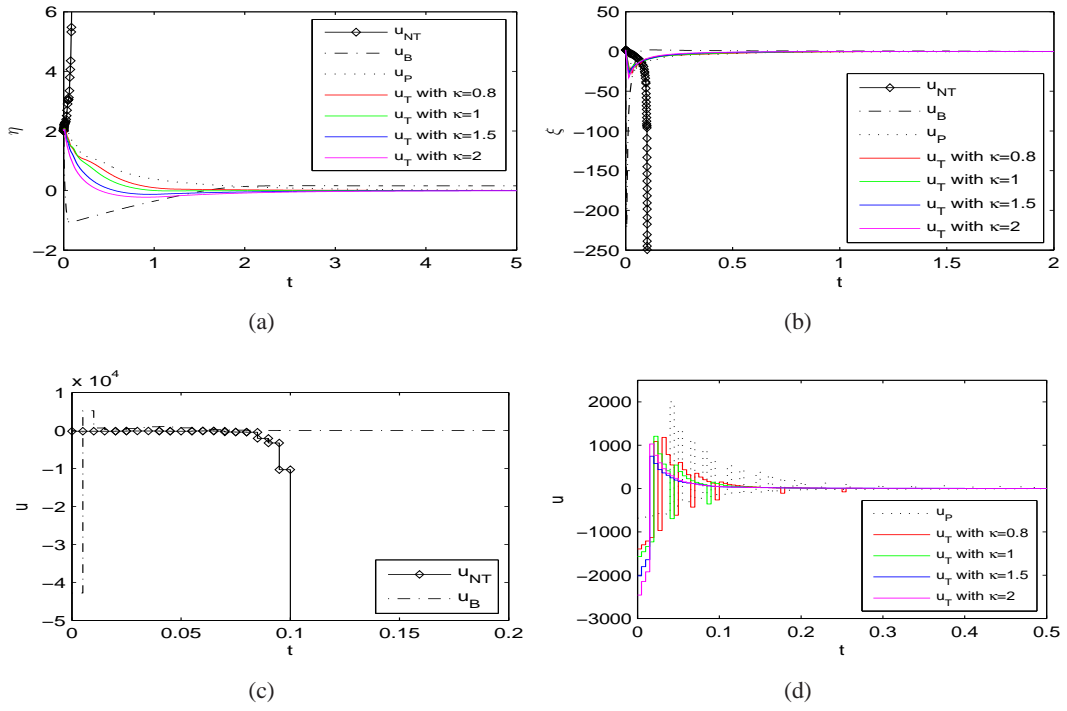


Figure 5.1: Time responses of  $\eta$ ,  $\xi$  and  $u$  with  $T = 0.005$ .

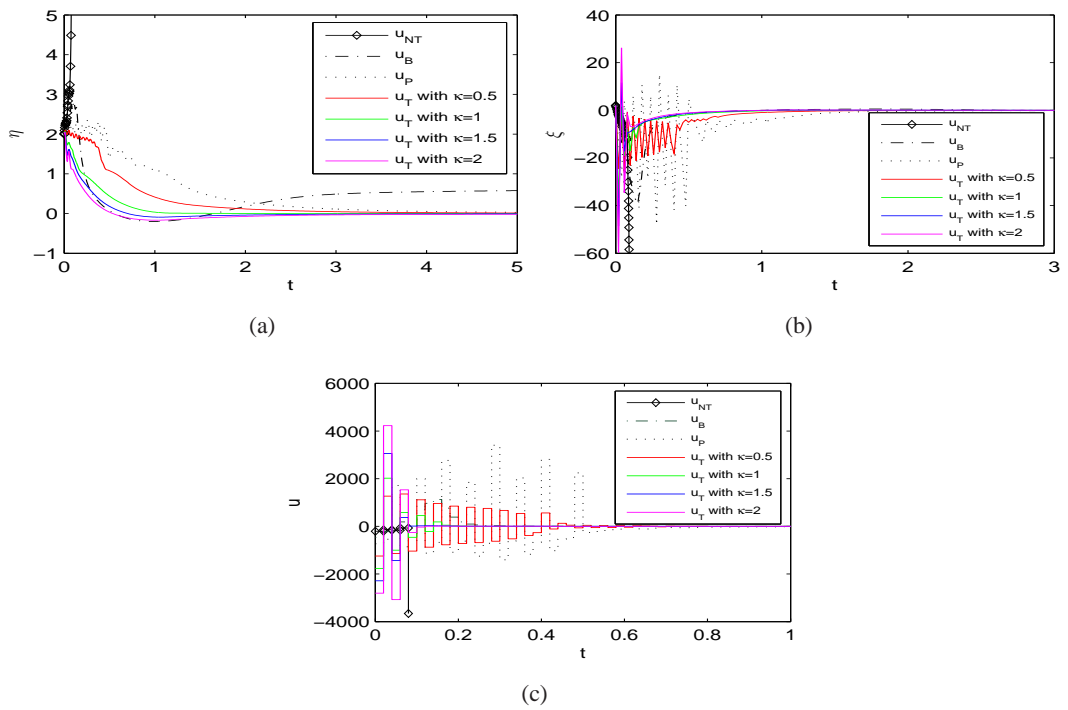


Figure 5.2: Time responses of  $\eta$ ,  $\xi$  and  $u$  with  $T = 0.02$ .

Next, the simulation is performed with the initial conditions given above and large sampling period  $T = 0.02$ . Simulation results are given in Figure 5.2. The parameter  $d$  in the controller  $u_B$  is chosen as  $d = 0.01$ . It is shown that the controllers  $u_{NT}$  and  $u_B$  give similar response with the first simulation. The controller  $u_T$  yields faster results when compared to the controller  $u_P$ . As the parameter  $\kappa$  increases, results of the controller  $u_T$  are faster. For  $\kappa > 2$ , the controller  $u_T$  cannot stabilize the system (5.24)-(5.25). Transient response of the controller  $u_P$  is degraded when the sampling period  $T$  is increased. The controllers  $u_T$  and  $u_P$  give unstable results for  $T > 0.03$ .

Then, the controllers are applied to the system (5.24)-(5.25) with the same sampling period  $T = 0.005$  as in the first simulation and large initial conditions  $\eta(0) = \xi(0) = 3$ . The parameter  $d$  in the controller  $u_B$  is chosen as  $d = 0.05$ . Simulation results are shown in Figure 5.3. The controllers  $u_{NT}$  and  $u_B$  give similar response with the first simulation again. The controllers  $u_T$  and  $u_P$  stabilize the system (5.24)-(5.25) successfully, but faster with the controller  $u_T$ .

As can be seen from figures, the control input  $u_T$  is produced with less energy when compared to the control input  $u_P$ . Therefore, the proposed method requires less control effort. Simulation results also show that when the parameter  $\kappa$  is increased, energy of the control input  $u_T$  decreases in general.

Moreover, when the sampling period  $T$  or the initial conditions are increased, the controller  $u_T$  gives faster results for cases where the parameter  $\kappa$  has smaller value.

Finally, by applying the controllers to the system (5.24)-(5.25) with different initial conditions, domain of attraction (DOA) estimates with the controllers  $u_T$  and  $u_P$  for the sampling period  $T = 0.005$  are given in Figure 5.4. In DOA estimate with the controller  $u_T$ , the parameter  $\kappa$  is chosen as  $\kappa = 0.05$ . As can be seen from figure, DOA for the system with the controller  $u_T$  is slightly larger than that with the controller  $u_P$ . For different controller parameters and sampling periods, much larger DOA estimate may be obtained with the controller  $u_T$  when compared to the estimate given in figure.

The last simulation is performed for the case of without disturbance or model uncertainty by taking  $d_1 = d_2 = 0$  in the system (5.24)-(5.25). The parameter  $d$  in the controller  $u_B$  and the parameter  $\kappa$  in the controller  $u_T$  are chosen as  $d = \kappa = 0.4$ . Simulation results are shown in Figure 5.5. The robust controllers  $u_T$  and  $u_P$  give faster results when compared to the their

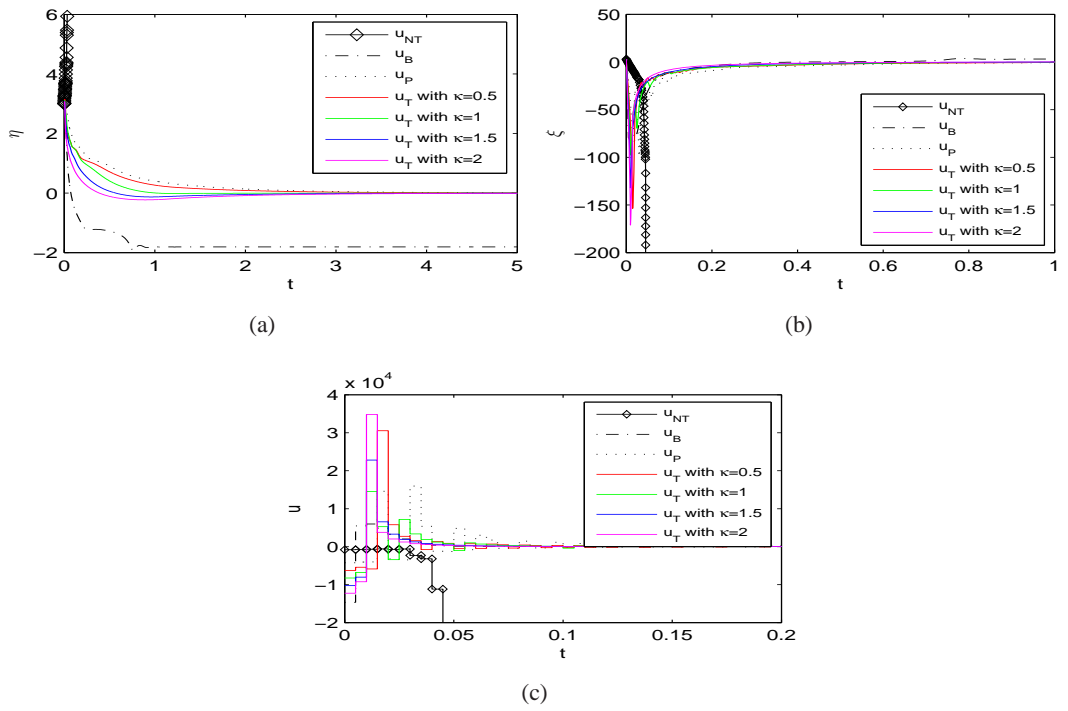


Figure 5.3: Time responses of  $\eta$ ,  $\xi$  and  $u$  with the initial conditions  $\eta(0) = \xi(0) = 3$  and  $T = 0.005$ .

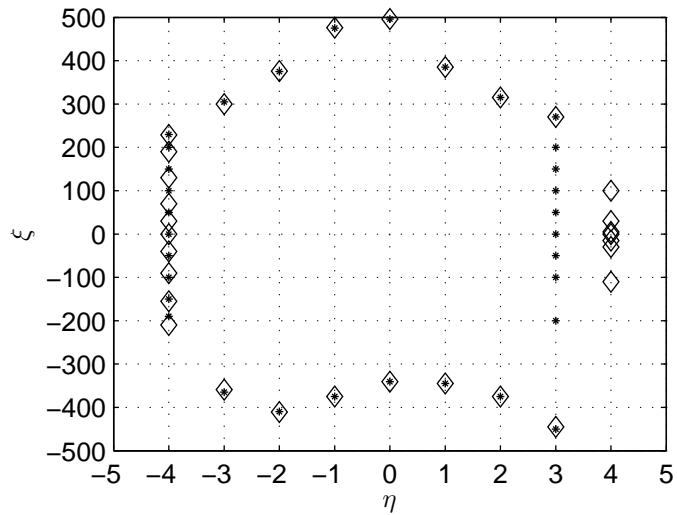


Figure 5.4: Domain of attraction estimates with  $T = 0.005$ . Diamond:controller  $u_T$ . Star:controller  $u_P$ .

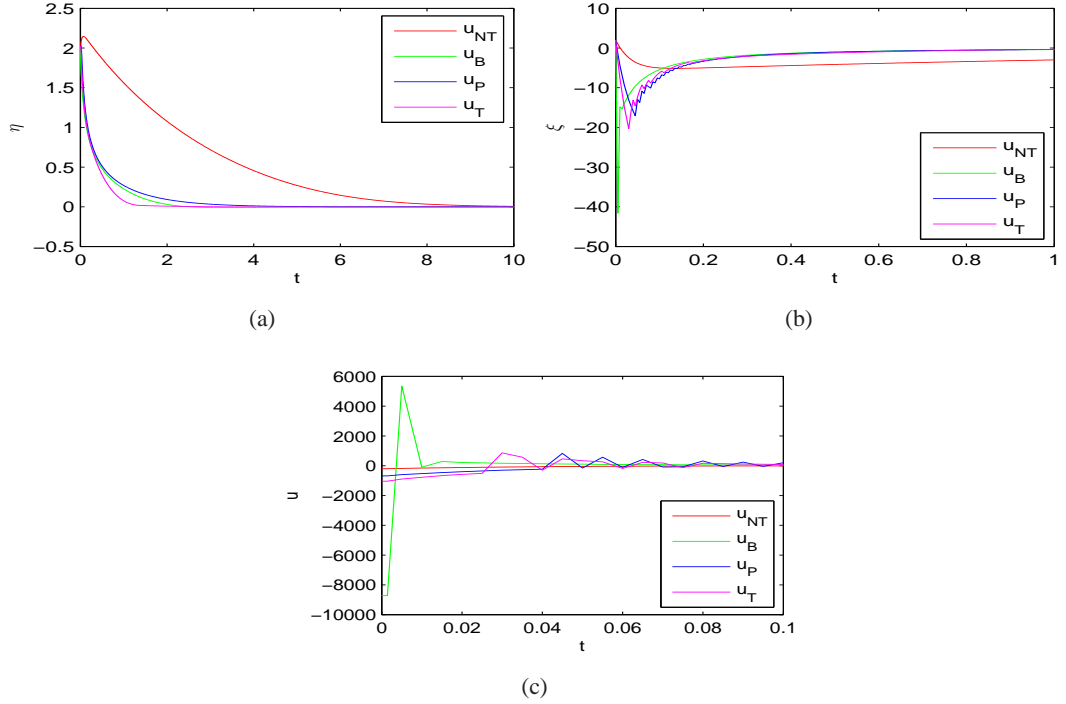


Figure 5.5: Time responses of  $\eta$ ,  $\xi$  and  $u$  with the initial conditions  $\eta(0) = \xi(0) = 3$  and  $T = 0.005$ .

nonrobust versions  $u_B$  and  $u_{NT}$ , respectively. In addition, the controllers  $u_T$  and  $u_B$  yield faster results than the controller  $u_P$ .

## 5.5 Conclusions

In this chapter, the problem of robust backstepping control has been considered for sampled-data nonlinear systems in strict feedback form. A controller design which is modified version of the method given in [58] has been presented based on the Euler approximate model. It has been shown that the designed controller SPA stabilizes the closed-loop sampled-data system based on the framework proposed in [46]. Also a numerical example has been given to illustrate the design method. The performances are analyzed with simulations.

Different from the controller given in [58], in this chapter, the controller was designed to compensate the effects of difference between disturbance or model uncertainty and their bounds. Therefore, simulation results have shown that the designed controller outperforms the controller in [58]. Moreover, in case of unstable results, the controller given in [58] can be tuned

to obtain stable results by adapting the controller gain. However, the controller designed by the proposed method can also be tuned adapting another parameter in addition to the controller gain. So the proposed method gives an additional flexibility for tuning the controller.

## CHAPTER 6

# REDUCED ORDER OBSERVER BASED OUTPUT-FEEDBACK CONTROL FOR THE EULER APPROXIMATE MODEL OF SAMPLED-DATA NONLINEAR SYSTEMS

### 6.1 Introduction

In this chapter, reduced order observer design and reduced order observer based output-feedback controller design methods are proposed. These methods are based on the approximate discrete-time model. It is shown that these controllers and observers semiglobally practically asymptotically (SPA) stabilize the sampled-data nonlinear systems.

In many applications only a part of the state vector is available from measurement. Thus control using output feedback or dynamic feedback is necessary. Designing an observer for unmeasured states is a useful method to be used for constructing an output feedback controller. Considering the output feedback tracking problem, observer-based output-feedback control design for continuous-time nonlinear systems using the observer backstepping procedure is proposed in [30]. On the other hand, the problem of output feedback stabilization of sampled-data nonlinear systems has not been studied much in the literature [10, 28, 65]. In particular, [10] and [28] showed that obtained sampled-data controllers using high gain observers can recover the performance of the continuous-time state feedback controllers.

In this chapter, the problem of reduced order observer-based output feedback control of sampled-data nonlinear systems in strict feedback form based on the Euler approximate model is considered. First, the design of reduced order observers for sampled-data nonlinear systems is presented, which is an extension of the reduced order observer given in [33] to a general

class of multi-input nonlinear systems. Then the design of reduced order observer based SPA stabilizing output-feedback controller for sampled-data nonlinear system in strict feedback form is discussed. For this problem, observer error behaves as disturbance. Even exponentially decaying disturbances can destabilize the sampled-data nonlinear system. Hence, in this chapter, the controller is designed to compensate the effects of this factor and this constitutes the difference from the controller in [25]. It is shown that the designed controllers SPA stabilize the closed-loop sampled-data system based on the framework proposed in [46]. Also numerical examples are given to illustrate the design method. Simulation results show that the designed controller outperforms the controllers given in [25].

The chapter is organized as follows. In Section 6.2 preliminaries are given. The main results are stated and proved in Section 6.3. Then, in Section 6.4, application examples are provided to illustrate the design method. Finally, conclusions are presented in the last section.

## 6.2 Preliminaries

This section provides technical preliminaries. Common definitions which will be used throughout the chapter are presented. For the sake of clarity and easy reading, some notions and definitions that have been introduced in Chapter 2 are repeated when necessary.

Consider the continuous-time nonlinear system

$$\dot{x} = f(x(t), u(t)), \quad y = Cx(t) \quad (6.1)$$

where  $x \in \mathbb{R}^n$  is the state,  $u \in \mathbb{R}^m$  is the control input,  $y \in \mathbb{R}^l$  is the output,  $C$  is a constant matrix of appropriate dimension and the function  $f$  is locally Lipschitz. The control input  $u$  is realized through a zero-order hold such that  $u(t) = u(kT) := u(k), \forall t \in [kT, (k+1)T), k \in \mathbb{N}$  and the output  $y$  is measured at sampling instants  $kT$ ; that is  $y(k) := y(kT)$  where  $T > 0$  is the sampling period.

The difference equations corresponding to the exact discrete-time model of (6.1) and its approximate discrete-time model are represented by:

$$x(k+1) = F_T^e(x(k), u(k)), \quad y(k) = Cx(k) \quad (6.2)$$

$$x(k+1) = F_T^a(x(k), u(k)), \quad y(k) = Cx(k) \quad (6.3)$$

respectively.

Now, consider the following family of observers:

$$\hat{x}(k+1) = G_T(\hat{x}(k), u(k)) \quad (6.4)$$

**Definition 6.2.1** [33] *The family of observers (6.4) is SPA stable observer for  $x(k+1) = F_T(x(k), u(k))$ , if for any compact sets  $\mathcal{X} \subset \mathbb{R}^n$ ,  $\hat{\mathcal{X}} \subset \mathbb{R}^p$ ,  $\mathcal{U} \subset \mathbb{R}^m$  and any strictly positive number  $\nu$ , there exists  $T^* > 0$  such that the followings hold.*

1. *For all  $x_0 \in \mathcal{X}$ ,  $u \in \mathcal{U}$  and  $T \in (0, T^*]$ , there exists  $\hat{x}_0 \in \hat{\mathcal{X}}$  such that  $|\hat{x}(k) - x(k)| \leq T\nu$ ,  $\forall k \geq 1$ .*
2. *For all  $x_0 \in \mathcal{X}$ ,  $\hat{x}_0 \in \hat{\mathcal{X}}$ ,  $u \in \mathcal{U}$  and all  $T \in (0, T^*]$ ,  $\limsup_{k \rightarrow \infty} |\hat{x}(k) - x(k)| \leq T\nu$ .*

To measure the discrepancy between the exact model and the approximate model, one step consistency property, as defined in [46], is used:

**Definition 6.2.2** ([46]) *The family  $F_T^a(x, u)$  is said to be one-step consistent with the exact discrete-time model  $F_T^e(x, u)$  if, for each compact set  $\Omega \subset \mathbb{R}^n \times \mathbb{R}^m$ , there exists a class- $\mathcal{K}$  function  $\rho(\cdot)$  and a constant  $T_0 > 0$  such that,  $|F_T^e(x, u) - F_T^a(x, u)| \leq T\rho(T)$  for all  $(x, u) \in \Omega$  and  $T \in (0, T_0]$ .*

**Definition 6.2.3** [3] *The family of observers (6.4) is SPA stable as in Definition 6.2.1 if there exists a family of Lyapunov functions  $V_T(x, \hat{x})$  and class- $\mathcal{K}_\infty$  functions  $\alpha_1(\cdot), \alpha_2(\cdot), \alpha_3(\cdot)$  such that for any compact sets  $\mathcal{X} \subset \mathbb{R}^n$ ,  $\hat{\mathcal{X}} \subset \mathbb{R}^p$ ,  $\mathcal{U} \subset \mathbb{R}^m$  and any strictly positive number  $\nu$ , there exist constants  $T^* > 0$  and  $M > 0$ , such that for all  $x, x_1, x_2 \in \mathcal{X}$ ,  $\hat{x} \in \hat{\mathcal{X}}$ ,  $u \in \mathcal{U}$ , and  $T \in (0, T^*]$ ,*

$$|V_T(x_1, \hat{x}) - V_T(x_2, \hat{x})| \leq M|x_1 - x_2|, \quad (6.5)$$

$$\alpha_1(|e|) \leq V_T(x, \hat{x}) \leq \alpha_2(|e|), \quad (6.6)$$

$$\frac{V_T(F_T(x, u), G_T(\hat{x}, u)) - V_T(x, \hat{x})}{T} \leq -\alpha_3(|e|) + \nu \quad (6.7)$$

where  $e$  is the observer error defined by the difference between the actual states and their estimates. Moreover, if  $F_T^a$  is consistent with  $F_T^e$  as in Definition 6.2.2 and the family of observers (6.4) is SPA stable observer for (6.3), then the family of observers (6.4) is also SPA stable observer for (6.2).

In order to shorten notations, the following definitions will be used:  $\tilde{x} := [\bar{x}^T, e^T]^T$ ,  $\tilde{F}_T(\tilde{x}) := \begin{bmatrix} \tilde{F}_T(\bar{x}, u) \\ E_T(x, \hat{x}, u) \end{bmatrix}$  with  $\bar{x} := [x^T, \hat{x}^T]^T$ ,  $\tilde{F}_T(\bar{x}, u) := \begin{bmatrix} F_T(x, u) \\ G_T(\hat{x}, u) \end{bmatrix}$  and  $E_T(x, \hat{x}, u) := F_T(x, u) - G_T(\hat{x}, u)$ .

**Definition 6.2.4** [3, 48] *The family of controllers  $u_T$  with observer (6.4) SPA stabilizes  $\tilde{F}_T$  if there exists  $\beta \in \mathcal{KL}$  such that for any pair of strictly positive real numbers  $(D, v)$  there exists  $T^* > 0$  such that for each  $T \in (0, T^*]$  the solutions of  $\tilde{x}(k+1) = \tilde{F}_T(\tilde{x}(k))$  satisfy:  $|\tilde{x}(k, \tilde{x}(0))| \leq \beta(|\tilde{x}(0)|, kT) + v$ , for all  $k \geq 0$ , whenever  $|\tilde{x}(0)| \leq D$ .*

**Definition 6.2.5** [48] *Let  $\hat{T} > 0$  be given and for each  $T \in (0, \hat{T}]$  let functions  $V_T : \mathbb{R}^{n+p} \rightarrow \mathbb{R}_{\geq 0}$  and  $u_T : \mathbb{R}^n \rightarrow \mathbb{R}^m$  be defined. The pair of families  $(u_T, V_T)$  with observer (6.4) is a SPA stabilizing pair for  $\tilde{F}_T$  if there exist  $\alpha_1, \alpha_2, \alpha_3 \in \mathcal{K}_\infty$  such that for any pair of strictly positive real numbers  $(\Delta, \delta)$  there exists a triple of strictly positive real numbers  $(T^*, L, M)$ , with  $T^* \leq \hat{T}$ , such that for all  $\tilde{x}_1, \tilde{x}_2 \in \mathbb{R}^{n+p}$  with  $\max\{|\tilde{x}_1|, |\tilde{x}_2|\} \leq \Delta$ , and  $T \in (0, T^*]$ :*

$$\alpha_1(|\tilde{x}|) \leq V_T(\tilde{x}) \leq \alpha_2(|\tilde{x}|) \quad (6.8)$$

$$V_T(\tilde{F}_T(\tilde{x})) - V_T(\tilde{x}) \leq -T\alpha_3(|\tilde{x}|) + T\delta \quad (6.9)$$

$$|V_T(\tilde{x}_1) - V_T(\tilde{x}_2)| \leq L|\tilde{x}_1 - \tilde{x}_2| \quad (6.10)$$

$$|u_T| \leq M \quad (6.11)$$

**Theorem 6.2.6** [45, 50, 51] *If  $(u_T, V_T)$  is a SPA stabilizing pair for  $\tilde{F}_T^a$ , then  $u_T$  stabilizes  $\tilde{F}_T^e$ .*

Then, stability properties of the sampled-data system (6.1) can be deduced from those of exact discretized system under certain conditions [51].

### 6.3 Main Results

In this section, the design of reduced order observers for sampled-data nonlinear systems using the Euler approximate discrete-time models is presented. This is an extension of the reduced order observer given in [33] to a general class of multi-input nonlinear systems. Then, the design of reduced order observer based SPA stabilizing output-feedback controller for sampled-data nonlinear system in strict feedback form using the Euler approximate model

is discussed. The controller is designed to compensate the effect of the observer error which behaves as disturbance and this is the main difference from the controller given in [25].

Consider the following strict feedback nonlinear system with sampled observation  $y(k) = \eta(k)$

$$\dot{\eta} = f(\eta) + g(\eta)\xi \quad (6.12)$$

$$\dot{\xi} = \alpha(\eta, \xi) + \beta(\eta)u \quad (6.13)$$

where  $x = [\eta^T \quad \xi^T]^T$  with  $\eta \in \mathbb{R}^n$  and  $\xi \in \mathbb{R}^m$  is the state vector,  $f(0) = 0$ ,  $g(0) \neq 0$ ,  $f, g, \alpha$  are differentiable sufficiently many times,  $g$  is invertible,  $\beta(\eta) \neq 0, \forall \eta$ ,  $\alpha$  is locally Lipschitz and the control input  $u \in \mathbb{R}^m$  is realized through a zero order hold such that  $u(t) = u(kT) := u(k), \forall t \in [kT, (k+1)T), k \in \mathbb{N}$  and the output  $y$  is measured at sampling instants  $kT$ ; that is  $y(k) := y(kT)$  where  $T > 0$  is the sampling period.

Suppose that family of exact discrete-time models of the system (6.12)-(6.13) is

$$\eta(k+1) = F_{\eta,T}^e(\eta, \xi, u) \quad (6.14)$$

$$\xi(k+1) = F_{\xi,T}^e(\eta, \xi, u) \quad (6.15)$$

with the output  $y(k) = \eta(k)$ . Since the exact discrete-time models (6.14)-(6.15) are not available in general, approximate discrete-time models are used. Hence the following Euler approximate discrete-time model of (6.12)-(6.13) is considered.

$$\eta(k+1) = \eta + T(f(\eta) + g(\eta)\xi) \quad (6.16)$$

$$\xi(k+1) = \xi + T(\alpha(\eta, \xi) + \beta(\eta)u) \quad (6.17)$$

Since the state  $\xi$  is not measured, its estimate  $\hat{\xi}$  is used where  $\xi = \hat{\xi} + \tilde{\xi}$ . Then, the following theorem provides the design of SPA stable reduced order observers.

**Theorem 6.3.1** *Given the exact discrete-time model (6.14)-(6.15) with the output  $y^e = \eta^e$ . For any triple of strictly positive numbers  $(\Delta_x, \Delta_{\hat{\xi}}, \Delta_u)$ , if there exists  $T^* > 0$  such that for all  $x, \hat{\xi}, u$  and  $T$  satisfying  $|x| \leq \Delta_x, |\hat{\xi}| \leq \Delta_{\hat{\xi}}, |u| \leq \Delta_u, T \in (0, T^*]$ , and if there exist matrices  $P = P^T > 0$  and  $R$  of appropriate dimensions such that the following linear matrix inequalities (LMIs) are feasible:*

$$\mathcal{A}^T(\gamma)P - R + P\mathcal{A}(\gamma) - R^T < 0, \forall \gamma \in \mathcal{V}_{\mathcal{H}_{m,m}}. \quad (6.18)$$

where  $\mathcal{V}_{\mathcal{H}_{m,m}} = \{\gamma = (\gamma_{11}, \dots, \gamma_{1m}, \dots, \gamma_{mm}) | \gamma_{ij} \in \{\bar{h}_{ij}, h_{ij}^*\}\}$  with  $h_{ij}^* = \max_k (h_{ij}(k))$  and  $\bar{h}_{ij} = \min_k (h_{ij}(k))$ , then the following reduced order observer is a SPA stable observer for the exact discrete-time model (6.15)

$$\hat{\xi}(k+1) = \hat{\xi} + T(\alpha(\eta, \hat{\xi}) + \beta(\eta)u + L\tilde{\xi}) \quad (6.19)$$

where  $\tilde{\xi} = g^{-1}(\eta)(\dot{\eta} - f(\eta)) - \hat{\xi}$ ,  $\dot{\eta} := \frac{\eta(k) - \eta(k-1)}{T}$  and the observer gain  $L$  is given by  $L = P^{-1}R^T$  when the LMIs in (6.18) are feasible.

**Proof.** The observer error is defined as  $\tilde{\xi} = \xi - \hat{\xi}$ . Considering the Euler approximate model (6.17) and the observer (6.19) the error dynamics could be written as:  $\tilde{\xi}(k+1) = \tilde{\xi} + T(\alpha(\eta, \xi) - \alpha(\eta, \hat{\xi}) - L\tilde{\xi})$ . Using the delta operator, the error dynamics are obtained as:

$$\delta\tilde{\xi} = \frac{\tilde{\xi}(k+1) - \tilde{\xi}(k)}{T} = \alpha(\eta, \xi) - \alpha(\eta, \hat{\xi}) - L\tilde{\xi}. \quad (6.20)$$

By the differential mean value theorem (DMVT), there exists  $z_i(k) \in Co(\xi, \hat{\xi})$  for all  $i = 1, \dots, m$ , such that:

$$\alpha(\eta, \xi) - \alpha(\eta, \hat{\xi}) = \left( \sum_{i,j=1}^{m,m} \varepsilon_m(i) \varepsilon_m^T(j) \frac{\partial \alpha_i}{\partial \xi_j}(z_i(k)) \right) \tilde{\xi}.$$

Then, using the notations:

$$\begin{aligned} h_{ij}(k) &= \frac{\partial \alpha_i}{\partial \xi_j}(z_i(k)), \\ h(k) &= (h_{11}(k), \dots, h_{1m}(k), \dots, h_{mm}(k)) \\ \mathcal{A}(h(k)) &= \sum_{i,j=1}^{m,m} h_{ij}(z_j(k)) \varepsilon_m(i) \varepsilon_m^T(j) \end{aligned}$$

the equation of the observer error dynamics can be rewritten as:

$$\delta\tilde{\xi} = (\mathcal{A}(h(k)) - L)\tilde{\xi} \quad (6.21)$$

It is assumed that the functions  $h_{ij}$  are bounded for all  $i, j = 1, \dots, m$ . Then the vector  $h(k)$  evolves in a bounded domain  $\mathcal{H}_{m,m}$  of  $\mathcal{V}_{\mathcal{H}_{m,m}} = \{\gamma = (\gamma_{11}, \dots, \gamma_{1m}, \dots, \gamma_{mm}) | \gamma_{ij} \in \{\bar{h}_{ij}, h_{ij}^*\}\}$  where  $h_{ij}^* = \max_k (h_{ij}(k))$  and  $\bar{h}_{ij} = \min_k (h_{ij}(k))$ .

Let  $T^* > 0$  and for each  $T \in (0, T^*)$  let the Lyapunov function  $V_o$  be defined as  $V_o = \tilde{\xi}^T P \tilde{\xi}$ . It is obvious that the conditions (6.5) and (6.6) are satisfied and hence, to prove SPA stability,

it is enough to show that condition (6.7) is satisfied.  $\delta V_o$  can be written, using delta operator and (6.21), as:

$$\begin{aligned}\delta V_o &= \frac{V_o(k+1) - V_o(k)}{T} = \frac{\Delta V_o}{T} = \tilde{\xi}^T P \delta \tilde{\xi} + (\delta \tilde{\xi})^T P \tilde{\xi} + T(\delta \tilde{\xi})^T P \delta \tilde{\xi} \\ &= \tilde{\xi}^T F(h(k)) \tilde{\xi} + T \tilde{\xi}^T (\mathcal{A}(h(k)) - L)^T P (\mathcal{A}(h(k)) - L) \tilde{\xi}\end{aligned}\quad (6.22)$$

where  $F(h(k)) = (\mathcal{A}(h(k)) - L)^T P + P(\mathcal{A}(h(k)) - L)$ . It is observed from (6.22) that condition (6.7) is satisfied if  $F(h(k)) < 0$  for all  $h(t) \in \mathcal{H}_{m,m}$ . Using the fact that  $F$  is affine in  $h(k)$  and the convexity principle ([6]), condition (6.7) holds if the following condition is satisfied:

$$F(\gamma) < 0 \quad \forall \gamma \in \mathcal{V}_{\mathcal{H}_{m,m}}. \quad (6.23)$$

If the notation  $R = L^T P$  is used, condition (6.23) is found to be equivalent to (6.18). Therefore, if (6.18) holds, then the inequality (6.23) is also verified. This implies that

$$\begin{aligned}\delta V_o &\leq -\tilde{\xi}^T L_o \tilde{\xi} + T \tilde{\xi}^T (\mathcal{A}(h(k)) - L)^T P (\mathcal{A}(h(k)) - L) \tilde{\xi} \\ \Delta V_o &\leq -T \alpha_3(|\tilde{\xi}|) + T \nu\end{aligned}$$

where  $\nu > 0$  is sufficiently small,  $\alpha_3 \in \mathcal{K}_\infty$  and  $L_o > 0$  is a matrix. Hence, condition (6.7) is satisfied for Euler model. Since the Euler model is one step consistent with the exact model, the same property holds for exact model. Consequently, the observer (6.19) is SPA stable observer for the exact model (6.15). ■

Consider the system represented by (6.12)-(6.13). Assume that a SPA stabilizing reduced-order observer for the system (6.13) is designed. Using this observer and Euler models, the closed-loop system can be written as:

$$\eta(k+1) = \eta + T(f(\eta) + g(\eta)(\hat{\xi} + \tilde{\xi})) \quad (6.24)$$

$$\hat{\xi}(k+1) = \hat{\xi} + T(\gamma(\eta, \hat{\xi}) + \beta(\eta)u) \quad (6.25)$$

$$\tilde{\xi}(k+1) = \tilde{\xi} + T(\alpha(\eta, \hat{\xi}) - \gamma(\eta, \hat{\xi})) \quad (6.26)$$

where the term  $\gamma(\eta, \hat{\xi})$  is obtained during the observer design.

**Hypothesis 6.3.2** [48] *There exist  $\hat{T} > 0$  and a pair  $(\phi_T, W_T)$  that is defined for each  $T \in (0, \hat{T})$  and that is a SPA stabilizing pair for the subsystem (6.24) with  $\hat{\xi} \in \mathbb{R}^m$  regarded as its control. Suppose also that the followings hold:*

1.  $\phi_T$  and  $W_T$  are twice differentiable for any  $T \in (0, \hat{T})$ ;

2. there exists  $\varphi \in \mathcal{K}_\infty$  such that  $|\phi_T(\eta)| \leq \varphi(|\eta|)$  for all  $\eta \in \mathbb{R}^n$ ,  $T \in (0, \hat{T})$ ;
3. for any  $\tilde{\Delta} > 0$  there exists a pair of strictly positive numbers  $(\tilde{T}, \tilde{M}_1)$  such that  $\max\{|\frac{\partial W_T}{\partial \eta}|, |\frac{\partial \phi_T}{\partial \eta}|, |\frac{\partial^2 \phi_T}{\partial \eta^2}|, |\frac{\partial^2 W_T}{\partial \eta^2}|\} \leq \tilde{M}_1$  for each  $T \in (0, \tilde{T})$  and  $|\eta| \leq \tilde{\Delta}$ .

Then, the following theorem provides the SPA stabilizing reduced order observer-based controller design.

**Theorem 6.3.3** *Assume that a SPA stabilizing reduced-order observer (6.25) for the system (6.13) is designed and Hypothesis 6.3.2 holds. Then the Euler model (6.24)-(6.26) is SPA stable with the following output-feedback controller  $u$ , and so is the exact discretized system (6.14)-(6.15).*

$$u = \beta^{-1}(\eta)(-c(\hat{\xi} - \phi_T(\eta)) - g(\eta)^T (\frac{\partial W_T}{\partial \eta}(\bar{\eta}_0^+))^T - d \left| (\frac{\partial \phi_T}{\partial \eta}(\eta_0^+)) \right|^2 (\hat{\xi} - \phi_T(\eta)) + \frac{\Delta \phi_T}{T} - \gamma(\eta, \hat{\xi})) \quad (6.27)$$

where  $c, d > 0$ ,  $\Delta \phi_T = \phi_T(\eta_0^+) - \phi_T(\eta)$ ,  $\eta_0^+ = \eta + T(f(\eta) + g(\eta)\hat{\xi})$  and  $\bar{\eta}_0^+ = \eta + T(f(\eta) + g(\eta)\phi_T)$ .

**Proof.** Let  $\Delta, \mu, \hat{\mu}, \tilde{\mu} \in \mathbb{R}_{>0}$ ,  $x = [\eta^T \ z^T \ \tilde{\xi}^T]^T \in \mathbb{R}^{n+2m}$  and  $\bar{x} = [\eta^T \ \tilde{\xi}^T]^T \in \mathbb{R}^{n+m}$  with  $|x| \leq \Delta$ ,  $z = \hat{\xi} - \phi_T$ . Consider the system given by (6.24). There exists  $\hat{T} > 0$  such that condition (6.9) holds for  $T \in (0, \hat{T})$  with  $\tilde{\alpha}_3 \in \mathcal{K}_\infty$  and  $\hat{\mu}$  when  $\hat{\xi} = \phi_T$  as input such that,

$$\Delta W_T = W_T(\bar{\eta}^+, \tilde{\xi}^+) - W_T(\eta, \tilde{\xi}) \leq -T\tilde{\alpha}_3(|\bar{x}|) + T\hat{\mu} \quad (6.28)$$

where  $\bar{\eta}^+ = \eta + T(f(\eta) + g(\eta)(\phi_T + \tilde{\xi}))$ .

Then, using delta operator the Euler approximate models for  $\eta$  and  $z$  can be written as:

$$\delta \eta = f(\eta) + g(\eta)(z + \phi_T(\eta) + \tilde{\xi}) \quad (6.29)$$

$$\delta z = \gamma(\eta, \hat{\xi}) + \beta(\eta)u - \frac{\phi_T(\eta^+) - \phi_T(\eta)}{T} \quad (6.30)$$

with  $\eta^+ = \eta + T(f(\eta) + g(\eta)(\hat{\xi} + \tilde{\xi}))$ . Let  $\Delta_1 = \sup_{|x| \leq \Delta, T \in (0, \hat{T})} \max\{|\eta^+|, |\eta_0^+|, |\bar{\eta}_0^+|, |\bar{\eta}^+|\}$  that is well defined since functions  $f, g, \phi_T$  are continuous. Let  $\bar{\Delta} = \max\{\Delta, \Delta_1\}$  generates  $\tilde{T}, \tilde{M}_1$  such that inequality 3 in Hypothesis 6.3.2 holds. Let  $\tilde{M} = \sup_{|x| \leq \Delta, T \in (0, \hat{T})} \max\{|\hat{\xi} - \phi_T|, |f(\eta) + g(\eta)\hat{\xi}|, |g(\eta)|, \tilde{M}_1, |\tilde{\xi}|, |\beta(\eta)|, |\alpha(\eta, \hat{\xi})|\}$  which is well defined since all the considered functions are continuous over the given compact set.

Let  $T^* > 0$  and for each  $T \in (0, T^*)$  let the Lyapunov function  $V$  be defined as  $V = V_T + V_e$  where  $V_e$  is the Lyapunov function for the observer error and  $V_T(x, \tilde{\xi}) = W_T(\eta, \tilde{\xi}) + \frac{1}{2}z^T z$ . It is obvious that conditions (6.8) and (6.10) are satisfied, (see [48]) and hence, to prove SPA stability, it is enough to show that conditions (6.9) and (6.11) are satisfied. First, it will be shown that condition (6.9) holds:

$$\delta V_T = \frac{\Delta V_T}{T} = \frac{V_T(k+1) - V_T(k)}{T} = \delta W_T + z^T \delta z + \frac{T}{2}((\delta z)^T \delta z).$$

$\delta W_T$  can be written, using the mean value theorem (MVT), as:

$$\begin{aligned} \delta W_T &= \frac{W_T(\eta^+) - W_T(\bar{\eta}^+, \tilde{\xi}^+) + W_T(\bar{\eta}^+, \tilde{\xi}^+) - W_T(\eta, \tilde{\xi})}{T} \\ &= \frac{\Delta W_T}{T} + (\hat{\xi} - \phi_T(\eta))^T g(\eta)^T \left( \frac{\partial W_T}{\partial \eta}(\eta^\diamond) \right)^T \end{aligned} \quad (6.31)$$

where  $\eta^\diamond = \bar{\eta}^+ + T\theta_1 g(\eta)(\hat{\xi} - \phi_T(\eta))$  and  $\theta_1 \in (0, 1)$ .

Then,  $\delta V_T$  can be written, using (6.29-6.31), as:

$$\delta V_T \leq \frac{\Delta W_T}{T} - cz^T z + z^T \Lambda + \frac{T}{2}((\delta z)^T \delta z) + z^T g(\eta)^T \left( \frac{\partial W_T}{\partial \eta}(\eta^\diamond) \right)^T - \frac{\partial W_T}{\partial \eta}(\bar{\eta}_0^+)^T$$

with  $\Lambda = -d \left| \left( \frac{\partial \phi_T}{\partial \eta}(\eta_0^+) \right) \right|^2 z + \frac{\phi_T(\eta_0^+) - \phi_T(\eta^+)}{T}$ .

Using MVT, it can be shown that

$$z^T g(\eta)^T \left( \frac{\partial W_T}{\partial \eta}(\eta^\diamond) \right)^T - \frac{\partial W_T}{\partial \eta}(\bar{\eta}_0^+)^T \leq T\tilde{M}^4. \quad (6.32)$$

Thanks to the use of MVT, the following equation can be written:

$$\frac{\phi_T(\eta_0^+) - \phi_T(\eta^+)}{T} = - \left( \frac{\partial \phi_T}{\partial \eta}(\eta^*) \right) g(\eta) \tilde{\xi} \quad (6.33)$$

where  $\eta^* = \eta_0^+ + T\ell_1 g(\eta) \tilde{\xi}$  and  $\ell_1 \in (0, 1)$ .

Then, using DMVT and (6.33),  $\Lambda$  can be written as:

$$\begin{aligned} \Lambda &= \left( \left( \frac{\partial \phi_T}{\partial \eta}(\eta_0^+) \right) - \left( \frac{\partial \phi_T}{\partial \eta}(\eta^*) \right) - \left( \frac{\partial \phi_T}{\partial \eta}(\eta_0^+) \right) \right) g(\eta) \tilde{\xi} - d \left| \left( \frac{\partial \phi_T}{\partial \eta}(\eta_0^+) \right) \right|^2 z \\ &= - \left( \frac{\partial^2 \phi_T}{\partial \eta^2}(\eta^{**}) \right) \ell_1 T \Omega (g(\eta) \tilde{\xi}) - \left( \frac{\partial \phi_T}{\partial \eta}(\eta_0^+) \right) g(\eta) \tilde{\xi} - d \left| \left( \frac{\partial \phi_T}{\partial \eta}(\eta_0^+) \right) \right|^2 z \end{aligned} \quad (6.34)$$

where  $\Omega = [\Omega_1^T, \Omega_2^T, \dots, \Omega_n^T]^T$ ,  $\Omega_i = g(\eta) \tilde{\xi}$ ,  $\eta^{**} = \eta_0^+ + T\ell_1 \ell_2 g(\eta) \tilde{\xi}$  and  $\ell_2 \in (0, 1)$ .

Using (6.28), (6.32), (6.34) and Young's inequality,  $\delta V_T$  can be written as:

$$\begin{aligned}
\delta V_T &\leq \frac{\Delta W_T}{T} + T\tilde{M}^4 + |z^T \frac{\partial^2 \phi_T}{\partial \eta^2}(\eta^{**}) \ell_1 T \Omega(g(\eta)\tilde{\xi})| - cz^T z + \frac{1}{4d} |g(\eta)\tilde{\xi}|^2 \\
&\quad - (\sqrt{d} |(\frac{\partial \phi_T}{\partial \eta}(\eta_0^+))z| + \frac{1}{2\sqrt{d}} |g(\eta)\tilde{\xi}|^2 + \frac{T}{2} | - cz - (\frac{\partial^2 \phi_T}{\partial \eta^2}(\eta^{**})) \ell_1 T \Omega(g(\eta)\tilde{\xi}) \\
&\quad - (\frac{\partial \phi_T}{\partial \eta}(\eta_0^+))g(\eta)\tilde{\xi} - g(\eta)^T (\frac{\partial W_T}{\partial \eta}(\bar{\eta}_0^+)) - d \left| (\frac{\partial \phi_T}{\partial \eta}(\eta_0^+)) \right|^2 |z|^2 \\
&\leq -\tilde{\alpha}_3(|\bar{x}|) + \hat{\mu} + T\tilde{M}^4 - cz^T z + \frac{1}{4d} \tilde{\xi}^T g(\eta)^T g(\eta)\tilde{\xi} + \frac{T}{2} ((c+1)\tilde{M} + 2\tilde{M}^2 + d\tilde{M}^3)^2 \\
&\leq -\tilde{\alpha}_3(|\bar{x}|) - cz^T z + \tilde{\mu} + \frac{1}{4d} \tilde{\xi}^T g(\eta)^T g(\eta)\tilde{\xi}.
\end{aligned}$$

Then, from SPA stability of the observer with a proper Lyapunov function  $V_e$  for observer error and Proposition 1 in [48], there exists  $\bar{\alpha}_3 \in \mathcal{K}_\infty$ , such that  $\Delta V \leq -T\bar{\alpha}_3(|x|) + T\mu$ .

Finally, the following equation shows that condition (6.11) holds,

$$\begin{aligned}
|u| &\leq |\beta(\eta)^{-1}|(c|\hat{\xi} - \phi_T(\eta)| + |g(\eta)^T \left\| (\frac{\partial W_T}{\partial \eta}(\bar{\eta}_0^+)) \right\|^T | + d \left| (\frac{\partial \phi_T}{\partial \eta}(\eta_0^+)) \right|^2 |z| \\
&\quad + |\alpha(\eta, \hat{\xi})| + \left| \frac{\Delta \phi_T}{T} \right| + L|\tilde{\xi}| \leq c + L + 1 + 2\tilde{M} + d\tilde{M}^4 = \bar{M}.
\end{aligned}$$

Consequently, the closed-loop system (6.24)-(6.26) is SPA stable. As a result of SPA stability of the observer, the Euler model (6.16)-(6.17) is SPA stable and the same property holds for the exact discretized system (6.14)-(6.15) due to the one-step consistency of the Euler model with the exact model. ■

## 6.4 Applications

In this section, design methods given in Theorems 6.3.1 and 6.3.3 are applied to various systems and the simulation results are analyzed.

### 6.4.1 Dynamically Positioned Ship

Consider the following equation of motion for the moored tanker in Example 11.4 in [12]

$$\dot{\eta} = R(\psi(t))\nu \tag{6.35}$$

$$\dot{\nu} = A_1 \eta + A_2 \nu + Bu \tag{6.36}$$

where  $y(k) = \eta(k)$ ,  $\eta = [n \ e \ \psi]^T$ ,  $v = [\mu \ v \ r]^T$ ,  $u = [u_1 \ u_2 \ u_3]^T$ ,  $A_1 = -M^{-1}K$ ,  $A_2 = -M^{-1}D$ ,  $B = M^{-1}$  and

$$M = \begin{bmatrix} 1.0852 & 0 & 0 \\ 0 & 2.0575 & -0.4087 \\ 0 & -0.4087 & 0.2153 \end{bmatrix}, \quad R(\psi) = \begin{bmatrix} \cos \psi & -\sin \psi & 0 \\ \sin \psi & \cos \psi & 0 \\ 0 & 0 & 1 \end{bmatrix},$$

$$D = \begin{bmatrix} 0.0865 & 0 & 0 \\ 0 & 0.0762 & 0.1510 \\ 0 & 0.0151 & 0.0031 \end{bmatrix}, \quad K = \text{diag}\{0.0389, 0.0266, 0\},$$

as given in [25].

First, the reduced observers given in Theorem 6.3.1 and [25] will be applied to the system (6.35)-(6.36). The reduced-order observer for (6.35) is designed in [25] as:

$$z(k+1) = M_1 z(k) + M_2 y(k) + T B u(k), \quad (6.37)$$

$$\hat{v}(k) = z(k) + G d y(k) \quad (6.38)$$

where  $d = [0 \ 0 \ 1]$ ,  $M_1 = I + T(A_2 - Gd)$ ,  $M_2 = T(A_1 + (A_2 - Gd)Gd)$  and  $G \in \mathbb{R}^{3 \times 1}$ .

Using (6.19) in Theorem 6.3.1, another reduced-order observer for (6.35) is designed as:

$$\hat{v}(k+1) = \hat{v} + T(A_1 \eta + A_2 \hat{v} + B u + L \tilde{v}) \quad (6.39)$$

with  $\tilde{v} = (R(\psi))^T \frac{\eta(k) - \eta(k-1)}{T} - \hat{v}$  and  $L = h + A_2$  where  $h$  can be chosen such that  $h = \text{diag}\{h_1, h_2, h_3\}$  with  $h_i > 0$  for sufficiently small  $T > 0$ .

Then, the observers given by (6.37)-(6.38) and (6.39) are applied to the system (6.35)-(6.36) with the following controller given in [25]:

$$u_E(y, \hat{v}) = B^{-1}[u_{aT}(y, \hat{v}) - A_1 y - A_2 \hat{v}] \quad (6.40)$$

where

$$u_{aT}(y, \hat{v}) = -c(\hat{v} - \phi_T(y)) - \frac{\Delta \bar{W}_T(y, \hat{v})}{T} + \frac{\Delta \bar{\phi}_T(y, \hat{v})}{T}$$

$$\Delta \bar{\phi}_T(y, \hat{v}) = \bar{\phi}_T(k+1) - \phi_T(y(k))$$

$$\phi_T(y(k)) = -R^T(\psi(k))K y(k)$$

$$\bar{\phi}_T(k+1) = -R^T(\hat{\psi}(k+1))K[y(k) + T R(\psi(k))K \hat{v}(k)]$$

$$\hat{\psi}(k+1) = \psi(k) + T \hat{r}(k)$$

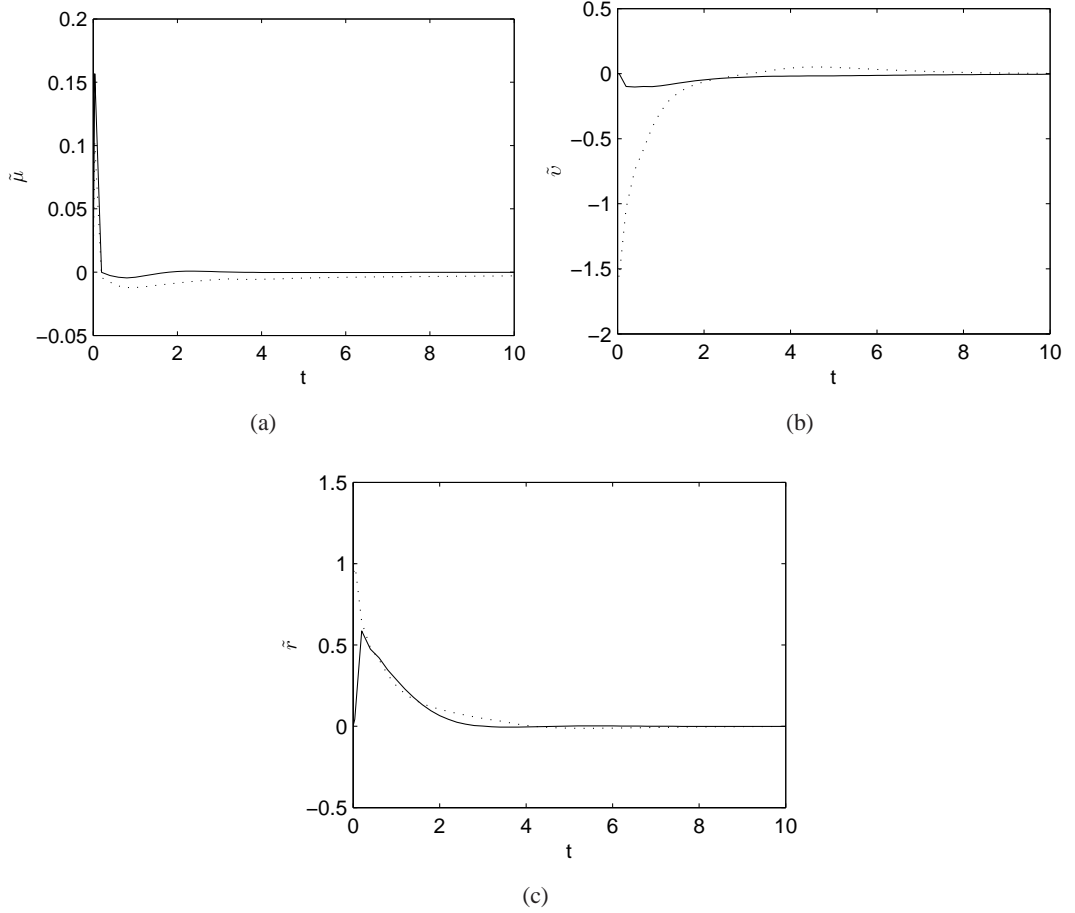


Figure 6.1: Time responses of observer errors with  $T = 0.2$ . Solid curve:observer (6.39). Dotted line:observer (6.37)-(6.38).

$$\Delta\tilde{W}_T(y, \hat{v}) = \begin{cases} \frac{\Delta\bar{W}_T(y, \hat{v})[\hat{v} - \phi_T(y)]}{\|\hat{v} - \phi_T(y)\|^2}, & \hat{v} \neq \phi_T(y) \\ TR^T(x_3)[y + TR(x_3)\hat{v}], & \hat{v} = \phi_T(y) \end{cases}$$

$$\Delta\bar{W}_T(y, \hat{v}) = W_T(y + TR(\psi)\hat{v}) - W_T((I + TK)y)$$

$W_T = \frac{1}{2}\eta^T\eta$  and  $c > 0$  is arbitrary.

In simulations, the following parameters are used:  $G = [0 \quad -1.8862 \quad 1.1358]^T$  and  $h = \text{diag}\{0.082, 0.25, 1\}$  for observers,  $K = \text{diag}\{0.5, 0.5, 0.5\}$  and  $c = 1$  for controller. The initial conditions are chosen as  $\eta(0) = [-2 \quad 2 \quad -\frac{\pi}{4}]^T$ ,  $v(0) = 0_{3 \times 1}$  and  $\hat{v}(0) = 0_{3 \times 1}$ . Simulation results with  $T = 0.2$  and  $T = 0.4$  are shown in Figures 6.1 and 6.2, respectively. It is shown that observer error  $\tilde{v} := v - \hat{v}$  converges to zero with both observers, but faster with (6.39). As the sampling period  $T$  increases, both observers give slower responses.

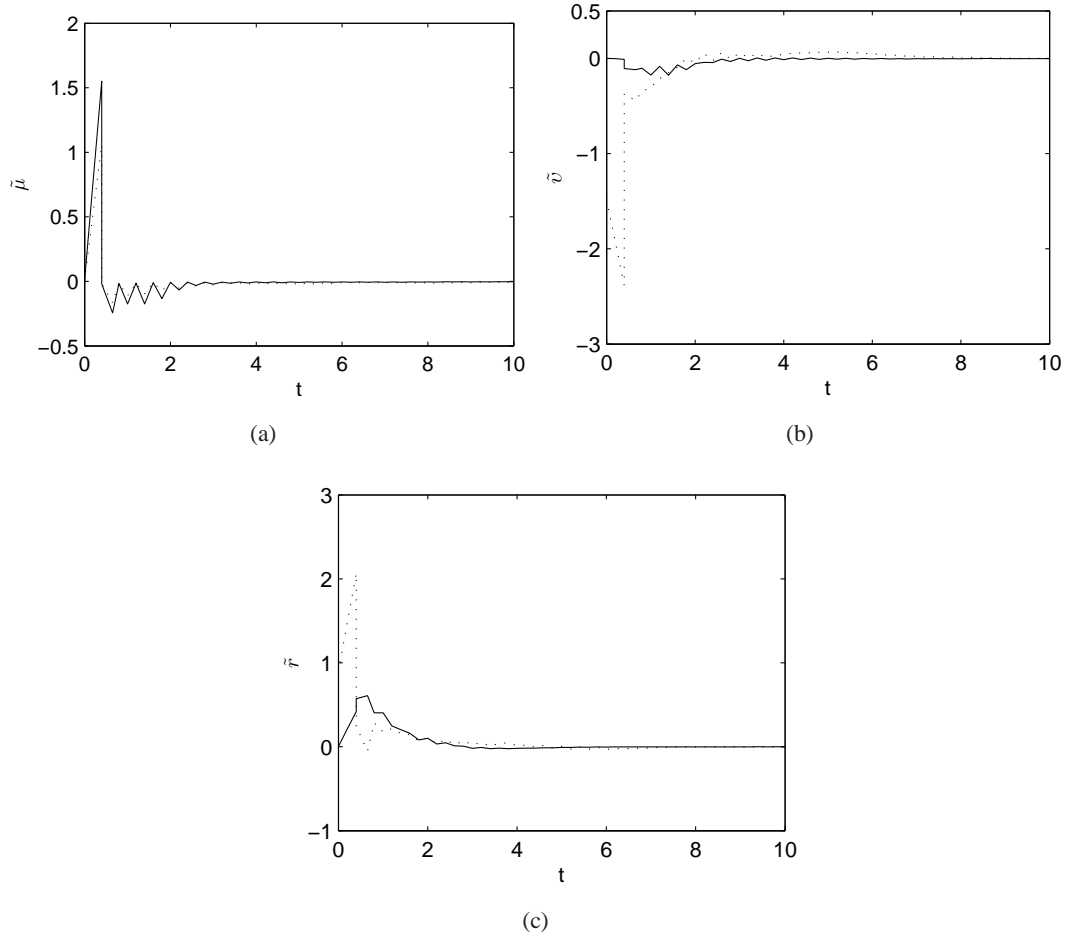
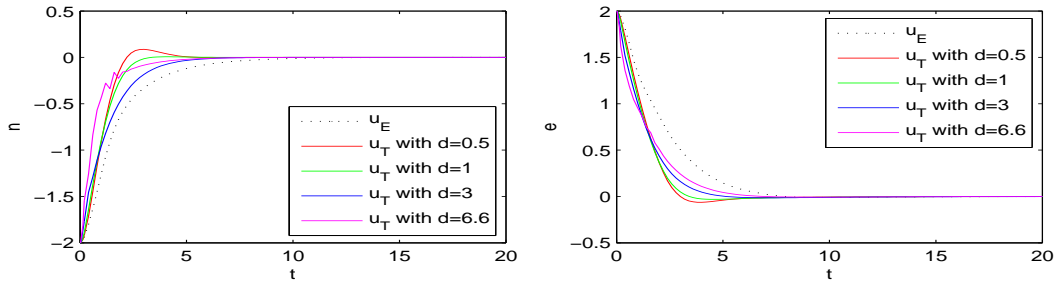


Figure 6.2: Time responses of observer errors with  $T = 0.4$ . Solid curve:observer (6.39). Dotted line:observer (6.37)-(6.38).

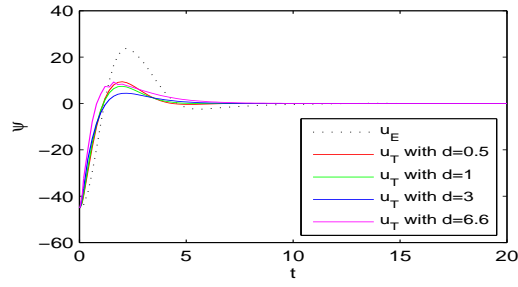
Second, the controller  $u_T$  designed using (6.27) in Theorem 6.3.3 and the controller  $u_E$  given by (6.40) will be applied to the system (6.35)-(6.36) with the observer (6.39). The controller  $u_T$  is designed with  $W_T = \frac{1}{2}\eta^T\eta + \frac{1}{2}\tilde{\nu}^T h^{-1}\tilde{\nu}$  and  $\phi_T(\eta) = -R^T(\psi)K\eta$  where  $K$  can be chosen such that  $K = \text{diag}\{k_1, k_2, k_3\}$  with  $|1 - Tk_i| < 1$  and  $k_i > 0$  for sufficiently small  $T > 0$ . The following simulation parameters are set:  $K = \text{diag}\{0.5, 0.5, 0.5\}$  and  $c = 1$  for controllers and  $h = \text{diag}\{0.082, 0.25, 1\}$  for observer. Then, simulations have been performed in order to compare the performances of the controllers  $u_T$  and  $u_E$  with different sampling periods and initial conditions.

In the first simulation, the controllers  $u_T$  and  $u_E$  are applied to the system (6.35)-(6.36) with the sampling period  $T = 0.2$  and the initial conditions,  $\eta(0) = [-2 \quad 2 \quad -\frac{\pi}{4}]^T$ ,  $\nu(0) = 0_{3 \times 1}$  and  $\hat{\nu}(0) = 0_{3 \times 1}$ . Simulation results with  $T = 0.2$  are given in Figure 6.3. As can be seen



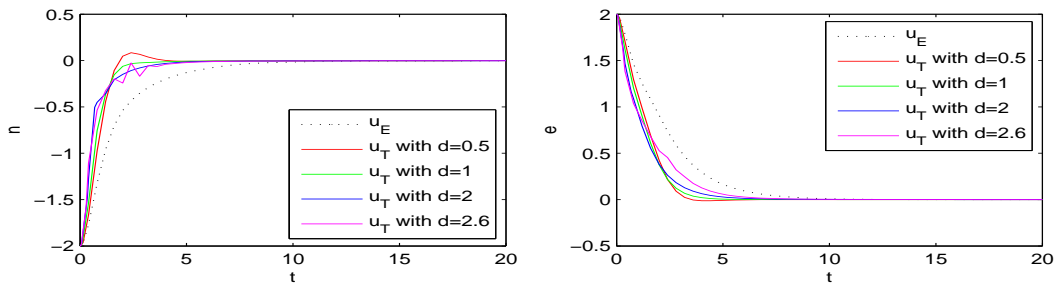
(a)

(b)



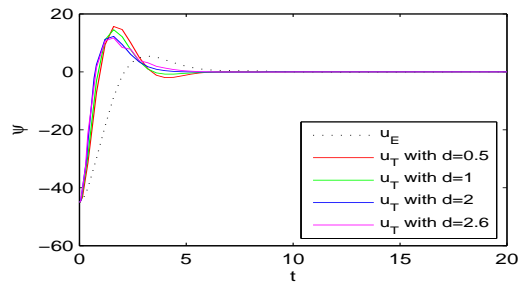
(c)

Figure 6.3: Time responses of yaw angle  $\psi$ , the North position  $n$  and the East position  $e$  with  $T = 0.2$ . Dotted line:controller  $u_E$ . Solid line:designed controller  $u_T$ .



(a)

(b)



(c)

Figure 6.4: Time responses of yaw angle  $\psi$ , the North position  $n$  and the East position  $e$  with  $T = 0.4$ . Dotted line:controller  $u_E$ . Solid line:designed controller  $u_T$ .

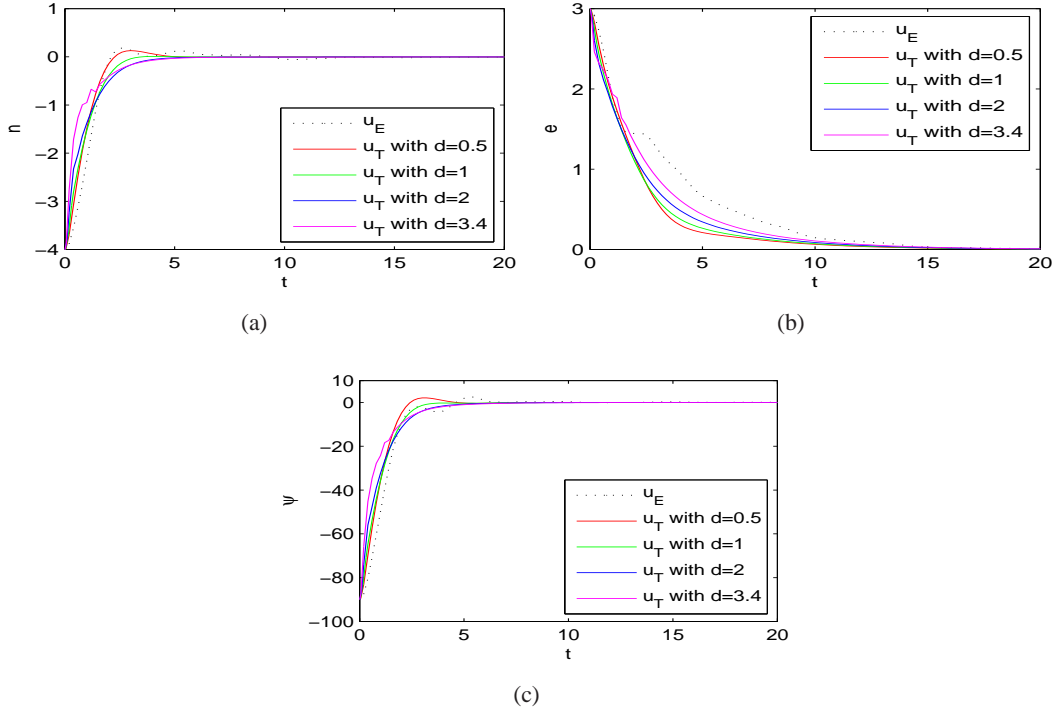


Figure 6.5: Time responses of yaw angle  $\psi$ , the North position  $n$  and the East position  $e$  with  $T = 0.2$  and large initial conditions. Dotted line:controller  $u_E$ . Solid line:designed controller  $u_T$ .

from figure, both controllers stabilize the system (6.35)-(6.36), but faster with  $u_T$ . Simulation results for the controller  $u_T$  show that as the parameter  $d$  increases, the performance of the controller  $u_T$  is faster. For  $d > 6.6$ , the controller  $u_T$  cannot stabilize the system (6.35)-(6.36).

Then, the simulation is performed with the initial conditions given above and large sampling period  $T = 0.4$ . Simulation results are given in Figure 6.3. It is shown that both controllers stabilize the system (6.35)-(6.36), but faster with  $u_T$  again. Faster results are obtained with the controller  $u_T$  until  $d = 2.6$  and the performance worsens after  $d = 2.6$ . For  $d > 2.6$ , the controller  $u_T$  cannot stabilize the system (6.35)-(6.36). Simulation results for the controller  $u_E$  show that increase in the sampling period  $T$  results in slightly slow response. While the controller  $u_E$  cannot stabilize the system (6.35)-(6.36) for  $T > 0.8$  with the initial conditions above, the controller  $u_T$  can stabilize the system until  $T = 1.2$ .

Finally, the controllers are applied to the system (6.35)-(6.36) with the same sampling period  $T = 0.2$  as in the first simulation and large initial conditions,  $\eta(0) = [-4 \ 3 \ -\frac{\pi}{2}]^T$ ,  $\nu(0) = 0_{3 \times 1}$  and  $\hat{\nu}(0) = 0_{3 \times 1}$ . Simulation results are given in Figure 6.5. It is shown that both

controllers stabilize the system (6.35)-(6.36) successfully, but faster with the controller  $u_T$ .

Moreover, when the sampling period  $T$  or the initial conditions are increased, the controller  $u_T$  gives faster results for cases where the parameter  $d$  has smaller value.

## 6.4.2 Two-Link Robot Manipulator

Consider the dynamic model of a two-link manipulator given in Subsection 3.4.2

$$\dot{\eta} = \xi \quad (6.41)$$

$$\dot{\xi} = M^{-1}(\eta)(u - C(\eta, \xi)\xi - G(\eta)) \quad (6.42)$$

where  $y(k) = \eta(k)$ , the state vectors are  $\eta := [q_1 \quad q_2]^T$  and  $\xi := [\dot{q}_1 \quad \dot{q}_2]^T$ ,  $M = \begin{bmatrix} M_1 & M_2 \\ M_3 & M_4 \end{bmatrix}$ ,  $C = \begin{bmatrix} C_1 & C_2 \\ C_3 & C_4 \end{bmatrix}$ ,  $G = \begin{bmatrix} G_1 \\ G_2 \end{bmatrix}$  and  $u = \begin{bmatrix} u_1 \\ u_2 \end{bmatrix}$  with  $M_1 = m_1 l_{c1}^2 + m_2(l_1^2 + l_{c2}^2 + 2l_1 l_{c2} \cos q_2)$ ,  $M_2 = M_3 = m_2 l_1 l_{c2} \cos q_2 + m_2 l_{c2}^2$ ,  $M_4 = m_2 l_{c2}^2$ ,  $C_1 = -m_2 l_2 l_{c2} \sin q_2 \dot{q}_2$ ,  $C_2 = -m_2 l_2 l_{c2} \sin q_2 (\dot{q}_1 + \dot{q}_2)$ ,  $C_3 = m_2 l_2 l_{c2} \sin q_2 \dot{q}_1$ ,  $C_4 = 0$ ,  $G_1 = m_1 g l_{c1} \cos q_1 + m_2 g (l_1 \cos q_1 + l_{c2} \cos(q_1 + q_2))$ ,  $G_2 = m_2 g l_{c2} \cos(q_1 + q_2)$ .  $l_{c1}$  and  $l_{c2}$  are the distances of the center of mass from the joint axes. The robot parameters are taken as  $m_1 = m_2 = 5$  [kg],  $l_1 = l_2 = 0.5$  [m],  $l_{c1} = l_{c2} = 0.25$  [m]. The control objective is to solve the trajectory tracking problem. Hence, the joint position tracking error  $e$  is defined as  $e := \eta - \eta_d$  where  $\eta_d := \begin{bmatrix} q_{1d} \\ q_{2d} \end{bmatrix}$  is the desired position trajectory. Then, the system dynamics can be written as:

$$\dot{e} = \xi - \dot{\eta}_d \quad (6.43)$$

$$\dot{\xi} = M^{-1}(\eta)(u - C(\eta, \xi)\xi - G(\eta)). \quad (6.44)$$

Using (6.19) in Theorem 6.3.1, the observer for (6.44) is designed as:

$$\hat{\xi}(k+1) = \hat{\xi} + T(M^{-1}(\eta)(u - C(\eta, \hat{\xi}) - G(\eta)) + K\tilde{\xi}) \quad (6.45)$$

with  $\tilde{\xi} = \frac{\eta(k) - \eta(k-1)}{T} - \hat{\xi}$  and where  $K$  can be chosen such that  $K = \text{diag}\{k_1, k_2\}$  with  $k_i > 0$  for sufficiently small  $T > 0$ .

Considering the observer (6.45), the controllers  $u_T$  and  $u_E$  are designed for the system (6.43)-(6.44) with  $\phi_T(\eta) = \begin{bmatrix} -c_1(q_1 - q_{1d}) + \dot{q}_{1d} \\ -c_2(q_2 - q_{2d}) + \dot{q}_{2d} \end{bmatrix}$ . The controller  $u_E$  for (6.43)-(6.44) is designed using the method given in [25] which was also presented in Theorem 2.3.3 with  $W_T(\eta) = \frac{1}{2}\eta^T \eta$ . The controller  $u_T$  is obtained using (6.27) in Theorem 6.3.3 with  $W_T(\eta) = \frac{1}{2}\eta^T \eta + \frac{1}{2}\tilde{\xi}^T L_o^{-1} \tilde{\xi}$  where  $L_o$  is a positive definite matrix. The following simulation parameters are set:  $c_1 = 2$ ,  $c_2 = 3$

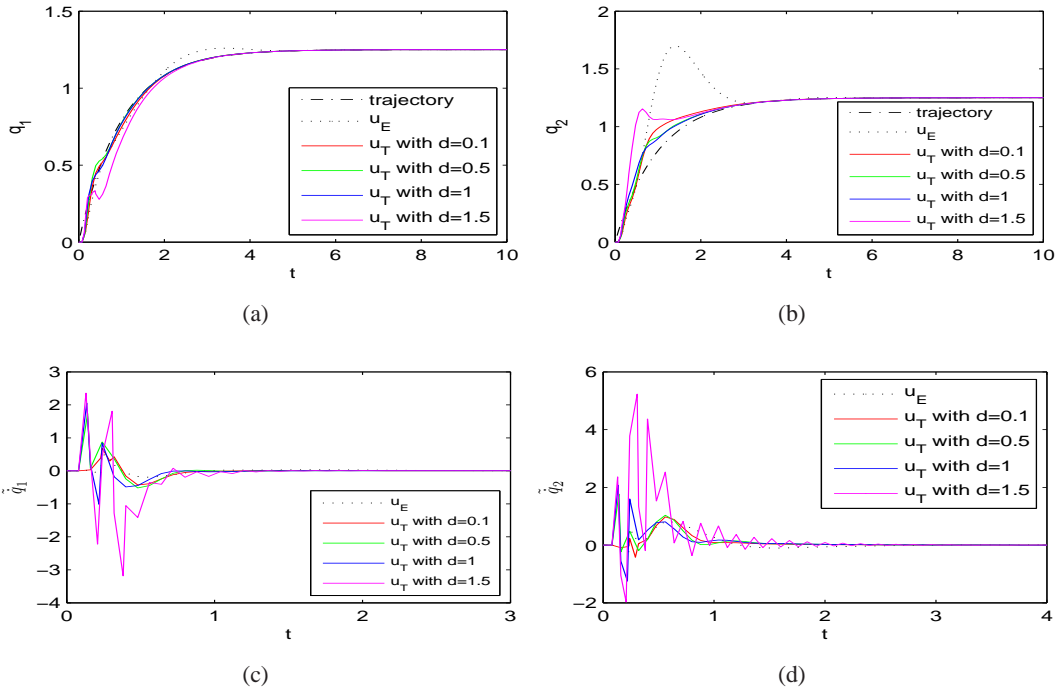


Figure 6.6: Responses of the system for the first trajectory with  $T = 0.08$ . Dotted line:controller  $u_E$ . Solid line:designed controller  $u_T$ . Dash-dotted line:desired trajectory.

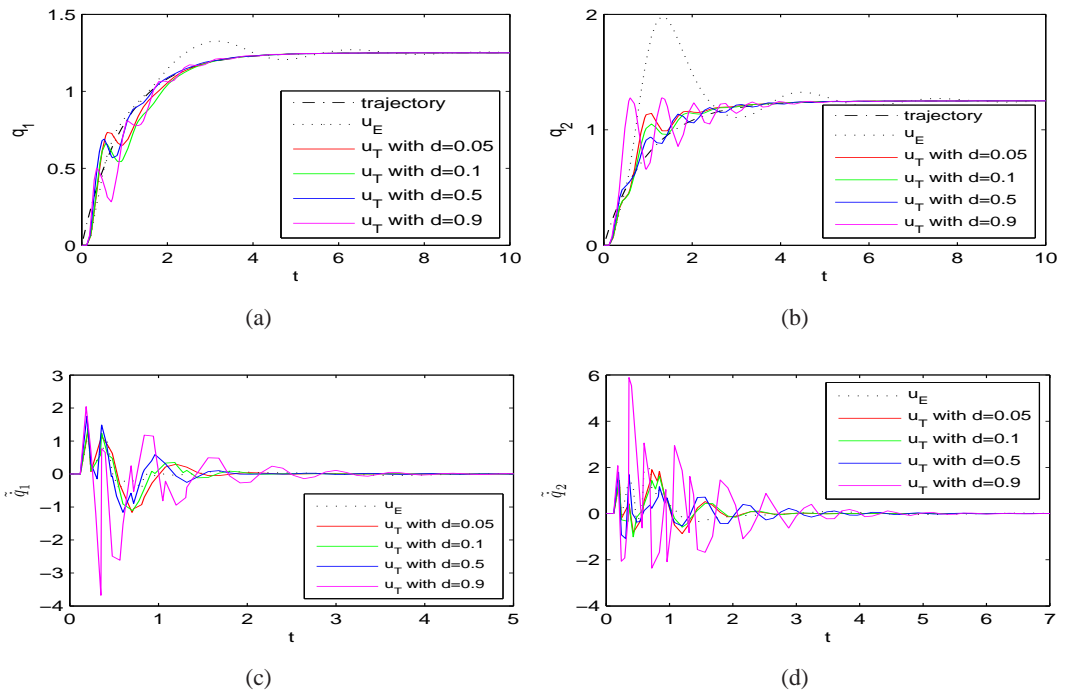


Figure 6.7: Responses of the system for the first trajectory with  $T = 0.12$ . Dotted line:controller  $u_E$ . Solid line:designed controller  $u_T$ . Dash-dotted line:desired trajectory.

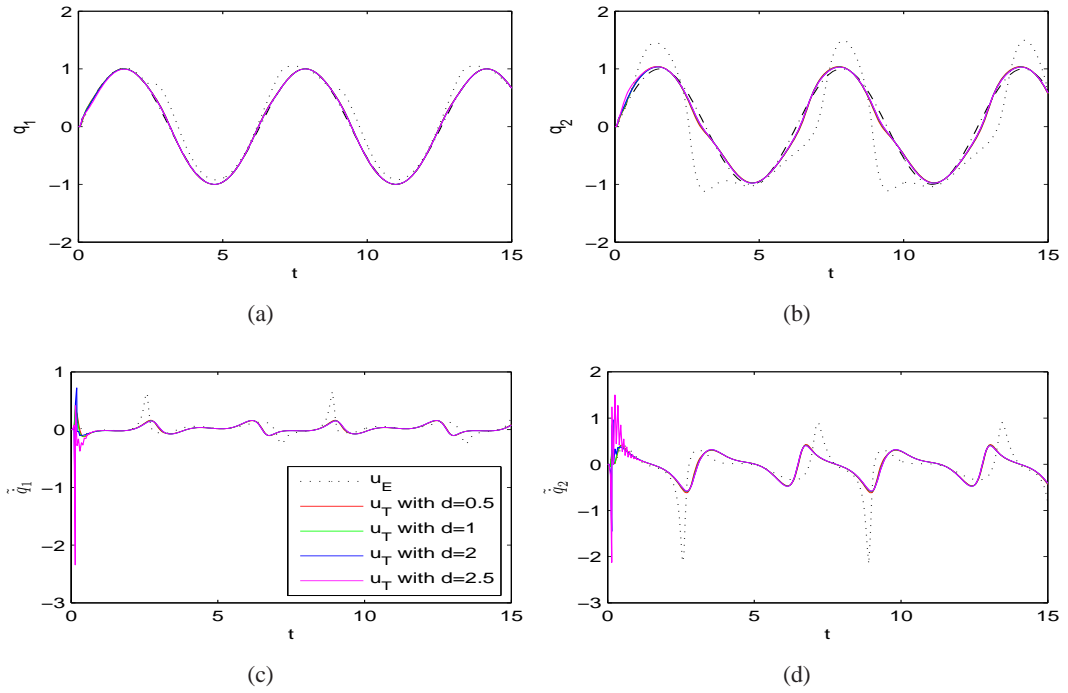


Figure 6.8: Responses of the system for the second trajectory  $T = 0.05$ . Dotted line:controller  $u_E$ . Solid line:designed controller  $u_T$ . Dash-dotted line:desired trajectory.

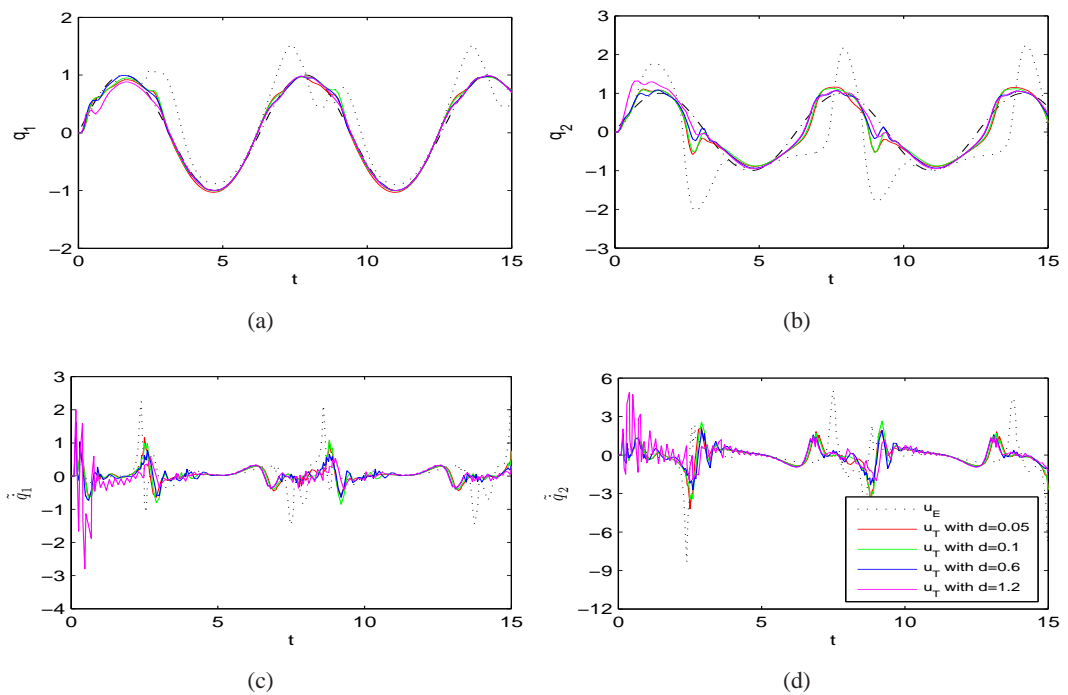


Figure 6.9: Responses of the system for the second trajectory  $T = 0.1$ . Dotted line:controller  $u_E$ . Solid line:designed controller  $u_T$ . Dash-dotted line:desired trajectory.

and  $c = 1$  for controllers and  $h = \text{diag}\{8, 9\}$  for observer. Two different reference trajectories,  $q_{d1} = q_{d2} = \frac{5}{4} - \frac{5}{4}e^{-t}$  and  $q_{d1} = q_{d2} = \sin(t)$ , are considered. Then, simulations have been performed in order to compare the performances of the controllers  $u_T$  and  $u_E$  with the initial conditions  $\eta(0) = \xi(0) = \hat{\xi}(0) = \begin{bmatrix} 0 \\ 0 \end{bmatrix}$  and different sampling periods.

First, the controllers  $u_T$  and  $u_E$  with the observer (6.45) are applied to the system (6.41)-(6.42) with the first reference trajectory,  $q_{d1} = q_{d2} = \frac{5}{4} - \frac{5}{4}e^{-t}$ .

Simulation results with  $T = 0.08$  are given in Figure 6.6. As can be seen from figure, both controllers track the desired trajectory, but the tracking error converges to zero faster with  $u_T$ . Simulation results for the controller  $u_T$  show that as the parameter  $d$  increases, the tracking error of the controller  $u_T$  is smaller. For  $d > 1.5$ , the controller  $u_T$  cannot stabilize the system (6.41)-(6.42).

Simulation results with  $T = 0.12$  are given in Figure 6.7. It is shown that both controllers track the desired trajectory, but the tracking error converges to zero faster with  $u_T$  again. Results with smaller tracking error are obtained with the controller  $u_T$  until  $d = 0.9$ . For  $d > 0.9$ , the controller  $u_T$  can not stabilize the system (6.41)-(6.42). Simulation results for the controller  $u_E$  show that increase in the sampling period  $T$  results in slower response. While the controller  $u_E$  cannot stabilize the system (6.41)-(6.42) for  $T > 0.14$ , the controller  $u_T$  can stabilize the system until  $T = 0.15$ .

Then, the controllers  $u_T$  and  $u_E$  with the observer (6.45) are applied to the system (6.41)-(6.42) with the second reference trajectory,  $q_{d1} = q_{d2} = \sin(t)$ .

Simulation results with  $T = 0.05$  are given in Figure 6.8. As can be seen from figure, the controller  $u_T$  tracks the desired trajectory with smaller tracking error when compared to the controller  $u_E$ . Simulation results for the controller  $u_T$  show that as the parameter  $d$  increases, the controller  $u_T$  tracks the desired trajectory with smaller error but for  $d = 2.5$  its performance is degraded. For  $d > 2.5$ , the controller  $u_T$  cannot stabilize the system (6.41)-(6.42).

Simulation results with  $T = 0.1$  are given in Figure 6.9. It is shown that the tracking error increases for both controllers when compared to the results with  $T = 0.05$ , but tracking error of the controller  $u_T$  is smaller than that of the controller  $u_E$ . Results with smaller tracking error are obtained with the controller  $u_T$  until  $d = 1.2$ . The performance of the controller  $u_T$  worsens after  $d = 1.2$ . For  $d > 1.2$ , the controller  $u_T$  cannot stabilize the system (6.41)-(6.42).

While the controller  $u_E$  cannot stabilize the system (3.28)-(3.29) for  $T > 0.13$ , the controller  $u_T$  can stabilize the system until  $T = 0.15$ .

Moreover, as the sampling period  $T$  increases, the controller  $u_T$  shows good performance for cases where the parameter  $d$  has smaller value.

### 6.4.3 Attitude Control of Rigid Artificial Satellite

Consider the following nonlinear equations for the digital attitude control of a rigid artificial satellite which were also given Subsection 3.4.3

$$\dot{\rho} = H(\rho)w, \quad (6.46)$$

$$\dot{w} = J^{-1}S(w)Jw + J^{-1}u \quad (6.47)$$

with sampled observation  $y(k) = \rho(k)$  where  $w := [w_1 \ w_2 \ w_3]^T \in \mathbb{R}^3$  is the angular velocity vector of the body in a body-fixed frame,  $\rho \in \mathbb{R}^3$  is the Cayley-Rodrigues parameters describing the body orientation,  $u \in \mathbb{R}^3$  is the control torque vector of the body,  $J = J^T = \text{diag}\{10, 15, 20\}$  is the inertia matrix of the body [31],  $S(w)$  is the skew-symmetric matrix given by  $S(w) = \begin{bmatrix} 0 & w_3 & -w_2 \\ -w_3 & 0 & w_1 \\ w_2 & -w_1 & 0 \end{bmatrix}$  and  $H(\rho) = \frac{1}{2}(I - S(\rho) + \rho\rho^T)$ .

Using (6.19) in Theorem 6.3.1, the observer for (6.47) is designed as:

$$\hat{w}(k+1) = \hat{w} + T(J^{-1}S(\hat{w})J\hat{w} + J^{-1}u + K\tilde{w}) \quad (6.48)$$

with  $\tilde{w} = H^{-1}(\rho)\frac{\eta(k)-\eta(k-1)}{T} - \hat{w}$  and where  $K$  can be chosen such that  $K = \text{diag}\{k_1, k_2, k_3\}$  with  $k_i > 0$  for sufficiently small  $T > 0$ .

Considering the observer (6.48), the controllers  $u_T$  and  $u_E$  are designed for the system (6.46)-(6.47) with  $\phi_T(\rho) = -H^{-1}(\rho)L\rho$  where  $L$  can be chosen such that  $L = \text{diag}\{l_1, l_2, l_3\}$  with  $|1 - Tl_i| < 1$  and  $l_i > 0$  for sufficiently small  $T > 0$ . The controller  $u_E$  is designed using the method given in [25] which was also presented in Theorem 2.3.3 with  $W_T(\eta) = \frac{1}{2}\rho^T\rho$ . The controller  $u_T$  is obtained using (6.27) in Theorem 6.3.3 with  $W_T(\eta) = \frac{1}{2}\rho^T\rho + \frac{1}{2}\tilde{w}^T L_o^{-1}\tilde{w}$  where  $L_o$  is a positive definite matrix. The following simulation parameters are set:  $L = \text{diag}\{0.5, 0.5, 0.5\}$  and  $c = 0.5$  for controllers and  $h = \text{diag}\{1, 4, 0.4\}$  for observer. Then, the controllers  $u_T$  and  $u_E$  with the observer (6.48) are applied to the system (6.46)-(6.47) in order to compare their performances with different sampling periods and initial conditions.

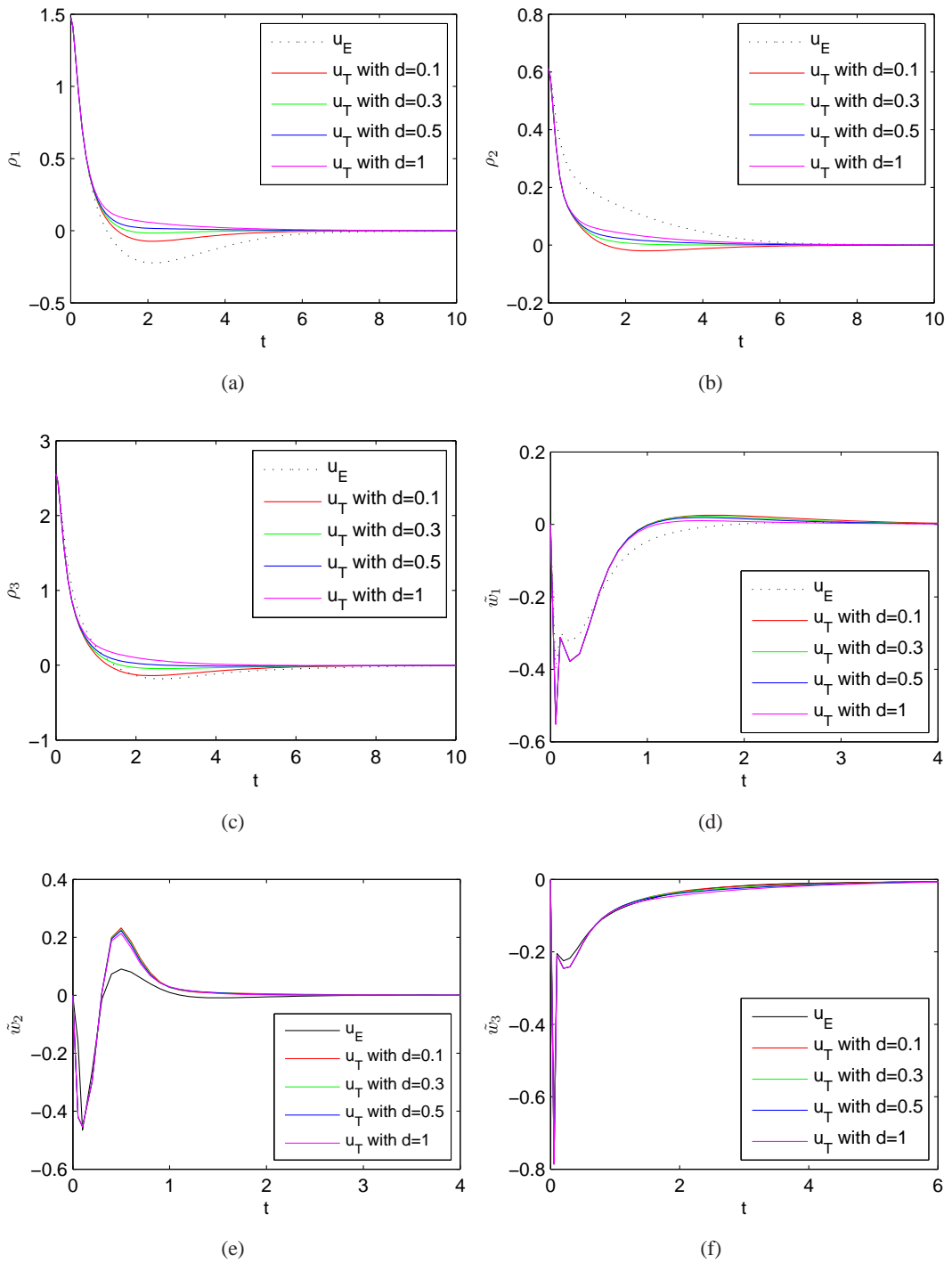


Figure 6.10: Time responses of  $\rho$  and  $\tilde{w}$  with  $T = 0.1$ . Dotted line:controller  $u_E$ . Solid line:designed controller  $u_T$ .

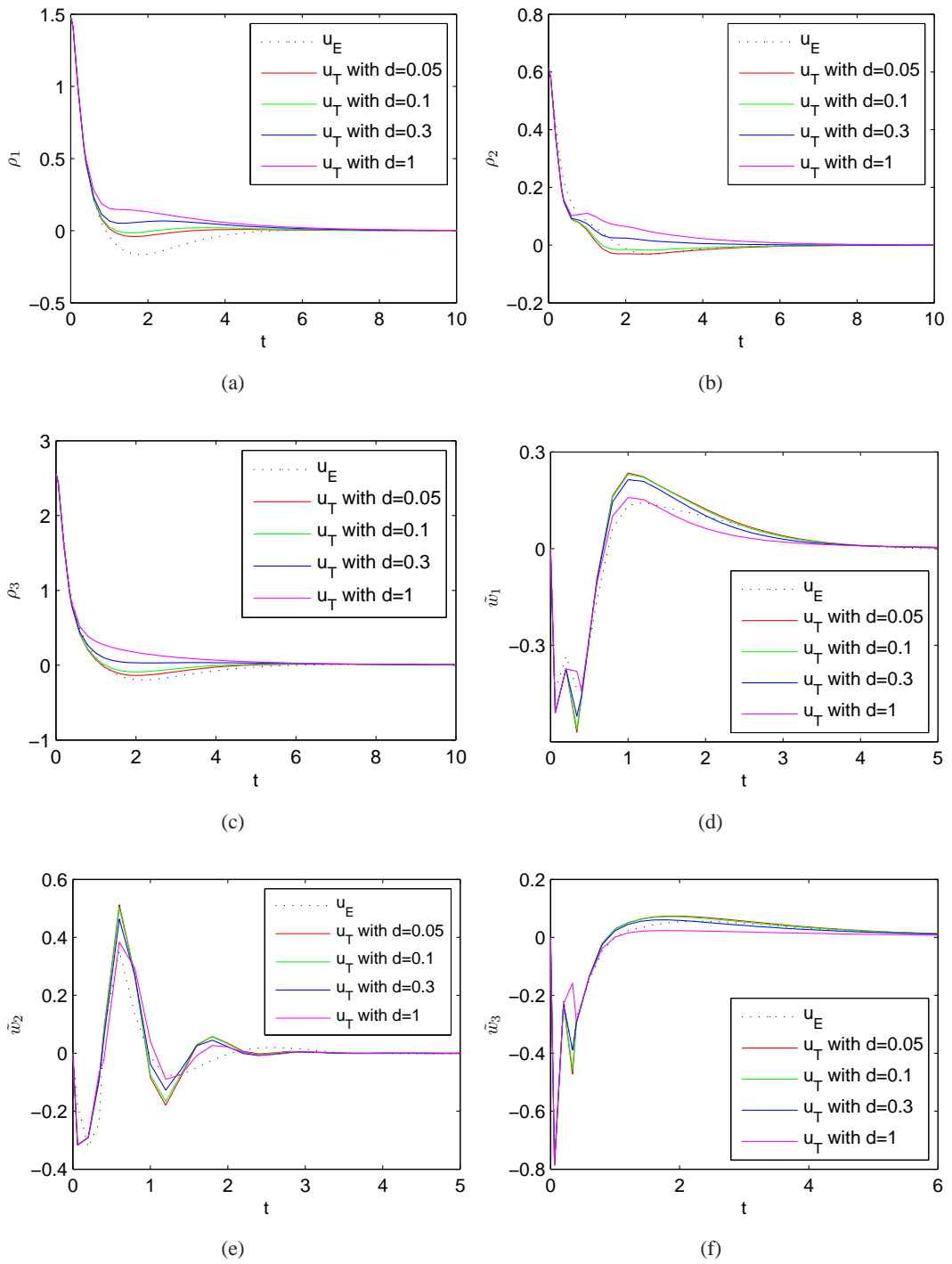


Figure 6.11: Time responses of  $\rho$  and  $\tilde{w}$  with  $T = 0.2$ . Dotted line:controller  $u_E$ . Solid line:designed controller  $u_T$ .

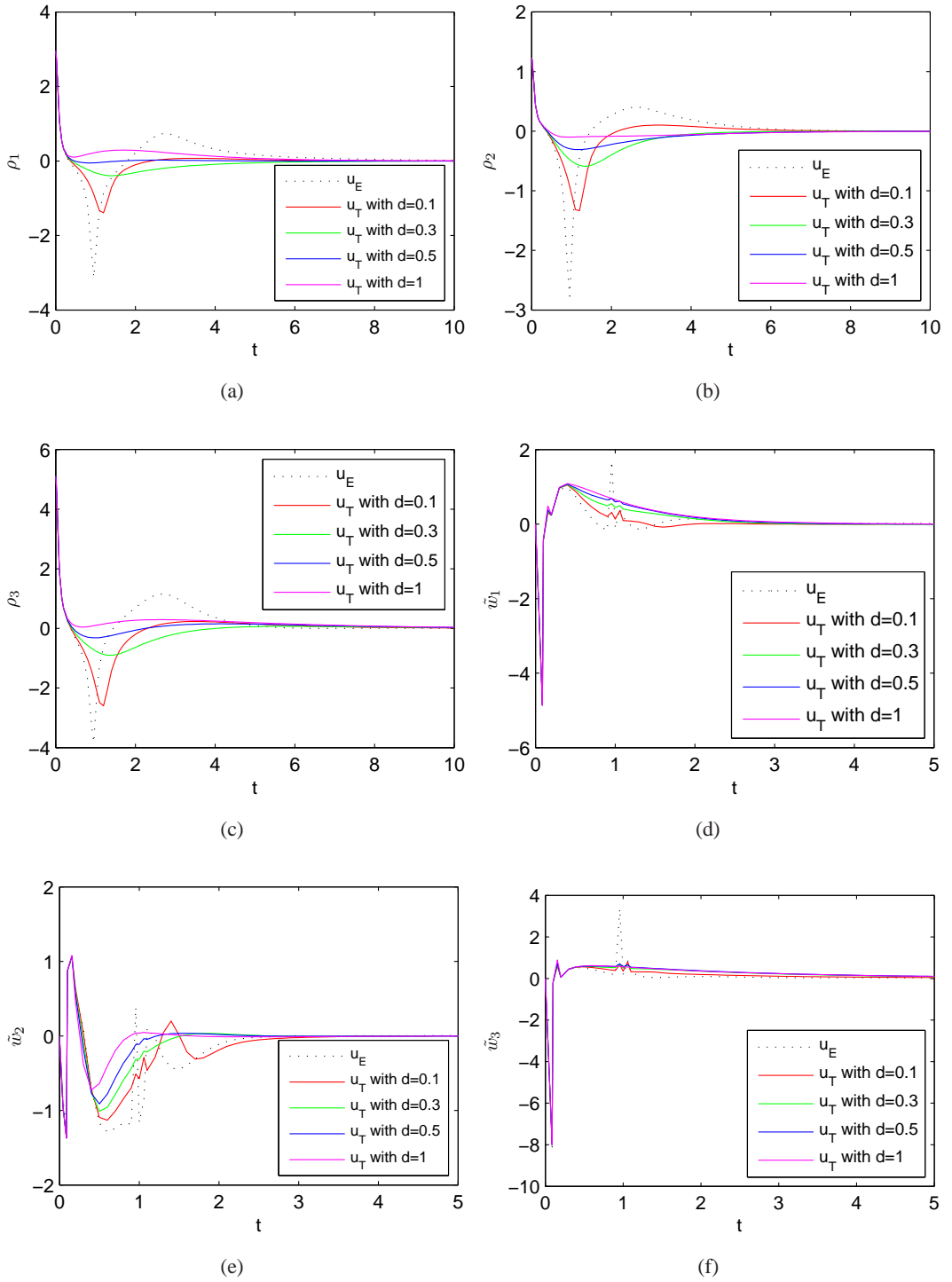


Figure 6.12: Time responses of  $\rho$  and  $\tilde{w}$  with  $T = 0.1$  and doubled initial conditions. Dotted line:controller  $u_E$ . Solid line:designed controller  $u_T$ .

In the first simulation, the initial conditions are chosen as  $\rho(0) = [1.4735 \quad 0.6115 \quad 2.5521]^T$ ,  $w(0) = 0_{3 \times 1}$  and  $\hat{w}(0) = 0_{3 \times 1}$ . Simulation results with the sampling period  $T = 0.1$  are given in Figure 6.10. As can be seen from figure, both controllers stabilize the system (6.46)-(6.47), but faster with  $u_T$ . As the parameter  $d$  increases, the performance of the controller  $u_T$  is faster but for  $d = 1$  performance degradation starts. For  $d > 7$ , the controller  $u_T$  cannot stabilize the system (6.46)-(6.47).

Then, the simulation is performed with the initial conditions given above and large sampling period  $T = 0.2$ . Simulation results are given in Figure 6.11. It is shown that the controller  $u_T$  gives faster results when compared to the controller  $u_E$ . The controller  $u_T$  shows a good performance until  $d = 1$  and the performance worsens after  $d = 1$ . For  $d > 2$ , the controller  $u_T$  cannot stabilize the system (6.46)-(6.47). The controller  $u_E$  gives slower response with larger overshoots when compared to results with  $T = 0.1$ . While the controller  $u_E$  cannot stabilize the system (6.46)-(6.47) for  $T > 0.37$ , the controller  $u_T$  can stabilize the system until  $T = 0.4$ .

Finally, the controllers are applied to the system (6.46)-(6.47) with the same sampling period  $T = 0.1$  as in the first simulation and initial conditions doubled. Simulation results are given in Figure 6.12. It is shown that the controller  $u_T$  gives faster results when compared to the controller  $u_E$  again.

Moreover, when the sampling period  $T$  or the initial conditions are increased, the controller  $u_T$  gives faster results for cases where the parameter  $d$  has smaller value.

#### 6.4.4 Second-Order Single-Input System

As a last example, consider the following continuous-time plant:

$$\dot{\eta} = \eta^2 + \xi \quad (6.49)$$

$$\dot{\xi} = u \quad (6.50)$$

where  $\eta \in \mathbb{R}$  and  $\xi \in \mathbb{R}$  are the state vectors,  $u \in \mathbb{R}$  is the control input and  $y(k) = \eta(k)$ .

Using (6.19) in Theorem 6.3.1, the observer for (6.50) is designed as:

$$\hat{\xi}(k+1) = \hat{\xi} + T(u + K\tilde{\xi}) \quad (6.51)$$

with  $\tilde{\xi} = \frac{\eta^{(k)} - \eta^{(k-1)}}{T} - \eta^2 - \hat{\xi}$  and where  $K > 0$  for sufficiently small  $T > 0$ .

Considering the observer (6.51), the controllers  $u_T$  and  $u_E$  are designed for the system (6.49)-(6.50) with  $\phi_T(\eta) = -\eta^2 - \eta$ . The controller  $u_E$  is designed using the method given in [25] which was also presented in Theorem 2.3.3 with  $W_T(\eta) = \frac{1}{2}\eta^2$ . The controller  $u_T$  is obtained using (6.27) in Theorem 6.3.3 with  $W_T(\eta) = \frac{1}{2}\eta^T\eta + \frac{1}{2}L_o^{-1}\tilde{\xi}^2$  where  $L_o > 0$ . The following simulation parameters are set:  $c = 1$  for controllers and  $K = 0.5$  for observer.

Then, the controllers  $u_T$  and  $u_E$  with the observer (6.51) are applied to the system (6.49)-(6.50) in order to compare their performances with different sampling periods and initial conditions.

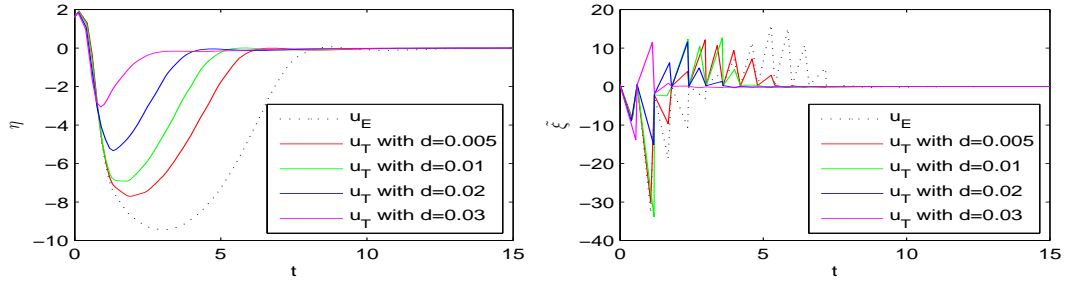
In the first simulation, the initial conditions are chosen as  $(\eta(0), \xi(0)) = (1.6, 0.5)$  and  $(\hat{\xi}(0)) = 0$ . Simulation results with  $T = 0.6$  are given in Figure 6.13. It is shown that the designed controller  $u_T$  works well and is faster than the controller  $u_E$ . As the parameter  $d$  increases, the performance of the controller  $u_T$  is faster but for  $d = 0.03$  performance degradation starts. For  $d > 0.03$ , the controller  $u_T$  cannot stabilize the system (6.49)-(6.50).

Next, the simulation is performed with the initial conditions given above and large sampling period  $T = 0.9$ . Simulation results are given in Figure 6.14. It is shown that the controller  $u_T$  yields faster results when compared to the controller  $u_E$ . The controller  $u_T$  shows a good performance until  $d = 0.006$  and the performance worsens after  $d = 0.006$ . For  $d > 0.006$ , the controller  $u_T$  can not stabilize the system (6.49)-(6.50). The controller  $u_E$  gives slower response with larger overshoots as the sampling period  $T$  is increased. Neither controller can stabilize the system (6.49)-(6.50) for  $T > 1$ .

Then, the controllers are applied to the system (6.49)-(6.50) with the same sampling period  $T = 0.6$  as in the first simulation and large initial conditions  $(\eta(0), \xi(0)) = (5, 5)$ . Simulation results are given in Figure 6.15. As can be seen from figure, while the controller  $u_E$  stabilize the system very slowly, the designed controller  $u_T$  stabilizes the system successfully.

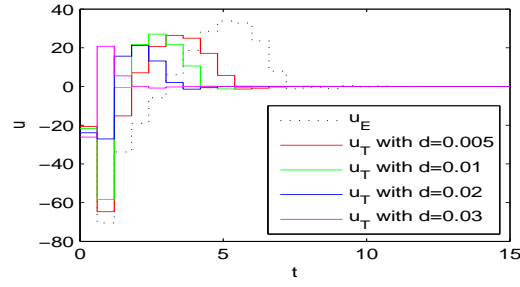
As can be seen from figures, the control input  $u_T$  is produced with less energy when compared to the control input  $u_E$ . Therefore, the proposed method requires less control effort. Simulation results also show that when the parameter  $d$  is increased, energy of the control input  $u_T$  decreases in general.

Moreover, when the sampling period  $T$  or the initial conditions are increased, the controller



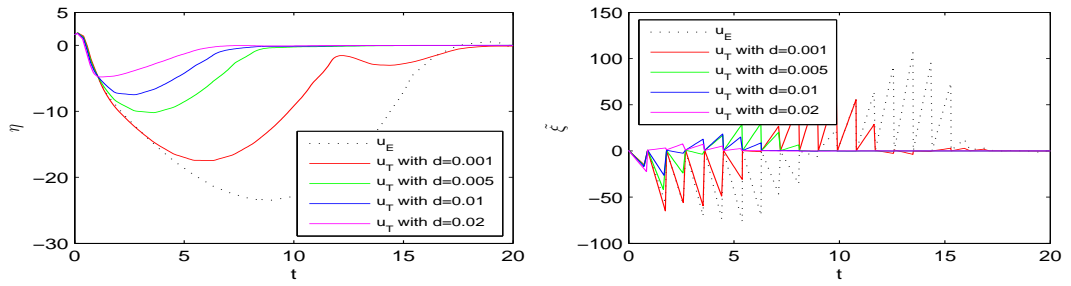
(a)

(b)



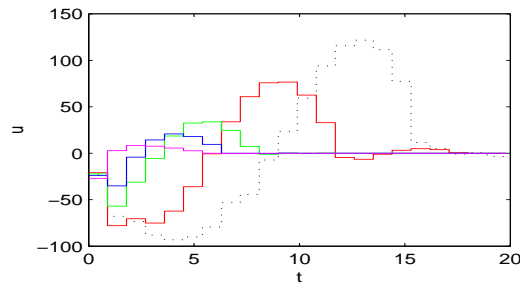
(c)

Figure 6.13: Time responses of  $\eta$ ,  $\hat{\xi}$  and  $u$  with  $T = 0.6$ . Solid line:controller  $u_T$ . Dotted line:controller  $u_E$ .



(a)

(b)



(c)

Figure 6.14: Time responses of  $\eta$ ,  $\hat{\xi}$  and  $u$  with  $T = 0.9$ . Solid line:controller  $u_T$ . Dotted line:controller  $u_E$ .

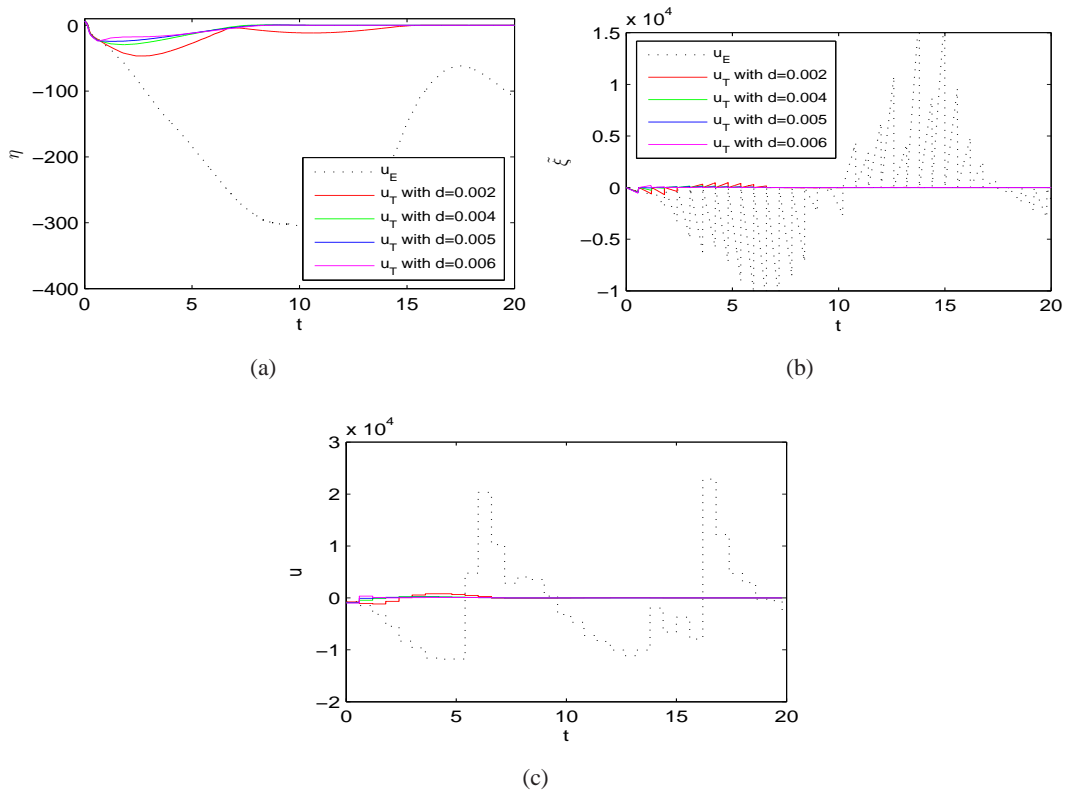


Figure 6.15: Time responses of  $\eta$ ,  $\hat{\xi}$  and  $u$  with  $T = 0.9$  and the initial condition  $(\eta(0), \xi(0)) = (5, 5)$ . Solid line:controller  $u_T$ . Dotted line:controller  $u_E$ .

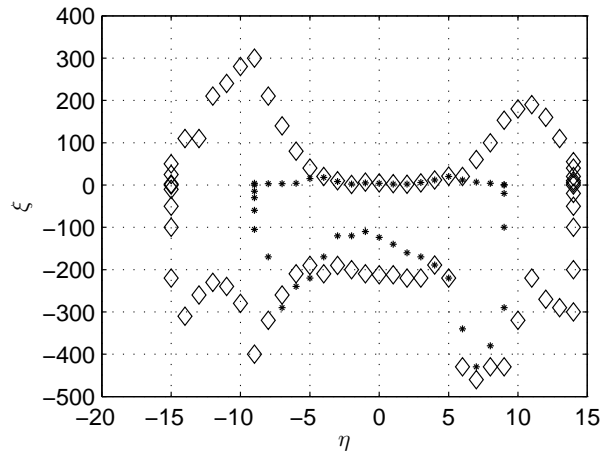


Figure 6.16: Domain of attraction estimates with  $T = 0.6$ . Diamond:controller  $u_T$ . Star:controller  $u_E$ .

$u_T$  gives faster results for cases where the parameter  $d$  has smaller value.

Finally, by applying the controllers to the system (6.49)-(6.50) with different initial conditions, domain of attraction (DOA) estimates with the controllers  $u_T$  and  $u_E$  for the sampling period  $T = 0.6$  are given in Figure 6.16. In DOA estimate with the controller  $u_T$ , the parameter  $d$  is chosen as  $d = 0.001$ . As can be seen from figure, DOA for the system with the controller  $u_T$  is much larger than that with the controller  $u_E$ . For different controller parameters and sampling periods, much larger DOA estimate may be obtained with the controller  $u_T$  when compared to the estimate given in figure.

## 6.5 Conclusions

In this chapter, the problem of reduced order observer-based output feedback control of sampled-data nonlinear systems in strict feedback form has been considered. First, a reduced order observer design has been presented based on the Euler approximate model, which is an extension of the reduced order observer given in [33] to a general class of multi-input nonlinear systems. Then, a reduced-order observer-based backstepping method has been given based on the Euler approximate model. It has been shown that the designed controllers SPA stabilize the closed-loop sampled-data system based on the framework proposed in [46]. The proposed design methods have been applied to several examples arising from the engineering practice. Their performances are analyzed with simulations.

For the problem considered, observer error behaves as disturbance. It is known that even exponentially decaying disturbances can destabilize the sampled-data nonlinear systems. Hence, in this chapter, the controllers were designed to compensate the effects of this factor. As a result of this, the results obtained are different from the controllers in [25]. Simulation results have shown that the controller designed by the proposed method gives better results than the controllers given in [25]. Moreover, in case of unstable results, the controller given in [25] can be tuned to obtain stable results by adapting the controller gain. However, the controller designed by the proposed method can also be tuned adapting another parameter in addition to the controller gain. So the proposed method gives an additional flexibility for tuning the controller.

The performance of the designed reduced order observer has been compared with the observer

given in [25]. It has been shown that observer error converges to zero with the designed observer faster than with the observer given in [25].

## CHAPTER 7

# OUTPUT-FEEDBACK STABILIZATION OF NONLINEAR DUAL-RATE SAMPLED-DATA SYSTEMS VIA APPROXIMATE DISCRETE-TIME MODEL

### 7.1 Introduction

In this chapter, the problem of output feedback stabilization of nonlinear sampled-data control systems is considered under the low measurement rate constraint. A dual-rate control scheme is proposed based on a numerical integration scheme which is used to approximately predict the missing output values between measured output samples. If an observer-based output feedback controller that semiglobally practically asymptotically (SPA) stabilizes the single-rate sampled-data plant model is given, then it is shown that SPA stability property will be preserved for the closed-loop dual-rate sampled-data system based on the proposed dual-rate control scheme under standard assumptions.

In Chapter 1, digital controller design methods for sampled-data nonlinear systems were mentioned such as emulation and direct discrete-time design methods. Although the emulation and direct discrete-time design allow multi-rate sampled-data systems, design methods using these approaches are single-rate in general, i.e. input and measurement sampling rates are assumed to be equal. For single-rate systems, [45, 46] showed that the input-to-state stabilization of exact model with the family of controllers which input-to-state stabilizes the approximate model is guaranteed under certain conditions. In [48], backstepping design is presented for a class of strict feedback nonlinear systems using Euler approximate discrete-time model. Robust backstepping method for sampled-data strict-feedback nonlinear system based on the Euler approximate model is given in [58]. However, these approaches may not perform well

in practice since the required sampling rate may exceed the hardware limitations.

In many applications only a part of the state vector is available from measurement. Thus control using output feedback or dynamic feedback is necessary. Designing an observer for unmeasured states is a useful method to be used for constructing an output feedback controller. Considering the output feedback tracking problem, observer-based output-feedback control design for continuous-time nonlinear systems using the observer backstepping procedure is proposed in [30]. On the other hand, the problem of output feedback stabilization of sampled-data nonlinear systems has not been studied much in the literature [10, 28, 65]. In particular, [10] and [28] showed that the obtained sampled-data controllers using high gain observers can recover the performance of the continuous-time state feedback controllers.

Moreover, in practical applications, hardware restrictions on input and measurement sampling rate can be different. Also, it is assumed that measurement result and the corresponding controller are available instantaneously. This assumption is unrealistic. Therefore, the use of multi-rate control scheme is proposed in [1, 56, 37, 38] to configure the control system so that several sample rates co-exist to achieve better performances. In [1] multi-rate sampled-data output feedback control of a class of nonlinear systems using high-gain observers where the analog-to-digital (A/D) sampling rate is faster than the digital-to-analog (D/A) sampling rate is considered. In [37, 38] the state feedback multi-rate controllers based on CTD and DTD methods, respectively, are discussed under the constraint that the D/A sampling rate is faster than the A/D sampling rate, called as low measurement rate constraint.

In this chapter, the problem of output feedback stabilization of sampled-data nonlinear systems under the low measurement rate constraint is considered. The design of semiglobally practically asymptotically (SPA) stabilizing dual-rate observer-based output feedback controllers is presented using single-rate observer-based output feedback controller and a fast-rate model based on the approximate discrete-time model to estimate the missing output values between measured output samples. It is shown that if a single rate observer-based output feedback controller SPA stabilizes a plant, then under some standard assumptions the proposed dual-rate observer-based output feedback controller makes the closed-loop dual-rate sampled-data system SPA stable. It is emphasized that the result is prescriptive since it can be used as a guide when designing observer-based output feedback controllers based on an approximate discrete-time model. Numerical examples are also included to illustrate the the-

oretical results obtained. Simulation results show that the dual-rate observer-based output feedback controller yields faster results when compared to the single-rate observer-based output feedback controller. However, the dual-rate design requires higher numerical effort.

The chapter is organized as follows. In Section 7.2 preliminaries are given. The main results are stated and proved in Section 7.3. Then, in Section 7.4, application examples are provided to illustrate the design method. Finally, conclusions are presented in the last section.

## 7.2 Preliminaries

This section provides technical preliminaries. Common notations and definitions which will be used throughout the chapter are presented. For the sake of clarity and easy reading, some notions and definitions that have been introduced in Chapter 2 are repeated when necessary.

Consider the nonlinear continuous-time system

$$\dot{x} = f(x(t), y(t), u(t)), \quad y(t) = H(x(t)) \quad (7.1)$$

where  $x \in \mathbb{R}^n$  is the state,  $u \in \mathbb{R}^m$  is the control input,  $y \in \mathbb{R}^l$  is the output and the functions  $f$  and  $H$  are locally Lipschitz. The control input  $u$  is realized through a zero-order hold such that  $u(t) = u(kT) := u(k), \forall t \in [kT, (k+1)T), k \in \mathbb{Z}^+$  and the output  $y$  is measured at sampling instants  $kT$ ; that is  $y(k) := y(kT)$  where  $T > 0$  is the sampling period. The difference equations corresponding to the exact discrete-time model of (7.1) and its approximate discrete-time model are represented by:

$$x(k+1) = F_T^e(x(k), y(k), u(k)), \quad y(k) = H(x(k)) \quad (7.2)$$

$$x(k+1) = F_T^a(x(k), y(k), u(k)), \quad y(k) = H(x(k)), \quad (7.3)$$

respectively.

Consider now the following family of observers

$$\hat{x}(k+1) = G_T(\hat{x}(k), y(k), u(k)) \quad (7.4)$$

**Definition 7.2.1** [33] *The family of observers (7.4) is SPA stable observer for  $x(k+1) = F_T(x(k), y(k), u(k))$ , if for any compact sets  $\mathcal{X} \subset \mathbb{R}^n, \hat{\mathcal{X}} \subset \mathbb{R}^p, \mathcal{U} \subset \mathbb{R}^m, \mathcal{Y} \subset \mathbb{R}^l$  and any strictly positive number  $\nu$ , there exists  $T^* > 0$  such that the followings hold.*

1. For all  $x_0 \in \mathcal{X}$ ,  $u \in \mathcal{U}$ ,  $y_0 \in \mathcal{Y}$  and  $T \in (0, T^*]$ , there exists  $\hat{x}_0 \in \hat{\mathcal{X}}$  such that  $|\hat{x}(k) - x(k)| \leq T\nu$ ,  $\forall k \geq 1$ .
2. For all  $x_0 \in \mathcal{X}$ ,  $\hat{x}_0 \in \hat{\mathcal{X}}$ ,  $u \in \mathcal{U}$ ,  $y_0 \in \mathcal{Y}$  and all  $T \in (0, T^*]$ ,  $\limsup_{k \rightarrow \infty} |\hat{x}(k) - x(k)| \leq T\nu$ .

**Definition 7.2.2**  $F_T^a(x, y, u)$  and  $F_{T,h}^a(x, y, u)$  is said to be one-step consistent with  $F_T^e(x, y, u)$  if for any positive real numbers  $(\Delta_1, \Delta_2, \Delta_3)$  there exist class- $\mathcal{K}$  functions  $\rho_1(\cdot), \rho_2(\cdot)$  and  $T^* > 0$  for each fixed  $T \in (0, T^*]$ , such that  $|F_T^e(x, y, u) - F_T^a(x, y, u)| \leq T\rho_1(T)$  and there exist  $h^* \in (0, T]$  such that  $|F_T^e(x, y, u) - F_{T,h}^a(x, y, u)| \leq T\rho_2(h)$  for all  $|x| \leq \Delta_1, |y| \leq \Delta_2, |u| \leq \Delta_3$  and  $h \in (0, h^*)$ .

**Definition 7.2.3** [3] The family of observers (7.4) is SPA stable as in Definition 7.2.1 if there exists a family of Lyapunov functions  $V_T(x, \hat{x})$  and class- $\mathcal{K}_\infty$  functions  $\alpha_1(\cdot), \alpha_2(\cdot), \alpha_3(\cdot)$  such that for any compact sets  $\mathcal{X} \subset \mathbb{R}^n, \hat{\mathcal{X}} \subset \mathbb{R}^p, \mathcal{U} \subset \mathbb{R}^m, \mathcal{Y} \subset \mathbb{R}^l$  and any strictly positive number  $\nu$ , there exist constants  $T^* > 0$  and  $M > 0$ , such that for all  $x, x_1, x_2 \in \mathcal{X}, \hat{x} \in \hat{\mathcal{X}}, u \in \mathcal{U}, y \in \mathcal{Y}$ , and  $T \in (0, T^*]$ ,

$$|V_T(x_1, \hat{x}) - V_T(x_2, \hat{x})| \leq M|x_1 - x_2|, \quad (7.5)$$

$$\alpha_1(|e|) \leq V_T(x, \hat{x}) \leq \alpha_2(|e|), \quad (7.6)$$

$$\frac{V_T(F_T(x, y, u), G_T(\hat{x}, y, u)) - V_T(x, \hat{x})}{T} \leq -\alpha_3(|e|) + \nu \quad (7.7)$$

where  $e$  is the observer error defined by the difference between the actual states and their estimates. Moreover, if  $F_T^a$  is consistent with  $F_T^e$  as in Definition 7.2.2 and the family of observers (7.4) is SPA stable observer for (7.3), then the family of observers (7.4) is also SPA stable observer for (7.2).

To shorten notation, the following definitions will be used:  $\tilde{x} := [\bar{x}^T, e^T]^T$ ,  $\tilde{F}_T(\tilde{x}) := \begin{bmatrix} \tilde{F}_T(\bar{x}, y, u) \\ E_T(\bar{x}, \hat{x}, y, u) \end{bmatrix}$  with  $\bar{x} := [x^T, \hat{x}^T]^T$ ,  $\tilde{F}_T(\bar{x}, y, u) := \begin{bmatrix} F_T(x, y, u) \\ G_T(\hat{x}, y, u) \end{bmatrix}$  and  $E_T(x, \hat{x}, y, u) := F_T(x, y, u) - G_T(\hat{x}, y, u)$ .

**Definition 7.2.4** [3, 48] The family of controllers  $u_T$  with observer (7.4) SPA stabilizes  $\tilde{F}_T$  if there exists  $\beta \in \mathcal{KL}$  such that for any pair of strictly positive real numbers  $(D, \nu)$  there exists  $T^* > 0$  such that for each  $T \in (0, T^*]$  the solutions of  $\tilde{x}(k+1) = \tilde{F}_T(\tilde{x}(k))$  satisfy:  $|\tilde{x}(k, \tilde{x}(0))| \leq \beta(|\tilde{x}(0)|, kT) + \nu$ , for all  $k \geq 0$ , whenever  $|\tilde{x}(0)| \leq D$ .

**Definition 7.2.5** [48] Let  $\hat{T} > 0$  be given and for each  $T \in (0, \hat{T}]$  let functions  $V_T : \mathbb{R}^{n+p} \rightarrow \mathbb{R}_{\geq 0}$  and  $u_T : \mathbb{R}^n \rightarrow \mathbb{R}^m$  be defined. We say that the pair of families  $(u_T, V_T)$  with observer (7.4) is a SPA stabilizing pair for  $\tilde{F}_T$  if there exist  $\alpha_1, \alpha_2, \alpha_3 \in \mathcal{K}_\infty$  such that for any pair of strictly positive real numbers  $(\Delta, \delta)$  there exists a triple of strictly positive real numbers  $(T^*, L, M)$ , with  $T^* \leq \hat{T}$ , such that for all  $\tilde{x}_1, \tilde{x}_2 \in \mathbb{R}^{n+p}$  with  $\max\{|\tilde{x}_1|, |\tilde{x}_2|\} \leq \Delta$ , and  $T \in (0, T^*]$ :

$$\alpha_1(|\tilde{x}|) \leq V_T(\tilde{x}) \leq \alpha_2(|\tilde{x}|) \quad (7.8)$$

$$V_T(\tilde{F}_T(\tilde{x})) - V_T(\tilde{x}) \leq -T\alpha_3(|\tilde{x}|) + T\delta \quad (7.9)$$

$$|V_T(\tilde{x}_1) - V_T(\tilde{x}_2)| \leq L|\tilde{x}_1 - \tilde{x}_2| \quad (7.10)$$

$$|u_T| \leq M \quad (7.11)$$

**Theorem 7.2.6** [45, 50, 51] If  $(u_T, V_T)$  is a SPA stabilizing pair for  $\tilde{F}_T^a$ , then  $u_T$  stabilizes  $\tilde{F}_T^e$ .

Then, stability properties of the sampled-data system (7.1) can be deduced from those of exact discretized system under certain conditions [51].

It is assumed that the single-rate SPA stabilizing output feedback controller  $u_T(\hat{x}, y)$  with observer (7.4) is given. Then, a dual-rate output feedback control scheme for system (7.1) is designed using the given single-rate observer-based output feedback controller. As in [38], it is chosen that the sampling period of (7.2) is equal to the input sampling period  $T_i$ , i.e.  $T = T_i$ . Suppose that measurement sampling period  $T_m$  is different from the input sampling period  $T_i$  due to the hardware restrictions and  $T_m > T_i$  due to the low measurement rate constraint. The main idea in the dual-rate output feedback control is to predict the unmeasured output samples between measured samples. Hence, the slow sampled measurement is used every  $T_m$  period such as  $y(0), y(T_m), y(2T_m)$ , etc., and the approximate model  $F_{T,h}^a$  of the plant is used to get the estimated output to fill in the missing samples. Let the measurement sampling period  $T_m$  be a multiple of  $T$ , i.e.  $T_m = lT$  for some integer  $l > 1$  without loss of generality. Then, to compensate for the lack of information about output which is fed back to controller and observer, a periodic switch is introduced which connects to the actual output  $y$  at times  $k/lT$  and connects to the estimate of the output at  $t = k/lT + jT$ ,  $j = 1, 2, \dots, l-1$  which is reconstructed by the approximate model with periodically updated initialization at sampling instant  $i = k/lT$  by the actual output. Then the output of the switch  $y_c(i+1) := y_c((i+1)T)$  can

be written as:

$$y_c(i+1) = \begin{cases} y(i+1), & \text{if } i+1 = kl, \\ H(F_{T,h}^a(\hat{x}(i), y(i), u(i))), & \text{if } i = kl \\ H(F_{T,h}^a(\hat{x}(i), y_c(i), u(i))), & \text{if } i+1 = kl + \tau \end{cases} \quad (7.12)$$

where  $k \in \mathbb{Z}^+$ ,  $\tau = 2, \dots, l-1$  and  $F_{T,h}^a$  is the approximate discrete-time model of (7.2) parameterized by the modeling parameter  $h > 0$  which may be different from the sampling period  $T$ . The parameter  $h$  represents the integration period of the numerical integration used to generate the approximate models. The following sampled-data closed loop system is considered which consists of the continuous-time plant and the dual-rate observer-based output feedback controller depending on the switch output  $y_c(k) := y_c(kT)$ :

$$\dot{x} = f(x(t), y(t), u(t)), \quad y(t) = H(x(t)) \quad (7.13)$$

$$\hat{x}(k+1) = G_{T,h}(\hat{x}, y_c, u) = G_T(\hat{x}, y_c, u) \quad (7.14)$$

$$u(k) = u_{T,h}(\hat{x}, y_c) = u_T(\hat{x}, y_c) \quad (7.15)$$

where  $G_{T,h}, u_{T,h}$  are zero at zero, the control  $u$  is implemented using a zero-order hold such that  $u(t) = u(kT_i) := u(k), \forall t \in [kT_i, (k+1)T_i), k \in \mathbb{Z}^+$  and the output  $y$  is measured at sampling instants  $kT_m$ ; that is  $y(k) := y(kT_m)$ . The discrete-time model of this sampled-data system consists of the exact discrete-time model (7.2), the controller (7.15), the observer (7.14) and the switch (7.12). To summarize, the dual rate output feedback control scheme uses a single-rate observer-based output feedback controller and a fast-rate model based on the approximate discrete-time model to estimate the missing output values between measured output samples.

The following definitions are now introduced.

**Definition 7.2.7** [50]  $F_T^a(x, u)$  is said to be multi-step consistent with  $F_T^e(x, u)$  if, for each  $L > 0, \eta > 0$  and each compact set  $\mathcal{X} \subset \mathbb{R}^n$ , there exist a function  $\alpha : \mathbb{R}_{\geq 0} \times \mathbb{R}_{\geq 0} \rightarrow \mathbb{R}_{\geq 0} \cup \{\infty\}$  and  $T^* > 0$  such that,  $\{x, z \in \mathcal{X}, |x - z| \leq \delta\}$  for all  $T \in (0, T^*]$  which implies  $|F_T^e(x, u) - F_T^a(z, u)| \leq \alpha(\delta, T)$  and  $k \leq L/T \Rightarrow \alpha^k(0, T) := \overbrace{\alpha(\dots\alpha(0, T), T)\dots, T}^k \leq \eta$ .

**Definition 7.2.8** The control law  $u_{T,h}$ , the observer dynamic  $G_{T,h}$  and the approximate model  $F_{T,h}^a$  are said to be uniformly locally Lipschitz if for any  $\Delta_1 > 0$  there exist  $L_u, L_f, L_g > 0$  and  $T^* > 0$  such that for each fixed  $T \in (0, T^*]$ , there exists  $h^* \in (0, T]$  such that for all  $|\xi_1|, |\xi_2| \leq$

$\Delta_1$  and  $h \in (0, h^*)$ , we have  $|u_{T,h}(\xi_1) - u_{T,h}(\xi_2)| \leq L_u |\xi_1 - \xi_2|$ ,  $|G_{T,h}(\xi_1) - G_{T,h}(\xi_2)| \leq L_g |\xi_1 - \xi_2|$  and  $|F_{T,h}^a(\xi_1) - F_{T,h}^a(\xi_2)| \leq L_f |\xi_1 - \xi_2|$ , where  $\xi := (\hat{x}^T, y_c^T)^T$ .

**Lemma 7.2.9** [38] *By the property that  $u_{T,h}$  is zero at zero and  $u_{T,h}, G_{T,h}$  are uniformly locally Lipschitz, given positive numbers  $(\Delta_1, \Delta_2, \Delta_3)$  there exist  $T^* > 0$ ,  $h^* > 0$  such that for all  $|\hat{x}| \leq \Delta_1, |y_c| \leq \Delta_2$ ,  $T \in (0, T^*]$  and  $h \in (0, h^*]$ ,  $|u_{T,h}(\hat{x}, y_c)| \leq \Delta_3$  holds. That is, the controller is locally uniformly bounded (see [27]).*

### 7.3 Main Results

In this section, it is shown that the dual-rate observer-based output feedback controller given in (7.12), (7.14) and (7.15) SPA stabilizes the closed loop sampled-data system if given single rate observer-based output feedback controller SPA stabilizes the closed loop sampled-data system. The stabilization problem is addressed under the following assumptions.

**Assumption .** (1) *The single-rate output feedback controller  $u_T(\hat{x}, y)$  with observer (7.4) SPA stabilizes the system (7.2). (2) The single-rate observer (7.4) is a SPA stable observer for (7.2). (3) The approximate models  $F_T^a$  and  $F_{T,h}^a$ , the controller (7.15) and the observer (7.14) are uniformly locally Lipschitz. (4) The approximate discrete-time models  $F_T^a$  and  $F_{T,h}^a$  are one-step consistent with the exact discrete-time model  $F_T^e$ .*

Next, two claims will be stated and their proofs will be given. These claims are to be used in the proofs of two theorems that follow.

**Claim 7.3.1** *Consider the exact model (7.2), the dual-rate output feedback control scheme (7.12), (7.14), (7.15) and Lemma 7.2.9. Given any strictly positive real numbers  $(\Delta_1, \varepsilon)$ , there exists  $T_1 > 0$  such that for any fixed  $T \in (0, T_1]$ , there exists  $h_1 \in (0, T]$  such that for all  $|\hat{x}(0)| \leq \Delta_1, |x(0)| \leq \Delta_1$  and  $h \in (0, h_1]$  the following holds under Assumptions 1-4: if  $\max_{i \in \{0, 1, \dots, k\}} |\hat{x}(i)| \leq \Delta_1$  and  $\max_{i \in \{0, 1, \dots, k\}} |x(i)| \leq \Delta_1$  for some  $k \in \{0, 1, \dots\}$  then the exact discrete-time output of the plant satisfies:  $|y(k) - y_c(k)| \leq T\varepsilon$  for all  $k$ .*

**Proof.** Let  $\Delta_1, \Delta_2, \Delta_3 \in \mathbb{R}_{\geq 0}$  be given. Using Assumption 3 and the fact that  $u_{T,h}$  is zero at zero, there exist  $T_{11} > 0$  and  $h_{11} > 0$  such that  $|u_{T,h}(\hat{x}, y_c)| \leq \Delta_3$  for all  $|\hat{x}| \leq \Delta_1, |y_c| \leq \Delta_2$

by Lemma 7.2.9. From Assumption 3, let  $T_{12} > 0$  and  $h_{12} > 0$  be generated using Definition 7.2.8. From Assumption 4, there exist  $T_{13} > 0$  and  $h_{13} > 0$  using Definition 7.2.2. Let  $L_F, L_f, L_H, L_g, L_u > 0$  be the Lipschitz constants of the functions  $F_T^a, F_{T,h}^a, H(\cdot), G_T$  and  $u_{T,h}$ , respectively. Using Definition 7.2.2, let  $\rho_1(\cdot), \rho_2(\cdot) \in \mathcal{K}_\infty$  be a function from Assumption 4 for one-step consistency of the approximate models  $F_T^a$  and  $F_{T,h}^a$  with the exact model  $F_T^e$ , respectively. Finally,  $T_1 = \min\{T_{11}, T_{12}, T_{13}\}$  and  $h_1 = \min\{h_{11}, h_{12}, h_{13}\}$  are defined. Suppose  $T \in (0, T_1]$ ,  $h \in (0, h_1]$ ,  $\max_{i \in \{0,1,\dots,k\}} |\hat{x}(i)| \leq \Delta_1$ ,  $\max_{i \in \{0,1,\dots,k\}} |x(i)| \leq \Delta_1$  and  $\max_{i \in \{0,1,\dots,k\}} |y(i)| \leq \Delta_2$  by the Lipschitzity of  $H(\cdot)$  for some  $k \in \{0, 1, \dots\}$ . First it is claimed that  $|y_c(k)| \leq \Delta_2$  follows by induction for some  $k \in \{0, 1, \dots\}$ . Consider  $k$  in the following three cases.

First, if  $k = jl$  for some  $j \in \{0, 1, \dots\}$  then it is obvious that  $|y(k) - y_c(k)| = 0$ . Since the single-rate observer (7.4) with initial condition  $|\hat{x}(0)| \leq \Delta_1$  is SPA stable by Assumption 2, it is obtained that  $|x(k) - \hat{x}(k)| \leq T\nu$  with  $\nu > 0$  using Definition 7.2.1 and the condition  $\max_{i \in \{0,1,\dots,k\}} |\hat{x}(i)| \leq \Delta_1$ .

Second, if  $k = jl + 1$ , then using Assumption 4 and triangle inequalities it can be written that

$$\begin{aligned} |y(k) - y_c(k)| &= |H(F_T^e(x(jl), y(jl), u_{T,h}(\hat{x}(jl), y(jl)))) - H(F_{T,h}^a(\hat{x}(jl), y(jl), u_{T,h}(\hat{x}(jl), y(jl))))| \\ &\leq L_H T \rho_2(h) + |H(F_{T,h}^a(x(jl), y(jl), u_{T,h}(\hat{x}(jl), y(jl)))) - H(F_{T,h}^a(\hat{x}(jl), y(jl), u_{T,h}(\hat{x}(jl), y(jl))))|. \end{aligned}$$

Hence, using Assumption 3 and  $|x(jl) - \hat{x}(jl)| \leq T\nu$ , it can be obtained that

$$|y(k) - y_c(k)| \leq L_H T \rho_2(h) + L_H L_f T \nu.$$

By Assumption 2 and Definition 7.2.1, one obtains that

$$|x(k) - \hat{x}(k)| = |F_T^e(x(jl), y(jl), u_{T,h}(\hat{x}(jl), y(jl))) - G_T(\hat{x}(jl), y(jl), u_{T,h}(\hat{x}(jl), y(jl)))| \leq T\nu$$

with  $\nu > 0$ .

Finally, using Assumption 3, it can be written for all  $k \in \{jl + 2, \dots, (j + 1)l - 1\}$  that

$$\begin{aligned} |x(k) - \hat{x}(k)| &= |F_T^e(x(k-1), y(k-1), u_{T,h}(\hat{x}(k-1), y_c(k-1))) \\ &\quad - G_T(\hat{x}(k-1), y_c(k-1), u_{T,h}(\hat{x}(k-1), y_c(k-1)))| \\ &\leq T\nu + |F_T^e(x(k-1), y(k-1), u_{T,h}(\hat{x}(k-1), y_c(k-1))) \\ &\quad - F_T^a(x(k-1), y(k-1), u_{T,h}(\hat{x}(k-1), y_c(k-1)))| \end{aligned}$$

$$\begin{aligned}
& + |F_T^a(x(k-1), y(k-1), u_{T,h}(\hat{x}(k-1), y(k-1))) \\
& - F_T^e(x(k-1), y(k-1), u_{T,h}(\hat{x}(k-1), y(k-1)))| \\
& + |F_T^a(x(k-1), y(k-1), u_{T,h}(\hat{x}(k-1), y_c(k-1))) \\
& - F_T^a(x(k-1), y(k-1), u_{T,h}(\hat{x}(k-1), y(k-1)))| \\
& + |G_T(\hat{x}(k-1), y(k-1), u_{T,h}(\hat{x}(k-1), y(k-1))) \\
& - G_T(\hat{x}(k-1), y_c(k-1), u_{T,h}(\hat{x}(k-1), y_c(k-1)))| \\
& \leq T\nu + 2T\rho_1(T) + (L_F L_u + L_g(1 + L_u))|y(k-1) - y_c(k-1)| \leq T\tilde{\nu}
\end{aligned}$$

with  $\tilde{\nu} > 0$ .

Then, it can be obtained by induction that

$$\begin{aligned}
|y(k) - y_c(k)| & = |H(F_T^e(x(k-1), y(k-1), u_{T,h}(\hat{x}(k-1), y_c(k-1)))) \\
& \quad - H(F_{T,h}^a(\hat{x}(k-1), y_c(k-1), u_{T,h}(\hat{x}(k-1), y_c(k-1))))| \\
& \leq L_H T \rho(h) + |H(F_{T,h}^a(x(k-1), y(k-1), u_{T,h}(\hat{x}(k-1), y_c(k-1)))) \\
& \quad - H(F_{T,h}^a(\hat{x}(k-1), y_c(k-1), u_{T,h}(\hat{x}(k-1), y_c(k-1))))| \\
& \leq L_H T \rho_2(h) + L_H L_f T \tilde{\nu} + L_H L_f |y(k-1) - y_c(k-1)|
\end{aligned}$$

Consequently, by the choice of  $T$  and  $h$  it is obtained that  $|y(k) - y_c(k)| \leq T\varepsilon$  for all  $k$ . This completes the proof of Claim 1.  $\blacksquare$

**Claim 7.3.2** [38] *Let  $\alpha_1, \alpha_2, \alpha_3 \in \mathcal{K}_\infty$  and strictly positive real numbers  $(\Delta, \delta)$  be such that  $\alpha_1(\Delta) \geq \delta$ . Let  $T_2 > 0$  be such that for each fixed  $T \in (0, T_2]$ , there exists  $h_2 \in (0, T]$  such that for any  $h \in (0, h_2]$  there exists a function  $V_T : \mathbb{R}^{n+p} \rightarrow \mathbb{R}_{\geq 0}$  such that  $\alpha_1(|\tilde{x}|) \leq V_T(\tilde{x}) \leq \alpha_2(|\tilde{x}|)$  for all  $\tilde{x} \in \mathbb{R}^{n+p}$  and  $V_T(\tilde{x}(i+1)) - V_T(\tilde{x}(i)) \leq -\frac{T}{4}\alpha_3(|\tilde{x}(i)|)$  holds for all  $\tilde{x} \in \mathbb{R}^{n+p}$  with  $|\tilde{x}| \leq \Delta$  and  $\max\{V_T(\tilde{x}(i+1)), V_T(\tilde{x}(i))\} \geq \delta$ . Then,  $|\tilde{x}(i)| \leq \delta$  holds for all  $|\tilde{x}(0)| \leq \alpha_2^{-1} \circ \alpha_1(\Delta)$  and all  $i \in \mathbb{Z}^+$ .*

**Proof.** By Assumption 1 and Definition 7.2.5, there exists a function  $V_T$  for all  $\tilde{x} \in \mathbb{R}^{n+p}$  such that  $\alpha_1(|\tilde{x}|) \leq V_T(\tilde{x}) \leq \alpha_2(|\tilde{x}|)$ . As stated in [38], the definitions of  $\delta$  and  $\Delta$  imply  $|\tilde{x}(0)| \leq \max\{\alpha_1^{-1} \circ V_T(\tilde{x}(0)), \alpha_1^{-1}(\delta)\} \leq \Delta$ . So either  $V_T(\tilde{x}(1)) \geq \delta$  which, from the condition of Claim 7.3.2, implies  $V_T(\tilde{x}(1)) \leq V_T(\tilde{x}(0))$  or else  $V_T(\tilde{x}(1)) \leq \delta$ . Then, in either case,  $V_T(\tilde{x}(1)) \leq \max\{V_T(\tilde{x}(0)), \delta\}$ . Hence  $V_T(\tilde{x}(i)) \leq \max\{V_T(\tilde{x}(0)), \delta\}$  follows by induction and  $|\tilde{x}(i)| \leq \Delta$  holds as well.  $\blacksquare$

In the following theorem, it is shown that the observer (7.14) is a SPA stable observer with (7.12) for the system (7.2) and this is proved using the conditions given in Definition 7.2.3.

**Theorem 7.3.3** *Consider the exact model (7.2), the dual-rate output feedback control scheme (7.12), (7.14), (7.15), Lemma 7.2.9, Claim 7.3.1 and Claim 7.3.2. Given any strictly positive real number  $\Delta_1$ , there exists  $T_1 > 0$  such that for any fixed  $T \in (0, T_1]$ , there exists  $h_1 \in (0, T]$  such that for all  $|\hat{x}(0)| \leq \Delta_1$ ,  $|x(0)| \leq \Delta_1$  and  $h \in (0, h_1]$ . Then, the observer (7.14) is a SPA stable observer with (7.12) for the system (7.2) under Assumptions 1-4.*

**Proof.** Let  $\Delta_1, \Delta_2, \Delta_3, \nu, \varepsilon \in \mathbb{R}_{\geq 0}$ ,  $|x| \leq \Delta_1$ ,  $|\hat{x}| \leq \Delta_1$ ,  $|y| \leq \Delta_2$  by the Lipschitzity of  $H(\cdot)$ ,  $|y_c| \leq \Delta_2$ . Using Assumption 3 and the fact that  $u_{T,h}$  is zero at zero, there exist  $T_{11} > 0$  and  $h_{11} > 0$  such that  $|u_{T,h}(\hat{x}, y_c)| \leq \Delta_3$  for all  $|\hat{x}| \leq \Delta_1$ ,  $|y_c| \leq \Delta_2$  by Lemma 7.2.9. From Assumption 3, let  $T_{12} > 0$  and  $h_{12} > 0$  be generated using Definition 7.2.8. From Assumption 4, there exist  $T_{13} > 0$  and  $h_{13} > 0$  using Definition 7.2.2. Let  $L_v, L_f, L_g, L_u > 0$  be the Lipschitz constants of the functions  $V_e, F_T^a, G_T$  and  $u_{T,h}$ , respectively. Using Definition 7.2.2, let  $\rho_1(\cdot) \in \mathcal{K}_\infty$  be a function from Assumption 4 for one-step consistency of  $F_T^a$  with  $F_T^e$ . From Claim 7.3.1 and Claim 7.3.2, let  $T_{14} > 0$ ,  $h_{14} > 0$  and  $T_{15} > 0$ ,  $h_{15} > 0$  be generated, respectively. Finally,  $T_1 = \min\{T_{11}, T_{12}, T_{13}, T_{14}, T_{15}\}$  and  $h_1 = \min\{h_{11}, h_{12}, h_{13}, h_{14}, h_{15}\}$  are defined. Suppose  $T \in (0, T_1]$ ,  $h \in (0, h_1]$ ,  $\max_{i \in \{0, 1, \dots, k\}} |\hat{x}(i)| \leq \Delta_1$ ,  $\max_{i \in \{0, 1, \dots, k\}} |x(i)| \leq \Delta_1$ . By Assumption 2, Lyapunov function  $V_e$  for the observer error  $e = x - \hat{x}$  satisfies

$$\Delta V_e = V_e(E_T^e(x, \hat{x}, y, u_T(\hat{x}, y))) - V_e(e) \leq -T\alpha(|e|) + T\nu \quad (7.16)$$

where  $\alpha \in \mathcal{K}_\infty$ ,  $\nu > 0$  is sufficiently small number and  $E_T^e(x, \hat{x}, y, u_T(\hat{x}, y)) := F_T^e(x, y, u_T(\hat{x}, y)) - G_T(\hat{x}, y, u_T(\hat{x}, y))$ .

Consider the observer (7.14). It is obvious that conditions (7.5) and (7.6) are satisfied and hence, to prove SPA stability, it is enough to show that condition (7.7) holds. First, the following equations are defined for the observer error dynamics:

$$E_{T,h}^e(x, \hat{x}, y_c, u_{T,h}(\hat{x}, y_c)) := F_T^e(x, y, u_{T,h}(\hat{x}, y_c)) - G_{T,h}(\hat{x}, y_c, u_{T,h}(\hat{x}, y_c)) \quad (7.17)$$

$$E_{T,h}^a(x, \hat{x}, y_c, u_{T,h}(\hat{x}, y_c)) := F_T^a(x, y, u_{T,h}(\hat{x}, y_c)) - G_{T,h}(\hat{x}, y_c, u_{T,h}(\hat{x}, y_c)) \quad (7.18)$$

$$E_T^a(x, \hat{x}, y, u_T(\hat{x}, y)) := F_T^a(x, y, u_T(\hat{x}, y)) - G_T(\hat{x}, y, u_T(\hat{x}, y)). \quad (7.19)$$

Using Assumption 4, (7.16)-(7.19) and continuity of  $V_e$ , the Lyapunov difference for the observer error can be written as:

$$\begin{aligned}
\Delta V_e &= V_e(E_{T,h}^e(x, \hat{x}, y_c, u_{T,h}(\hat{x}, y_c))) - V_e(e) \\
&= V_e(E_{T,h}^e(x, \hat{x}, y_c, u_{T,h}(\hat{x}, y_c))) - V_e(E_T^e(x, \hat{x}, y, u_T(\hat{x}, y))) + V_e(E_T^e(x, \hat{x}, y, u_T(\hat{x}, y))) - V_e(e) \\
&\leq V_e(E_{T,h}^e(x, \hat{x}, y_c, u_{T,h}(\hat{x}, y_c))) - V_e(E_{T,h}^a(x, \hat{x}, y_c, u_{T,h}(\hat{x}, y_c))) + V_e(E_T^a(x, \hat{x}, y, u_T(\hat{x}, y))) \\
&\quad - V_e(E_T^e(x, \hat{x}, y, u_T(\hat{x}, y))) + V_e(E_{T,h}^a(x, \hat{x}, y_c, u_{T,h}(\hat{x}, y_c))) - V_e(E_T^a(x, \hat{x}, y, u_T(\hat{x}, y))) - T\alpha(|e|) \\
&\quad + T\nu \leq -T\alpha(|e|) + T\nu + V_e(E_{T,h}^a(x, \hat{x}, y_c, u_{T,h}(\hat{x}, y_c))) - V_e(E_T^a(x, \hat{x}, y, u_T(\hat{x}, y))) + 2L_\nu T\rho_1(T)
\end{aligned}$$

Then, using continuity of  $V_e$ , Claim 7.3.1, Claim 7.3.2 and Assumption 3, it can be written that

$$\begin{aligned}
\Delta V_e &\leq -T\alpha(|e|) + T\nu + 2L_\nu T\rho_1(T) + L_\nu L_f L_u |y_c - y| + L_\nu L_g |y_c - y| + L_\nu L_g L_u |y_c - y| \\
&\leq -T\alpha(|e|) + T\nu + 2L_\nu T\rho_1(T) + (L_\nu L_f L_u + L_\nu L_g + L_\nu L_g L_u) T\varepsilon
\end{aligned}$$

A sufficiently small  $\tilde{\nu} > \nu$  can be picked such that there exists  $T^1 > 0$  such that for each  $T \in (0, T^1]$ , there exists  $h^1 \in (0, T]$  such that  $T\nu + 2L_\nu T\rho_1(T) + (L_\nu L_f L_u + L_\nu L_g + L_\nu L_g L_u) T\varepsilon \leq T\tilde{\nu}$  for all  $h \in (0, h^1]$  and hence  $\Delta V_e \leq -T\alpha(|e|) + T\tilde{\nu}$ . Consequently, condition (7.7) is satisfied and this completes the proof.  $\blacksquare$

In the following theorem, it is shown that the dual-rate observer-based output feedback controller (7.14), (7.15) and (7.12) SPA stabilizes the system (7.2) and this is proved using the conditions given in Definition 7.2.5.

**Theorem 7.3.4** *Consider the exact model (7.2), the dual-rate output feedback control scheme (7.12), (7.14), (7.15), Lemma 7.2.9, Claim 7.3.1 and Claim 7.3.2. Given any strictly positive real numbers  $\Delta_1$ , there exists  $T_1 > 0$  such that for any fixed  $T \in (0, T_1]$ , there exists  $h_1 \in (0, T]$  such that for all  $|\hat{x}(0)| \leq \Delta_1$ ,  $|x(0)| \leq \Delta_1$  and  $h \in (0, h_1]$ . Then the system (7.2) is SPA stable with the dual-rate observer-based output feedback controller (7.14), (7.15) and (7.12) under Assumptions 1-4.*

**Proof.** Let  $\Delta_1, \Delta_2, \Delta_3, \delta, \varepsilon \in \mathbb{R}_{\geq 0}$ ,  $|x| \leq \Delta_1$ ,  $|\hat{x}| \leq \Delta_1$ ,  $|y| \leq \Delta_2$  by the Lipschitzity of  $H(\cdot)$  and  $|y_c| \leq \Delta_2$ . Using Assumption 3 and the fact that  $u_{T,h}$  is zero at zero, there exist  $T_{11} > 0$  and  $h_{11} > 0$  such that  $|u_{T,h}(\hat{x}, y_c)| \leq \Delta_3$  for all  $|\hat{x}| \leq \Delta_1$ ,  $|y_c| \leq \Delta_2$  by Lemma 7.2.9. From Assumption 3, let  $T_{12} > 0$  and  $h_{12} > 0$  be generated using Definition 7.2.8. From Assumption

4, there exist  $T_{13} > 0$  and  $h_{13} > 0$  using Definition 7.2.2. Let  $L_v, L_f, L_g, L_u > 0$  be the Lipschitz constants of the functions  $V_T, F_T^a, G_T$  and  $u_{T,h}$ , respectively. Using Definition 7.2.2, let  $\rho_1(\cdot) \in \mathcal{K}_\infty$  be a function from Assumption 4 for one-step consistency of  $F_T^a$  with  $F_T^e$ . From Claim 7.3.1 and Claim 7.3.2, let  $T_{14} > 0, h_{14} > 0$  and  $T_{15} > 0, h_{15} > 0$  be generated, respectively. Finally,  $T_1 = \min\{T_{11}, T_{12}, T_{13}, T_{14}, T_{15}\}$  and  $h_1 = \min\{h_{11}, h_{12}, h_{13}, h_{14}, h_{15}\}$  are defined. Suppose  $T \in (0, T_1], h \in (0, h_1], \max_{i \in \{0, 1, \dots, k\}} |\hat{x}(i)| \leq \Delta_1, \max_{i \in \{0, 1, \dots, k\}} |x(i)| \leq \Delta_1$ . Let the Lyapunov function  $V(\tilde{x})$  be defined as  $V(\tilde{x}) = V_T(\tilde{x}) + V_e(e)$ . By Assumption 1, the Lyapunov difference can be written as

$$\begin{aligned} \Delta V &= V(\tilde{F}_T^e(\tilde{x})) - V(\tilde{x}) = V_T(\tilde{F}_T^e(\tilde{x}, y, u_T(\hat{x}, y))) - V_T(\tilde{x}) + V_e(E_T^e(x, \hat{x}, y, u_T(\hat{x}, y))) - V_e(e) \\ &\leq -T\tilde{\alpha}(|\tilde{x}|) + T\delta \end{aligned} \quad (7.20)$$

where  $\tilde{\alpha} \in \mathcal{K}_\infty, \delta > 0$  is a sufficiently small number.

Consider the output feedback controller (7.14)-(7.15). It is obvious that conditions (7.8) and (7.10) are satisfied and hence it is enough to show that condition (7.9) holds. The Lyapunov difference can be written using continuity of  $V_T$ , Assumption 4, Theorem 7.3.3 and (7.20) as:

$$\begin{aligned} \Delta V &= V_T(\tilde{F}_T^e(\tilde{x}, y, u_{T,h}(\hat{x}, y_c))) - V_T(\tilde{x}) + V_e(E_{T,h}^e(x, \hat{x}, y_c, u_{T,h}(\hat{x}, y_c))) - V_e(e) \\ &\leq V_T(\tilde{F}_T^e(\tilde{x}, y, u_{T,h}(\hat{x}, y_c))) - V_T(\tilde{F}_T^e(\tilde{x}, y, u_T(\hat{x}, y))) + V_T(\tilde{F}_T^e(\tilde{x}, y, u_T(\hat{x}, y))) - V_T(\tilde{x}) \\ &\quad - T\alpha(|e|) + T\tilde{v} \leq V_T(\tilde{F}_T^e(\tilde{x}, y, u_{T,h}(\hat{x}, y_c))) - V_T(\tilde{F}_T^e(\tilde{x}, y, u_T(\hat{x}, y))) - T\tilde{\alpha}(|\tilde{x}|) + T\bar{\delta} \\ &\leq -T\tilde{\alpha}(|\tilde{x}|) + T\bar{\delta} + 2L_v T \rho_1(T) + V_T(\tilde{F}_T^a(\tilde{x}, y, u_{T,h}(\hat{x}, y_c))) - V_T(\tilde{F}_T^a(\tilde{x}, y, u_T(\hat{x}, y))) \end{aligned}$$

where  $\bar{\delta} > 0$  is a sufficiently small number.

Then, using Claim 7.3.1, Claim 7.3.2, Assumption 3 and continuity of  $V_T$ , it can be written that

$$\begin{aligned} \Delta V &\leq -T\tilde{\alpha}(|\tilde{x}|) + T\bar{\delta} + L_v(L_f L_u + L_g + L_g L_u)|y_c - y| + 2L_v T \rho_1(T) \\ &\leq -T\tilde{\alpha}(|x|) + T\bar{\delta} + 2L_v T \rho_1(T) + L_v(L_f L_u + L_g + L_g L_u)T\varepsilon. \end{aligned}$$

A sufficiently small  $\tilde{\delta} > \bar{\delta}$  can be picked such that there exists  $T^1 > 0$  such that for each  $T \in (0, T^1]$ , there exists  $h^1 \in (0, T]$  such that for all  $h \in (0, h^1]$  it can be obtained that  $T\bar{\delta} + 2L_v T \rho_1(T) + L_v(L_f L_u + L_g + L_g L_u)T\varepsilon \leq T\tilde{\delta}$  and hence  $\Delta V \leq -T\tilde{\alpha}(|\tilde{x}|) + T\tilde{\delta}$ . Hence condition (7.9) is satisfied. By Lemma 7.2.9, condition (7.11) holds and this completes the proof.  $\blacksquare$

**Remark 7.3.5** *The proposed dual-rate output feedback control scheme can be applied to general output dynamical controllers (not necessarily observer-based) by predicting the unmeasured output samples between measured samples. Hence, a periodic switch is used which connects the slow sampled measurement every  $T_m$  period and uses the approximate model  $F_{T,h}^a$  of the output dynamics of  $y$  to get the estimated output to fill in the missing samples.*

## 7.4 Applications

In this section, dual-rate output feedback control scheme given in (7.14), (7.15) and (7.12) is applied to various systems and the simulation results are analyzed.

### 7.4.1 Dynamically Positioned Ship

Consider the following system equations for the moored tanker in Example 11.4 in [12]

$$\dot{\eta} = R(x_3(t))\nu \quad (7.21)$$

$$\dot{\nu} = A_1\eta + A_2\nu + Bu \quad (7.22)$$

where  $y(k) = \eta(k)$ ,  $\eta = [x_1 \ x_2 \ x_3]^T$ ,  $\nu = [x_4 \ x_5 \ x_6]^T$ ,  $u = [u_1 \ u_2 \ u_3]^T$ ,  $A_1 = -M^{-1}K$ ,

$$M = \begin{bmatrix} 1.0852 & 0 & 0 \\ 0 & 2.0575 & -0.4087 \\ 0 & -0.4087 & 0.2153 \end{bmatrix}, \quad R(x_3) = \begin{bmatrix} \cos x_3 & -\sin x_3 & 0 \\ \sin x_3 & \cos x_3 & 0 \\ 0 & 0 & 1 \end{bmatrix},$$

$$D = \begin{bmatrix} 0.0865 & 0 & 0 \\ 0 & 0.0762 & 0.1510 \\ 0 & 0.0151 & 0.0031 \end{bmatrix}, \quad K = \text{diag}\{0.0389, 0.0266, 0\},$$

$A_2 = -M^{-1}D$  and  $B = M^{-1}$  as given in [25].

In [25], single-rate reduced order observer based SPA stabilizing output feedback controller for the system (7.21)-(7.22) is designed using the Euler approximate model. The single-rate output feedback controller is obtained using  $W_T = \frac{1}{2}y^T y$  as:

$$u_T(y, \hat{\nu}) = B^{-1}[u_{aT}(y, \hat{\nu}) - A_1y - A_2\hat{\nu}] \quad (7.23)$$

$$z(k+1) = M_1z(k) + M_2y(k) + TBu(k), \quad (7.24)$$

$$\hat{\nu}(k) = z(k) + Gd y(k) \quad (7.25)$$

where

$$\begin{aligned}
u_{aT}(y, \hat{v}) &= -c(\hat{v} - \phi_T(y)) - \frac{\Delta \bar{W}_T(y, \hat{v})}{T} + \frac{\Delta \bar{\phi}_T(y, \hat{v})}{T} \\
\Delta \bar{\phi}_T(y, \hat{v}) &= \bar{\phi}_T(k+1) - \phi_T(y(k)) \\
\phi_T(y(k)) &= R^T(x_3(k))Ly(k) \\
\bar{\phi}_T(k+1) &= R^T(\hat{x}_3(k+1))L[y(k) + TR(x_3(k))L\hat{v}(k)] \\
\hat{x}_3(k+1) &= x_3(k) + T\hat{x}_6(k) \\
\Delta \bar{W}_T(y, \hat{v}) &= \begin{cases} \frac{\Delta \bar{W}_T(y, \hat{v})[\hat{v} - \phi_T(y)]}{\|\hat{v} - \phi_T(y)\|^2}, & \hat{v} \neq \phi_T(y) \\ TR^T(x_3)[y + TR(x_3)\hat{v}], & \hat{v} = \phi_T(y) \end{cases} \\
\Delta \bar{W}_T(y, \hat{v}) &= W_T(y + TR(x_3)\hat{v}) - W_T((I + TL)y)
\end{aligned}$$

and  $c > 0$  is arbitrary,  $d = [0 \ 0 \ 1]$ ,  $M_1 = I + T(A_2 - Gd)$ ,  $M_2 = T(A_1 + (A_2 - Gd)Gd)$  and  $G \in \mathbb{R}^{3 \times 1}$ .

Then, the dual-rate SPA stabilizing reduced order observer-based output feedback controller is designed as:

$$u_{T,h} = u_T(y_c(k), \hat{v}(k)) \quad (7.26)$$

$$z(k+1) = M_1 z(k) + M_2 y_c(k) + T B u_{T,h}(k) \quad (7.27)$$

$$\hat{v}(k) = z(k) + G d y_c(k) \quad (7.28)$$

$$y_c(i+1) = \begin{cases} y(i+1), & \text{if } i+1 = kl, \\ F_{T,h}^a(y(i), \hat{v}(i)), & \text{if } i = kl \\ F_{T,h}^a(y_c(i), \hat{v}(i)), & \text{if } i+1 = kl + \tau \end{cases} \quad (7.29)$$

where  $k \in \mathbb{Z}^+$ ,  $\tau = 2, \dots, l-1$ . The numerically integrated approximate model  $F_{T,h}^a(y_c, \hat{v})$  can be written as:

$$\begin{aligned}
f_h^1(y_c, \hat{v}) &= f_h(y_c, \hat{v}) = y_c + hR(x_3)\hat{v} \\
f_h^{k+1}(y_c, \hat{v}) &= f_h(f_h^k, \hat{v}) \\
F_{T,h}^a(y_c, \hat{v}) &= f_h^N(y_c, \hat{v}), \quad k = 1, 2, \dots, N-1
\end{aligned}$$

where  $h$  is the integration period,  $T$  is the sampling period and  $N = \frac{T}{h}$ . The consistency of approximation scheme is checked. By Lemma II.2 in [45],  $f_h$  is one-step consistent with  $F_h^e$  where  $F_h^e$  is the exact discrete-time model with the sampling period  $h$ . Also, the multi-step

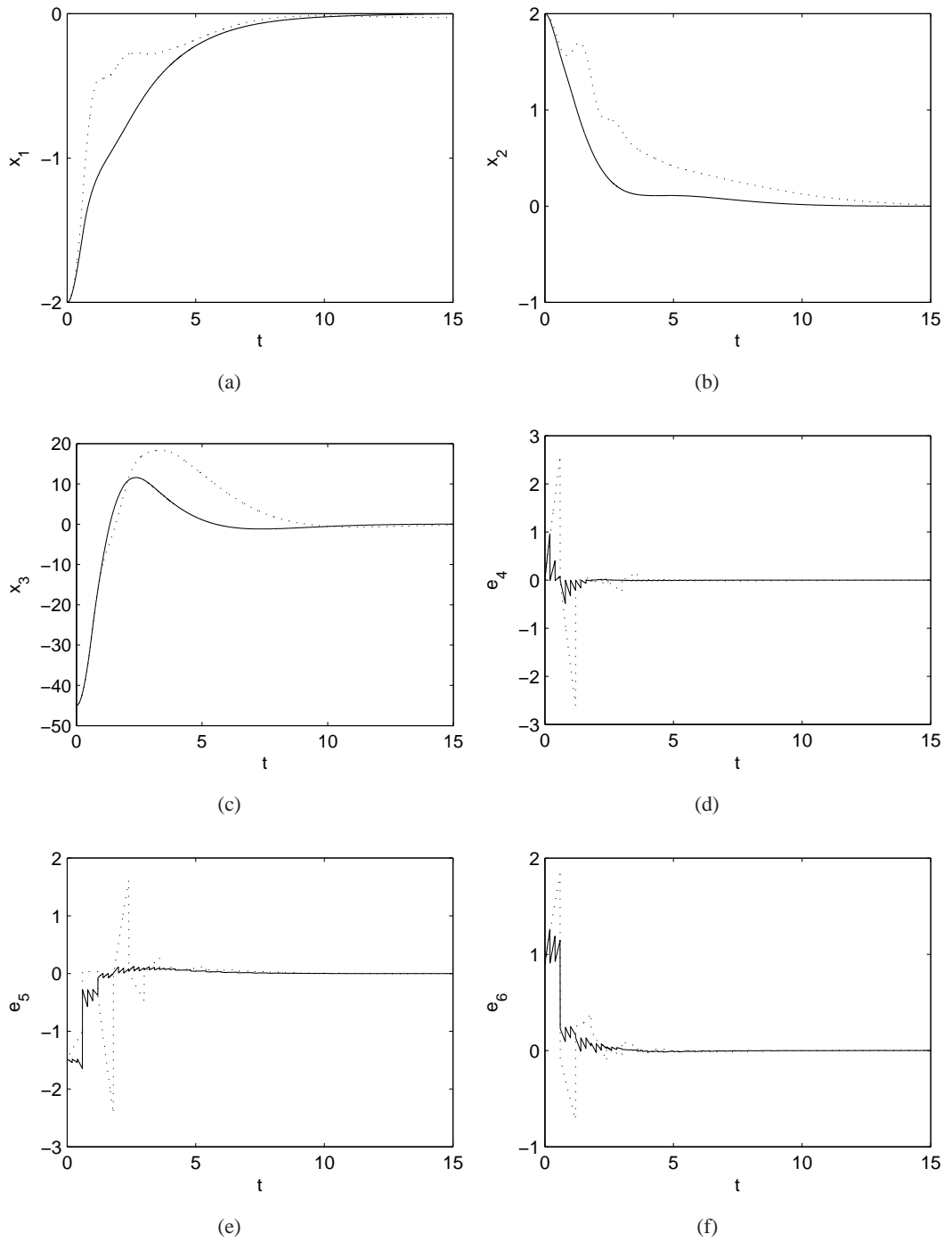


Figure 7.1: Time responses of yaw angle  $x_3$ , the North position  $x_1$ , the East position  $x_2$  and the observer errors for  $x_4$ ,  $x_5$  and  $x_6$  with  $T_m = 0.6$ ,  $T_i = 0.2$ ,  $h = 0.005$  and  $T = 0.6$ . Dotted line: Single-rate controller. Solid line: Dual-rate controller.

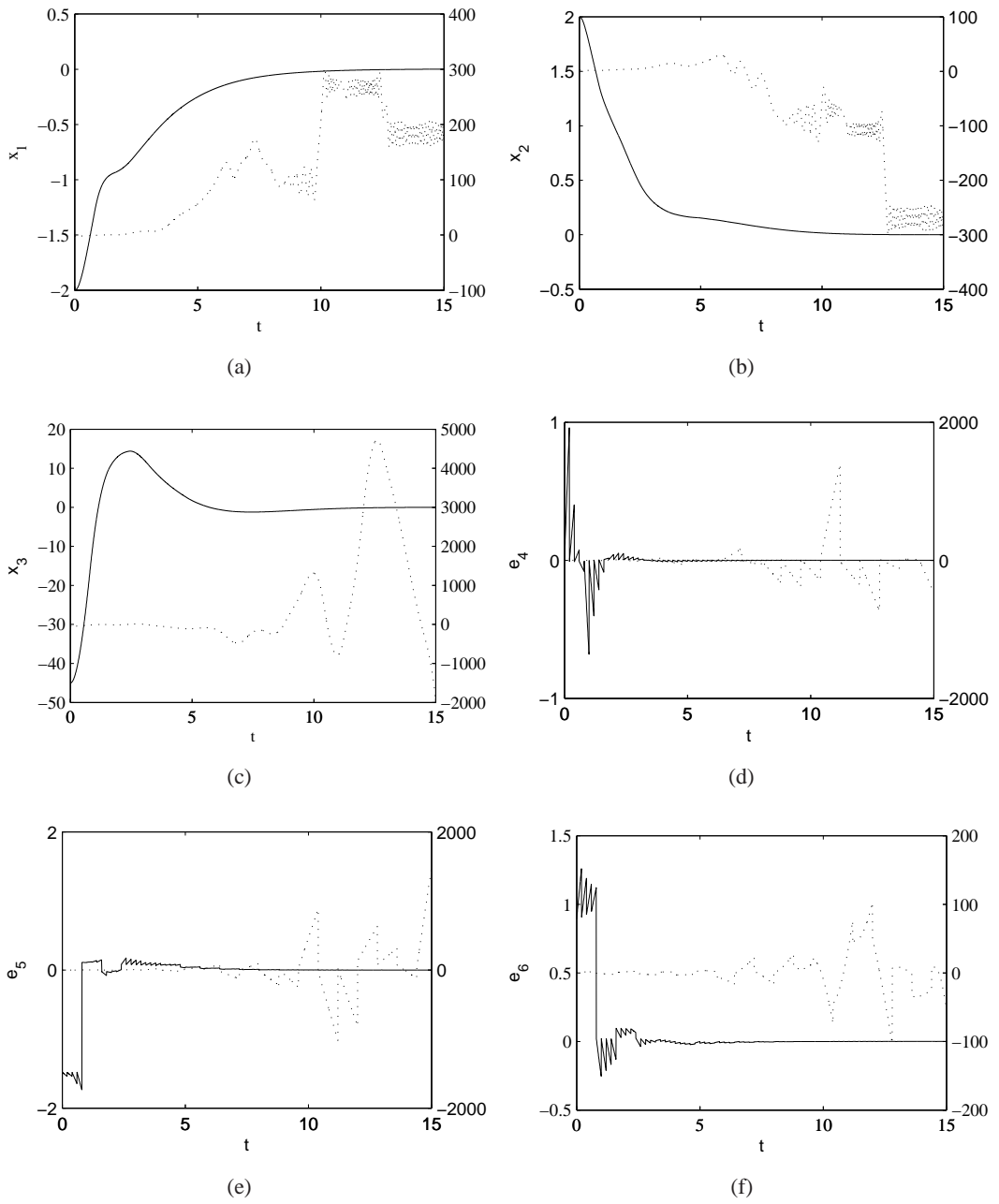


Figure 7.2: Time responses of yaw angle  $x_3$ , the North position  $x_1$ , the East position  $x_2$  and the observer errors for  $x_4$ ,  $x_5$  and  $x_6$  with  $T_m = 0.8$ ,  $T_i = 0.2$ ,  $h = 0.005$  and  $T = 0.8$ . Dotted line and right y-axis: Single-rate controller. Solid line and left y-axis: Dual-rate controller.

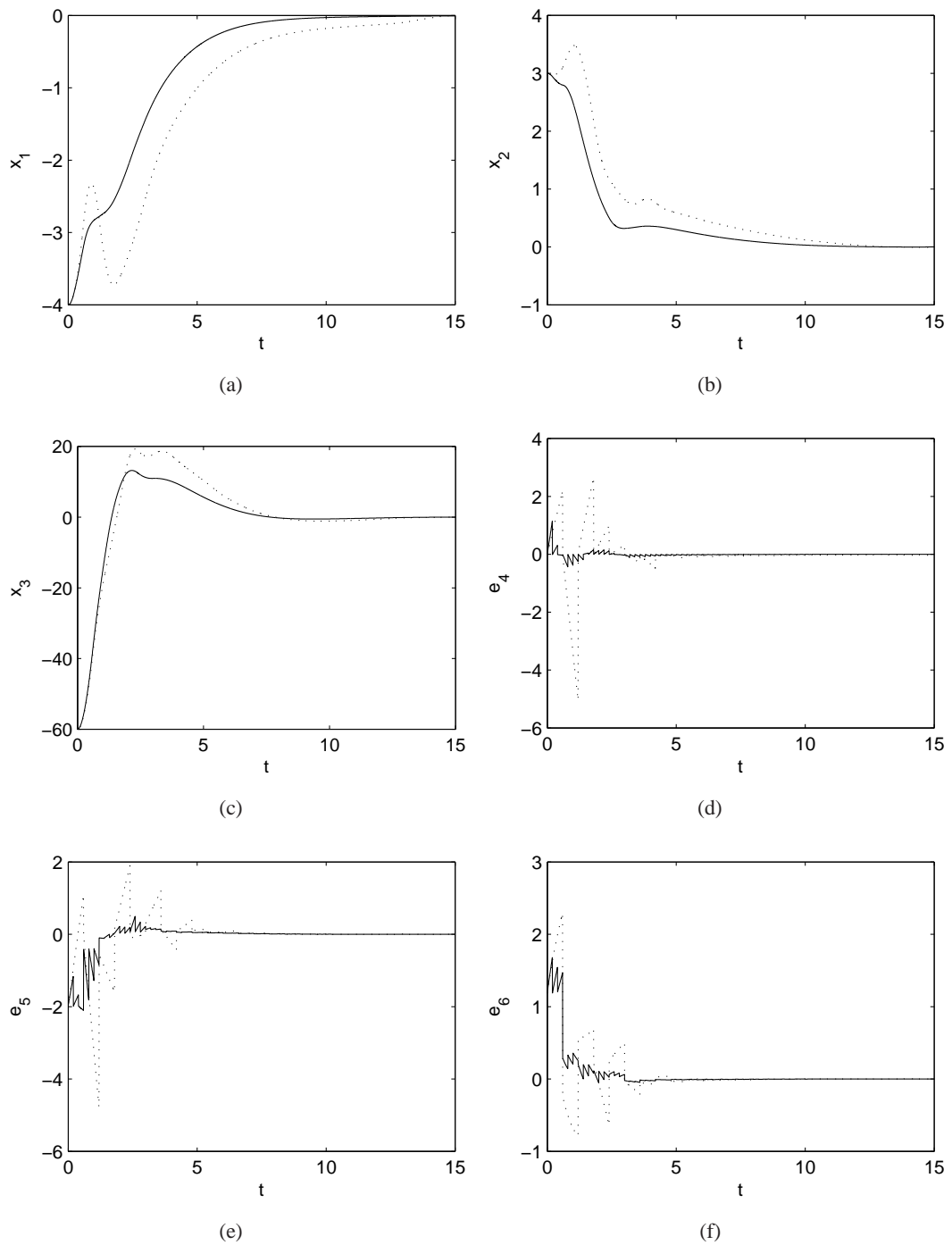


Figure 7.3: Time responses of yaw angle  $x_3$ , the North position  $x_1$ , the East position  $x_2$  and the observer errors for  $x_4$ ,  $x_5$  and  $x_6$  with and large initial conditions,  $T_m = 0.6$ ,  $T_i = 0.2$ ,  $h = 0.005$  and  $T = 0.6$ . Dotted line: Single-rate controller. Solid line: Dual-rate controller.

consistency is guaranteed by the one-step consistency plus the uniform Lipschitz condition on  $f_h$  (see Remark 13 in [46]). Then, following closely the conclusions of Corollary 4 and Remark 14 in [46], it is shown that  $F_{T,h}^a(\eta, \nu)$  is one-step consistent with  $F_T^e(\eta, \nu)$ . Moreover it is easy to see that Assumption 3 is also satisfied.

As in [25], it is set that  $G = [0 \quad -1.8862 \quad 1.1368]^T$  for observer and  $L = -diag\{0.5, 2, 1\}$  and  $c = 0.2$  for controller. Simulations have been performed to compare the dual-rate controller (7.26)-(7.28) with the single-rate controller (7.23)-(7.25).

First, the single-rate and dual-rate controllers are applied to the system (7.21)-(7.22) with the initial conditions,  $\eta(0) = [-2 \quad 2 \quad -\frac{\pi}{4}]^T$ ,  $\nu(0) = [0 \quad 0 \quad 0]^T$  and  $\hat{\nu}(0) = [0 \quad 0 \quad 0]^T$ . Simulation results with the sampling periods  $T = 0.6$  for the single-rate controller and  $T_m = 0.6$ ,  $T_i = 0.2$ ,  $h = 0.005$  for the dual-rate controller are given in Figure 7.1. It is shown that the dual-rate controller (7.26)-(7.28) works well and is faster than the single rate controller (7.23)-(7.25). Also, observer errors converge to zero faster with the dual-rate controller.

Then, the simulation is performed with the initial conditions given above and large sampling periods. Simulation results with the sampling periods  $T = 0.8$  for the single-rate controller and  $T_m = 0.8$ ,  $T_i = 0.2$ ,  $h = 0.005$  for the dual-rate controller are shown in Figure 7.2. While the single-rate controller (7.23)-(7.25) cannot stabilize the system, the dual-rate controller (7.26)-(7.28) stabilizes the system successfully.

Finally, the controllers are applied to the system (7.21)-(7.22) with the same sampling periods as in the first simulation and large initial conditions  $\eta(0) = [-4 \quad 3 \quad -\frac{\pi}{3}]^T$  and  $\nu(0) = \hat{\nu}(0) = 0_{3 \times 1}$ . Simulation results with the sampling periods  $T = 0.6$  for the single-rate controller and  $T_m = 0.6$ ,  $T_i = 0.2$ ,  $h = 0.005$  for the dual-rate controller are given in Figure 7.3. It is shown that the dual-rate controller gives faster results compared to the single-rate controller again.

## 7.4.2 Two-Link Robot Manipulator

Consider the dynamic model of the two-link manipulator given in Subsection 3.4.2

$$\dot{\eta} = \xi \quad (7.30)$$

$$\dot{\xi} = M^{-1}(\eta)(u - C(\eta, \xi)\xi - G(\eta)) \quad (7.31)$$

with sampled measurement  $y(k) = \eta(k)$  where the state vectors are  $\eta := [q_1 \quad q_2]^T$  and  $\xi := [\dot{q}_1 \quad \dot{q}_2]^T$ ,  $M = \begin{bmatrix} M_1 & M_2 \\ M_3 & M_4 \end{bmatrix}$ ,  $C = \begin{bmatrix} C_1 & C_2 \\ C_3 & C_4 \end{bmatrix}$ ,  $G = \begin{bmatrix} G_1 \\ G_2 \end{bmatrix}$  and  $u = \begin{bmatrix} u_1 \\ u_2 \end{bmatrix}$  with  $M_1 = m_1 l_{c1}^2 + m_2(l_1^2 + l_{c2}^2 + 2l_1 l_{c2} \cos q_2)$ ,  $M_2 = M_3 = m_2 l_1 l_{c2} \cos q_2 + m_2 l_{c2}^2$ ,  $M_4 = m_2 l_{c2}^2$ ,  $C_1 = -m_2 l_2 l_{c2} \sin q_2 \dot{q}_2$ ,  $C_2 = -m_2 l_2 l_{c2} \sin q_2 (\dot{q}_1 + \dot{q}_2)$ ,  $C_3 = m_2 l_2 l_{c2} \sin q_2 \dot{q}_1$ ,  $C_4 = 0$ ,  $G_1 = m_1 g l_{c1} \cos q_1 + m_2 g (l_1 \cos q_1 + l_{c2} \cos(q_1 + q_2))$ ,  $G_2 = m_2 g l_{c2} \cos(q_1 + q_2)$ .  $l_{c1}$  and  $l_{c2}$  are the distances of the center of mass from the joint axes. The robot parameters are given as  $m_1 = m_2 = 5$  [kg],  $l_1 = l_2 = 0.5$  [m],  $l_{c1} = l_{c2} = 0.25$  [m]. The control objective is to solve the trajectory tracking problem.

The single-rate output feedback controller  $u_T$  with the observer (6.45) is designed in Subsection 6.4.2. Then the dual-rate output feedback controller is designed as:

$$u_{T,h} = u_T(y_c(k), \hat{\xi}(k)) \quad (7.32)$$

$$\hat{\xi}(k+1) = \hat{\xi} + T(M^{-1}(y_c) (u_{T,h} - C(y_c, \hat{\xi})\hat{\xi} - G(y_c)) + K\tilde{\xi}) \quad (7.33)$$

$$y_c(i+1) = \begin{cases} y(i+1), & \text{if } i+1 = kl, \\ F_{T,h}^a(y(i), \hat{\xi}(i)), & \text{if } i = kl \\ F_{T,h}^a(y_c(i), \hat{\xi}(i)), & \text{if } i+1 = kl + \tau \end{cases} \quad (7.34)$$

where  $k \in \mathbb{Z}^+$ ,  $\tau = 2, \dots, l-1$ . The numerically integrated approximate model  $F_{T,h}^a(y_c, \hat{\xi})$  can be written as:

$$\begin{aligned} f_h^1(y_c, \hat{\xi}) &= f_h(y_c, \hat{\xi}) = y_c + h(\hat{\xi}) \\ f_h^{k+1}(y_c, \hat{\xi}) &= f_h(f_h^k, \hat{\xi}) \\ F_{T,h}^a(y_c, \hat{\xi}) &= f_h^N(y_c, \hat{\xi}), \quad k = 1, 2, \dots, N-1 \end{aligned}$$

where  $h$  is the integration period,  $T$  is the sampling period and  $N = \frac{T}{h}$ . The following simulation parameters are set:  $c_1 = 2, c_2 = 3, c = 1$  and  $d = 0.5$  for controllers and  $h = \text{diag}\{5, 6\}$  for observer. Two different reference trajectories,  $q_{d1} = q_{d2} = \frac{5}{4} - \frac{5}{4}e^{-t}$  and  $q_{d1} = q_{d2} = \sin(t)$ , are considered. Then, simulations have been performed in order to compare performances of the single-rate and dual-rate output feedback controllers with the initial conditions  $\eta(0) = \xi(0) = \hat{\xi}(0) = \begin{bmatrix} 0 \\ 0 \end{bmatrix}$  and different sampling periods.

First, the single-rate and dual-rate controllers are applied to the system (7.30)-(7.31) with the first reference trajectory,  $q_{d1} = q_{d2} = \frac{5}{4} - \frac{5}{4}e^{-t}$ .

Simulation results with sampling periods  $T = 0.15$  for the single-rate controller and  $T_m = 0.15$ ,  $T_i = 0.01$ ,  $h = 0.001$  for the dual-rate controller are given in Figure 7.4. It is shown

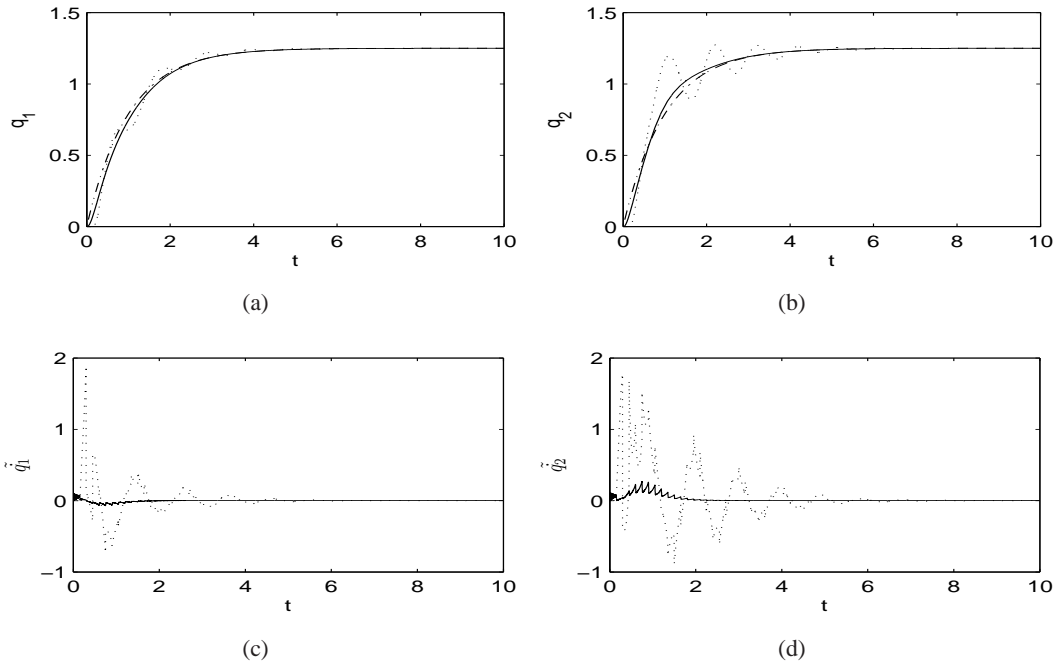


Figure 7.4: Responses of the system for the first trajectory with  $T_m = 0.15$ ,  $T_i = 0.01$ ,  $h = 0.001$  and  $T = 0.15$ . Dotted line: Single-rate controller. Solid line: Dual-rate designed controller. Dash-dotted line:desired trajectory.

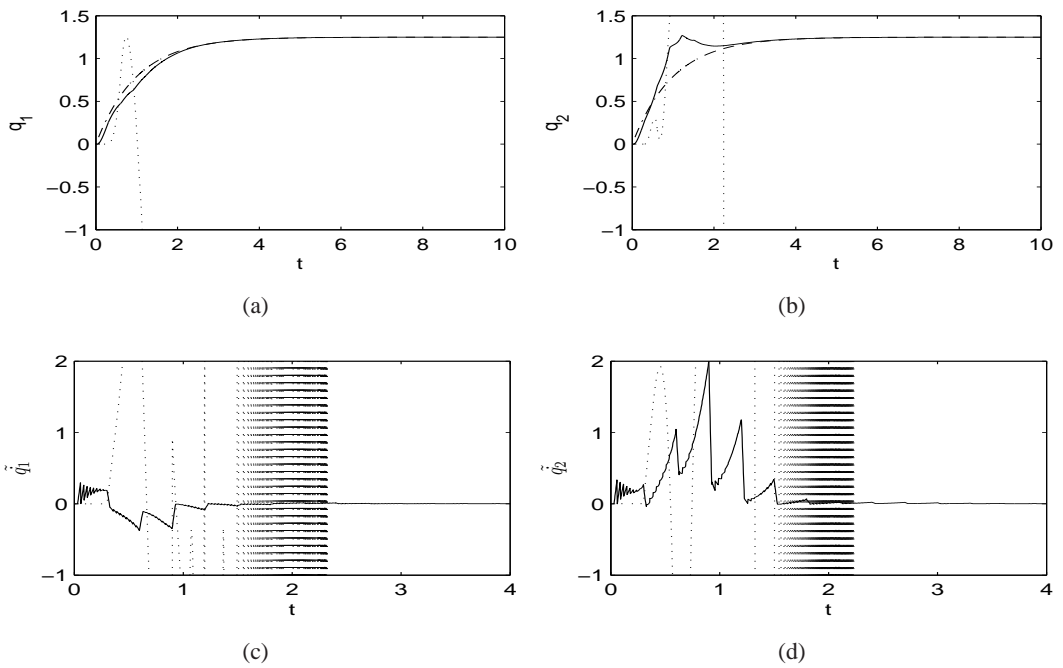


Figure 7.5: Responses of the system for the first trajectory with  $T_m = 0.3$ ,  $T_i = 0.03$ ,  $h = 0.003$  and  $T = 0.3$ . Dotted line: Single-rate controller. Solid line: Dual-rate designed controller. Dash-dotted line:desired trajectory.

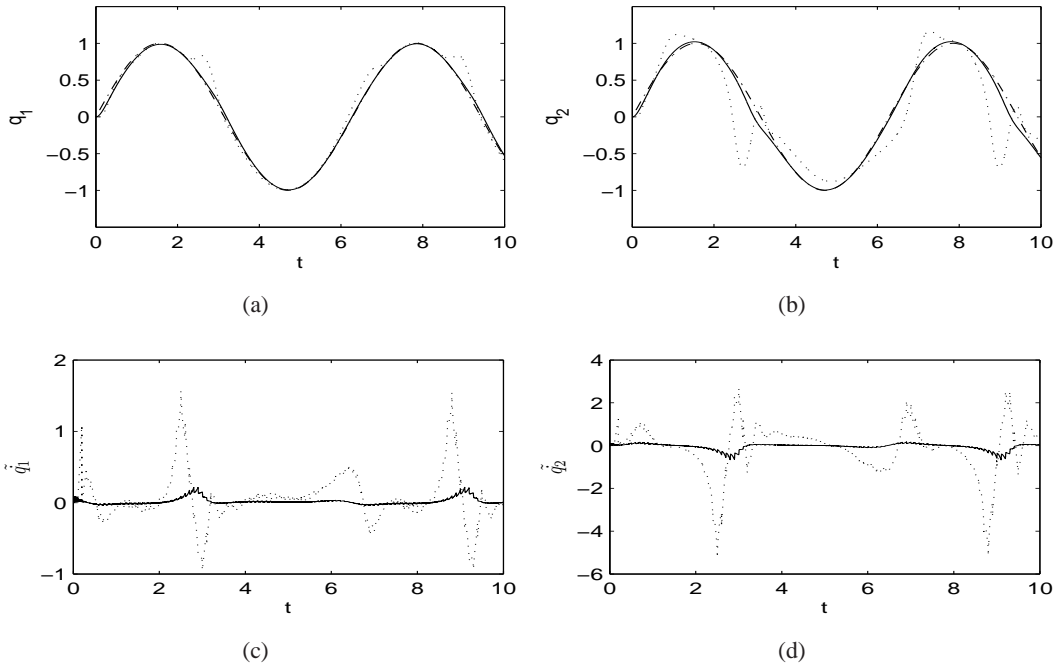


Figure 7.6: Responses of the system for the second trajectory with  $T_m = 0.1$ ,  $T_i = 0.01$ ,  $h = 0.001$  and  $T = 0.1$ . Dotted line: Single-rate controller. Solid line: Dual-rate designed controller. Dash-dotted line:desired trajectory.

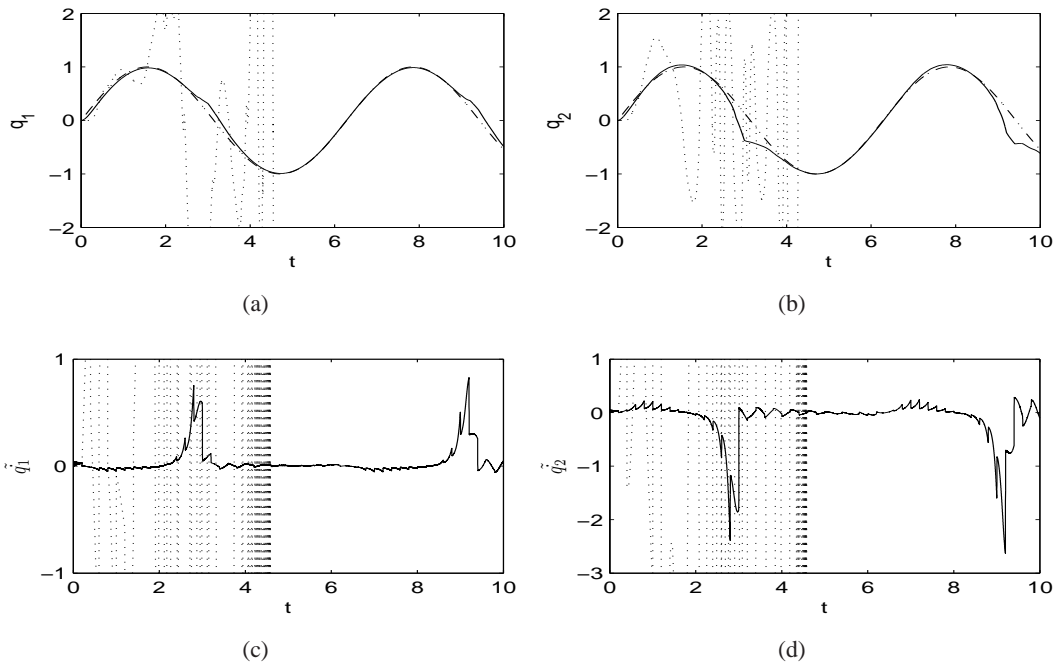


Figure 7.7: Responses of the system for the second trajectory with  $T_m = 0.2$ ,  $T_i = 0.005$ ,  $h = 0.0005$  and  $T = 0.2$ . Dotted line: Single-rate controller. Solid line: Dual-rate designed controller. Dash-dotted line:desired trajectory.

that both controllers track the desired trajectory, but the tracking error converges to zero faster with dual-rate controller.

Simulation results with sampling periods  $T = 0.3$  for the single-rate controller and  $T_m = 0.3$ ,  $T_i = 0.03$ ,  $h = 0.003$  for the dual-rate controller are given in Figure 7.5. While the single-rate controller cannot track the trajectory, the dual-rate controller tracks the trajectory successfully.

Then, the single-rate and dual-rate controllers are applied to the system (7.30)-(7.31) with the second reference trajectory,  $q_{d1} = q_{d2} = \sin(t)$ .

Simulation results with sampling periods  $T = 0.1$  for the single-rate controller and  $T_m = 0.1$ ,  $T_i = 0.01$ ,  $h = 0.001$  for the dual-rate controller are given in Figure 7.6. It is shown that the dual-rate controller track the desired trajectory with smaller tracking error when compared to the single-rate controller.

Simulation results with sampling periods  $T = 0.2$  for the single-rate controller and  $T_m = 0.2$ ,  $T_i = 0.005$ ,  $h = 0.0005$  for the dual-rate controller are shown in Figure 7.7. While the single-rate controller cannot track the trajectory, the dual-rate controller tracks the trajectory successfully.

### 7.4.3 Attitude Control of Rigid Artificial Satellite

Consider the following nonlinear equations for the digital attitude control of a rigid artificial satellite which were also given Subsection 3.4.3

$$\dot{\rho} = H(\rho)w, \quad (7.35)$$

$$\dot{w} = J^{-1}S(w)Jw + J^{-1}u \quad (7.36)$$

with sampled observation  $y(k) = \rho(k)$  where  $w := [w_1 \ w_2 \ w_3]^T \in \mathbb{R}^3$  is the angular velocity vector of the body in a body-fixed frame,  $\rho \in \mathbb{R}^3$  is the Cayley-Rodrigues parameters describing the body orientation,  $u \in \mathbb{R}^3$  is the control torque vector of the body,  $J = J^T = \text{diag}\{10, 15, 20\}$  is the inertia matrix of the body [31],  $S(w)$  is the skew-symmetric matrix given by  $S(w) = \begin{bmatrix} 0 & w_3 & -w_2 \\ -w_3 & 0 & w_1 \\ w_2 & -w_1 & 0 \end{bmatrix}$  and  $H(\rho) = \frac{1}{2}(I - S(\rho) + \rho\rho^T)$ .

The single-rate output feedback controller  $u_T$  with the observer (6.48) is designed in Subsec-

tion 6.4.3. Then the dual-rate output feedback controller is designed as:

$$u_{T,h} = u_T(y_c(k), \hat{w}(k)) \quad (7.37)$$

$$\hat{w}(k+1) = \hat{w} + T(J^{-1}S(\hat{w})J\hat{w} + J^{-1}u_{T,h} + K\tilde{w}) \quad (7.38)$$

$$y_c(i+1) = \begin{cases} y(i+1), & \text{if } i+1 = kl, \\ F_{T,h}^a(y(i), \hat{w}(i)), & \text{if } i = kl \\ F_{T,h}^a(y_c(i), \hat{w}(i)), & \text{if } i+1 = kl + \tau \end{cases} \quad (7.39)$$

where  $k \in \mathbb{Z}^+$ ,  $\tau = 2, \dots, l-1$ .

The numerically integrated approximate model  $F_{T,h}^a(y_c, \hat{w})$  can be written as:

$$\begin{aligned} f_h^1(y_c, \hat{w}) &= f_h(y_c, \hat{w}) = y_c + hH(y_c)\hat{w} \\ f_h^{k+1}(y_c, \hat{w}) &= f_h(f_h^k, \hat{w}) \\ F_{T,h}^a(y_c, \hat{w}) &= f_h^N(y_c, \hat{w}), \quad k = 1, 2, \dots, N-1 \end{aligned}$$

where  $h$  is the integration period,  $T$  is the sampling period and  $N = \frac{T}{h}$ . The following simulation parameters are set:  $L = \text{diag}\{0.5, 0.5, 0.5\}$ ,  $c = 1$  and  $d = 0.5$  for controllers and  $h = \text{diag}\{1, 2, 0.4\}$  for observer. Then, simulations have been performed in order to compare performances of the single-rate and dual-rate output feedback controllers with different sampling periods and initial conditions.

In the first simulation, the initial conditions are chosen as  $\rho(0) = [1.4735 \quad 0.6115 \quad 2.5521]^T$ ,  $w(0) = 0_{3 \times 1}$  and  $\hat{w}(0) = 0_{3 \times 1}$  as the initial conditions of the observer. Simulation results with the sampling periods  $T = 0.5$  for the single-rate controller and  $T_m = 0.5$ ,  $T_i = 0.1$ ,  $h = 0.001$  for the dual-rate controller are given in Figure 7.8. It is shown that both controllers stabilize the system (7.35)-(7.36), but faster with  $u_T$ .

Then, the simulation is performed with the initial conditions given above and large sampling periods. Simulation results with the sampling periods  $T = 0.8$  for the single-rate controller and  $T_m = 0.8$ ,  $T_i = 0.1$ ,  $h = 0.001$  for the dual-rate controller are shown in Figure 7.9. While the single-rate controller cannot stabilize the system, the dual-rate controller stabilizes the system successfully.

Finally, the controllers are applied to the system (7.35)-(7.36) with the same sampling periods as in the first simulation and large initial conditions. Simulation results with 1.5-fold initial

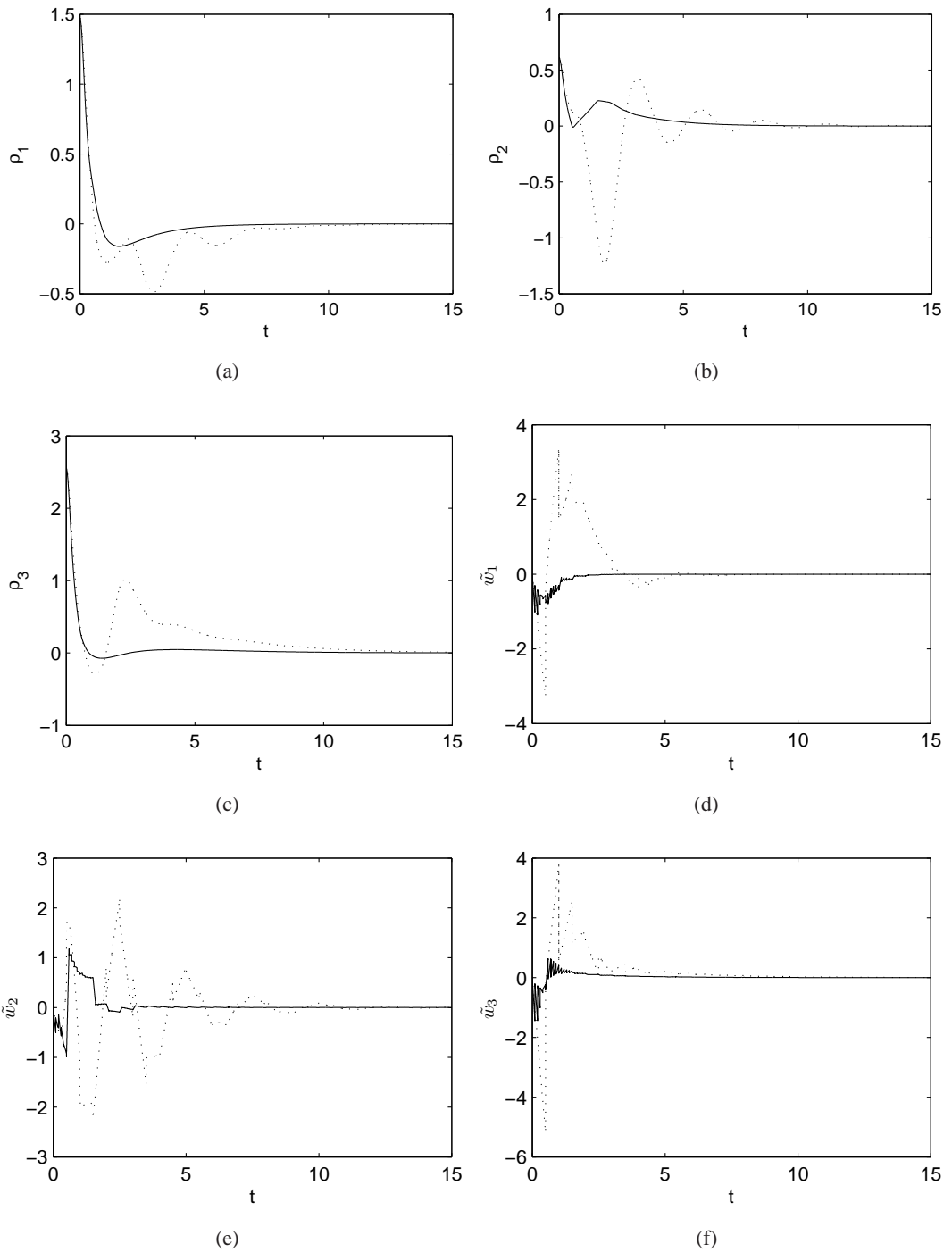


Figure 7.8: Time responses of  $\rho$  and  $\tilde{w}$  with  $T_m = 0.5$ ,  $T_i = 0.1$ ,  $h = 0.001$  and  $T = 0.5$ . Dotted line: Single-rate controller. Solid line: Dual-rate controller.

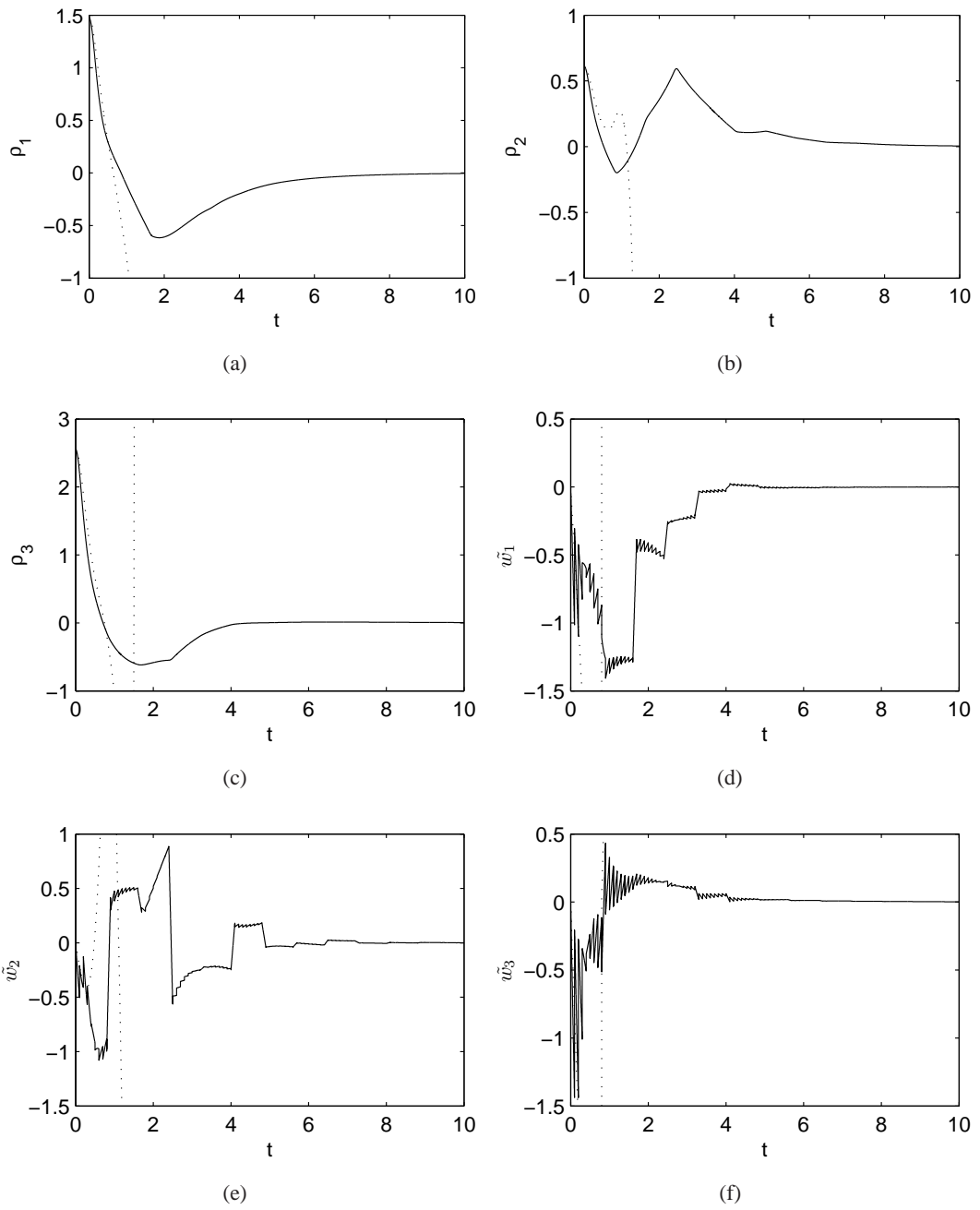


Figure 7.9: Time responses of  $\rho$  and  $\tilde{w}$  with  $T_m = 0.8$ ,  $T_i = 0.1$ ,  $h = 0.001$  and  $T = 0.8$ . Dotted line: Single-rate controller. Solid line: Dual-rate controller.

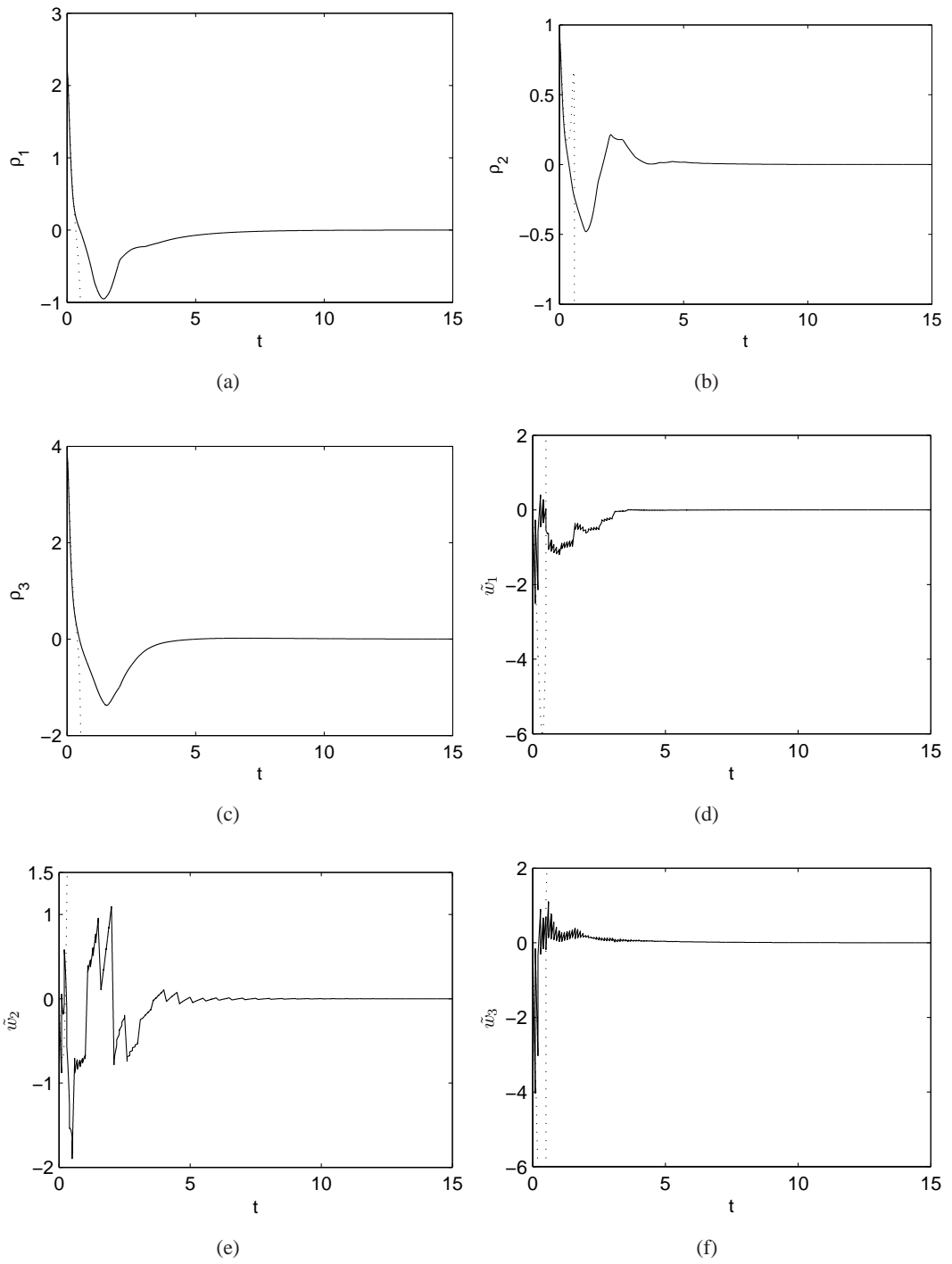


Figure 7.10: Time responses of  $\rho$  and  $\tilde{w}$  with 1.5-fold initial conditions and  $T_m = 0.5$ ,  $T_i = 0.1$ ,  $h = 0.001$ ,  $T = 0.5$ . Dotted line: Single-rate controller. Solid line: Dual-rate controller.

conditions and sampling periods  $T = 0.5$  for the single-rate controller and  $T_m = 0.5$ ,  $T_i = 0.1$ ,  $h = 0.001$  for the dual-rate controller are given in Figure 7.10. It is shown that while the single-rate controller cannot stabilize the system, the dual-rate controller stabilizes the system successfully again.

#### 7.4.4 Second-Order Single-Input System

As a last example, consider the following continuous-time plant:

$$\dot{\eta} = \eta^2 + \xi \quad (7.40)$$

$$\dot{\xi} = u \quad (7.41)$$

where  $\eta \in \mathbb{R}$  and  $\xi \in \mathbb{R}$  are the state vectors,  $u \in \mathbb{R}$  is the control input and  $y(k) = \eta(k)$ .

The single-rate output feedback controller  $u_T$  with the observer (6.51) is designed in Subsection 6.4.4. Then the dual-rate output feedback controller is designed as:

$$u_{T,h} = u_T(y_c(k), \hat{\xi}(k)) \quad (7.42)$$

$$\hat{\xi}(k+1) = \hat{\xi} + T(u_{T,h} + K\tilde{\xi}) \quad (7.43)$$

$$y_c(i+1) = \begin{cases} y(i+1), & \text{if } i+1 = kl, \\ F_{T,h}^a(y(i), \hat{\xi}(i)), & \text{if } i = kl \\ F_{T,h}^a(y_c(i), \hat{\xi}(i)), & \text{if } i+1 = kl + \tau \end{cases} \quad (7.44)$$

where  $k \in \mathbb{Z}^+$ ,  $\tau = 2, \dots, l-1$ . The numerically integrated approximate model  $F_{T,h}^a(y_c, \hat{\xi})$  can be written as:

$$\begin{aligned} f_h^1(y_c, \hat{\xi}) &= f_h(y_c, \hat{\xi}) = y_c + h(\eta^2 + \hat{\xi}) \\ f_h^{k+1}(y_c, \hat{\xi}) &= f_h(f_h^k, \hat{\xi}) \\ F_{T,h}^a(y_c, \hat{\xi}) &= f_h^N(y_c, \hat{\xi}), \quad k = 1, 2, \dots, N-1 \end{aligned}$$

where  $h$  is the integration period,  $T$  is the sampling period and  $N = \frac{T}{h}$ . The following simulation parameters are set:  $c = 1$  and  $d = 0.01$  for controllers,  $K = 1$  for observer. Then, simulations have been performed in order to compare performances of the single-rate and dual-rate output feedback controllers with different sampling periods and initial conditions.

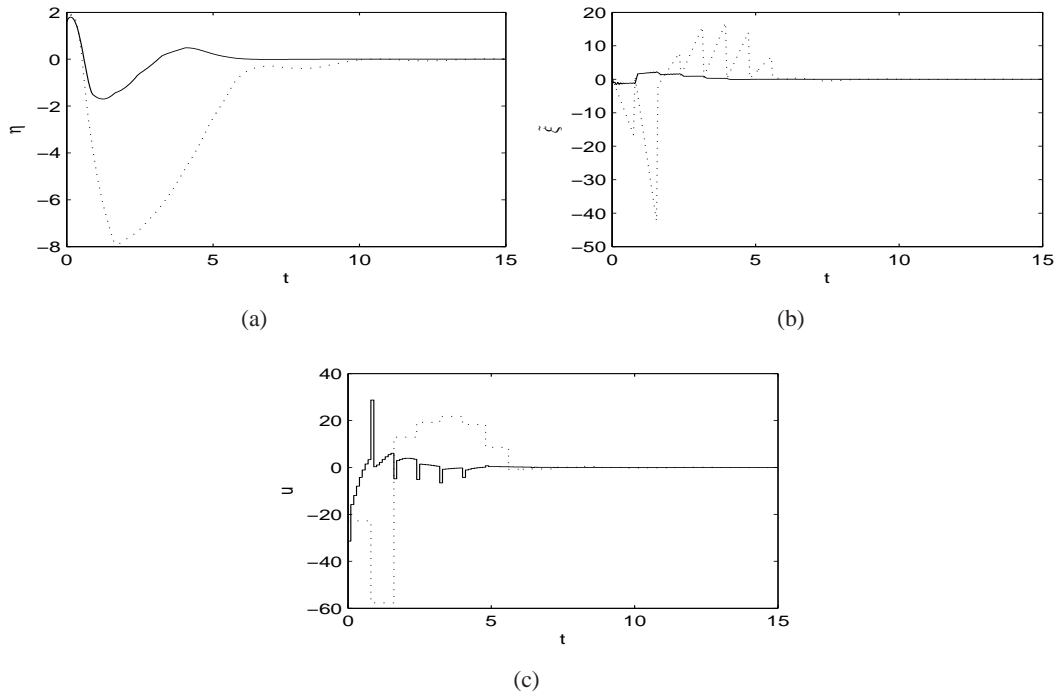


Figure 7.11: Time responses of  $\eta$ , the observer error  $\tilde{\xi}$  and  $u$  with  $T_m = 0.8$ ,  $T_i = 0.1$ ,  $h = 0.05$  and  $T = 0.8$ . Solid line: Dual-rate controller. Dotted line: Single-rate controller.

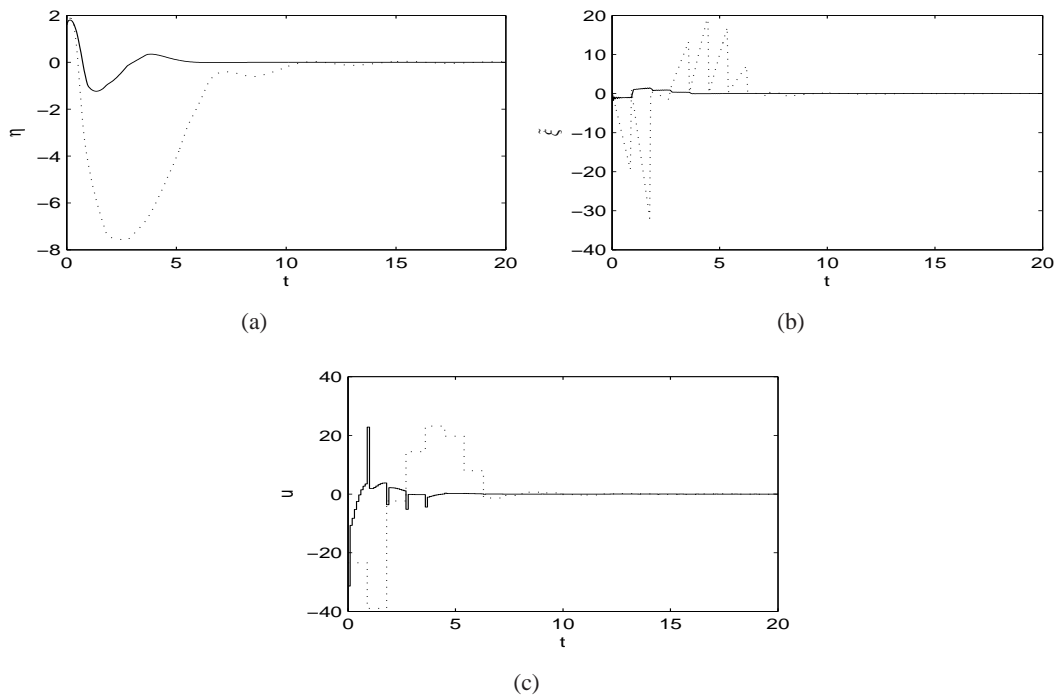


Figure 7.12: Time responses of  $\eta$ , the observer error  $\tilde{\xi}$  and  $u$  with  $T_m = 0.9$ ,  $T_i = 0.1$ ,  $h = 0.05$  and  $T = 0.9$ . Solid line: Dual-rate controller. Dotted line: Single-rate controller.

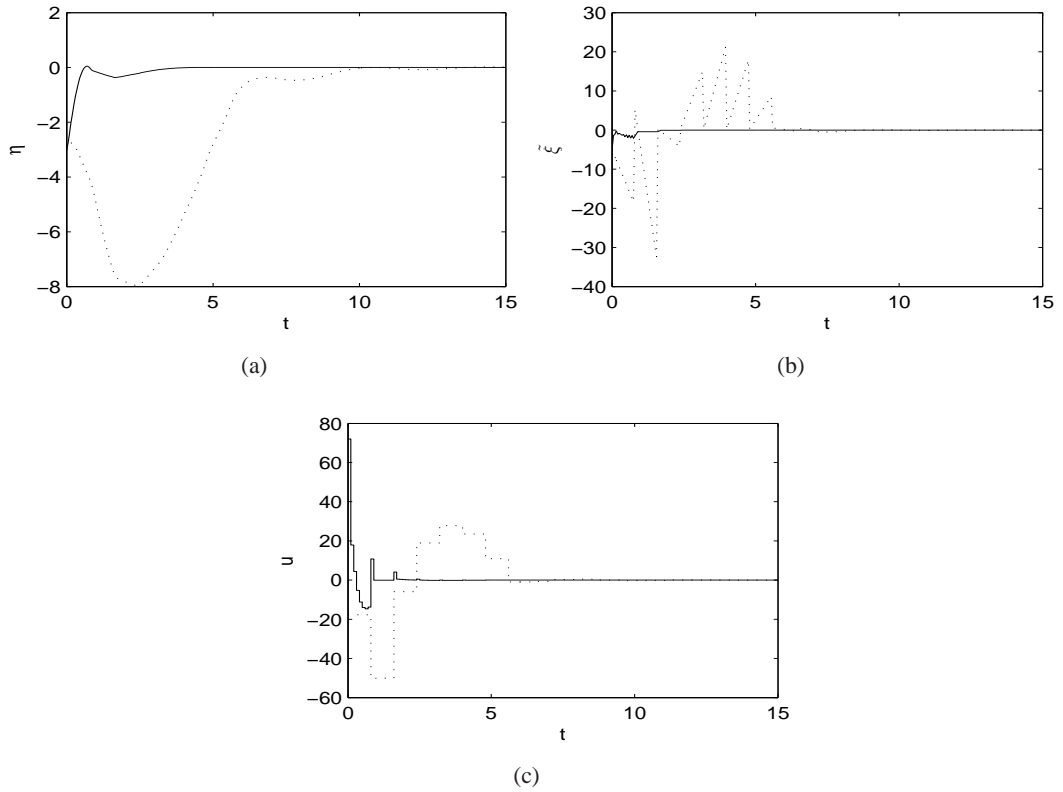


Figure 7.13: Time responses of  $\eta$ , the observer error  $\xi_{\tilde{}}$  and  $u$  with the initial conditions  $(\eta(0), \xi(0)) = (-3, -5)$  and  $T_m = 0.8$ ,  $T_i = 0.1$ ,  $h = 0.05$ ,  $T = 0.8$ . Solid line: Dual-rate controller. Dotted line: Single-rate controller.

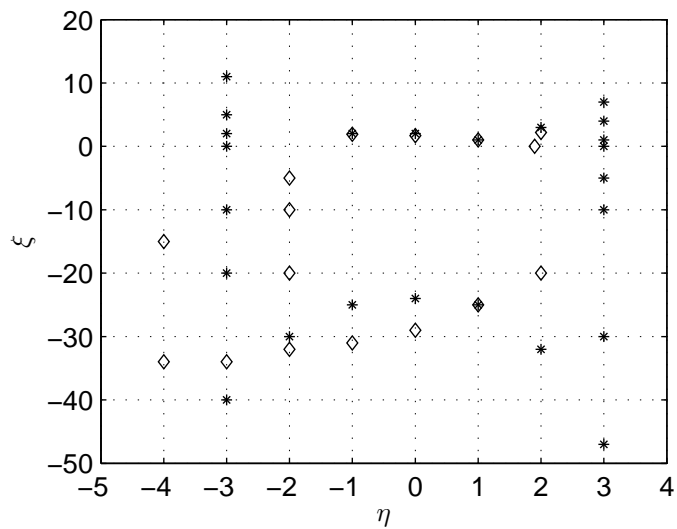


Figure 7.14: Domain of attraction estimates with  $T_m = 0.8$ ,  $T_i = 0.1$ ,  $h = 0.05$ ,  $T = 0.8$ . Diamond: Dual-rate controller. Star: Single-rate controller.

First, the single-rate and dual-rate controllers are applied to the system (7.40)-(7.41) with the initial conditions  $(\eta(0), \xi(0)) = (1.6, 0.5)$  and  $(\hat{\xi}(0)) = 0$ . Simulation results with the sampling periods  $T = 0.8$  for the single-rate controller and  $T_m = 0.8, T_i = 0.1, h = 0.05$  for the dual-rate controller are shown in Figure 7.11. It is observed that both controllers stabilize the system (7.40)-(7.41), but faster with  $u_T$ .

Next, the simulation is performed with the initial conditions given above and large sampling periods. Simulation results with the sampling periods  $T = 0.9$  for the single-rate controller and  $T_m = 0.9, T_i = 0.1, h = 0.05$  for the dual-rate controller are can be seen from Figure 7.12. It is shown that both controllers stabilize the system (7.40)-(7.41), but the dual-rate controller yields better performance when compared to the single-rate controller.

Then, the controllers are applied to the system (7.40)-(7.41) with the same sampling periods as in the first simulation and large initial conditions  $(\eta(0), \xi(0)) = (-3, -5)$  and  $(\hat{\xi}(0)) = 0$ . Simulation results with the sampling periods  $T = 0.8$  for the single-rate controller and  $T_m = 0.8, T_i = 0.1, h = 0.05$  for the dual-rate controller are given in Figure 7.13. It is shown that the dual-rate controller gives faster results when compared to the single-rate controller.

Moreover, as can be seen from figures, the dual-rate controller produces the control input with less energy when compared to the single-rate controller. Therefore, the dual-rate control method requires less control effort.

Finally, by applying the controllers to the system (7.40)-(7.41) with different initial conditions, domain of attraction (DOA) estimates with the single-rate and dual-rate controllers are given in Figure 7.14. In DOA estimates, the sampling periods are chosen as  $T = 0.8$  for the single-rate controller and  $T_m = 0.8, T_i = 0.1, h = 0.05$  for the dual-rate controller. As can be seen from figure, DOA for the system with the dual-rate controller is almost same as that with the single-rate controller. For different controller parameters and sampling periods, much larger DOA estimate may be obtained with the dual-rate controller when compared to the estimate given in figure.

## 7.5 Conclusions

In this chapter, the problem of dual-rate output feedback stabilization of sampled-data nonlinear systems has been considered under the low measurement rate constraint. The dual-rate control scheme has been presented based on estimation of the missing output values between measured output samples using approximate discrete-time model. It is shown that if one designs a single-rate observer-based output feedback controller which SPA stabilizes the sampled-data nonlinear system, then the dual-rate observer-based output feedback controller will also SPA stabilize the exact discrete-time plant model. Then, numerical examples have been given to illustrate the design method.

Using simulations, the performance of the designed dual-rate controller has been compared with the single-rate controller. It was observed that the dual-rate controller yielded better performance. The dual-rate controller can stabilize the systems with larger sampling periods.

## CHAPTER 8

### CONCLUSIONS & FURTHER RESEARCH

Because of technological advances in computer technology, nowadays controllers are implemented using a digital computer in most control engineering systems. Therefore sampled-data systems have received much attention in recent years. Although sampled-data nonlinear control has attracted much attention in recent years, the controller design methods for sampled-data nonlinear systems are still limited.

In this thesis, digital controller design methods for sampled-data nonlinear systems have been investigated. The direct discrete-time design, one of the main approaches to sampled-data design, based on approximate plant models has been the focus of this research.

In this chapter, the main contributions of the thesis will be summarized and the topics for further research will be stated.

#### 8.1 Conclusions

In this thesis, a reduced order observer design and a range of controller design tools have been proposed for sampled-data nonlinear systems in strict feedback form. Then, a dual-rate control scheme has been presented for the problem of dual-rate output feedback stabilization of sampled-data nonlinear systems under the low measurement rate constraint. To illustrate the tools in this thesis, these tools were applied to several examples arising from the engineering practice. Their performances were analyzed with simulations. The conclusions from each part of the thesis are the following.

In Chapter 3, a backstepping design method has been developed for sampled-data nonlinear

systems in strict feedback form. Different from the backstepping controller given in [48], the controller in this thesis is designed for multi-input sampled-data nonlinear systems to compensate the effects of the discrepancy between the Euler approximate model and exact discrete time model by adding a nonlinear damping term. It was shown by simulations that the designed controller outperforms the controllers given in [48] and [26] which is an extension of the controller in [48] to multi-input sampled-data nonlinear systems. This method can be used for sampled-data nonlinear systems in strict feedback form when all the states are measured.

In Chapter 4, two SPA stabilizing adaptive backstepping design methods have been presented for sampled-data nonlinear systems in strict feedback form. The controllers are designed to compensate the effect of the error in parameter estimation. It was shown by simulations that the designed controllers outperform the emulation controllers. These controllers can be applied to the sampled-data nonlinear systems in strict feedback form in case of parameter uncertainty.

In Chapter 5, a robust backstepping method has been developed for sampled-data nonlinear systems in strict feedback form. This controller is a modified version of the controller given in [58]. Different from the controller in [58], the controller in this thesis is designed to compensate the effect of difference between disturbance or model uncertainty and their bounds. It was shown by simulations that the designed controller outperforms the controller given in [58]. To deal with model uncertainty and disturbances, this controller can be used for sampled-data nonlinear systems in strict feedback form.

In Chapter 6, a reduced order observer design has been presented, which is an extension of the reduced order observer given in [33] to a general class of multi-input nonlinear systems. The observer error converges to zero by the designed observer. It was shown by simulation that the designed observer gives faster results than the observer given in [25].

Then, a reduced-order observer-based SPA stabilizing backstepping method has been given for sampled-data nonlinear systems in strict feedback form in Chapter 6. Different from the backstepping controller given in [25], the controller in this thesis is designed to compensate the effects of observer error. It was shown by simulations that the designed controller outperforms the controller given in [25]. This method can be applied to the applications where only a part of the state vector is available from measurement.

In Chapter 7, for the problem of dual-rate output feedback stabilization of sampled-data nonlinear systems under the low measurement rate constraint, a dual-rate control scheme has been presented based on estimation of the missing output values between measured output samples using approximate discrete-time model. It was shown that if one designs a single-rate observer-based output feedback controller which SPA stabilizes the sampled-data nonlinear system, then the SPA stability property will be preserved by the dual-rate observer-based output feedback controller. This control scheme can be used in applications where hardware restrictions on input and measurement sampling rate is different. Also network load minimization can be achieved by this method.

Consequently, the proposed design tools have been applied to the practical applications such as, ship, robot manipulator, satellite, etc. Simulation results have shown that the controllers designed by the proposed tools yield better results when compared to the controllers existing in the literature. The controllers designed by the proposed methods enlarge the domain of attraction and stabilize the sampled-data nonlinear systems with larger sampling periods in general. When the simulation results with the proposed methods are compared, it can be observed that observer-based output feedback controller given in Chapter 6 gives slightly faster results when compared to the state feedback controller given in Chapter 3. In Chapter 7, it was shown that the dual-rate output-feedback controller outperforms the single-rate output-feedback controller. As a result, it can be said that dual-rate output-feedback controller yields faster results when compared to the other controllers proposed in this thesis.

## **8.2 Further Research**

Although this thesis has developed some design methods, there seems to be still a lot of work to be done to develop a comprehensive set of tools that control engineers can use directly for sampled-data controller design.

In this thesis, design tools based on the Euler approximate model have been given for sampled-data nonlinear systems in strict feedback form. Hence, design tools for other types of sampled-data nonlinear systems which cannot be expressed in strict feedback form may be developed. Also, controllers may be designed using the approximate discrete-time models different from the Euler approximate model.

In this research, reduced order observer-based controller design has been presented. Therefore, for general output dynamical controllers (not necessarily observer-based), sampled-data control design methods can be developed. Also dual-rate control scheme given in this thesis can be applied to sampled-data systems with general output dynamical controllers.

In this thesis, a reduced order observer design has been presented, which is an extension of the reduced order observer given in [33] to a general class of multi-input nonlinear systems. New observer design methods for sampled-data nonlinear systems using the approximate model can be studied. Moreover, the reduced observer-based controller given in this thesis can be applied with the new observers designed and their performances can be analyzed.

The design tools have been applied to the practical applications such as, ship, robot manipulator, satellite, etc. Application of these tools to other practical applications which can be expressed in strict feedback form may be a further research topic.

## REFERENCES

- [1] AHRENS, J., AND KHALIL, H. Multirate sampled-data output feedback using high-gain observers. In *Proceedings of the 45th IEEE Conference on Decision and Control* (San Diego, CA, USA, 2006), pp. 4885–4890.
- [2] ARAPOSTATHIS, A., JACUBCZYK, B., LEE, H. G., MARCUS, S. I., AND SONTAG, E. D. The effect of sampling on linear equivalence and feedback linearization. *Systems and Control Letters* 13 (1989), 373–381.
- [3] ARCAK, M., AND NEŠIĆ, D. A framework for nonlinear sampled-data observer design via approximate discrete-time models and emulation. *Automatica* 40 (2004), 1931–1938.
- [4] ASTOLFI, A., AND ORTEGA, R. Immersion and invariance: A new tool for stabilization and adaptive control of nonlinear systems. *IEEE Transactions on Automatic Control* 48 (2003), 590–606.
- [5] ASTRÖM, K., AND WITTEMARK, B. *Computer-controlled system, Theory and design*. PHI, 1997.
- [6] BOYD, S., AND VANDENBERGHE, L. *Convex optimization with engineering applications*. Lecture Notes, Stanford University, Stanford, 2001.
- [7] CASTILLO, B., DI GENNARO, S., MONACO, S., AND NORMAND-CYROT, D. On regulation under sampling. *IEEE Transactions on Automatic Control* 42 (1997), 864–868.
- [8] CHEN, T., AND FRANCIS, B. A. *Optimal Sampled-Data Control Systems*. Springer-Verlag, London, 1995.
- [9] CRAIG, J. *Adaptive Control of Mechanical Manipulators*. Addison-Wesley, 1988.
- [10] DABROOM, A., AND KHALIL, H. Output feedback sampled-data control of nonlinear systems using high-gain observers. *IEEE Transactions on Automatic Control* 46 (2001), 1712–1725.
- [11] ELAIW, A. *Stabilization of sampled-data nonlinear systems by receding horizon control via discrete-time approximations*. PhD thesis, Budapest University of Technology and Economics, 2005.
- [12] FOSSEN, T. *Marine Control Systems*. Marine Cybernetics, 2002.
- [13] FRANKLIN, G. F., POWEL, J. D., AND WORKMAN, M. *Digital Control of Dynamic Systems*, 3rd ed. Addison-Wesley, 1997.
- [14] FREEMAN, R., AND KOKOTOVIC, P. Backstepping design of robust controllers for a class of nonlinear systems. In *Preprints of second IFAC nonlinear control systems design symposium* (Bordeaux, France, 1992), pp. 307–312.

- [15] FREEMAN, R., AND KOKOTOVIC, P. Design of softer robust nonlinear control laws. *Automatica* 29 (1993), 1425–1437.
- [16] FREEMAN, R., AND KOKOTOVIC, P. *Robust Nonlinear Control Design: State-Space and Lyapunov Techniques*. Birkhauser, 1996.
- [17] GRÜNE, L., WORTHMANN, K., AND NEŠIĆ, D. Continuous-time controller redesign for digital implementation: a trajectory based approach. *Automatica* 44 (2008), 225–232.
- [18] GUGLIERI, G., AND QUAGLIOTTI, F. Analytical and experimental analysis of wing rock. *Nonlinear Dynamics* 24 (2001), 129–146.
- [19] GUILLAUME, A., BASTIN, G., AND CAMPION, G. Sampled-data adaptive control of a class of continuous nonlinear systems. *International Journal of Control* 60 (1994), 569–594.
- [20] HSU, C., AND LAN, C. Theory of wing rock. *Journal of Aircraft* 22 (1985), 920–924.
- [21] ISIDORI, A. *Nonlinear Control Systems II*. Springer-Verlag, New York, 1999.
- [22] KARAGIANNIS, D., AND ASTOLFI, A. Nonlinear adaptive control of systems in feedback form: An alternative to adaptive backstepping. *Syst. Contr. Lett.* 57 (2008), 733–739.
- [23] KARAGIANNIS, D., ORTEGA, R., AND ASTOLFI, A. *Nonlinear adaptive stabilization via system immersion: Control design and applications*, vol. 311 of *In: F. Lamnabhi-Lagarrigue, A. Loría, E. Panteley (Eds.), Lecture Notes in Control and Information Sciences*. Springer-Verlag, Berlin, 2005, pp. 1–21.
- [24] KATAYAMA, H. Nonlinear sampled-data stabilization control for ships. In *American Control Conference* (Seattle, Washington, USA, 2008), pp. 550–555.
- [25] KATAYAMA, H. Nonlinear sampled-data stabilization of dynamically positioned ships by reduced order observer-based controllers. In *European Control Conference* (Budapest, Hungary, 2009), pp. 4883–4888.
- [26] KATAYAMA, H. Nonlinear sampled-data stabilization of dynamically positioned ships. *IEEE Transactions on Control Systems and Technology* 18 (2010), 463–468.
- [27] KHALIL, H. *Nonlinear Control Systems*, 2nd ed. Springer, 1996.
- [28] KHALIL, H. Performance recovery under output feedback sampled-data stabilization of a class of nonlinear systems. *IEEE Transactions on Automatic Control* 49 (2004), 2173–2184.
- [29] KOKOTOVIC, P. The joy of feedback: Nonlinear and adaptive. *IEEE Control Systems Magazine* 12 (1992), 7–17.
- [30] KRSTIĆ, M., KANELAKOPOULOS, I., AND KOKOTOVIĆ, P. *Nonlinear and adaptive control design*. J. Wiley & Sons, New York, 1995.
- [31] KRSTIC, M., AND TSOTRAS, P. Inverse optimal stabilization of a rigid spacecraft. *IEEE Transactions on Automatic Control* 44 (1999), 1042–1049.
- [32] LAILA, D. *Design and analysis of nonlinear sampled-data control systems*. PhD thesis, University of Melbourne, 2003.

- [33] LAILA, D., AND GRÜNBAKER, E. Discrete-time nonlinear observer and output feedback design for a combustion engine test bench. In *Proceedings of the 47th IEEE Conference on Decision and Control* (Cancun, Mexico, 2008), pp. 5718–5723.
- [34] LAILA, D., NAVARRO-LOPEZ, E., AND ASTOLFI, A. Sampled-data adaptive control for a class of nonlinear systems with parametric uncertainties. In *18th IFAC World Congress* (Milan, Italy, 2011).
- [35] LAILA, D., AND NEŠIĆ, D. Changing supply rates for input-output to state stable discrete-time nonlinear systems with applications. *Automatica* 39 (2003), 821–835.
- [36] LAILA, D., NEŠIĆ, D., AND TEEL, A. Open and closed loop dissipation inequalities under sampling and controller emulation. *Europ. J. Contr.* 8 (2002), 109–125.
- [37] LIU, X., AND MARQUEZ, H. Preservation of input-to-state stability under sampling and emulation: multi-rate case. *International Journal of Control* 80 (2007), 1944–1953.
- [38] LIU, X., MARQUEZ, H., AND LIN, Y. Input-to-state stabilization of nonlinear dual-rate sampled-data systems via approximate discrete-time model. *Automatica* 44 (2008), 3157–3161.
- [39] MARINO, R., AND TOMEI, P. Robust stabilization of feedback linearizable time-varying uncertain systems. *Automatica* 29 (1993), 181–189.
- [40] MARINO, R., AND TOMEI, P. *Nonlinear Control Design: Geometric, Adaptive and Robust*. Prentice Hall, London, 1995.
- [41] MONACO, S., AND NORMAND-CYROT, D. Minimum phase nonlinear discrete-time systems and feedback stabilization. In *Proceedings of 26th IEEE Conf. Decis. Contr.* (1987), pp. 979–986.
- [42] MONAHEMI, M., AND KRSTIC, M. Control of wing rock motion using adaptive feedback linearization. *J. Guidance, Control and Dynamics* 19 (1996), 905–912.
- [43] NEŠIĆ, D., AND ANGELI, D. Integral versions of iss for sampled-data nonlinear systems via their approximate discrete-time models. *IEEE Trans. Automat. Contr.* 47 (2002), 2033–2037.
- [44] NEŠIĆ, D., AND GRÜNE, L. Lyapunov based continuous-time nonlinear controller redesign for sampled-data implementation. *Automatica* 41 (2005), 1143–1156.
- [45] NEŠIĆ, D., AND LAILA, D. A note on input-to-state stabilization for nonlinear sampled-data systems. *IEEE Trans. Automat. Contr.* 47 (2002), 1153–1158.
- [46] NEŠIĆ, D., AND TEEL, A. A framework for stabilization of nonlinear sampled-data systems based on their approximate discrete-time models. *IEEE Trans. Automat. Contr.* 49 (2004), 1103–1122.
- [47] NEŠIĆ, D., AND TEEL, A. Matrosov theorem for parameterized families of discrete-time systems. *Automatica* 40 (2004), 1025–1034.
- [48] NEŠIĆ, D., AND TEEL, A. Stabilization of sampled-data nonlinear systems via backstepping on their euler approximate model. *Automatica* 42 (2006), 1801–1808.

- [49] NEŠIĆ, D., TEEL, A., AND CARNEVALE, D. Explicit computation of the sampling period in emulation of controllers for nonlinear sampled-data systems. *IEEE Transactions on Automatic Control* 54 (2009), 619–624.
- [50] NEŠIĆ, D., TEEL, A., AND KOKOTOVIĆ, P. Sufficient conditions for stabilization of sampled-data nonlinear systems via discrete-time approximations. *Syst. Contr. Lett.* 38 (1999), 259–270.
- [51] NEŠIĆ, D., TEEL, A., AND SONTAG, E. Formulas relating KL stability estimates of discrete-time and sampled-data nonlinear systems. *Sys. Contr. Lett.* 38 (1999), 49–60.
- [52] NISOSIA, S., AND TOMEI, P. Robot control by using joint position measurements. *IEEE Transactions on Automatic Control* 35 (1990), 1058–1061.
- [53] OGATA, K. *Discrete-Time Control Systems*, 1st ed. PHI, New Jersey, 1987.
- [54] OWENS, D., ZHENG, Y., AND BILLINGS, S. Fast sampling and stability of nonlinear sampled-data systems: part 1. existence theorems. *IMA Journal of Mathematics, Control and Informations* 7 (1990), 1–11.
- [55] PERTEW, A., MARQUEZ, H. J., AND ZHAO, Q. Direct sampled-data design approach for robot stabilization. In *Proc. of the American Control Conference* (Seattle, WA, 2008), pp. 369–374.
- [56] POLUSHIN, I., AND MARQUEZ, H. Multirate versions of sampled-data stabilization of nonlinear systems. *Automatica* 40 (2004), 1035–1041.
- [57] POSTOYAN, R., AHMED-ALI, T., BURLION, L., AND LAMNABHI-LAGARRIGUE, F. On the lyapunov-based adaptive control redesign for a class of nonlinear sampled-data systems. *Automatica* 44 (2008), 2099–2107.
- [58] POSTOYAN, R., AHMED-ALI, T., AND LAMNABHI-LAGARRIGUE, F. Robust backstepping for the euler approximate model of sampled-data strict feedback systems. *Automatica* 45 (2009), 2164–2168.
- [59] QU, Z. *Robust control of nonlinear uncertain systems*. Wiley, New York, 1998.
- [60] SASTRY, S. *Nonlinear Systems. Analysis, Stability and Control*. Springer, 1999.
- [61] SASTRY, S., AND BODSON, M. *Adaptive Control: Stability, Convergence and Robustness*. Prentice Hall, London, 1989.
- [62] SEPULCHRE, R., JANKOVIĆ, M., AND KOKOTOVIĆ, P. *Constructive Nonlinear Control*. Springer, London, 1997.
- [63] WARSHAW, G., AND SCHWARTZ, H. Sampled-data robot adaptive control with stabilizing compensation. *The International Journal of Robotic Research* 15 (1996), 78–91.
- [64] WU, B., AND DING, Z. A sampled-data scheme for adaptive control of nonlinear systems. In *Proceedings of the 2007 American Control Conference* (Newyork, USA, 2007), pp. 2893–2898.
- [65] WU, B., AND DING, Z. Semi-global asymptotic stability of a class of sampled-data nonlinear systems in output feedback form. In *Proceedings of the 47th IEEE Conference on Decision and Control* (Cancun, Mexico, 2008), pp. 5420–5425.

- [66] ZEMOUCHE, A., BOUTAYEB, M., AND BARA, G. Observer design for nonlinear systems:an approach based on the differential mean value theorem. In *Proceedings of the 44th IEEE Conference on Decision and Control* (Seville, Spain, 2005), pp. 6353–6358.
- [67] ZHENG, Y., OWENS, D., AND BILLINGS, S. Fast sampling and stability of nonlinear sampled-data systems:part 2. sampling rate estimation. *IMA Journal of Mathematics, Control and Informations* 7 (1990), 13–33.

## CURRICULUM VITAE

### AHMET ÜSTÜNTÜRK

Date/Place of Birth: 1981/ Konya  
Marrital Status: Married  
email: a\_ustunturk@yahoo.com

### EDUCATION

| Degree | Institution                               | Year of Graduation |
|--------|---|--------------------|
| PhD    | METU Electrical & Electronics Engineering | 2012               |
| B.Sc   | METU Electrical & Electronics Engineering | 2002               |

### WORK EXPERIENCE

| Year          | Place                      | Enrollment        |
|---------------|----------------------------|-------------------|
| 2005- Present | Türk Telekomünikasyon A.Ş. | Team Leader       |
| 2003-2004     | Karel Elektronik           | Software Engineer |
| 2002-2003     | Vestel Elektronik          | Hardware Engineer |

### FOREIGN LANGUAGES

Advanced English, Beginner French

### PUBLICATIONS

1. Üstüntürk, A., Output-feedback stabilization of nonlinear dual-rate sampled-data systems via approximate discrete-time model, Accepted by Automatica, 2011.
2. Üstüntürk, A., Kocaođlan, E., Backstepping designs for the stabilization of nonlinear sampled-data systems via approximate discrete-time model, Submitted to International Journal of Control, 2011, Under review.